Real Time PCR-Based Infectivity Assay and Characterization of Cell Surface Receptors for Turkey Hemorrhagic Enteritis Virus

Hassan M. Mahsoub

Dissertation submitted to the faculty of the Virginia Polytechnic Institute and State University in partial fulfillment of the requirements for the degree of

Doctor of Philosophy
In
Biomedical and Veterinary Sciences

F. William Pierson, Chair
Roger J. Avery
Kurt L. Zimmerman
Lijuan Yuan

Dec 9, 2015
Blacksburg, Virginia

Keywords: Hemorrhagic Enteritis, THEV, *Siadenovirus*, titration, receptor

Real Time PCR-Based Infectivity Assay and Characterization of Cell Surface Receptors for Turkey Hemorrhagic Enteritis Virus

Hassan M. Mahsoub

ABSTRACT

Turkey hemorrhagic enteritis virus (THEV) is responsible for the hemorrhagic enteritis (HE) disease in commercial turkeys through infections by its virulent strains. HE is an acute condition characterized by depression, immunosuppression, bloody droppings, intestinal hemorrhage, and death. THEV (also known as turkey adenovirus 3) is an official member of the family *Adenoviridae*, genus *Siadenovirus*, species *Turkey siadenovirus A*.

Two main types of live vaccines are currently used for the protection of turkeys against HE; a crude splenic vaccine propagated in live turkeys, and a cell culture-based vaccine generated in RP19 cells. The only laboratory-adapted tests for assessing the titers of these vaccines are agar gel immunodiffusion test and cell culture endpoint dilution, respectively. The assays suffer from low sensitivity, inaccuracy, and time consumption.

A SYBR Green-based real time PCR assay for determining the genomic titer of THEV through the quantification of its hexon gene was developed. The assay was applied as a quality control for the titration of splenic vaccines and was found useful in distinguishing the differences in virus titer among many vaccine batches. Additionally, using the qPCR assay along with a cell culture system, a novel infectivity assay was developed for the titration of THEV, as an alternative for the endpoint dilution assay. Applying the assay on nine batches of commercial HE cell culture vaccines, high variations in infectious virus titers were detected. The new method is rapid, sensitive, and very accurate. A strong correlation was found between the genomic titer and qPCR infectious titer in HE cell culture vaccines. Moreover, the qPCR infectivity assay proved as an instrumental research tool. It was used to measure the effect of several treatments of RP19 cells on virus infection.

The main target cell type for THEV infection and replication is B-lymphocytes, which are represented in vitro by the B lymphoblastoid, RP19 cells. The cellular surface components used by the virus to gain entry into cells are unknown. As an adenovirus, we hypothesized that THEV uses two different molecules on RP19 cells for the attachment and internalization. A recent study has shown that the synthesized THEV fiber knob domain binds to sialyllactose, based on a glycan array analysis. In our studies, the treatment of RP19 cells with neuraminidases and lectins resulted in high reduction of virus entry, which provide a strong evidence of the utilization of cell surface sialic acids as attachment receptor for THEV. Destruction of surface carbohydrates and proteins on RP19 cells also reduced virus entry, indicating that these components are part of the THEV receptor. Using virus overlay protein blot assay, THEV was found to specifically bind to two RP19 surface membrane proteins, most likely, representing primary and secondary receptors for virus entry. Further studies are required to identify these proteins and verify their role in THEV endocytosis in host cells.

Dedication

This dissertation is dedicated to

My wife Marwa Elsenderissy
My sons Mohamed and Hamza
My daughter Khadija

My beloved uncle Hassan Mahsoub
&
My grandfather Mohamed E. Shoaib

Acknowledgements

First and foremost, I praise ALLAH (God) for guiding me throughout my work on this dissertation until I achieved it and for blessing me with the many people who helped me and encouraged me to accomplish this work in the best form it could be.

I would like to thank my supervisor, Dr. Pierson. He provided me with exceptional guidance throughout my dissertation work. Dr. Pierson has always been very supportive of me individually or when I have gone before my PhD advising committee. He knows very well how to make his students self-confident, self-sufficient, and creative researchers. He appreciates my strengths and works with me to improve my weaknesses. Dr. Pierson has never put unnecessary pressure on my shoulders and always shows appreciation for my work. He understands that trial and error is an important part of professional development. When I reached the end of my knowledge and experience, he has always put me back on the right path. As an emeritus professor here at VA Tech once said to me "if your advisor does not consider you as his son, you will find it hard to succeed". This statement is positively applied to Dr. Pierson.

A lot of thanks go to my committee members, Dr. Avery, Dr. Zimmerman, and Dr. Yuan. I could have never imagined having an advisory committee better than this. Every time I went to a committee meeting, I had concerns about the quality and quantity of the lab work I did. However, they always surprised me with their appreciation of what I have accomplished. From my first committee meeting till the day of my dissertation defense, their criticism has been always constructive and friendly, and their words have been always encouraging. I do appreciate all kind of support and advising they have provided me throughout my PhD studies and dissertation writing.

I feel obliged to thank Becky Jones, our BMVS program coordinator, for her extraordinary effort and advices which kept my visa paperwork in a good shape, although not part of her responsibilities. Thanks again for keeping me safe and keeping my assistantship uninterrupted during the last three years. I am also thankful to Cyndi Booth for her administrative roles.

Special thanks are to Dr. Nathan Beach, a previous member in our lab, for his great help during my first year in the lab and afterwards. I thank him also for teaching me lab techniques and troubleshooting, and for continuous encouragement.

I would like also to thank Dr. Sriranganathan for his friendly scientific and non-scientific discussions, and Nancy Tenpenny and Paige Smith for their efforts to make my stay at CMMID as comfortable as possible.

I would like to express my appreciation to all the friendly and lovely faces I have met in CMMID and the College of Veterinary Medicine (faculty, staff, and students). You have truly made my life very pleasant and I really enjoyed the good times we spent together.

I would like also to say thank you to Dr. Nicholas Evans for keeping our research uninterrupted during the last few years through his efficient management of our laboratory financial and organizational matters. Also, he has never hesitated to give help in explaining things that I did not understand and reviewing my abstracts, presentations, and other stuff, when asked to do so.

I am so grateful to Kay Carlson, a previous lab manager at CMMID, for her tremendous effort in reviewing and proofreading the majority of my dissertation.

I am thankful to many friends in and out of Blacksburg: Dr. Mohamed Seleem, Mostafa Ali, Abdullah Awaysheh, Tariq Abuhamdia, Michael Tomaszewicz, and many others. You have been great friends. I would like also to thank my best friends in Egypt: Mahmoud Hafez, Hassan Eltaweell, and Fahmy Abdelaziz.

My first four years in the graduate school at Virginia Tech was supported by a scholarship from the Egyptian Ministry of Higher Education and Scientific Research. I gratefully acknowledge this support. Thanks also to the staff of the Egyptian Cultural and Educational Bureau in Washington, DC, for facilitating my paperwork until I finished my degree.

I am exceptionally thankful to my father Mostafa Mahsoub, my mother Kawthar Shoaib, my brother Mohamed, my sisters Wesam and Reham and their husbands Mohamed Elian and Mohamed Motawea, my parents-in-law Taiseer Eltahawy and Salaheldin Elsenderissy, and my sisters-in-law Maiada, Mai, Mona, and Mariam. Thanks to those family members and all friends in Egypt who remembered me in their prayers all the time and wished me success in my PhD and future profession.

Finally, I will never be able to find the suitable words to express how grateful I am to my wife Marwa, who kept my life in the past seven years the easiest one possible. She has exerted a tremendous effort in taking care of me and our three. God bless you my wife and reward you for all what you have done and are still doing for us. I love you. My gorgeous kids (Mohamed, Hamza, and Khadija), your smiles were a major reason that I have survived my long-term stress until finished my PhD work. May Allah bless you all!

Table of Contents

List of Figures

List of Tables

List of Abbreviations

A	
aa	Amino acid(s)
AAS	Avian adenovirus group II associated splenomegaly of chickens
AASV	Avian adenovirus group II associated splenomegaly virus
Ad(s)	Adenovirus(es)
AGID	Agar gel immunodiffusion / precipitation test
AUN	Neuraminidase from *Arthrobacter ureafaciens*
B	
bp	DNA base pair(s)
BF	Bursa of Fabricius
BM	Bone marrow
C	
Cº	Celsius degrees
CC	Cell culture
$CCID_{50}$	Cell culture infectious dose 50
CPN	Neuraminidase from *Clostridium perfringens*
CV	Coefficient of variation
D	
d	Day(s)
DNA	Deoxyribonucleic acid
dpc	Day(s) post-challenge
dpi	Day(s) post-inoculation
dpv	Day(s) post-vaccination
H	
h	Hour(s)
HAdV(s)	Human adenovirus(es)
HBSS	Hank's balanced salt solution
HE	Hemorrhagic enteritis of turkeys
I, K, L	
IFN	Interferon
IIN	Intranuclear inclusions / inclusion bodies
iv	Intravenous
kDa	Kilo Dalton
LDV	Leucine–aspartic acid–valine motif
M	
min	Minute(s)
mpi	Minute(s) post-inoculation
MSD	Marble spleen disease of pheasants
MSDV	Marble spleen disease virus
mU	Milliunit = 0.0001 unit
N, O	
NA	Neuraminidase / sialidase

nm	Nanometer(s)
nt	Nucleotide
ORF	Open reading frame
P	
PAGE	Polyacrylamide gel electrophoresis
PBS	Phosphate buffered saline
PCR	Polymerase chain reaction
pi	Post-inoculation
pv	Post-vaccination
Q, R, S	
qPCR	Quantitative (real-time) PCR
RGD	Arginine-glycine-aspartic acid motif
RP19	MDTC-RP19, B lymphoblastoid turkey cell line
rpm	Rotation per minute
RT	Room temperature
SA(s)	Sialic acid(s)
ScCl	Cesium chloride
SDS	Sodium dodecyl sulfate
T	
$TCID_{50}$	Tissue culture infectious dose 50%
THEV	Turkey hemorrhagic enteritis virus
THEV-A	Avirulent THEV
THEV-V	Virulent THEV
TID_{50}	Turkey infectious dose 50
Tm	Melting temperature
TNF	Tumor necrosis factor
UVW	
µm	Micrometer(s) / micron(s)
VCN	Neuraminidase from *Vibrio cholerae*
wk	Week(s)

Chapter 1

Introduction

1.1. Background

Turkey hemorrhagic enteritis virus (THEV) is the etiologic agent of hemorrhagic enteritis (HE), an economically important disease in commercial turkeys. HE is characterized by splenomegaly, immunosuppression, acute intestinal hemorrhage, and death in turkeys 6 weeks of age or older. Two serologically indistinguishable and genetically similar viruses to THEV are responsible for causing marble spleen disease (MSD) in pheasants and avian adenovirus splenomegaly (AAS) in chickens, which are characterized by splenomegaly, respiratory edema and congestion (Pierson and Fitzgerald, 2008). Avirulent strains of THEV (THEV-A) have been used in vaccine production both *in vivo*, i.e., in live turkeys, and *in vitro*, i.e., in susceptible leukocytes / lymphocytes, since the late 1970s and the early 1980s, respectively. The vaccines against HE and MSD are able to confer a rapid protection inoculated birds against the virulent strains-induced disease through yet-unknown mechanisms. This protection is known to be not humorally-dependent. Anecdotally, we have observed that vaccination in the face of virulent infection prevents clinical disease. Although studies have shown that lesions caused by THEV and related viruses are immune-mediated, the actual mechanisms by which these lesions form are not well-defined. Also, the mechanism(s) by which the live vaccines protect the birds within a short period after vaccination are not well understood. This lack of understanding is partially due to the absence of knowledge about the changes occurring in the subcellular pathways during the infection process or virus entry and trafficking into target immune cells.

1.2. Previous status of THEV research

HE was reported for the first time in turkeys in 1937 and again in 1957 (Gale and Wyne, 1957; Pomeroy and Fenstermacher, 1937). Thereafter, the pathology of natural and experimental infections of HE and MSD, as well their inter- and intra-species transmission, have been extensively studied. The causative agents were also found to

have typical adenovirus morphology. Results of these studies have been reviewed by multiple works (Fitzgerald and Reed, 1989; Pierson and Fitzgerald, 2008; Sharma, 1991). Several studies have also investigated the potential mechanisms by which the HE and MSD viruses induce deadly clinical lesions in the host species. Although some progress has been made and the clinical lesions are now known to be mediated by the host immune responses/immune system (Rautenschlein and Sharma, 2000; Rautenschlein et al., 2000; Saunders et al., 1993; Suresh and Sharma, 1995), a clear understanding on how these responses are triggered is still lacking.

THEV was found to have a typical morphology of an adenovirus featuring non-enveloped icosahedron composed of three types of capsomers (major surface proteins): the hexon protein (the major capsomer), the penton base protein, and the fiber protein (Davison and Harrach, 2001). The major structural proteins, the complete nucleotide sequence, and the genomic organization of virulent (THEV-V) and avirulent (THEV-A) strains of THEV have been reported (Beach, 2006; Jucker et al., 1996; Nazerian et al., 1991; Pitcovski et al., 1998; van den Hurk, 1992; van den Hurk and van Drunen Littel-van den Hurk, 1988; Zhang et al., 1991). Regarding THEV receptor work, one study, based on the analyses of the predicted amino acid (aa) sequence of the penton base protein, revealed the presence of a leucine-aspartic acid-valine (LDV) motif similar to that of fibronectin. The latter protein is known to use the LDV motif to bind to the alpha(4)beta(1) integrin on the surface of cells. Therefore, it was speculated that THEV could be using the same motif to facilitate its entry into cells (Suresh et al., 1995). However, this hypothesis has not yet been empirically examined. In 2000, the virus was found to be phylogenetically related to frog adenovirus 1 and were then put together into one species designated *Siadenovirus*. The new species was so named because of the presence of an unusual sialidase homolog in the viral genomes of its members (Davison and Harrach, 2001; Davison and Harrach, 2011; Davison et al., 2000; Mayo, 2002). The actual role of this enzyme and whether it is expressed during the infectious cycle of the virus has not been studied.

Recently, the genetic differences in several THEV strains of varying virulence have been reported. Strains were found to share 99.9% DNA sequence homology, but changes (point mutations) in the sequence of three ORFs were suggested to contribute to

the differences in virulence (Beach et al., 2009a). Another study has provided evidence that THEV infection may persist in inoculated turkeys at a low level, undetectable by the common immunoassays, as an explanation of the long-term immunity in one-time vaccinated birds (Beach et al., 2009b). Information concerning the crystallization of THEV fiber protein knob domain was also reported (Singh et al., 2013). In 2015, X-ray crystallography and glycan array binding studies have shown that THEV fiber knob domain binds to 3'- and 6'-sialyllactose; a lactose with sialic acid connected to its galactose unit at the 3 or 6 position, respectively (Singh et al., 2015).

1.3. Scope of the problem

THEV is one of the first two recognized members in the genus *Siadenovirus* and was identified as the etiologic agent of HE in 1974 (Tolin and Domermuth, 1975). In the 1990s, B lymphocytes were confirmed to be the primary cell type for virus infection and replication in various host species (Rautenschlein et al., 1998; Suresh and Sharma, 1996; Suresh and Sharma, 1995). As an adenovirus, THEV is expected to enter target cells through receptor-mediated endocytosis: a process that has not been experimentally investigated for this virus. To date, cellular molecules involved in THEV-cell attachment and internalization, i.e., primary and secondary receptors, have not been characterized or identified. The study of virus entry is the next logical step towards the advancement in Siadenovirology and THEV biology. Therefore, we were interested in investigating how THEV gains entry into target B cells. The intended research focused specifically on the characterization of cellular surface molecules, i.e., receptors, utilized by the virus to facilitate its entry into susceptible B lymphocytes.

1.4. Overall research approach

Molecular studies of virus-cell interactions require the availability of convenient tools and techniques in order to be performed efficiently. First, the presence of an appropriate susceptible cell line(s) is a major requirement for the study of viruses. Fortunately, the establishment of MDTC-RP19 B lymphoblastoid cell line-hereafter referred to as RP19-from turkey liver tumor (Nazerian et al., 1982; Nazerian and Fadly, 1982) has made possible the *in vitro* molecular studies of THEV. This cell line was

deposited in the American Type Culture Collection and made commercially available for use in THEV propagation for vaccine production and experimental purposes. Second, efficient *in vitro* infectivity assays are another necessary research tool to help study virus-cell interactions. These assays are means of verifying successful infection, active virus replication and propagation, which is normally conducted through visual examination of inoculated host, e.g., cells and animals, either *in vivo* or *in vitro* (Villegas, 2008). An accurate and rapid infectivity assay to evaluate the infectivity and determine the titer of THEV is lacking. During the period from 1970s to 1980s, several infectivity assays have been developed for THEV or adapted from general virology procedures. The most common *in vitro* method relies solely on using light microscopy to monitor the development of cytopathic effect (CPE; enlargement and ballooning of cells) in susceptible cells after inoculation with virus (Nazerian and Fadly, 1987). This assay is used by most vaccine companies for virus titration of cell culture-based HE vaccine products. Immunofluorescence assay and agar gel immunodiffusion tests have been established and electron microscopy has been utilized to study and confirm viral replication (Domermuth et al., 1977; Domermuth et al., 1973; Nazerian and Fadly, 1982), under certain experimental conditions and requirements. Regardless of their usefulness, these assays are not suitable for certain types of research, such as when virus binding and infectivity need to be verified within a few hours of viral inoculation into cells. Therefore, a new assay for the quantitative assessment of virus infectivity is needed. Third, identification of cellular proteins that interact with certain viruses necessitates the use of well-described methods and protocols that have shown satisfactory results with relevant viruses. Sodium dodecyl sulfate-polyacrylamide gel electrophoresis (SDS-PAGE), virus overlay protein blot assay (VOPBA), and mass spectrometry have been used in recent years to characterize receptors for several viruses, including a human adenovirus (Jindadamrongwech and Smith, 2004; Karger and Mettenleiter, 1996; Koudelka et al., 2009; Trauger et al., 2004; Wu et al., 2001). These methods were used in the present work for the identification of the cell surface protein molecules that interact with THEV.

1.5. Hypotheses

Based on published research and preliminary data, I hypothesize that:

1. There are considerable lot-to-lot variations in virus titers, i.e., content of infectious virus particles, of live HE vaccines among the different manufacturers and within the same manufacturer.
2. THEV uses two cell surface molecules on target cells, e.g., RP19 cells, most likely a sugar and a polypeptide, as receptors for attachment and internalization.

Aims and Objectives

Aim 1: To devise a novel qPCR-based assay for accurate titration of THEV and studying virus attachment/infectivity

Objectives:

1. To establish a real-time quantitative PCR (qPCR) assay for accurate quantification of THEV genome copy number.
2. To optimize the new assay for use with various biological samples, e.g., tissues, solutions, cell cultures, vaccines, etc.
3. To validate the new assay as a tool for verifying virus attachment/entry into infected RP19 cells as well as active virus replication through one-step growth curve experiments.
4. To employ the new assay for the titration of HE cell culture vaccines and determine the differences in virus titers among different vaccine products.

Aim 2: To determine the structural components of potential THEV receptor(s) on RP19 cells.

Objectives:

1. To investigate the role, if any, of cell surface sialic acids -used as functional receptors by some human adenoviruses- in virus entry.
2. To determine whether the receptor contains a carbohydrate moiety.
3. To determine whether the receptor contains a protein component.

4. To identify any cellular membrane proteins which may interact with the virus on RP19 cells, using VOPBA.

Chapter 2 discusses the literature review related to 3 main areas: 1) titration of live virus vaccines, 2) siadenoviral infections, including THEV, and 3) adenovirus receptors. Chapter 3 describes the results from Aim1, objectives 1 and 2 about the establishment and optimization of a new THEV-qPCR assay. Chapter 4 describes the results from Aim 1, objectives 3 and 4 regarding the development of a novel qPCR-based procedure for the quantification of THEV infectivity in cell cultures and its use in vaccine titration. The findings from Aim 2 regarding the THEV cellular receptor(s) on B cells are described in Chapter 5. This chapter also discusses the expected overall structure of the potential viral receptor(s) in the light of the experimental information obtained. Chapter 6 contains general conclusions of results and their significance, and proposed future research.

1.6. References

Beach, N.M. 2006. Characterization of avirulent turkey hemorrhagic enteritis virus: a study of the molecular basis for variation in virulence and the occurrence of persistent infection, Virginia Polytechnic Institute and State University, Blacksburg, VA, USA, pp. 207.

Beach, N.M., Duncan, R.B., Larsen, C.T., Meng, X.-J., Sriranganathan, N. and Pierson, F.W., 2009a. Comparison of 12 turkey hemorrhagic enteritis virus isolates allows prediction of genetic factors affecting virulence. J Gen Virol 90, 1978-1985.

Beach, N.M., Duncan, R.B., Larsen, C.T., Meng, X.J., Sriranganathan, N. and Pierson, F.W., 2009b. Persistent Infection of Turkeys with an Avirulent Strain of Turkey Hemorrhagic Enteritis Virus. Avian Diseases 53, 370-375.

Davison, A. and Harrach, B. 2001. Siadenovirus. In: Tidona, C., Darai, G. and Büchen-Osmond, C. (Eds), The Springer Index of Viruses, Springer Berlin Heidelberg, pp. 29-33.

Davison, A. and Harrach, B. 2011. Siadenovirus. In: Tidona, C. and Darai, G. (Eds), The Springer Index of Viruses, Springer New York, pp. 49-56.

Davison, A.J., Wright, K.M. and Harrach, B., 2000. DNA sequence of frog adenovirus. J Gen Virol 81, 2431-2439.

Domermuth, C.H., Gross, W.B., Douglass, C.S., Dubose, R.T., Harris, J.R. and Davis, R.B., 1977. Vaccination for hemorrhagic enteritis of turkeys. Avian Dis 21, 557-565.

Domermuth, C.H., Gross, W.B. and DuBose, R.T., 1973. Microimmunodiffusion Test for Hemorrhagic Enteritis of Turkeys. Avian Diseases 17, 439-444.

Fitzgerald, S.D. and Reed, W.M., 1989. A review of marble spleen disease of ring-necked pheasants. J Wildl Dis 25, 455-61.

Gale, C. and Wyne, J.W., 1957. Preliminary Observations on Hemorrhagic Enteritis of Turkeys. Poultry Science 36, 1267-1270.

Jindadamrongwech, S. and Smith, D.R., 2004. Virus Overlay Protein Binding Assay (VOPBA) Reveals Serotype Specific Heterogeneity of Dengue Virus Binding Proteins on HepG2 Human Liver Cells. Intervirology 47, 370-373.

Jucker, M.T., McQuiston, J.R., van den Hurk, J.V., Boyle, S.M. and Pierson, F.W., 1996. Characterization of the haemorrhagic enteritis virus genome and the sequence of the putative penton base and core protein genes. J Gen Virol 77, 469-479.

Karger, A. and Mettenleiter, T.C., 1996. Identification of cell surface molecules that interact with pseudorabies virus. Journal of Virology 70, 2138-45.

Koudelka, K.J., Destito, G., Plummer, E.M., Trauger, S.A., Siuzdak, G. and Manchester, M., 2009. Endothelial Targeting of Cowpea Mosaic Virus (CPMV) via Surface Vimentin. PLoS Pathog 5, e1000417.

Mayo, M.A., 2002. ICTV at the Paris ICV: Results of the Plenary Session and the Binomial Ballot. Archives of Virology 147, 2254-2260.

Nazerian, K., Elmubarak, A. and Sharma, J.M., 1982. Establishment of B-lymphoblastoid cell lines from Marek's disease virus-induced tumors in turkeys. International Journal of Cancer 29, 63-68.

Nazerian, K. and Fadly, A.M., 1982. Propagation of virulent and avirulent turkey hemorrhagic enteritis virus in cell culture. Avian Diseases 26, 816-27.

Nazerian, K. and Fadly, A.M., 1987. Further studies on in vitro and in vivo assays of hemorrhagic enteritis virus (HEV). Avian Diseases 31, 234-40.

Nazerian, K., Lee, L.F. and Payne, W.S., 1991. Structural polypeptides of type II avian adenoviruses analyzed by monoclonal and polyclonal antibodies. Avian Diseases 35, 572-8.

Pierson, F.W. and Fitzgerald, S.D. 2008. Hemorrhagic Enteritis and Related Infections. In: Saif, Y.M., Fadly, A.M., Glisson, J.R., McDougald, L.R., Nolan, L.K. and Swayne, D.E. (Eds), Diseases of Poultry, Wiley-Blackwell, Iowa, pp. 276-286.

Pitcovski, J., Mualem, M., Rei-Koren, Z., Krispel, S., Shmueli, E., Peretz, Y., Gutter, B., Gallili, G.E., Michael, A. and Goldberg, D., 1998. The Complete DNA Sequence and

Genome Organization of the Avian Adenovirus, Hemorrhagic Enteritis Virus. Virol 249, 307–315.

Pomeroy, B.S. and Fenstermacher, R., 1937. Hemorrhagic Enteritis in Turkeys. Poultry Science 16, 378-382.

Rautenschlein, S. and Sharma, J.M., 2000. Immunopathogenesis of haemorrhagic enteritis virus (HEV) in turkeys. Dev Comp Immunol 24, 237-46.

Rautenschlein, S., Suresh, M., Neumann, U. and Sharma, J.M., 1998. Comparative pathogenesis of haemorrhagic enteritis virus (HEV) infection in turkeys and chickens. J Comp Pathol 119, 251-61.

Rautenschlein, S., Suresh, M. and Sharma, J.M., 2000. Pathogenic avian adenovirus type II induces apoptosis in turkey spleen cells. Arch Virol 145, 1671-83.

Saunders, G.K., Pierson, F.W. and Hurk, J.V.v.d., 1993. Haemorhagic enteritis virus infection in turkeys: A comparison of virulent and avirulent virus infections, and a proposed pathogenesis. Avian Pathology 22, 47 - 58.

Sharma, J.M., 1991. Hemorrhagic enteritis of turkeys. Vet Immunol Immunopathol 30, 67-71.

Singh, A.K., Ballmann, M.Z., Benko, M., Harrach, B. and van Raaij, M.J., 2013. Crystallization of the C-terminal head domain of the fibre protein from a siadenovirus, turkey adenovirus 3. Acta Crystallographica Section F 69, 1135-1139.

Singh, A.K., Berbis, M.A., Ballmann, M.Z., Kilcoyne, M., Menendez, M., Nguyen, T.H., Joshi, L., Canada, F.J., Jimenez-Barbero, J., Benko, M., Harrach, B. and van Raaij, M.J., 2015. Structure and Sialyllactose Binding of the Carboxy-Terminal Head Domain of the Fibre from a Siadenovirus, Turkey Adenovirus 3. PLoS One 10, e0139339.

Suresh, M., Cyr, S.S. and Sharma, J.M., 1995. Molecular cloning and sequence analysis of the penton base genes of type II avian adenoviruses. Virus Res 39, 289-297.

Suresh, M. and Sharma, J., 1996. Pathogenesis of type II avian adenovirus infection in turkeys: in vivo immune cell tropism and tissue distribution of the virus. J. Virol. 70, 30-36.

Suresh, M. and Sharma, J.M., 1995. Hemorrhagic enteritis virus induced changes in the lymphocyte subpopulations in turkeys and the effect of experimental immunodeficiency on viral pathogenesis. Vet Immunol Immunopathol 45, 139-150.

Tolin, S.A. and Domermuth, C.H., 1975. Hemorrhagic Enteritis of Turkeys: Electron Microscopy of the Causal Virus. Avian Diseases 19, 118-125.

Trauger, S.A., Wu, E., Bark, S.J., Nemerow, G.R. and Siuzdak, G., 2004. The Identification of an Adenovirus Receptor by Using Affinity Capture and Mass Spectrometry. ChemBioChem 5, 1095-1099.

van den Hurk, J.V., 1992. Characterization of the structural proteins of hemorrhagic enteritis virus. Arch Virol 126, 195-213.

van den Hurk, J.V. and van Drunen Littel-van den Hurk, S., 1988. Characterization of group II avian adenoviruses with a panel of monoclonal antibodies. Can J Vet Res 52, 458-67.

Villegas, P. 2008. Titration of biological suspensions. In: Dufour-Zavala, L. (Ed), Isolation, Identification, and Characterization of Avian Pathogens, The American Association of Avian Pathologists, Athens, GA, pp. 217-221.

Wu, E., Fernandez, J., Fleck, S.K., Von Seggern, D.J., Huang, S. and Nemerow, G.R., 2001. A 50-kDa membrane protein mediates sialic acid-independent binding and infection of conjunctival cells by adenovirus type 37. Virology 279, 78-89.

Zhang, C.L., Nagaraja, K.V., Sivanandan, V. and Newman, J.A., 1991. Identification and characterization of viral polypeptides from type-II avian adenoviruses. Am J Vet Res 52, 1137-41.

Chapter 2

Review of Literature

Review outline

2.1. Current taxonomy of adenoviruses

2.2. Section I: Turkey hemorrhagic enteritis virus (THEV) and other siadenoviral infections

- THEV and related infections in pheasant and chicken
- Siadenoviral infections of avian and non-avian species

2.3. Section II: Virus titration and infectivity assays

- Background
- Traditional titration methods for THEV and other viruses
  - Common techniques and culture systems found unsuitable for THEV
  - Infectivity assays and titration procedures for THEV
  - Most common infectivity assays and titration procedures for viruses
- Modern titration methods
- Overall advantages and disadvantages of virus titration methods

2.4. Section III: Adenovirus cell receptors

- Adenovirus structure and genomic composition
- Adenovirus receptors and cell / tissue tropism
- The use of virus overlay protein blot assay (VOPBA) for identifying novel viral receptors

2.5. References

2.1. Current taxonomy and nomenclature of adenoviruses

In 1971, the genus adenovirus was established without an assigned family. It contained only Adenovirus type 1 (AdV-1) which was also designated as the type species. In 1975, the genus was upgraded to family *Adenoviridae* and it involved two genera; *Mastadenovirus* (type species AdV-1) and *Aviadenovirus* (type species chicken embryo lethal orphan [CELO]). Since then, several species have been discovered and

added to these genera, other genera have been created, and the naming of viruses has been changed multiple times. According to the most recent release from the International Committee on Taxonomy of Viruses (ICTV; EC 46, Montreal, Canada, July 2014, Email ratification 2015 [MSL #29]) available at http://www.ictvonline.org/index.asp, the virus family *Adenoviridae* is composed of the following five genera based on phylogenetic analyses: *Mastadenovirus*, established in 1975, contains 25 species including all human adenoviruses (type species *Human mastadenovirus C*); *Aviadenovirus* established in 1975, contains 8 species (type species *Fowl aviadenovirus A*); *Atadenovirus*, proposed in 1998 (Benkö and Harrach; Dan et al.) and established in 2002, contains 5 species (type species *Ovine atadenovirus D*); *Siadenovirus*, proposed in 2000 (Davison et al.) and officially recognized in 2002, contains 5 species (type species *Frog siadenovirus A*); and *Ichtadenovirus*, established in 2009, contains 1 (type) species *Sturgeon ichtadenovirus A*.

In 2002, a new species named *Turkey adenovirus A* was created and contained turkey adenovirus 3 (TAdV-3), which is the official name for turkey hemorrhagic enteritis virus (THEV) and marble spleen disease virus (MSDV). In this year, the genus *Siadenovirus* was also established to include this species along with the "frog" species. Before that, THEV was located under the genus *Aviadenovirus*. Until recently, the *Siadenovirus* genus has been solely composed of the above two species. Starting 2009, several reports have been made on the discovery of new siadenoviruses, three of which are now official species in the genus: *Raptor adenovirus A*, *Great tit siadenovirus A*, and *Skua siadenovirus A*. The rest of the newly discovered siadenoviruses have not been officially accepted. All of these viruses are reviewed in the following pages.

2.2. Section I: Turkey hemorrhagic enteritis virus and other siadenoviral infections

Siadenoviral infections have been reported in a variety of animal classes including amphibians, birds, and reptiles. All the discovered infections are described below. The clinical presentations, histopathological findings and results from genetic and phylogenetic analyses are detailed where available.

2.2.1. Turkey hemorrhagic enteritis virus (THEV) and related strains

Historically, three serologically and antigenically indistinguishable THEV isolates were described and originally referred to as the group II aviadenoviruses. These were named turkey hemorrhagic enteritis virus (THEV), marble spleen disease virus (MSDV), and avian adenovirus splenomegaly virus (AASV) causing disease in turkeys, pheasants, and chickens, respectively.

2.2.1.1. History of incidence, current status of HE, and potential economic impact

HE disease was recognized for the first time in turkeys (7-12 weeks [wk] of age) in 1936; occurring on several different farms in Minnesota (Pomeroy and Fenstermacher, 1937). Mortality as high as 10% was noted. In the late 1950s, two outbreaks of HE were reported over a 3-year period in turkeys, 7 and 11 wk of age, raised in confinement at the Ohio Agricultural Experiment Station (Gale and Wyne, 1957). Mortality rates of 1.6% and 3.5% were reported in the two flocks, respectively. In the 1960s, THEV was identified in Virginia and other states with flock mortality rates exceeding 60% (Gross and Moore, 1967). Also, THEV infections were seen in association with other health problems in Iowa, Illinois, and California (Ianconescu et al., 1985; Trampel et al., 1992). Outside of the US, occurrences of HE have been reported in Canada (Ontario) (Itakura and Carlson, 1975b), Japan (Fujiwara et al., 1975), Australia (Arzey and Cross, 1990; Tham and Critchley, 1981), Poland (Koncicki, 1990; Koncicki et al., 2012), Spain (Gómez-Villamandos et al., 1994), and Croatia (Lojkić et al., 2010). More recently, HE outbreaks complicated with secondary E. coli infection have been reported in Hungary in turkeys 6-8 wk of age (Palya et al., 2007) and Italy in 52-wk old turkey breeders, causing a drop in egg production for 5 weeks (Ceruti et al., 2007).

In the 1980s, economic losses to the turkey industry due to HE and accompanying secondary infections were estimated to be in the tens of millions of dollars (Nagaraja et al., 1985). THEV is widely spread in the environment (Ceruti et al., 2007) and, therefore, represents a continuous threat to the turkey industry. However, with the advent of vaccination in the 1970s, losses have been dramatically curtailed.

2.2.1.2. Etiology of HE and characteristics of the causal pathogen

Virus discovery

Although HE has been observed in turkey flocks since the mid-1930s, the true nature of the causative agent remained unknown for decades. The earliest investigations using microscopic examination of the intestinal contents and the mucosa of dead birds ruled out protozoa and vibrionic bacteria. An attempt to isolate virus from purified intestinal contents in chicken embryos was unsuccessful (Gale and Wyne, 1957). Moderate progress was made when Gross and Moore (1967) were able to experimentally produce HE in turkeys by the inoculation with a 0.22 µm filterable agent they speculated to be a bacterial toxin or a streptococci-specific bacteriophage that could be serially passed along with the bacterial culture. In the early 1970's, additional filtration studies suggested that the HE-causing pathogen could be a virus. The agent was found to readily pass through a 100-nm filter and it was speculated that the particle was approximately 50 nm in diameter (Domermuth and Gross, 1971; Domermuth et al., 1972). Confirmation of the identity of the HE pathogen as a virus was presented by Carlson et al. (1974) who noted intranuclear inclusion (INI) bodies in markedly enlarged nuclei of ballooned cells in the spleen and the intestinal lamina propria. Transmission electron microscopy revealed viral particles occurring in 3 forms in the nucleus: rows, crystalline arrays, and loosely scattered. Remnants of ruptured cells containing virus particles were seen in splenic tissue (Carlson et al., 1974). Virus particles similar to those in the spleen where also observed in other tissues, e.g., cecal tonsils, liver, and bone marrow (Itakura and Carlson, 1975a).

Virus morphology

Transmission electron microscopy of the nuclei of infected cells showed THEV particles which differed in core density: dense osmiophilic nucleoid cores (presumably mature virions), loose osmiophilic cores, and empty capsids containing no cores. The buoyant density of the virus band separated by sucrose-cesium chloride (ScCl) gradient centrifugation was determined to be 1.33-1.34 g/cm3 (Iltis et al., 1977), although slightly higher values have been observed, i.e., 1.4 g/cm3 (van den Hurk, 1992). The size of purified THEV particles was determined to be in the range of 70-90 nm. Electron

micrographs of negatively-stained splenic extracts purified from infected spleens displayed nonenveloped, icosahedral virus particles similar to those seen in mammalian, but not fowl, adenoviral infection (Carlson et al., 1974; Trampel et al., 1992). The number of capsomers was estimated to be 252. However, in early studies, the adenoviral penton fibers were not seen; apparently being lost during staining (Carlson et al., 1974; Iltis et al., 1975; Itakura and Carlson, 1975a; Ossa et al., 1983b; Tolin and Domermuth, 1975; van den Hurk, 1992). These were later identified as single rather than double fibers as is seen with the fowl adenoviruses (van den Hurk, 1992).

Structural proteins

Three studies were conducted to investigate the structural components of the THEV/MSDV/AASV virion. In one study, THEV-V or MSDV was propagated in RP19 cells, followed by disruption with a lysis buffer. Using sodium dodecyl sulfate-polyacrylamide gel electrophoresis (SDS-PAGE), immunoblotting and immunoprecipitation assays, eleven polypeptides were identified in the lysates of both. Molecular weights of detected polypeptides ranged from 14 to 97 kDa (Nazerian et al., 1991). SDS-PAGE and western blot analysis of virus purified from infected spleens using polyclonal and monoclonal THEV-specific antibodies revealed the presence of eleven viral polypeptides in THEV, ranging in size between 9.5 and 96 kDa. These proteins were identified as the outer capsid proteins: hexon (96 kDa), penton (~52 kDa), fiber (29 kDa); two core proteins: 9.5 kDa and 12.5 kDa; IIIa (HAdV-2 homologue; 57 kDa); and five more proteins of the following molecular weights: 44, 37, 34, 24, and 21 kDa. No major differences were found between THEV-A and THEV-V strains. Variations in molecular weights between this study and the previous one were thought to be due to differences in preparation of viral proteins, PAGE conditions, and staining protocols. Zhang et al. (1991) propagated THEV, MSDV and AASV in turkeys and purified virus using sucrose-CsCl gradients. SDS-PAGE stained with Coomassie blue revealed eight polypeptides in THEV and only six in MSDV and AASV. The molecular weights of these polypeptides ranged from 18 to 97 kDa. Immunoblots using THEV polyclonal antibody from turkeys and HRP-conjugated goat-anti-turkey antibodies was performed. Four polypeptides, namely II (97 kDa), V (48 kDa), VI (25 kDa), and VII (18 kDa) were detected in all three viruses, and two more, namely III (70 kDa) and IV (60 kDa), were

detected only in THEV. Again, the difference between this and previous studies was likely the result of methodological issues such as low proteins concentration, low sensitivity of detection, reagent variation, protein sample preparation, and PAGE conditions.

Genomic composition and genetic features

Several studies have been conducted to determine the genetic characteristics of THEV, MSDV, and AAVS. The first was an attempt to determine differences among strains based on restriction endonuclease fingerprinting (Zhang and Nagaraja, 1989). The restriction patterns were useful in differentiating the genome of the group II aviadenoviruses from other aviadenoviruses; but of little value relative to determining strain variations. Although complete genomic DNA was presumably isolated from purified virions, a genome size was not determined. A 2500-bp EcoRI restriction fragment of THEV DNA, which reacted positively with a penton base gene probe, was cloned and sequenced (Suresh et al., 1995). Comparisons of the nucleotide and projected amino acid (aa) sequences showed strong homology with fowl adenovirus 10 (FAdV-10) and several human adenoviruses (HAdVs). The fragment was found to contain the full length of 1344 bp of the putative penton base ORF, which is ~370 bp or 230 bp shorter than that of HAdVs type 2 and 5 or FAdV-10, respectively. A restriction digest of MSDV DNA yielded similar results. Alignment and analysis of the predicted THEV penton protein aa sequence revealed that it lacked the arginine-glycine-aspartic acid (RGD) motif present on HAdVs penton proteins e.g., HAdV-2, resembling FAdV-10; however, a motif of leucine–aspartic acid–valine (LDV) was identified. It was further speculated that this motif may mediate the internalization of THEV into host cells through binding to the surface α4β1 integrin receptor, which is expressed on several cell types including lymphocytes, monocytes, and bone marrow progenitors (Suresh et al., 1995). This hypothesis has not been experimentally tested. A genomic restriction map of THEV DNA, purified from a Virginia isolate of low virulence, was constructed. The genome length was estimated to be 25.5 kb; making it the shortest adenoviral genome reported (Jucker et al., 1996). A central EcoRI restriction fragment of 2643 bp was cloned and sequenced. It was found to have a remarkably low G+C content of 34% as compared to other adenoviruses. Based on the analysis of its deduced aa sequence, this fragment was

found to contain a partial ORF, followed by the coding sequences of putative penton base (pIII), two core proteins (pVII and p-mu), and partial putative pVI (hexon associated protein). Comparison of the projected aa sequences of these ORFs with those of FAdV-10, HAdV-2, and HAdV-40 indicated that THEV truly belonged to a classification distinct from aviadenoviruses and mastadenoviruses (Jucker et al., 1996). Two years later, the complete nucleotide sequence of the THEV genome was published for a virulent field isolate referred to as Israeli virulent strain (IVS); GenBank accession # AF074946.1 (Pitcovski et al., 1998), validating the previous claim that it was in fact the shortest adenovirus genome identified. Several years later, Beach et al. (2009a) sequenced the full genome of the naturally occurring, Virginia avirulent strain (VAS) of THEV; GenBank accession # AY849321.1. The overall features of the two genomes were: genome size is 26,263 bp and 26,266 bp respectively; G+C content is 34.9%, both; length of inverted terminal repeats (ITR), 39 and 40, respectively. A comparison of the two genomes revealed 49 point mutations, 14 of which were believed to result in changes in the aa sequence of THEV proteins. Further comparisons of partial genomic sequences from twelve THEV field strains of varying virulence revealed that the majority of mutations were present in two ORFs of yet unknown function; ORF1 and E3, and the fiber knob domain. Consequently, these ORFs/genes were suggested to play a role in the phenotypic differences in virulence among the strains (Beach, 2006; Beach et al., 2009a).

Susceptibility and tropism

Host susceptibility

Most of the natural clinical cases and outbreaks of HE have been reported in turkey poults 4 wk of age or older; (Pierson and Fitzgerald, 2008). Only one case was reported where an HE outbreak occurred in 2.5 wk old poults (Harris and Domermuth, 1977). In general, turkeys of 2-4 wk of age are refractory to clinical disease, depending on the level of maternal antibodies (mAbs) (Sharma, 1991), but they are still susceptible to THEV infection. Fadly and Nazerian (1989) found that poults without mAbs against THEV were much more susceptible to THEV infection if older than 15 days. Resistance to HE was seen in poults up to 13 days of age regardless of their mAb levels. However, mAb-free embryos were susceptible to infection with THEV-V and -A strains, developed

protective Abs post-hatch upon inoculation, but showed no evidence of clinical disease. In another study, SPF turkey embryos were injected at day 24 of incubation with MSDV. The virus was detected in the spleen and other organs starting 4 days post-inoculation (dpi) and reached its peak replication in the spleen at 6 dpi (Ahmad and Sharma, 1993). Results from the last two studies indicate that the host cells in young turkeys support virus replication. However, the immune system is not mature enough to trigger the acute, likely immune mediated responses (manifested by clinical HE) seen in older birds (Rautenschlein and Sharma, 2000).

Tissue and cell tropism

Viral antigens and DNA distribution in various tissues of THEV-infected birds have been studied using a variety of techniques including transmission electron microscopy, immunostaining, and PCR (Beach et al., 2009b; Fasina and Fabricant, 1982a; Fasina and Fabricant, 1982b; Saunders et al., 1993; Suresh and Sharma, 1996). However, the specific types of cells susceptible to THEV infection and replication have only been partially investigated. Regardless of the pathology caused by THEV strains of varying virulence, the spleen has been shown to be the primary site of tropism and viral replication. Splenomegaly with INIs has been consistently seen in all affected species (Domermuth et al., 1982; Suresh and Sharma, 1996; Tolin and Domermuth, 1975; Veit et al., 1981). Although virus particles and in several cases INIs, were observed in the intestinal lamina propria, liver, lungs, bone marrow, and kidneys of naturally and experimentally THEV-infected turkeys and MSDV-infected pheasants (Carlson et al., 1974; Fitzgerald et al., 1992; Suresh and Sharma, 1996), it was suggested that the virus-infected cells (mainly lymphocytes) from the spleen circulated through these sites rather than being indigenous (Saunders et al., 1993). In addition to the spleen, cecal tonsils were reported to be another location having high levels of THEV replication (Suresh and Sharma, 1996). In a recent study, the distribution of THEV DNA was studied over time in various organs of inoculated poults (Beach et al., 2009b). THEV DNA was detected in bone marrow for up to 15 wk post-inoculation (pi); however, it was not verified whether this was related to active virus replication or not. Because of the long-lasting immune responses and high antibody titers, it was suggested that THEV could be constantly infecting a small population of B lymphocytes in this location.

In regard to cell tropism, early electron microscopic studies on THEV cytopathology suggested two types of cells as targets for THEV replication/infection based on the presence of INIs and viral particles. Their morphological characteristics were consistent with lymphocytes and macrophages (Itakura and Carlson, 1975a). Fasina and Fabricant (1982b) studied the susceptibility of various primary cultures of splenic lymphocytes collected from chickens, pheasants, and turkeys at various ages to the infection with THEV. Positive cells were identified by the presence of intranuclear viral antigen visualized using immunofluorescence. Splenic lymphocytes from 1 to 5 wk old chicks were positive, while those from 18 d old embryos and 1 d old chicks were negative when examined at 45 and 70 hours post-inoculation (hpi). Overall, THEV antigens were detected in inoculated lymphocytes as early as 24 hpi and increased by 48 hpi. When compared together, pheasant and turkey splenic lymphocytes where much more susceptible to THEV infection than those of chickens. In another study, splenic leukocytes (lymphocytes and other white blood cells) from turkeys 5-12 wk of age and peripheral blood leukocytes from turkeys 8-20 wk of age were isolated, cultured, and inoculated with THEV. Adherent and nonadherent cells were harvested 2-3 dpi and subject to THEV-fluorescent staining and electron microscopy (van den Hurk, 1990b). The non-adherent susceptible cell type was described as smooth, immature (blast-like) and non-phagocytic. Using fluorescent microscopy, the infection of THEV in large adherent granular leukocytes having the properties of monocyte-macrophage-type of cells was verified. THEV particles were seen in the nucleus as well as in the cytoplasm of these adherent cells. It was also noted that viral antigen and infectious virions gradually increased as measured by FA assay and titration experiments up to 3 dpi. Further evidence fueled speculation that the non-adherent THEV-susceptible cells were lymphocytes. In one study, THEV-infected turkeys showed a reduction in the number of IgM^+ B lymphocytes in spleens and peripheral blood. Also, cyclophosphamide-induced B cell depletion was found to dramatically impair THEV replication in the spleen. These observations and other in vitro studies clearly suggested that B cells were the major target of THEV replication (Nazerian et al., 1982; Nazerian and Fadly, 1987; Rautenschlein and Sharma, 2000; Suresh and Sharma, 1995). Splenic macrophages were also believed to

support replication based on viral DNA content (Rautenschlein et al., 2000b; Suresh and Sharma, 1996).

Other proposed sites of replication include alveolar epithelial cells, lung atrial histiocytes (tissue-bound macrophages), liver cells "adjacent to hepatic sinusoids", and bone marrow (INIs were "scattered among hematopoietic cells"). INIs have also been seen in high numbers in cells found in the intestinal lamina propria and ceca of turkeys (Fitzgerald et al., 1992; Itakura et al., 1974). Based on in vivo and in vitro studies, it was shown that the different T-cell populations (CD4+ and CD8+) are resistant to THEV infection (Nazerian and Fadly, 1982; Rautenschlein et al., 2000b), even though they were suggested to have a considerable role in the viral immunopathogenicity (Rautenschlein and Sharma, 2000; Suresh and Sharma, 1995).

2.2.1.3. Pathology of HE

The natural route of THEV infection is fecal-oral; however, HE has been reproduced successfully in susceptible turkeys by various routes of inoculation, i.e., cloacal, intraperitoneal, intravenous, and intramuscular (Arzey and Cross, 1990; Gross and Moore, 1967; Rautenschlein et al., 1998; Silim and Thorsen, 1981). A difference of up to 2 days in the virus incubation period was observed depending on the route of infection. Lesions caused by THEV infections in turkeys can be generally divided into two types: 1) primary lesions, which occur in the spleen and small intestines of affected turkeys; and 2) secondary lesions observed in other internal organs.

HE primary lesions

Splenic lesions

During natural outbreaks of virulent HE reported in the 1930s and 1950s, splenomegaly, was not seen in autopsied birds. The main reason was believed to be splenic contraction due to significant blood loss (60-70%) although dark discoloration and congestion was occasionally noticed (Gale and Wyne, 1957; Pomeroy and Fenstermacher, 1937). Early studies looking at experimental reproduction of HE in the 1960s focused mainly on the intestinal lesions, while other organs were not investigated (Gross, 1967; Gross and Moore, 1967). The first observations of HE splenic lesions were

in field cases of dead and dying turkeys, in the 1970s. Shrunken pale spleens were noted in some cases, but enlargement, severe congestion, and focal necrosis were seen in others (Carlson et al., 1974). Experimentally infected 7-wk old turkeys displayed splenomegaly and hypertrophy of the "white pulp" (Itakura et al., 1974). In a postmortem examination of spontaneously infected turkeys, spleens showed varying degrees of enlargement, had a soft texture and mottling (Itakura and Carlson, 1975b). Histology revealed necrotic foci containing degenerated "reticular" cells and necrotic lymphoid cells. Cells with ballooned nuclei and eccentrically marginated chromatin were observed (Carlson et al., 1974). Microscopically, in experimentally infected turkeys, by day 3 pi, "reticular" cells around the sheathed arteries showed some proliferation. The red pulp and the area around the sheathed arteries had swollen "reticuloendothelial" cells and increased numbers of medium sized mononuclear cells. Also, the "reticuloendothelial" cells in the red pulp contained INIs. At day 5 and 6 pi, "reticuloendothelial" cells around the sheathed arteries had proliferated and contained INIs. Hyperplastic "white pulp" containing numerous large lymphoid cells and ballooned "reticular" cells was noted. By day 7 pi, these lesions were reduced and INIs had disappeared and by day 9 pi the spleen returned to its normal appearance (Itakura et al., 1974). In another report on naturally infected turkeys, the spleen showed enlarged "white pulp" with large lymphoid cells and congested red pulp. Proliferation of swollen "reticular" cells was seen around the sheathed arteries along with numerous large mononuclear cells containing INI and plasma cells (Itakura and Carlson, 1975b). Hypertrophy of mononuclear phagocytic cells with marginated chromatin and INIs were also reported in the spleens of naturally affected turkeys (Meteyer et al., 1992).

Intestinal lesions

A detailed description of the sequence of pathological events occurring in the gut of naturally and experimentally infected turkey poults has been described by several authors. The first report was in 1937. Grossly, the intestinal tract of turkey poults was found distended with sanguineous contents and the mucosa highly congested. Inflammation was more pronounced in the duodenum. Cecal congestion and hemorrhage was noted in some birds. Microscopically, the pathological process in the intestines was described as occurring in two stages. First, the lamina propria became infiltrated with red blood cells and round cells, leading to villus distention. Second, there was loss of the

mucosal lining from villi (Pomeroy and Fenstermacher, 1937). The next report on intestinal lesions of HE appeared in the 1950s. The intestinal tract (small intestines and ceca) showed no distension or dilation, but the lumen was filled with blood. The mucosa was slightly edematous and markedly congested (Gale and Wyne, 1957). Ten years later, the first experimental reproduction of HE was reported. In one experiment, turkey poults at 8 wk of age were inoculated via the cloaca with serial dilutions (1, 0.1, or 0.001 ml) of gut contents from a naturally infected turkey. The percentage of birds with intestinal lesions was found to be dose dependent; however, the onset of lesions (i.e., virus incubation period) was not affected by the dose (Gross and Moore, 1967). In another experiment, the birds were rectally inoculated with 0.5 ml of gut contents. The lesions in the intestinal tract progressed gradually from nothing on the 1st day to localized congestion in the duodenum which progressed to the entire small intestine over the next 2-3 days; culminating with frank hemorrhage throughout the intestinal tract and death on the 5th day. By day 6 pi, the intestinal lesions in surviving birds showed evidence of healing until they disappeared by day 9. In a separate experiment, the authors detected a decrease in the percentage of lymphocytes in peripheral blood 6 days pi which returned to normal by day 8 pi. The percentage of heterophils decreased 7 days pi, rose to 60% 11 days pi, and then normalized by 15 days pi (Gross and Moore, 1967). A more detailed histopathological description of the development of HE intestinal lesions over 2-10 days was provided after experimental inoculation of SPF poults with filtered (0.22 μm) gut contents (Gross, 1967). Apparently, no lesions were observed until day 4 pi. On day 5 pi, the tips of villi were slightly congested with free red blood cells seen in the lamina propria. Next, the mucosa became congested, with many erythrocytes leaving the blood vessels and entering the lamina propria. Villus thickness increased due to edema. Congestion and hemorrhage became severe, the epithelial layer at the tips of the villi separated and openings formed; allowing blood to leak into the intestinal lumen. At the outset of day 6 pi, the mucosa was severely congested and the villus tips were necrotic and blunted; however, hemorrhage began to regress by mid-day and the epithelium reattached to the villi. The area between live and necrotic villi was infiltrated with heterophils. On day 7 pi the villi began to heal and macrophages containing hemosiderin were seen in the congested areas. By day 8 and 9 pi, the mucosal congestion and

hemorrhage were greatly reduced. On day 10 pi, lesions were no longer apparent (Gross, 1967). The author suggested that the luminal hemorrhage was due to diapedesis of red blood cells rather than complete vascular disruption.

In another report on a spontaneous HE infection, lesions similar to those described above were found upon postmortem examination of turkey poults. These were seen in the duodenum, jejunum, and cecal tonsils. Moreover, lymphocytic hyperplasia was observed in the lamina propria along the entire length of the intestines and cecal tonsils with increased numbers of large lymphoid cells, plasma cells, and heterophils. Lymphocytic hyperplasia (follicular) was seen in the duodenum. Swollen "reticular" cells containing hemosiderin were occasionally noticed in the lamina propria. Large mononuclear cells containing INIs were observed throughout the lamina propria of the intestines and the cecum, but were highest in the cecal tonsils (Itakura and Carlson, 1975b). In orally inoculated turkeys, THEV was detected at 3-8 dpi by immunofluorescence in cecal tonsils, duodenum, jejunum, ileum, and cecum (Fasina and Fabricant, 1982a). In intraperitoneally inoculated turkeys, THEV was detected in cells within the duodenal lamina propria by immunoperoxidase staining at 4 dpi (Silim and Thorsen, 1981).

HE secondary lesions

Gross and histopathological/microscopic lesions in organs other than the spleen and the GI tract have been observed in turkeys infected either naturally or experimentally with THEV-V strains. These organs and lesions include thymus (lymphocytic depletion), bursa of Fabricius (BF; lymphocytic depletion), bone marrow (BM; paleness), kidney (paleness, petechial hemorrhages, intertubular hemorrhage), liver (paleness, petechia, ecchymosis, congestion, and focal hepatic coagulation necrosis), lung (paleness, petechia, edema, congestion), heart (petechial hemorrhages), and gizzard (hemorrhages in the confined epithelium) (Gale and Wyne, 1957; Itakura and Carlson, 1975b; Palya et al., 2007; Pomeroy and Fenstermacher, 1937; Wilcock and Thacker, 1976). Microscopically, a few INIs were detected 3-6 dpi in a small number of hepatic sinusoidal endothelial cells (3/14 birds), "reticular" cells of the lungs (3/14), BF (2/14), thymic reticulum (1/14), "reticuloendothelial" cells in the BM (3/14), and in the testicles (1/14). Additionally,

lymphocytic reactions of varying degrees e.g., a proliferation of lymphocytes followed by aggregation or follicle formation, or an increase of heterophil counts were observed in several organs including the liver, lungs, BF, BM, and thymus starting 5 dpi and continued for multiple days. Also, lymphocytes were aggregated in the interstitial connective tissue of the kidneys, testicles, ovary, and adrenal glands, and the proventriculus lamina propria (Itakura et al., 1974). Similar observations have been made in naturally affected turkeys with INIs found in large immature cells/lymphocytes and (swollen) "reticular" cells in H & E-stained tissue sections from the liver and BM. Some of these cells showed varying degrees of degeneration. Aggregated and/or marginated chromatin was also seen in infected cells. Electron microscopy revealed that these INIs contain icosahedral viral particles similar to those associated with other adenoviral infections. The medulla of the lymphoid follicles in the BF contained a few large mononuclear cells with INIs (Itakura and Carlson, 1975a; Itakura and Carlson, 1975b). INIs were also noted in hepatocytes of intraperitoneally-inoculated turkeys 4-5 dpi, in the nuclei of tubular epithelial cells 4 dpi, and in BM 5 dpi (Silim and Thorsen, 1981). In orally inoculated turkeys, THEV was detected at 3-8 dpi by immunofluorescence in thymus, liver, and BM (Fasina and Fabricant, 1982a).

2.2.1.4. Pathogenesis of HE

Early studies on HE have shown that the major target sites of THEV-induced pathology are the small intestines in turkeys which die from intestinal hemorrhage (Gross and Moore, 1967), and the lung in pheasants and chickens which die from pulmonary hemorrhage and edema (Domermuth et al., 1982; Wyand et al., 1972). Several studies have provided strong evidence that the clinical symptoms (mainly immunosuppression) and intestinal lesions of HE are immune-mediated. THEV-induced immunosuppression in infected birds has been attributed to the direct effect of the virus on B lymphocytes and macrophages. THEV infections were found to cause apoptosis and necrosis of splenic IgM^+ B lymphocytes and potentially by-stander cells. Also, a considerable, though transient reduction in the peripheral blood B and T cell populations has been noticed in virus-infected poults (Koncicki et al., 2012; Rautenschlein et al., 2000a; Rautenschlein et al., 2000b; Saunders et al., 1993; Suresh and Sharma, 1996). For the intestinal lesions,

various explanations have been provided for the development of intercellular and intracellular pathology. Bursectomy, immediately after hatching, has been found to abolish the occurrence of clinical signs, lesions, and death in antibody-free poults orally inoculated with THEV-V at 2 or 5 wk of age (Fadly and Nazerian, 1982). Normal birds had 38-100% mortality after virus inoculation. In the same study, normal poults inoculated at 3 d of age showed successful virus infection and replication, but not pathological lesions. This suggested that HE pathogenesis was age-related, i.e., mainly dependent on the maturity of the immune system, rather than on the level of maternal antibodies. In another study, poults less than 2 wk of age were reported to be resistant to the development of HE lesions (Beasley and Wisdom, 1978). Surgical splenectomy at 5 wk of age prevented the development of HE lesions and death in poults, when inoculated intravenously with THEV 1 d post-surgery (Ossa et al., 1983a). It is worth noting that splenectomy did not affect the development of anti-THEV antibodies in infected poults, which suggested that replication of THEV could alternately occur in B cells of peripheral blood and/or BF. The first notion that intestinal hemorrhage was inflammatory in origin was made by Saunders et al. (1993). The authors found clear microscopic evidence of erythrocyte diapedesis without noticeable vascular damage. In a previous study, an increase in the permeability of blood vessels within the lamina propria of the duodenum was reported in THEV-infected poults (Opengart et al., 1992). The authors linked observation to significantly increased numbers of the duodenal mucosal mast cells which contain vasoactive chemokines. Likewise, T lymphocytes were also shown to play a major role in HE pathogenesis, providing strong support to the hypothesis of an immune-mediated process for THEV-induced intestinal lesions (Suresh and Sharma, 1995). Turkeys at 4 wk of age were treated with cyclosporine A to selectively suppress T cell mitogenesis, followed by THEV inoculation. The treatment completely prevented HE lesions, without affecting THEV replication in the spleen. A more-detailed mechanism of immunopathogenesis of HE splenic and intestinal lesions has been proposed by Rautenschlein and Sharma (2000) i.e., after oral exposure, THEV is believed to either replicate in B cells of the intestine, BF or make its way directly to the spleen through the bloodstream. In the spleen, the virus replicates rapidly in B lymphocytes and macrophages. Hyperplasia of the white pulp then occurs as a result of infiltration with

high numbers of macrophages and lymphocytes, including CD4+ T cells. The interplay among these various types of immune cells within the site of viral replication leads to the production of very high levels of proinflammatory cytokines e.g., interleukin 6 (IL-6) and tumor necrosis factor (TNF) as well as the anti-inflammatory cytokines of type I and II interferons (IFN). The latter activates macrophages, inducing the production of the antiviral and immunosuppressive nitric oxide (NO). Most likely, IFN-I and NO play a role in clearing the virus later from the spleen.

2.2.1.5. Assays for specific detection THEV antigens and genetic material

Several methods have been developed or adapted for the detection or quantification of THEV antigens, i.e., capsid proteins; mainly hexon, and genetic material, i.e., DNA. The methods developed for the detection of THEV antigens include: 1) agar gel immunodiffusion tests (Domermuth et al., 1973; Domermuth et al., 1972); 2) immunoperoxidase staining (Silim and Thorsen, 1981); 3) immunofluorescence staining (Fasina and Fabricant, 1982a; Fasina and Fabricant, 1982b); 4) an ELISA using anti-THEV antibodies and peroxidase-linked goat anti-mouse IgG (van den Hurk, 1986); 5) a double-antibody ELISA using monoclonal antibody and turkey antiserum against THEV (Nazerian et al., 1990); and 6) an immunohistochemical staining technique using a pool of monoclonal (primary) antibodies, secondary anti-mouse antibody, streptavidin-peroxidase conjugate, and substrate-chromagen mixture, followed by counterstaining with hematoxylin (Fitzgerald et al., 1992). Methods for the detection or quantification of virus DNA have been developed including: 1) in situ hybridization for the detection of viral DNA in cells and tissues using a digoxigenin-labeled 564-bp probe (Suresh and Sharma, 1996); 2) standard PCR for the amplification of a 234-bp THEV DNA fragment, followed by detection with electrophoresis on 2% agarose gel stained with ethidium bromide (EtBr) (Suresh and Sharma, 1996); 3) a standard PCR for the amplification of 1647-bp hexon fragment, followed by detection on 0.5% agarose gel electrophoresis stained with EtBr (Hess et al., 1999); 4) hexon-based nested PCR / competitive PCR (Beach, 2006; Beach et al., 2009b); 5) hexon-based real-time quantitative PCR (Beach, 2006; Beach et al., 2009b; Shah et al., 2013); and 6) real-time fluorescence loop-mediated isothermal amplification (LAMP) (Liu et al., 2014).

2.2.1.6. Protection and vaccination

Before the advent of HE vaccines, convalescent antiserum obtained from apparently healthy turkeys that had been exposed to THEV proved successful in controlling HE in susceptible 6-wk old turkey poults. HE gut lesions were prevented when 0.5-1 ml of convalescent antisera were used intravenously or subcutaneously a few hours before or even 24-48 h after challenge with THEV-V (Domermuth and Gross, 1975). In another study, the same concept of passive protection was proven. HE hyperimmune serum given 1 h after or up to 5 wk before challenging poults with THEV-V prevented HE lesions and death (Fadly and Nazerian, 1989). Furthermore, treatment of poults with a high dose of THEV hexon-specific monoclonal antibodies protected them from the clinical HE disease and reduced the replication of the challenge virus in the spleen (van den Hurk and van Drunen Littel-van den Hurk, 1993).

During the period from 1977 to 2005, several types of vaccines were developed in an effort to protect the domestic turkey population from the intestinal lesions and death caused by THEV-V infections. The production of the first HE vaccines was described by Domermuth et al. (1977). Two virus strains were used: the first was isolated from enlarged spleens of pheasants suspected of having MSD and the second was isolated from contaminated litter of a poultry house where clinical, HE-seropositive turkeys had been raised. A preparation of each of these viruses was given orally to two separate groups of 6-wk-old poults for 6 days, after which the spleens were removed and homogenized. This was diluted in drinking water and administered to a second group of turkey poults from which the spleens were again removed and homogenized. The resultant vaccine was administered to 4.5 wk old turkey flocks on farms with a history of recurring 10-15% mortality. Both vaccines successfully prevented the HE intestinal lesions. No mortality was seen in flocks receiving the vaccine made from the MSDV isolate and only 0.15% mortality was seen in flocks that received vaccine made from the turkey isolate (Domermuth et al., 1977). The MSDV-based splenic vaccine also proved effective following experimental challenge with a virulent field strain of THEV (Thorsen et al., 1982).

Currently, the crude splenic vaccine is produced by IV or oral inoculation with a THEV-A inoculum into susceptible turkey poults of 5-6 wk-of-age, birds are euthanized 3-5 dpi, their spleens are harvested and ground, and a crude splenic homogenate is made in PBS at 1:1 (v/v) ratio and frozen until needed. The splenic vaccine is administered via unchlorinated drinking water (Pierson and Fitzgerald, 2008). The second type of HE vaccine is a cell culture (CC)-propagated live vaccine. A B-lymphoblastoid cell culture system (MDTC-RP19) established from a Marek's disease virus induced liver tumor in turkeys (Nazerian et al., 1982) was found to be highly susceptible to THEV and MSDV infection (Nazerian and Fadly, 1982). The methods for virus propagation and vaccine production were patented through the U.S. Department of Agriculture (USDA) (Nazerian, 1983). The vaccine was found to be efficacious and safe (Fadly and Nazerian, 1984). In field trials, when applied in drinking water to 4-5.5 wk-old poults, CC HE induced a high level of seroconversion (88-91 %) and protected the turkey poults against HE intestinal lesions and death (Fadly et al., 1985). Unlike the splenic vaccine, CC HE vaccines, which are cell-free products in liquid or lyophilized form, are USDA-licensed, commercially produced and distributed by multiple companies in the U.S. and Europe.

In 1993, two separate studies were conducted to compare the performance of splenic and CC HE vaccines. In the first study, both vaccine types were evaluated under laboratory and field conditions and found to produce high levels of seroconversion (97% vs 98.5%, CC and splenic vaccine, respectively). They produced protection from virulent challenge, inhibiting replication in the spleen as well as GI lesions (Barbour et al., 1993). In the second study, when given to 4-wk old commercial poults, the splenic vaccine outperformed the CC vaccine in terms of protection from splenic and GI lesion development (splenic *vs*. CC, 97 *vs*. 61%, respectively); however, no such differences were found when the vaccines were given to SPF poults of the same age (Hussain et al., 1993). Apparently, the residual maternal antibodies in commercial 4-wk old poults had a stronger neutralizing effect on CC-propagated viruses.

Another method for producing a CC HE vaccine was described by van den Hurk (1990a). Primary cultures of mixed adherent and nonadherent turkey peripheral blood leukocytes were evaluated to determine if they would support THEV replication (van den

Hurk, 1990b). The author used these cultures for the propagation of THEV-A extracted from infected splenic homogenate or infected cell culture. Both preparations were provided in the drinking water to 4.5-5 wk old turkeys and produced 96% seroconversion after 3 weeks. Vaccinated birds were successfully protected against clinical HE.

Three alternative products were developed in an attempt to avoid the mild transient immunosuppression seen with the live vaccines. The trimeric hexon protein (96 kDa) was immunoaffinity purified from a THEV-A stock prepared from an infected splenic homogenate and used as a subunit vaccine. The purified native viral hexon emulsified in Freund's adjuvants was injected twice subcutaneously, 2 wk apart, in 6-wk-old poults and found to induce high levels of THEV-neutralizing antibodies. The product protected challenged birds against clinical HE and virus replication in the spleen (van den Hurk and van Drunen Littel-van den Hurk, 1993). A recombinant fowl poxvirus (rFPV) expressing the native THEV hexon protein has also been used as a vaccine for 5-6 wk-old poults. rFPV administered via wing-web stick elicited anti-THEV antibodies similar to the commercial CC vaccine and prevented the HE lesions (splenic and GI), but did not completely prevent replication of the challenge virus. It did however cause less immunosuppression (Cardona et al., 1999). Finally, the fiber knob domain and adjacent 48 aa of the shaft domain were expressed in E. coli and used as a recombinant subunit vaccine. When administered to turkey poults, this vaccine was found to induce protection against challenge with virulent THEV at 3 wk post-vaccination (Pitcovski et al., 2005).

As with HE, MSD in pheasants was initially controlled by the MSDV-specific convalescent antiserum obtained from pheasants and from turkeys that had HE (Domermuth et al., 1975). An avirulent THEV isolate propagated in turkeys was found to protect susceptible pheasants against MSD. Moreover, the vaccine was found to mitigate clinical disease and mortality in pheasant flocks actively experiencing virulent outbreaks (Domermuth et al., 1979a). As for the AAS in chickens, no vaccine has been developed due to the apparently low incidence of disease (Pierson and Fitzgerald, 2008).

Maternal antibodies can protect poults for a few weeks post-hatch (wph), after which birds must be vaccinated for protection against THEV-V infection. Maternal antibodies were found to greatly interfere with HE vaccination and subsequent protection

(Fadly and Nazerian, 1989). The optimal age for vaccination against HE in commercial turkeys, hatched from seropositive hens was determined to be 5-6 wph. This age correlated with a decline in the titer of THEV-specific material antibodies below 40; the level at which no interference with vaccine- induced protection was detected (van den Hurk, 1990a).

Marble spleen disease virus (MSDV) of pheasants and Aviadenovirus type II-associated splenomegaly virus (AASV) of chickens

The spread of MSD in the U.S. and worldwide, etiology, clinical signs and pathology, and disease prevention have been reviewed in detail by Fitzgerald and Reed (1989); Pierson and Fitzgerald (2008). The first outbreak of MSD was reported in 1966 in Italy and thereafter in the U.S. (Virginia, Pennsylvania, California, Michigan, and Connecticut) and many other countries where pheasants are commonly reared for sport hunting. The last report of MSD to appear in the literature occurred in outdoor, pen-raised pheasants in Korea (Lee et al., 2001). Due to its mild symptoms, very little information exists regarding AASV. MSD occurs in confined pheasants of 3-8 months of age, while AAS occurs in chickens of 20 wk of age or older (Domermuth et al., 1979b; Domermuth et al., 1982). Based on electron microscopy studies, AGID and other serology tests, MSDV and AASV are morphologically, serologically, and antigenically indistinguishable from THEV (Domermuth et al., 1979b; Iltis et al., 1977; Jakowski and Wyand, 1972; Wyand et al., 1972). However, slight differences were noted on restriction endonuclease fingerprinting (Zhang and Nagaraja, 1989). As observed with HE in turkeys, MSDV and AASV cause transient immunosuppression and splenomegaly with lymphocytic hyperplasia, necrosis of "white pulp" and the presence of INIs in splenic "reticuloendothelial" cells (Veit et al., 1981). Secondary lesions and large monocytes with INIs were seen in other organs / tissues (Carlson et al., 1973; Fitzgerald and Reed, 1989). MSD and AAS differ from HE in that the effected birds die from acute pulmonary edema, congestion, and hemorrhage with lymphocytic degeneration (Cowen et al., 1988; Domermuth et al., 1982; Veit et al., 1981). As previously noted, effective vaccines for MSD have been developed (Domermuth et al., 1979a; Fadly et al., 1988).

2.2.2. Frog adenovirus 1 (FAdV-1)

2.2.2.1. Virus discovery and primary features

FAdV-1 was discovered when histopathological examination of a leopard frog (sacrificed in 1966) revealed a granulomatous nodule in one swollen, tumor-free kidney. As an initial attempt for virus isolation, a sample of digested kidney tissue was inoculated onto a culture of TH-1 cells and incubated at 23°C. TH-1 is a continuous cell line established from the heart of an Eastern box turtle (Clark and Karzon, 1967). Characteristic cytopathic effect (CPE) in inoculated cell cultures was first observed 16 dpi in the form of cell enlargement and roundness, and then progressed over a period of up to 10 wk to cell destruction, without forming syncytia or virus-specific inclusions. In following experiments, the isolate-infected TH-1 cells, incubated at 30°C, developed "pale eosinophilic intranuclear inclusions" after 20 passages, confirming the recovery of the new virus. The virus titer was found to increase over 1000-fold when grown in TH-1 at 30°C compared to 23°C (Clark et al., 1973).

2.2.2.2. Biological characteristics

Although FrAdV-1 replicates well in the turtle TH-1 cells, attempts to cultivate the virus in two cell lines from frog species: RP132 and FT, did not succeed. Additionally, cells from 6 reptilian, 3 piscine, 6 mammalian (including human) species as well as primary chicken embryo fibroblasts did not support virus replication as CPE was not observed in inoculated cells after a minimum of 14 days in culture. Also, the virus was incapable of forming plaques on monolayers of TH-1 cells overlaid with gel and incubated at two different temperatures (Clark et al., 1973). Furthermore, inoculated via two different routes, the virus neither affected the mortality of 9-day-old chick embryos, nor caused observable pathologic lesions over a course of 8 dpi. FrAdV-1 has the ability to agglutinate rat erythrocytes at 37°C (Clark et al., 1973), a feature shared with other adenoviruses such as human adenovirus type 37 and bovine adenovirus type 3 (Arnberg et al., 2000a; Arnberg et al., 2002b; Li et al., 2009).

2.2.2.3. Physico-chemical characteristics

Filtration experiments showed that the virus size is expected to be between 50 and 100 nm. The absence of CPE in infected TH-1 culture treated with 5 bromo-2'-dexoyuridine, as compared to untreated culture that displayed CPE, suggested that the virus is of the DNA type. Morphologically, electron microscopy on virus-infected cells revealed the presence of many "complete" and "incomplete" viral capsids as well as condensed virus particles forming crystalline-like arrays in the nuclei of numerous cells. The outer diameter of virions in thin sections of infected TH-1 cell culture was about 78 nm. Based on various capsomere measurements, the virus was estimated to contain a total of 252 capsomers. Taken together, this information concluded that the new virus isolate is an "adeno-type virus".

Serologically, complement fixation and serum neutralization tests confirmed that the virus is antigenically different from mammalian and avian adenoviruses. This was the first report on the isolation of an adenovirus from poikilothermic vertebrates; the virus was designated frog adenovirus 1 (FrAdV-1) (Clark et al., 1973).

2.2.2.4. Genomic and phylogenetic findings

In 2000, the complete DNA sequence and the deduced genomic organization of FrAdV-1 was reported (Davison et al., 2000). The virus was found to hold the smallest adenovirus genome to date with a size of 26,163 bp. The G+C content is 37.9% and the ITR length at both ends of the genome is 36 bp. FrAdV-1 genome is composed of 24 genes/ORFs, 2 of which were not identified before in the virulent strain of TAdV-3 by Pitcovski et al. (1998). Based on full-genome comparisons, 16 of these genes were found common among members of the family *Adenoviridae*, while the other 6-8 ORFs were restricted to these two viruses. Because of their high sequence similarity between TAdV-3 and FrAdV-1, four ORFs (i.e., ORFs 1, 7, 8, and E3) were expected to encode proteins. Among the distinct genes was ORF1, the deduced protein product of which was linked substantially to bacterial sialidases, with the highest sequence similarity found with *Clostridium sordellii*. Also, the nucleotide composition and genetic layout were found similar between FrAdV-1 and TAdV-3. Furthermore, phylogenetic analyses, based on aa sequences deduced from hexon and other genes, grouped FrAdV-1 and TAdV-3 together,

distally from the two adenoviral recognized genera (i.e., *Mastadenovirus* and *Aviadenovirus*) and the third proposed genus, *Atadenovirus*. Collectively, this information led the authors to propose a fourth adenoviral genus (i.e., *Siadenovirus*) to contain the two aforementioned virus species (Davison et al., 2000).

2.2.3. Raptor adenovirus 1 (RAdV-1)

2.2.3.1. Virus discovery

In 2006, novel siadenoviral infections were described in three different raptor species that died while being held in captivity in the United Kingdom: a 20-wk-old Harris hawk, a 1-year-old Bengal eagle owl, and a 3-year-old Verreaux's eagle owl (Zsivanovits et al., 2006). Immediately prior to death, one hawk had a 10-min seizure, while the other two were clinically lethargic for 24 to 48 hours. Necropsy findings varied amongst the three cases/species with affected organs including liver (3/3 hepatomegaly with mottling and necrosis), spleen (2/3 splenomegaly with necrosis), proventriculus (1/3 dilation and necrosis), ventriculus (2/3 dilation, ulceration, erythema, and necrosis), intestines (2/3), lungs/air sacs (3/3 congestion and airsacculitis), heart (1/3), and kidney (3/3 renomegaly). Histologically, the liver and spleen of one case had severe necrosis with basophilic INIs and large nuclei in some hepatocytes (liver) or reticular (spleen) cells. In another case, disseminated epithelial and lymphoreticular cell nuclear atypia with inclusion bodies were seen in liver, spleen, kidneys, and pancreas. The mildest case showed INIs in necrotizing ventriculus tissue. No histological abnormalities were found in the proventriculus, intestines and pancreas, lungs/air sacs, and heart of 2/3 cases/species and in the kidneys of 1 case/species.

2.2.3.2. Genomic and phylogenetic findings

DNA was extracted from pooled tissues of the three bird species and used to amplify a short fragment within the adenovirus DNA-dependent DNA polymerase (POL) gene by a nested PCR and degenerate consensus primers. The three amplicons were sequenced, and with a phylogenetic analysis based on the predicted 91- aa sequence the novel virus was grouped with other *Siadenovirus* members with the closest relative found

to be THEV. Attempts failed to isolate the virus in chicken embryo liver cells. Also, the virus could not be detected by electron microscopy, apparently due to the low virus titers in examined tissues as a concentration of $>10^6$ viral particles/ml is generally required for positive electron microscopic results (Zsivanovits et al., 2006). RAdV-1 has not been reported in new cases or species since 2006.

After three years of the initial recognition of raptor siadenoviral infection, a DNA stretch of ~12.3 kb central region of RAdV-1 that covers nine full and two partial genes was sequenced. Phylogenetic analyses confirmed the identity of the virus as a new siadenovirus species, which was clustered in a common branch with THEV reflecting the high aa sequence similarity between both viruses (Kovács and Benkő, 2009). Attempts for virus isolation in RP19 cells were unsuccessful. Two years later, the full genome sequence of RAdV-1 (26,284 nt, the 3rd siadenovirus to be fully sequenced) and its genomic organization and genetic features were determined (Kovács and Benkő, 2011). The genome is only 18 nt longer than THEV-A strain and has a higher G+C content (38.5%) and a considerably shorter ITR (29 *vs.* 39 nt). Genetic analysis revealed the presence of the previous genus-specific genes/ORFs described in THEV and FrAdV-1 with some sequence differences, in addition to a new putative gene, ORF9. The putative sialidase protein encoded by RAdV-1-ORF1 gene exhibited higher similarity to the bacterial sialidase of *Bacteroides vulgatus*, unlike THEV and FrAdV-1 bacterial sialidase homologs (i.e., *Clostridium* and *Akkermansia* sialidases, respectively).

2.2.4. Budgerigar adenovirus 1 (BuAdV-1)

2.2.4.1. Virus discovery

In a breeding facility in Japan, four budgerigars with no previous clinical signs were found dead and one with ruffled feathers was euthanized. Three cases including the killed bird were valid for investigation. The two dead birds had splenomegaly with lymphoid depletion and increased macrophages. In the 3 cases, congestions in lung, liver, kidney, and/or brain as well as inflammatory cells in livers and kidneys were noticed. The euthanized bird had hepatic and renal necrosis. Moreover, using H & E staining,

basophilic INIs were detected in the renal tubular epithelial cells, suggesting an adenoviral infection (Katoh et al., 2009).

2.2.4.2. Genomic and phylogenetic findings

DNA purified from liver, spleen, kidney tissues was used in a PCR targeting the L1 region of adenoviral hexon gene and resulted in the generation of one product from a kidney sample. The amplicon was sequenced and phylogenetic analysis with the deduced 176-aa sequence clustered the novel virus, named as budgerigar adenovirus 1 (BuAdV-1), with siadenoviruses. BuAdV-1 exhibited the highest aa sequence similarity with RAdV-1 (60.5%) as compared to 53.7% with THEV. Using a different pair of primers, an identical BuAdV infection of the kidney was confirmed in the 5 birds (Katoh et al., 2009).

2.2.5. Sulawesi tortoise adenovirus 1 (STAdV-1)

2.2.5.1. Case description and clinical findings

A systemic viral infection characterized by inflammation and necrosis along with viral INIs in many tissues including intestine (often seen in enterocytes), spleen, pancreas, testis, ovary, kidney and renal epithelium, respiratory epithelium, vascular and cardiac epithelium, cerebral glia and choroid plexus was observed in a group of sick Sulawesi tortoises illegally imported to the U.S. (Rivera et al., 2009). Thirty tortoises died before being subjected to any clinical or diagnostic investigations and most of the remaining animals died within 3 to 8 wk after starting medical treatments. The majority of examined cases had bone marrow necrosis associated with INs and marginated chromatin in a number of myeloid cells of the hematopoietic tissue. INs that were detected hispathologically in the examined tissues were shown by transmission electron microscopy (TEM) to contain nonenveloped viral particle of 70-90 nm diameter. TEM performed on spleen sections revealed the presence of marginated chromatin and paracrystalline arrays of nonenveloped, hexagonal, viral particles of ~70 nm diameter in the oval-shaped nucleus of an infected cell. Interestingly, similar splenic observations to

what is described here have been seen in THEV-infected turkeys, where the spleen is the major site for virus replication.

2.2.5.2. Genomic and phylogenetic findings

Forty two DNA samples were extracted from various tissues (mainly liver, kidney, spleen, and oral/nasal mucosa) of deceased tortoises, or from choanal swabs and plasma samples of live tortoises. A nested PCR assay with consensus adenoviral primers was used to amplify a 272-bp fragment of the POL gene. Forty one positive (i.e., 97%) adenoviral amplicons were detected, directly sequenced, and used in phylogenetic analyses on the basis of their predicted aa sequence. The analyses positioned the new virus, designated as Sulawesi tortoise adenovirus 1, within the genus *Siadenovirus* and the aa sequence comparison with other adenoviruses showed its highest similarity with FrAdV-1 (Rivera et al., 2009).

As the bone marrow was involved in many deceased cases, it was suggested that STAdV-1 has an immunosuppressive nature (Rivera et al., 2009). It is worth mentioning that THEV, MSDV, and AASV have always shown a period of immunosuppression in infected birds at the beginning of the infectious cycle (Pierson and Fitzgerald, 2008).

Although siadenovirus infection was confirmed in all dead tortoises, the main cause(s) of death was difficult to recognize since the animals were concurrently infected with other bacterial and parasitic pathogens. These infections might be secondary to an initial viral immunosuppressive effect and other stress factors such as bad housing, poor transportation, unfavorable environmental conditions, and malnutrition. As opportunistic pathogens cause severe tissue damages, the virus could be able to extend its infection to other tissues and organs that may not be reachable in normal conditions. A tightly controlled infection experiment is, therefore, desirable to define the target organs for STAdV-1 infection as well as its pathogenicity in tortoises.

2.2.6. Psittacine adenovirus 2 (PsAdV-2)

2.2.6.1. Case description and clinical findings

Two birds from different psittacine species, an 8-year male plum-headed parakeet and a 20-year old female umbrella cockatoo, displaying no characteristic clinical signs, were found unhealthy, based on physical examination and general laboratory blood services (Wellehan et al., 2009). The parakeet died about 34 days from initial examination regardless of offered therapies, while the cockatoo was euthanized after about 1 year and seven months after losing the ability to walk independently due to neurological problems.

2.2.6.2. Genomic and phylogenetic findings

DNA was extracted from cloacal swabs from both birds and an adenoviral consensus nested PCR for the amplification of a fragment of the POL gene was run. The two 269-bp PCR products were sequenced and the predicted aa sequences were subjected to sequence comparison and phylogenetic analyses, which revealed that the novel virus had the highest similarity with RAdV-1 from gnus *Siadenovirus*. Moreover, the nt sequence of the partial PsAdV-2 DNA polymerase was found rich in A and T content (62.1%) as other known siadenoviruses, which ranged from 62.5% in FrAdV-1 to 65.8% in TAdV-3 (Wellehan et al., 2009). A new virus species containing PsAdV-1 and named Psittacine adenovirus B was proposed.

The histopathology on the parakeet liver and the liver, brain, and heart of cockatoo showed inflammation and lymphocyte infiltration but did not reveal a specific etiologic cause.

2.2.7. Great tit adenovirus 1 (GTAdV-1)

2.2.7.1. Case description and clinical findings

The total nucleic acids were extracted from a tissue homogenate made from the internal organs (lung, liver, spleen, & intestine) of a dead great tit bird in Hungary for use in an avian influenza surveillance program started in 2006. The clinical, condition, and

necropsy findings on the carcass were not reported and, therefore, the potential target organs or tissues of this virus species are still unknown. Using a consensus nested PCR assay targeting the adenoviral POL gene on the stored DNA, the bird was found adenovirus-positive (Kovács et al., 2010).

2.2.7.2. Genomic and phylogenetic findings

A genomic portion of about 13.6 kb in size (~50% of the genome) spanning the region from adenoviral IVa2 to hexon genes was PCR-amplified and sequenced. This central genomic part contained the full sequence of eight (polymerase, pTp, 52K, pIIIa, III, pVII, pX, pVI) and the partial sequence of two (Iva2 and hexon) adenoviral genes. Phylogenetic analysis based on deduced hexon protein aa sequences revealed the discovery of a novel siadenovirus which was thus named great tit adenovirus 1. The existence of this new virus was confirmed through additional phylogenetic analyses using penton and DNA polymerase predicted aa sequences. A new siadenovirus species, Tit adenovirus A, was also proposed.

2.2.8. South Polar skua adenovirus 1 (SPSAdV-1)

2.2.8.1. Case description and clinical findings

A small group of the large predatory seabirds, South Polar skuas, was found dead in Lake King Sejong in Antarctica between 2007 and 2009. There were no obvious signs of disease. The adenoviral DNA was PCR-detected in frozen samples of one or more of the following tissues: heart, lung, liver, kidney, intestine, and trachea, but most frequently seen in the kidney (5 out of 6 birds). Since the virus was present in several organs, a systemic or disseminated infection with viremia was suggested to have occurred in birds before death (Park et al., 2012). Virus isolation from the positively infected organs was not attempted by authors

2.2.8.2. Genomic and phylogenetic findings

Using PCR, nucleotide sequencing, and phylogenetic analyses based on deduced aa sequences, a novel siadenovirus was identified. The complete genome sequence of

SPSAdV-1 was then accomplished and found to be 26,340 bp (74 nt longer than THEV-A strain) with a G+C content of 34.2% (Park et al., 2012). These values are very similar to those determined for THEV (~ 26,266 bp and 37.9%, respectively) (Beach, 2006) and two other siadenoviruses. The genome of SPSAdV-1 (the 4th siadenovirus to be fully sequenced) encodes 24 genes and ORFs. Nucleotide sequence comparison revealed higher sequence similarities (68-75%) between the SPSAdV-1 polymerase, penton base, and hexon genes and those of THEV, while the fiber gene displayed a lower similarity (< 50%) (Park et al., 2012). We may speculate that the low homology in fiber gene sequences indicates a difference in the primary tissue tropism between SPSAdV-1 and THEV; however, this needs to be experimentally verified as the spleen was not amongst the organs examined for infection with SPSAdV-1.

2.2.9. Gouldian finch adenovirus 1 (GFAdV-1)

2.2.9.1. Virus discovery

Six cases of Gouldian finches (1 in the U.S. and 5 in Hungary) tested positive for adenovirus by a nested PCR assay targeting the adenoviral DNA polymerase gene that was run on DNA extracts from 3 liver, 2 fecal material, and 1 kidney samples taken from suspect finches in 2010-2011 (Joseph et al., 2014). Total DNA purified from the liver of a Hungarian case was used to partially amplify 3 adenoviral genes: polymerase, pTP, and hexon, which were sequenced, and used in predicted aa-based phylogenetic analyses that clustered the discovered virus into the genus *Siadenovirus* (Joseph et al., 2014).

2.2.9.2. GFAdV-1 pathology

From the clinical side, the conditions of the birds varied from being "clinically healthy" to being "lethargic, fluffed", having "respiratory crackles", and death 3 days post-treatment. The U.S. dead finch was used to histologically examine this siadenoviral infection of the kidney that showed no obvious clinical signs of renal disease. H & E staining showed large basophilic INIs, mild lymphocytic inflammation, and blood vessel congestion in the kidney. Transmission electron microscopy revealed icosahedral, adenoviral particles and marginated chromatin in the nucleus of renal tubular epithelial

cell (Joseph et al., 2014). Pulmonary parasitic, proventricular and ventricular protozoal, and duodenal bacterial infections were concurrent with this adenoviral infection.

2.2.10. Chinstrap penguin adenovirus 1 (CSPAdV-1)

2.2.10.1. Virus discovery

Adenoviral infections were verified by nested PCR targeting a 1240-bp siadenoviral pVI-hexon genomic region in various tissues collected from Chinstrap penguins found dead in King Georg Island, Antarctica during 2009-2010 (Lee et al., 2014). Within the eight out of ten birds found AdV-positive, the viral DNA was detected most frequently in the lung (6/8), kidney (6/8), and intestines (5/8). Due to the existence of viral DNA in 6 different internal organs/tissues throughout the body, a systemic infection was proposed. On the other hand, PCR performed on DNA from brains, lymph nodes, spleens, and colons of six birds was AdV-negative.

2.2.10.2. Phylogenetic analysis

Comparing a deduced 285-aa region of the hexon protein, 6 to 12 sequence differences were found between a CSPAdV-1 strain from one bird and those from seven other birds. Also, one aa deletion and one insertion were revealed in some CSPAdV-1 variants. Attempts for virus isolation from CSPAdV-positive kidney homogenates via the MDTC-RP19 cell culture system have failed (Lee et al., 2014).

2.3. Section II: Virus titration methods and infectivity assays

2.3.1. Background

Titration can generally be defined as the process of determining the concentration (or titer) of a particular substance (e.g., virus, bacteria, chemical element, etc.) in a given sample or solution. Estimating the accurate concentration of virus infectious particles is of significant importance for many fields. In the vaccine industry, manufacturers need to precisely determine the optimal dose of a vaccine which should be high enough to sufficiently provide the desired level of protection and, at the same time, not so high that it compromises the host immune system due to immunosuppression or other side effects.

Likewise, precise live-virus enumeration is necessary in virus research, where tightly controlled infection experiments are frequently conducted and an exact number of virus particles are needed to infect cells or animals.

The history of the virus titration process can be tracked back to the late 1930s when Reed and Muench published a "rapid" procedure to estimate the dilution of a biological solution (e.g., sera or viruses) at which half of test animals react or die, and called it 50% endpoint (Reed and Muench, 1938). They chose this percentage because it is less affected by "small chance variations" than is any other point. This 50% endpoint titration became the most popular method in calculating the titers of numerous bacterial and viral agents existing in a solution form.

Titration of an infectious virus is dependent on the existence of a suitable infectivity assay, which in turn relies on the availability of an authentic virus detection technique. Over the past seven to eight decades, various *in vitro* and *in vivo* methods have been developed to estimate the concentration of "viable" virus particles or virus infectious doses in biological suspensions, including vaccines and infected tissues. In the beginning, the titration process relied solely on live animals and embryonated eggs from poultry species such as chicken (the most common), duck, turkey, and goose. Upon the appearance of cell culture techniques and the establishment of susceptible continuous or semi-continuous cell lines, several *in vitro* infectivity assays and titration methods have been devised by virology investigators to quantify viruses of interest. In a given virus sample, two types of titration strategies can be carried out: 1) infectious doses of the virus can be determined with techniques based on infection of cell culture, and 2) virus particles can be enumerated directly by electron microscopy. Here we will discuss in some detail the titration procedures and infectivity assays, both *in vivo* and *in vitro*, which have been developed for THEV. Also, some light will be shed on the major traditional methods and infectivity assays, as well as the modern ones established for the quantification of viable viruses. In this review section, for each titration/infectivity assay discussed, examples of viruses affecting avian species will be shown, unless the method has been exclusively applied to a "mammalian" virus.

2.3.2. Traditional titration methods for THEV and other viruses

2.3.2.1. Common techniques and culture systems found unsuitable for THEV

Although numerous avian adenoviruses, including those infecting fowls and other avian species, can be readily propagated in epithelial cell lines of their host counterparts (e.g., CrFK, feline kidney cortex cells; and Vero, African green monkey kidney cells which are commonly used for human adenoviruses), similar epithelial systems failed to support the replication of THEV (Nazerian and Fadly, 1982; Taharaguchi et al., 2012; van den Hurk, 1990). Because most of the standard *in vitro* infectivity assays that are employed in common titration methods, such as the plaque assay and focus formation assays, require the use of adherent cells, these assays cannot be applied to THEV due to the lack of an established susceptible and commercially available, adherent cell line. Two early studies noted that attempts for THEV propagation in embryonated eggs or in embryo fibroblast cell cultures from chicken and turkey were unsuccessful (Carlson et al., 1974; Thorsen et al., 1982). No explanations were given for the failure of virus propagation in these systems; thus, we may speculate that it could be either procedural problems or absence of susceptibility. However, further studies are needed to verify this speculation. A few studies to establish THEV-susceptible adherent or non-adherent cell cultures were performed by Nazerian and Fadly (1982). Spleen cell suspensions, extracted from enlarged THEV-infected spleens, have died within 48 hours of culturing and thus, failed to support virus replication. Likewise, no cytopathology was observed in kidney monolayer cultures extracted from THEV-infected turkeys, indicating no virus replication. Similarly, no cytopathic effects (CPEs) were seen in two chicken T-lymphoblastoid cell lines (transformed with Marek's disease virus), when co-cultivated with infective splenic extracts, indicating their non-susceptibility to THEV infection (Nazerian and Fadly, 1982). Another study demonstrated that chicken kidney cells are refractory to infection with avirulent and virulent THEV strains (Nazerian and Fadly, 1987). Attempts to establish cell lines susceptible for THEV infection from bone marrow-derived leukocytes have failed. Grown cultures showed a maximum susceptibility of only 2%, which was lost completely after 4 weeks of culturing (van den Hurk, 1990).

2.3.2.2. Infectivity assays and titration procedures developed or adapted for THEV

Many traditional methods have been developed and/or adapted for the titration of THEV in live-virus vaccines, either splenic or cell culture-based types. By convention, as indicated in the literature, live bird titration is the gold standard assay for reliably determining the titers of HE vaccines propagated in either live birds (crude splenic vaccine) or in cell culture systems. However, upon the establishment of a semi-continuous THEV-susceptible cell line, multiple variants of *in vitro* titration assays were developed. Below are descriptions of such assays as well as the cell culture systems used for virus infectivity procedures. Generally, a chronological order will be followed, unless otherwise dictated by the context.

In 1977, Domermuth et al. described the first *in vivo* procedure to be used for titration of virulent and avirulent THEV/MSD isolates (Domermuth et al., 1977). Five birds per group of six-week-old HE-susceptible poults were inoculated with 200 µl of 1:10-diluted (v/v with saline)–supernatants from ground spleens (to be titrated). Six dpi spleens were collected from euthanized birds and scored individually by microimmunodiffusion / agar precipitation test (Domermuth et al., 1973) to detect virus-positive poults. The procedure was done in duplicate (i.e., 10 birds total were used per each vaccine stock tested) and titers were expressed as poult-infective doses/ml; the actual method/ formula used for titer calculations, however, was not revealed by authors. A similar procedure was later followed by Hussain et al. (1993) for titration of a splenic vaccine and a commercial cell culture vaccine in specific-pathogen-free (SPF) poults and the titers were expressed as mean turkey infective doses (TID_{50}).

A more detailed procedure for titration of a live-bird MSDV-based HE vaccine propagated in susceptible turkey poults was described by Thorsen et al. (1982). A tenfold dilution series ranging from 10^{-1} to 10^{-6} was made from prepared splenic vaccine suspension, and a group of three turkeys (4.5 to 6 weeks of age) per dilution was inoculated with 5 ml via the intraperitoneal route. Five dpi, the spleens were collected from euthanized birds. Enlarged spleens were scored as positively-infected, and titers were calculated using Karber formula (Kärber, 1931) and expressed as median turkey infectious doses (TID_{50})/ml.

The first attempts to propagate THEV in cell culture systems were reported by Fasina and Fabricant (1982). They successfully verified the infection of splenic lymphocyte suspension cultures prepared from SPF chickens, turkeys, or pheasants with a THEV preparation from infected-splenic homogenates but failed to prove active virus replication. It may be suitable to mention that turkey and pheasant splenic cultures were much more susceptible to THEV than the chicken splenic culture. Although successful infection was confirmed by detecting intranuclear THEV antigens in inoculated cultures, primary lymphocytes failed to support serial virus passaging, making them inadequate for mass virus production. In the same study, Fasina and Fabricant (1982) developed an infectivity assay for the quantification of THEV-infected cells based on the detection of intranuclear viral antigens through an immunofluorescence staining protocol. The authors established the first *in vitro* titration method for THEV and also described another variant of a live-bird titration method, in which they applied the same infectivity assay. In the *in vitro* assay, aliquots of 1 ml of splenic lymphocyte suspension from SPF chickens were inoculated with tenfold serial dilutions (from 10^{-1}-10^{-4}) of a THEV inoculum; 100 µl each, and incubated at 41°C. At 30-hour pi (hpi), inoculated cells were harvested; from which smears were made on glass slides, fixed in acetone, and reacted with fluorescein isothiocyanate (FITC)-conjugated THEV antiserum. Stained smears were then examined with a fluorescent microscope for specific intranuclear viral antigens to verify and count the number of positively infected cells in each smear. In the *in vivo* assay, isolated groups of SPF chickens were orally inoculated with 1 ml each of a virus dilution made above and were euthanized 5 dpi to evaluate the infectivity titer. Spleens from inoculated chickens were harvested and frozen, and thin sections were made and fixed in acetone. Sections were stained with fluorescent-labeled antibodies and specific intranuclear viral antigens were detected fluorescently. Based on the numbers of positive samples per each dilution, the titers were calculated according to the Reed-Muench method and expressed as median infective dose (ID_{50}) per ml. Comparing the two titration methods of THEV, the titer estimated by the *in vivo* method was $10^{5.6}$ ID_{50} per ml, while that determined by the *in vitro* method was $10^{3.5}$ ID_{50} per ml (Fasina and Fabricant, 1982).

In 1982, the establishment of the only reliable cell culture system that supports the replication of THEV was introduced. Initially, four cell lines were established (two from

spleen tumors (MDTC-RP16 and 18) and two from liver tumors (MDTC-RP17 and 19). The tumors were induced by Marek's disease virus. Cytogenetic and immunofluorescence studies showed that all four cell lines have normal turkey chromosomes and express surface immunoglobulins, i.e., IgM and IgG (Nazerian et al., 1982). Infection experiments found that RP19 cells, established from a turkey liver tumor, are the most susceptible to the *in vitro* infection with THEV and have been used for large-scale propagation of virus and HE vaccine production since the early 1980s (Fadly and Nazerian, 1984; Fadly et al., 1985; Nazerian and Fadly, 1982; Nazerian, 1983).

After establishing the THEV-susceptible RP19 cell line, Nazerian and Fadly (1982) demonstrated an *in-vitro* infectivity assay for THEV. In that procedure, cultures of RP19 cells were co-cultivated with spleen preparations from virulent and avirulent THEV-infected turkeys. Four days post-cultivation, adenovirus-specific antigens were shown in the nucleus and cytoplasm by immunofluorescence. THEV-specific antigens were detected in cell extracts and supernatants by agar gel precipitation (AGP) test, and INIs containing typical adenovirus particles were viewed by electron microscopy. These techniques demonstrated, for the first time, *in vitro* virus replication of virulent and avirulent THEV isolates, as indicated by the authors. The assay was used in several studies for the titration of various preparations of virulent and apathogenic THEV strains (Fadly and Nazerian, 1984; Fadly et al., 1985; Nazerian and Fadly, 1987). The titers were expressed as tissue-culture-infectious-doses (TCID)/ml. It is worth noting that the THEV specific CPE, i.e., cell enlargement / ballooning, may take up to 12 days to occur in cell cultures (Fadly et al., 1985).

In 1983, Ossa et al., developed an *in vivo* titration method based on the body/spleen ratio to quantify virus purified from infected spleens. This method may be referred to as "50% body/spleen ratio" (B/S_{50}) and is performed as follows. Tenfold dilutions of virus stock ranging from 10^{-3} to 10^{-8} are made and each of 5-week-old poults (six per dilution) is inoculated intravenously with 0.5 ml. At 80-hpi, birds are killed, body and spleen are weighed, and the percentage of body/spleen ratio (% B/S) is calculated for each dilution. Values of % B/S are then graphically plotted against the associated

dilutions and the titer is determined as the dilution corresponding to a 50% reduction in B/S ratio as compared to a control group (Ossa et al., 1983).

van den Hurk (1990) reported the successful propagation of virulent and avirulent THEV strains in primary leukocyte cultures prepared from turkey spleens and blood taken from susceptible birds at 8-to-20 weeks of age. The author then described a titration procedure in which blood leukocyte cultures were inoculated with the virus suspensions to be titrated. At 3 dpi, smears of inoculated cells were made on microscopic slides by cytocentrifuge, and the infected cells were confirmed by the presence of group II avian adenoviral hexon antigens in the nuclei using an antigen-specific indirect immunofluorescence assay (IFA). The percentage of infected cells in a total of 500 to 1000 cells examined per smear was calculated and used to determine the 50% tissue-culture-infectious-doses ($TCID_{50}$s) according to Dulbecco (1980).

New *in vitro* and *in vivo* titration procedures for MSDV and THEV were described by Sharma (1994). For the *in vitro* assay, RP19 cells were cultured in 96-well plates, inoculated with serial dilutions of the virus (six wells per dilution), and checked for virus-specific cytopathic effect at 5 dpi. Wells were scored as negative or positive, and $TCID_{50}$ was calculated. The *in vivo* assay was used to determine the 50% turkey infectious doses (TID_{50}) of virulent THEV and avirulent THEV and MSDV strains. A dilution series was made from each virus and was used to inoculate groups of 4-week-old SPF poults (3 birds per dilution). After five days, spleens were individually harvested and homogenized and virus antigens were detected by ELISA to determine the infected birds.

Rautenschlein and Sharma (1999) described another variant of the *in vitro* titration procedure which they used with a MSDV vaccine and an avirulent THEV strain. Tenfold serial dilutions were made from each virus and RP19 cells were prepared in 96-well culture plates (5×10^3 cells in 50 µl/well). To each of six wells of cells, 50 µl of a virus dilution were added followed by incubation for 7 days. Inoculated wells were then scored based on the presence of CPE and virus titers were calculated. Additionally, the authors used a peroxidase-linked antibody assay (PLA), originally developed by Rautenschlein et al. (1996), as an alternative method to verify virus infectivity in the same experiment. In this assay, the plates were centrifuged at day 7 pi; supernatants were removed followed by drying and fixation of the cells. An overnight incubation of fixed

cells with diluted polyclonal rabbit anti-THEV serum was performed followed by a 1 h-incubation with goat anti-rabbit peroxidase-conjugated antiserum. After development of the enzymatic reaction with 3-amino-9-ethylcarbazol, the positively stained wells per each virus dilution were detected with light microscopy, and counts were taken and used to determine $TCID_{50}$. PLA assay was also used by Chary et al. (2002) for the titration of virulent THEV, cell culture-attenuated THEV, and commercial MSDV vaccine strains in RP19 cells.

To conclude, multiple traditional methods have been developed for THEV titration in cell culture or live birds, which may be sufficient for titration of a limited number of vaccine/virus suspensions (one or two at maximum), due to the inherent limitations of these assays (discussed below). If comparing among several batches of vaccines or virus inocula, these assays will be feasibly impossible to use. Therefore, a new, high throughput titration/quantification assay for THEV could be an urgent tool required to facilitate the progress in recent virus research, especially in the *in vitro* systems. Rapidity, accuracy, precision, throughput, and feasibility are all important factors that are lacking in previous traditional assays and should be considered in the new virus titration method to be developed.

2.3.2.3. Overview of common infectivity assays and titration procedures for viruses

The general procedures for the most frequently used infectivity assays in virus biology, i.e., tissue culture infectious dose, plaque assays, and infectivity assays in chicken embryonated eggs, have been extensively demonstrated by several authors including Hierholzer and Killington (1996), Villegas (2008), and Senne (2008). Although established many years ago, some traditional infectivity assays have continued be adapted or optimized for use in titration of viruses in recent years.

Titration in embryonated chicken eggs (ECEs)

Prior to the advent of cell culture systems, besides live animals, ECE was the only alternative for virus propagation and titration. ECE has been used to determine the infectivity titers of numerous viral pathogens from a wide range of virus families, including, for instance, *Paramyxoviridae* (e.g. Newcastle disease virus [NDV]),

Orthomyxoviridae (e.g., Avian Influenza virus [AIV]), *Adenoviridae* (e.g. fowl adenoviruses,), *Herpesviridae* (e.g., Marek's disease virus [MDV]), and *Poxviridae* (e.g., Avian pox viruses) (Bankowski, 1958; Cowen, 1988; Grimes, 2002; Sharma et al., 1976; Spackman and Killian, 2014; Yadav et al., 2007).

Before starting the titration procedure, some viruses may be subjected to primary isolation in ECE or cell culture. AIV is usually isolated first in ECEs; the isolate is kept frozen at ~ -80°C or in liquid nitrogen, in the form of infectious allantoic fluid (AF) or embryonic homogenate. Other viruses (e.g., fowl adenoviruses) may be isolated in cell culture before their infectivity titers are determined in ECE. Briefly, serial tenfold dilutions of virus isolate are prepared in sterile brain-heart infusion (HBI) broth or phosphate-buffered saline (PBS) containing a mixture of antibiotics. Three routs of ECE inoculation can be used: 1) chorioallantoic sac (CAS), which is the standard route for several viruses the most common of which are AIV and NDV; 2) yolk sac (YS), some virus types showed better replication capabilities in theYS as compared to CAS, e.g. fowl adenoviruses; 3) chorioallantoic membrane (CAM), which is used for some poxviruses. A total of thirty susceptible SPF-ECEs (6 eggs per dilution) are required for each virus isolate; embryos at 9-11 d of age are used with the CAS or CAM route and at 5-7 d of age with the YS route. Eggs are candled to determine and mark the air cell position and to check for viability that is verified by the healthy spread of blood vessels. After appropriately disinfecting the egg shell area, a 3-4 mm hole is drilled at the marked air cell for YS, at a lower position for CAS inoculation, or on the egg side for CAM inoculation. Each egg is then injected at a blood vessel-free area through the preferred route with 100-200 µl of infectious material, using an appropriate syringe and needle size, followed by sealing the hole with glue and incubation. For AIV and NDV titration, after 4-7 d of inoculation the AFs are collected from eggs with dead and surviving embryos and tested individually for virus infectivity/replication using hemagglutination (HA) and HA inhibition (HI) assays. The method of Reed and Muench was used to calculate virus titers based on the results of HA and HI assays. Virus titers are usually expressed as 50% embryo infectious doses (EID_{50}) or 50% embryo lethal dose (ELD_{50}) depending on the pathogenicity of the isolate examined (e.g., low *vs*. high pathogenic AIV and avirulent *vs*. virulent NDV) (Grimes, 2002; King and Seal, 1997; Spackman

and Killian, 2014; Young et al., 2002). A similar procedure was followed by Ahmad et al. (2005) to determine the EID_{50} titers of virulent strains of infectious bursal disease virus (IBDV) through CAM inoculation. At 4 dpi, CAMs and embryos were grossly examined for pathological abnormalities, AFs were harvested and embryonic homogenates were made and used to verify the infection by reverse passive HA assay, followed by titer calculations with the method of Reed-Muench. Cowen (1988) applied this assay on fowl adenoviruses, where the EID_{50} was determined for many cell-culture propagated strains of several serotypes. Nine days pi, the infectivity and replication of examined viruses were verified by gross (e.g., death, stunting and curling, overall congestions and hemorrhage, hepatitis, splenomegaly, kidney urates) and microscopic (hepatocellular IIBs) lesions in the inoculated embryos. Using the Reed-Muench method, EID_{50} titer was calculated for each virus strain based on lesion scores per virus dilution.

Pock formation assay (PkFA)

As mentioned above, poxviruses have demonstrated higher infectivity when inoculated in CAMs of ECEs. The viruses replicate in epithelial cells of CAMs and form lesions as plaques or pocks, and thus the protocol is called "pock formation assay". MDV was titrated with PkFA through the inoculation of test material intravenously in the YS (Katz and Kohn, 1971; Sharma et al., 1976). In general, a tenfold dilution series is prepared from the suspension to be titrated and aliquots are used for ECE inoculation. After the incubation of inoculated ECEs (2-5 d depending on the virus type), the CAMs or other membranes are carefully harvested in sterile petri dishes, washed well, and then virus-specific pocks are enumerated and used for titer calculation, which is expressed as pock-forming units (pkfu) per ml. PkFA has been recently employed in the titration of four different avipoxviruses (Yadav et al., 2007).

Tissue culture infectious dose (TCID)

Tissue culture infectious dose endpoint dilution assay has been interchangeably referred to in the literature using different abbreviations, such as TCID, CCID, or TCD assay (the first is now used more frequently), with $TCID_{50}$ the most commonly used type. TCID50 determines the dilution point at which half (50%) of the inoculated subjects is positively infected with the test pathogen under test (Reed and Muench, 1938). This

infectivity assay can be used for titration of virtually any virus as long as susceptible cells are available or can be obtained and prepared from target organs/tissues of host species. The TCID method has a substantial advantage over the common plaque assay, in addition to being more sensitive, TCID can be applied for viruses that cannot replicate in cell monolayers, i.e., viruses that only infect suspension cell cultures.

In the beginning, before the manufacturing of the multiwell culture plates, TCID assays have been performed in glass tissue culture tubes as reported for the titration of smallpox vaccine in Cynomolgus monkey kidney cells by Espmark (1964) and of infectious bursal disease virus (IBDV) in lymphoblastoid cells by Yamaguchi et al. (1981). In this "tube" method, 10-fold serial dilutions are made from virus material, and aliquots of 100 µl from each dilution are inoculated into 100 µl of suspended cells (10^5 to 10^5 cells) in 4 to 10 tube replicates. Inoculated cells are mixed well in the tubes and allowed to adsorb for 1 h, followed by the addition of 800 µl growth media to each tube and further incubation for several days while the tubes are in a standing position. At the end of the incubation period, virus titers can be assessed in two ways based on the virus and cell types. For some viruses like IBDV, which is titrated in lymphoblastoid suspension cells, inoculated cells are harvested from tubes by centrifugation, smears are made on cover glasses, and infected cells are detected by staining with fluorescein-conjugated virus-specific serum and a fluorescent microscope. The positive cells and number of positive tubes per dilution are counted and used for $TCID_{50}$ calculation using Karber's formula (Kärber, 1931). For other viruses like smallpox, the infected cultures are subjected to hemagglutination and hemadsorption tests with susceptible chick erythrocytes. Positive tubes per dilution are counted and used for titer calculation.

The use of microculture systems for virus and antibody titration assays has been reported as early as the 1950s (Melnick and Opton, 1956; Rightsel et al., 1956). Later, the technique became popular and was employed in the infectivity titration of viruses with the endpoint dilution assay for different virus groups (e.g., avian paramyxoviruses and human and avian adenoviruses) (Elazhary and Derbyshire, 1979; Grimes et al., 1976; Katz et al., 1976; Schmidt et al., 1966).

In general, the typical TCID infectivity assay is carried out in 96-well, flat-bottom tissue culture plates. Aliquots of susceptible cell culture are dispensed into each plate-

well and incubated for a period of time based on the protocol requirements; generally, for adherent cells the plate is incubated for 24-48 h until the cells are attached to the plate surface; whereas suspended cells may be incubated for only a few hours. Five to eight successive serial dilutions, normally at 10-fold steps or at least covering 1 $\log_{10}$ range of virus concentrations, are made from the tested virus suspension in low-serum cell culture growth media. Aliquots of each virus dilution are used to inoculate 10 wells of cells in one row of the plate, and 2 wells per row receive virus-free media as negative control. The titer plate is then placed in the incubator for several days and checked daily for the development of virus-specific CPE using an inverted light microscope. Because some viruses may not develop evident CPE in a reasonable time, variations of TCID protocols have been developed by investigators to accommodate the special features of these viruses. The main focus in these assays was on the technique for detection of virus replication and infectivity. A prominent example of such techniques is the titration of Dengue viruses in microtiter plates by indirect immunofluorescence. The procedure is performed in a similar way to what is described above until the end of the incubation period for virus-inoculated cells (from 5-7 days). The cells are then fixed (e.g., in acetone solution), blocked in bovine serum albumin (BSA) solution, and stained with FITC-labeled antibodies specific for virus antigens. The cells per each dilution are examined by fluorescent microscope and scored as negative or positive based on the fluorescence emitted as compared with a positive and negative control (Lambeth et al., 2005; Schoepp and Beaty, 1984). The assay can also be performed in 48-well culture plates as reported for different virus species (Malenovska, 2013).

Regardless of the time it takes to perform the assay and obtain final results, the relatively simple procedure of TCID and no need of sophisticated equipment, all encourage workers to continue improving and evaluating it for use in their research (LaBarre and Lowy, 2001; Malenovska, 2013; Smither et al., 2013).

Plaque assay

The assay of plaque formation is one of the oldest, widely used, gold standard methods that have been devised for the titration of viruses. It was originally described by Dulbecco in the early 1950s (Dulbecco, 1952). Shortly after its initial reporting, the plaque-formation assay (PFA) was employed in studying the replication of several

viruses in different types of cells as well as determining their infectivity titers, as reported by several workers (Bachrach et al., 1957; Cruz and Shin, 2007; Dulbecco and Freeman, 1959; Dulbecco and Vogt, 1954a; Dulbecco and Vogt, 1954b; Furness and Youngner, 1959; Sellers, 1955; Taylor and Graham, 1961; Youngner, 1956). Also, the assay was applied for the titration of common avian viruses including MDV in duck embryo fibroblasts (DEF) (Sharma et al., 1976) and NDV in LLC-MK2 (rhesus monkey kidney) cell line (Kournikakis and Fildes, 1988). Theoretically, PFA can be used for the titration of any virus that can replicate in monolayers of adherent cells and cause discernible cytopathology.

PFA procedure essentially involves the following steps: 1) seeding of susceptible adherent cells into Petri dishes or six-well plates, 2) incubation of cells until forming 90-100% confluent monolayers, 3) inoculation of cells with aliquots of virus dilutions (usually 10-fold diluted solutions) that are spread evenly on the cell monolayers followed by a short incubation (i.e., 30 min to 2 h) allowing virus attachment to cells, 4) spreading a layer of agar-containing culture media over the inoculated cells followed by incubation for a certain period of time sufficient for the development of macroscopically recognizable "plaques" that take the form of bright round areas of 2-4 mm in diameter on a dark background (Dulbecco, 1952; Winocour and Sachs, 1959).

Multiple variations of the PFA procedure have been developed for many viruses; two representative examples covering viruses from two different families are explained next. In 1977, a plaque assay was developed for cricket paralysis virus (positive, ssRNA) titration (Scotti). *Drosophila melanogaster*, embryo epithelial cells were seeded into and allowed to attach to plastic tissue culture dishes or glass Petri dishes. After removing the culture media, 100 µl of diluted virus was added to a cell monolayer, allowed to adsorb for 1 h, and followed by adding a layer of media containing methylcellulose and incubation for 40-48 h. For visualization of infected cells, the methylcellulose layers were removed and cell monolayers were stained with neutral red for 2-3 h. With this stain the plaques were still hard to distinguish and therefore, the contrast between plaques (infected) and uninfected cells was enhanced by a 10-minute staining with a crystal violet solution (Scotti, 1977).

More recently, plaque assays were developed for the titration of enteric human adenoviruses 40 and 41 (Cromeans et al., 2008). A549 (epithelial lung carcinoma) cells were seeded into culture dishes for 2-3 days. Virus dilutions (250 µl) in low serum culture media were added to the cell monolayers and allowed to adsorb for 1 h. An overlay of media containing 0.5% agarose was spread over the plates of inoculated cells, which were then incubated for various periods of up to 17 days depending on the virus serotype. Fresh media/agarose overlays were added every 5-7 days. Right before the staining procedure, agarose overlays were removed, and dishes were allowed to dry. Infected monolayers were stained in two ways: 1) using crystal violet containing formaldehyde for about 2 min; the plaques can be kept for direct counting for a few weeks; 2) using a thiazolyl blue tetrazolium (MTT), viable stain (5 µg/ml) for 2-4 h; the plaques should be counted within 24 h on a light box. This plaque assay was adapted as an alternative to the end-point assay of species F viruses in G293 cells which requires up to 4 weeks to perform (Cromeans et al., 2008). Virus titers are expressed as plaque forming units (PFU)/ml and can be calculated by multiplying the number of plaques per well by dilution factor and then dividing the product by the inoculum volume used (Lambeth et al., 2005).

Furthermore, PFA has recently been either modified to enhance the titration of certain viruses (Juarez et al., 2013) or evaluated for different groups of viruses to compare with modern techniques under development (Calgua et al., 2011; Cruz and Shin, 2007; Lambeth et al., 2005; Payne et al., 2006).

Focus formation assay (FFA)

FFA is an improved variation of the plaque assay and has been favorably used for titration of viruses that do not lyse or kill infected cells. Instead of forming easily recognizable plaques representing a patch of lysed infected cells, non-lytic viruses form limited-size, clusters (foci) of infected cells that are too difficult to distinguish by naked eye. Also, FFA can detect infected cells, through immunostaining for virus antigens, at much earlier stages of infection than plaque assay can do.

In the assay procedure, adherent cells are seeded onto Petri dishes (Thiel and Smith, 1967) or cell culture plates (Cruz and Shin, 2007) at a high enough density to reach confluence after incubation for about 24 h. After the cells are attached, the growth

media is removed and replicate cell monolayers are inoculated with aliquots of virus serial dilutions (commonly tenfold dilutions) in low-serum growth media, and the virus is allowed to adsorb for 1 to 2 h. Virus inocula are washed away and the inoculated cell monolayers are overlaid with a medium containing low percentage of gelling agents such as agarose agar, methyl cellulose, or carboxy methyl cellulose. After incubation of cells for the desired period, ranging from 24 to 96 h depending on the application, the gel overlays are removed, and the inoculated cell monolayers are fixed in a fixing agent like methanol, formalin, or formaldehyde. Some protocols, e.g., rotavirus FFA, may skip the gel overlaying to the fixation step directly. Different staining and visualization procedures may be followed, depending on the availability of reagents and ease of virus detectability. The infected cells can be detected by immunostaining with virus-specific FITC-conjugated antibodies and visualized with a microscope equipped with a UV light source; alternatively, cells can be stained with horseradish peroxidase-labeled reagents or with crystal violet and examined by an inverted microscope (Cruz and Shin, 2007; Thiel and Smith, 1967; Winship and Thacore, 1980). Foci of infected cells are counted and virus titers are calculated and expressed as focus forming units (FFU)/ml. Recently, a more sophisticated variation of FFA was developed, in which images are captured for the FITC-stained cell monolayers and stored by a special computer program. The foci of infected cells can be counted later and used for virus titer estimation (Payne et al., 2006).

More recently, a simple IFA-based method was adapted by Calgua et al. (2011) for quantifying infectious human adenoviruses (HAdV serotypes 2 and 41) and JC polyomaviruses in river water and sewage samples. First, the collected samples were treated to concentrate the virus particles in small volumes. For virus titration, adherent cell lines susceptible to HAdVs or polyomavirus were added to multi-well chamber slides, and aliquots of virus dilutions were mixed with corresponding cells and incubated overnight. Virus inocula were discarded and inoculated cells were incubated in growth media for 4 or 8 days depending on virus type. The cell monolayers were fixed in methanol, blocked in BSA with Tween, and indirectly stained with virus-specific FITC-conjugated antibodies. Cells were examined daily using fluorescent microscopy with a UV light source, infected foci of cells were counted per well and the virus titers were expressed as focus forming units (FFU)/ml (Calgua et al., 2011).

2.3.2.4. Modern titration methods for viruses

Reliable and rapid titration of infectious viruses in live virus vaccines is of great importance to both human and animal recipients. In the past few years and with the advancement in technology and scientific industry, novel techniques have been devised, and new instruments have been manufactured to save researchers' time and effort and to increase the expected throughput from scientific applications. Virus and vaccine titration have benefited greatly from this scientific and technological progress as indicated by the numerous reports related to the establishment and application of new techniques in quantification of viable viruses. In this section of the review, light will be shed on a few of these techniques that have been developed to determine the content of infectious virus particles in live vaccines. It is worth noting that all of the modern virus titration approaches are *in vitro*-based, i.e., they require no use of live animals at any point during the procedure.

Virus titration on the basis of real-time qPCR assays

In recent years a new trend for quantifying infectious virus particles by using infectivity assays based on PCR applications has emerged. The novel techniques were implemented extensively in developing potency tests for the evaluation of the quality features of live virus vaccines. The use of PCR technology throughout the multiple phases of vaccine development and assessment, as well as its weaknesses and strengths, have been recently reviewed (Wolf et al., 2007). Below is a description of examples of applying qPCR techniques in the enumeration of infective viruses in two live vaccines.

Schalk et al. (2004) developed a Light Cycler RT-qPCR-based infectivity assay to estimate the potency of live attenuated measles (single stranded, RNA) virus in trivalent (mumps, rubella, and measles) virus vaccines. The method was used for counting viable viruses in infected cell cultures, as an alternative for the prolonged $CCID_{50}$ protocol and the measles virus plaque assay which require cultivation for 7 or 9 days, respectively. In a 96-well plate, triplicate wells of African green monkey kidney (Vero) cell culture (3.5×10^4 cells in 50 µl/well) were inoculated with 0.25 $\log_{10}$-based serial dilutions of vaccine (50 µl of dilution per well). At 3 dpi, total RNA was extracted from inoculated

cultures using a commercial kit. qPCR with primers and hybridization probes for detection and amplification of a 413 bp-fragment of the measles nucleoprotein gene were used, and the cycle threshold (Ct) values were obtained from the LightCycler software. Using these values, a parallel line analysis of the sample and reference dilutions was run with Combistats software to determine the potency of the sample. Results of the new assay developed by Schalk et al. (2004) were statistically comparable to that of the plaque assay with the advantage of being rapid and less laborious.

Kallesh et al. (2009) established a TaqMan qPCR assay targeting a sequence in the conserved capripoxvirus DNA polymerase gene and used it for determining viable goatpox (double stranded, DNA) virus content in monovalent live attenuated goatpox or divalent goatpox and peste de petits ruminants (PPR) vaccines. To determine the best harvest time for cells post-inoculation, a batch of freeze-dried vaccine was reconstituted, tenfold dilutions from undiluted to 10^{-4} were made, and six-well plates containing confluent Vero cell monolayers were inoculated with 100 µl of each dilution (one dilution per plate). The inoculated cells were harvested at different time points from 24 to 72 hpi and freeze-thawed twice. DNA was extracted and qPCR assays were run. The standard curve for each time point was plotted and the slope was calculated; the maximum slope was obtained from the 36 hpi point. The same infection protocol (i.e., inoculating Vero cells with tenfold vaccine dilutions and harvest at 36 h for DNA and qPCR) was then used to determine the titers of 3 batches each of attenuated monovalent goatpox vaccine and divalent goatpox and PPR vaccine using a reference goatpox vaccine. The goatpox virus titers in test vaccines were calculated by interpolating the qPCR Ct values of their 10-fold dilutions into the standard curve of the reference vaccine; the latter was established by plotting its Ct values against the known $\log_{10}$ virus titers.

An important pitfall of using a reference vaccine in the qPCR-based infectivity assay is that the replication rate of sample and reference viruses may not be exactly the same, which will result in discrepancy in vaccine titration. In order to overcome this, the vaccine/virus production conditions of both sample and reference batches should be homologous (Schalk et al., 2004). Several variations of the virus infectivity assay based on the combination of qPCR techniques and cell culture systems have been recently found in the scientific literature. Applications of such assays encompassed the assessment

of vaccines potency, estimation of viable virus content in live vaccines, and quantification of recombinant virus particles (Bora et al., 2012; Mayginnes et al., 2006; Prabhu et al., 2012; Ranheim et al., 2006; Rohr et al., 2005; Wang et al., 2005). A variety of viruses (virus genera) were involved in these studies including orf virus (*Parapoxvirus*), adeno-associated viruses (*Dependoparvovirus*), camelpox and buffalopox viruses (*Orthopoxvirus*), rotaviruses (*Reovirus*), and human adenoviruses (*Mastadenovirus*).

Virus titration on the basis of fluorescent cell imaging and analysis

In 2005, a flow cytometry-based assay was developed for the titration of dengue virus (DENV) as an alternative for the traditional end point dilution and plaque assays (Lambeth et al.). In this protocol, DENV-susceptible mosquito cells were seeded in six-well culture plates and incubated until nearly confluent. The cells were inoculated with serial tenfold dilutions of test virus and adsorbed for 1 h with rocking every 15 min. The virus was removed from each well and inoculated cells were incubated in growth media for 24 h. Cells from each well were then scraped, washed in PBS, counted by a hemocytometer, and then fixed for 20 min in a commercial fixation buffer. Subsequently, cell samples were stained with FITC-labeled monoclonal antibody against a DENV antigen and analyzed with a flow cytometer. The percentage of infected cells was calculated and the virus titer was estimated using the following formula: "FACS infectious units/ml = [(% of infected cells) × (total number of cells in well) × (dilution factor)]/(volume of inoculum added to cell). The detection limit for FACS assay is ≥ 10,000 cells (Lambeth et al., 2005).

Clinical isolates of yellow fever virus (YFV) are often found unable to form plaques; thus, their titers cannot be evaluated through standard plaque assay or focus forming assay. Therefore, a new virus quantification method was needed. A flow cytometry-based tissue culture limiting dilution assay (TC-LDA) was optimized by Hammarlund et al. (2012) in order to estimate the level of infectious yellow fever virus in a given sample. In this assay, YFV-permissive C6/36 cells were incubated with serial dilutions of virus in a 96-well flat-bottom plate (10 wells/ dilution) for 7 to 10 days after which inoculated cells were resuspended, and aliquots were moved to the wells of a 96-

well round-bottom plate containing 6% formaldehyde solution for virus inactivation. Next, cells were permeabilized with 0.1% saponin solution and blocked with mouse IgG, incubated (1 h) with biotinylated YFV-specific monoclonal antibodies for intracellular staining. A second incubation (30 min) was performed with Strep-Avidin PE. Finally, cells from each well were resuspension in 70 µl of 2% formaldehyde and assayed with a FACSCaliber flow cytometer; acquired data was analyzed with FlowJo software. Negative and positive-stained wells were determined and counted based on a cut-off value of 0.02% background staining for uninfected/negative cells. The virus titer estimated by TC-LDA was calculated as "the reciprocal of the dilution at which 37% of the wells are negative" and was found to give titer values comparable to what were obtained by standard $TCID_{50}$ method (Hammarlund et al., 2012).

2.3.2.5. Overall advantages and disadvantages of virus titration methods

Traditional methods

Advantages: The following points may be favorable in certain situations when running a traditional titration assay: 1) Some of the classic assays require inexpensive reagents and supplies, and therefore the overall running cost is low compared to high-tech methods, particularly when testing small numbers of samples, 2) most of these assays do not require expensive or sophisticated lab equipment, and 3) assays can be easily learned and may not require highly skilled individuals to perform.

Disadvantage: An inherent pitfall observed early in the *in vivo* titration assays is that the susceptibility to pathogenic agents (viral or bacterial) may vary significantly from animal to animal and batch to batch, and therefore not recommended to be used as a reliable and decisive method for accurate virus titration. Rather, these assays can be considered an alternative or temporary method until an appropriate *in vitro* one is developed (Ossa et al., 1983). Furthermore, reviewing the *in vivo* virus titration methods described in the literature and what they entail, one can perceive the following generic downsides: 1) they are cost-prohibitive, as many assays require the use of expensive SPF animals; 2) they require the use of animals at infection-susceptible ages which may not be readily available; 3) they are time-consuming, as one or multiple organs should be inspected for infection-specific lesions; 4) the potential need for growing animals/birds

till a certain age to be valid for use in the titration procedure; 5) they require killing of many animals / birds or chick embryos; and 6) they are labor-intensive as considerable care is needed for animal husbandry throughout the titration procedure which normally extends for several weeks. Additionally, investigating several *in vivo* protocols individually, one can reveal much more concerns to be considered before running them in research nowadays.

Additional disadvantages for in vitro titration methods: 1) Some viruses, like adenoviruses, replicate very slowly and it may take up to 1-2 weeks or one month to perform a plaque assay or a standard CPE-based endpoint dilution assay, respectively (Weber, 1972); 2) in a typical endpoint dilution assay, a tedious microscopic examination of at least 72 wells per titration plate (6 dilution × 10 wells+2 negative control wells) for several days is necessary before obtaining a final result; and 3) judging the cellular pathologic changes due to viral infection is highly subjective and may strongly lead to inaccuracy and inconsistency of calculated titers.

More concerns about the traditional, widespread $TCID_{50}$ endpoint assays are briefly discussed here. It was stated that "to cover a wide range of possible variations in titer, it is generally necessary to use a large number of small groups of test animals at different dilutions" (Reed and Muench, 1938). This is not in concordance with the new recommendations for minimizing animal use. Moreover, the accuracy of the endpoint dilution for virus titration was statistically evaluated and compared with the traditional plaque assay. Since the $TCID_{50}$ method was originally developed using a two-fold dilution series and the titer was estimated based on a graphical interpolation, applying the same procedure to commonly used ten-fold dilutions dramatically affects the accuracy of the assay (Nielsen et al., 1992). Therefore, authors recommended a two-stage assay to overcome this defect and to reach a better accuracy; the first stage is to run a standard one-plate endpoint assay (6 dilutions; 10 wells/ dilution) and choose the two most significant dilutions; the second stage is to run a plaque assay on the selected dilutions or to run another endpoint titration assay using 30 wells/dilution. Although this proposed methodology will increase the accuracy of titers estimated, it will take twice the time needed to perform the original one-stage assays (Nielsen et al., 1992).

Modern methods

Advantages: The modern titration assays have the following advantages over the traditional *in vitro* assays: 1) high throughput, 2) less time-consuming, 3) more accurate and precise with higher reproducibility due to minimizing the intervention of the human factor in assessing the infectivity, and 4) less laborious, as the assessment of virus infectivity is often done mechanically by a piece of equipment and analytical software.

Disadvantages: The following factors may limit the spread of using some of the modern titration methods: 1) reagents and supplies may be relatively expensive as compared with those for *in vitro* assays; 2) assay materials may not be provided by suppliers in certain locations of the world; and 3) the equipment may not be readily available for use, especially in limited-budget institutions.

2.4. Section III: Adenovirus cellular receptors

2.4.1. Overview of the adenovirus structure and genomic composition

Adenoviruses (AdVs) are non-enveloped, icosahedral viral particles with size ranging from 60 to 90 nm and a molecular mass of 150 mega Daltons. The virion capsid is composed of three major structural units (capsomere): trimeric hexon, pentameric penton base, and trimeric fiber proteins. The hexon is the most abundant capsomere (n = 240 units) and it constitutes the main structure of the virion forming 20 triangular facets, each containing 12 hexons. This structure leads to the formation of 12 vertices, each arranged in a five-fold symmetry; at each vertex the penton base is located, where it is surrounded by five hexon protein units. From each vertex protrudes one (in most AdVs, including THEV) or two (long and short; in human AdVs types 40, 41, and 52 and all fowl AdVs) fiber proteins that are anchored in the center of the penton. The estimated fiber length is ~30 nm based on X-ray crystallography and cryoelectron microscopy analyses of human AdVs (Guardado-Calvo et al., 2007; Kidd et al., 1993; Lenman et al., 2015; Nemerow et al., 2012). Each fiber monomer is composed of three domains: C-terminal knob, long shaft, and N-terminal tail. The predicted aa composition of the corresponding domains in THEV are 45, 258, and 151, respectively. The fiber rod is connected directly to the penton base protein through its tail domain (Singh et al., 2013).

The fiber is the primary determinant of the cell and tissue tropism of adenoviruses. This is because, by virtue of its exceptionally elongated structure, it is responsible for the initial interaction between the virus particle and the host cell. Significant sequence variation in fiber genes as well as structural variations in fiber proteins has been found among different AdV members. These differences were strongly linked to variations in tissue tropism and disease potential of an adenoviral infection (Arnberg et al., 1997; Burmeister et al., 2004; Durmort et al., 2001; Shayakhmetov et al., 2003). The penton base is the second essential AdV protein required for successful internalization of the virus into susceptible cells. It is responsible for the interaction of the AdV particle with a second receptor molecule on host cells, upon which interaction the endocytosis process initiates leading eventually to virus entry (Nemerow et al., 2009).

The adenoviral genome is lineal, non-segmented, dsDNA molecule and is terminated at its both 5' ends with terminal proteins to maintain its stability. The genome size varies widely ranging from ~26 kb for most members of genus *Siadenovirus* to ~45 kb for mammalian and other adenoviruses. It features an inverted terminal repeat of 36-200 nt. There are 16 common genes shared by all AdVs. Genus *Siadenovirus* was found to have 8-9 genus-specific ORFs of yet unknown functions; of which ORF1 was found to share a high homology with bacterial sialidases (Davison et al., 2003).

2.4.2. Adenovirus receptors and cell tropism

The cellular receptors identified for different adenovirus species, especially those belonging to the genus *Mastadenovirus*, have been reviewed several times in the recent years (Arnberg, 2009; Cupelli and Stehle, 2011; Jeffrey M, 1999; Nemerow, 2000; Sharma et al., 2009; Zhang and Bergelson, 2005). Here we will focus on adenovirus receptors of members from various genera of the family *Adenoviridae* in the context of their cell and tissue tropism with a mention of the diseases/conditions they cause. Genus *Mastadenovirus*, which contains the majority of HAds, is the most extensively-studied and well-characterized genus in family *Adenoviridae* in terms of virus-host interaction. Only a few studies have been conducted to address the structural basis of virus-cell interaction on members from the other four adenoviral genera. Adenoviral receptors are divided into two types: attachment and internalization receptors, which are required for

productive infection. Members of the family *Adenoviridae* have been shown to utilize a wide variety of cell membrane components as receptors for their attachment and internalization into host cells. Typically, these receptor molecules play important physiological or developmental roles that are important for cell life. Often times, within the same adenoviral genus, viruses have shown considerable diversity in the cell surface molecules utilized to mediate entry into cells.

2.4.2.1. Attachment receptors

Coxsackievirus and adenovirus receptor (CAR): Early studies showed, through competition / saturation experiments on HeLa (human adenocarcinoma epithelial) cells, that HAd type 2 (HAd-2) and Coxsackie virus type B3 (CV-B3) reciprocally prevented the attachment of one other to cell surface. This led to the conclusion that HAdV-2 and CV-B3 share the same attachment receptor on HeLa cells (Lonberg-Holm et al., 1976). Also, it was previously known that HAdV-2 and -5 utilize similar attachment receptor on HeLa cells as the purified HAd-2 fiber inhibited HAdV-5 binding to cells (Philipson et al., 1968). In 1997, the cell surface receptor protein of yet unknown cellular functions was purified from HeLa cells and designated coxsackievirus and adenovirus receptor (CAR). The isolation of cDNAs encoding CAR from human (HeLa) and mouse (TCMK-1; SV40 transformed mouse kidney) epithelial cells and the successful expression of CAR on CAR-negative cells (i.e., NIH 3T3 and Chinese hamster ovary [CHO]) transfected with CAR-cDNA were reported (Bergelson et al., 1997; Tomko et al., 1997). The immunoprecipitation of CAR from HeLa cell lysates with a monoclonal antibody showed a 46-kDa band of a surface glycoprotein. The deduced amino acid (aa) sequence of this membrane glycoprotein indicated 365 residues that are divided into three domains: an N-terminal extracellular domain (222 aa), a single transmembrane helical domain, and a C-terminal cytoplasmic domain (107 aa). Further sequence analyses revealed that CAR belongs to the immunoglobulin superfamily and its extracellular part contains two immunoglobulin-like domains (Bergelson et al., 1997; Tomko et al., 1997). Recently, CAR was reported to play substantial roles in early development of heart in embryos through experiments on mice. Also CAR interacts with junctional adhesion molecule-like

protein to facilitate the migration of immune cells though epithelial tight junctions and endothelial cells (Houri et al., 2013).

By far, CAR is the most popular and well-characterized attachment receptor molecule used by the majority of HAdVs. Further studies using A549 (human lung carcinoma) cells revealed that more HAdVs utilize CAR for attachment which include HAdV-12 and 31 (subgroup A), HAdV-9 and 15 (subgroup D), HAdV-4 (subgroup E), and HAdV-41 (via its long, but not short, fiber; subgroup F), in addition to the subgroup C HAdV-2 and 5 (Roelvink et al., 1998). These HAdVs are widely spread on epithelial cells in various types of tissues and are responsible for a variety of respiratory, gastrointestinal, and genital infections (Biere and Schweiger, 2010; Shinozaki et al., 1991; Swenson et al., 1995). Due to the shortage of research on non-HAdVs, only a few animal adenoviruses were found to use CAR for attachment and these include canine AdV type 2 on CAR-expressing CHO cells (Soudais et al., 2000), CELO virus (FAdV-1) (Tan et al., 2001), and chimpanzee AdV type 68 on CHO cells expressing human or murine CAR (Cohen et al., 2002).

CD46: CD46 is a membrane glycoprotein that functions as a cofactor of the serine protease factor I of complement system. In the presence of CD46, factor I cleaves and therefore deactivates the complement components C3b and C4b which may bind to host cells, preventing them from being destroyed by effector cells. CD46 is ubiquitously expressed on all nucleated cells, including lymphocytes and intercellular junctions of normal and tumor epithelial cells. It is present on cells at densities of 5,000-10,000 molecules / cell (Seya et al., 1998; Strauss et al., 2009). In 2001, (Wu et al.) reported the attachment of HAdV-37 (subgroup D) to a 50-kDa protein on Chang C conjunctival cells and independent of CAR expression. The identity of that protein has not been discovered by that time, but the virus-cell binding was shown to be sialic acid-independent. The same research group has described the isolation and identification of two HAdV-37-binding isoforms of CD46 (MW: 50 and 60 kDa) from Chang C cells using virus overlay protein blot assay, liquid chromatography, and mass spectrometry (Trauger et al., 2004; Wu et al., 2004). HAdV-37 is a major cause of the eye condition called keratoconjunctivitis (Inflammation of the cornea and conjunctiva). Unlike most of the HAdV subgroups, subgroup B virus types do not use CAR as a primary receptor.

Different research groups have demonstrated that members of the HAdV subgroup B (i.e., type 3, 7, 11, 21, and 35) utilize CD46 for the attachment using a variety of techniques and different approaches such as the interaction of purified wild-type or recombinant AdV fiber knobs with CD46 proteins, crystallography and structural analyses, western blot analysis, or virus-cell infectivity assays (Cupelli et al., 2010; Fleischli et al., 2007; Segerman et al., 2003; Sirena et al., 2004; Wang et al., 2007). Subgroup B HAdVs are responsible for causing respiratory and urinary tract infections. Several studies have demonstrated that subgroup B HAdVs can bind to non-CD46 expressing cells, which indicate that these viruses may use alternative cell surface molecules for attachment (Hall et al., 2009; Sirena et al., 2004; Wang et al., 2011).

Sialic acid: Sialic acids (SAs) are monosaccharides that are expressed on almost every mammalian cell, with higher expression on lymphocytes than most of other cells. They are found attached to the termini of surface carbohydrate chains as well as to the side of the chains. Early studies on mouse immune cells revealed that the surface of B-cell, T-cell, and thymocyte contains 70-90%, 60-70%, and 80-100, respectively, of total SAs content in the cell (Wiig and Mæhle, 1975). Other studies have shown similar findings (Boulanger et al., 1972). SAs are crucial components to a variety of functions of the immune system as they are involved in the regulation of T cell/B cell interactions and adhesion, lymphocyte development and maturation, among several other functions (Bagriaçik and Miller, 1999). SAs have been also reported to play roles in the function and maturation of dendritic cells, to have anti-inflammatory effects, and to be expressed on epithelial cells and tissues (Carbone and Heath, 2003; Crespo et al., 2009; Crespo et al., 2013; Görög and Kovács, 1978; Ulloa and Real, 2001).

Around the 1970s, the role of SA in adenovirus adsorption has been reported from studies on the agglutination of erythrocytes (Boulanger et al., 1972). Later on, several studies have shown that members of subgroup D HAdVs (e.g, HAdV-8, -9, -19a, and -37) use surface SAs (mainly α2,3 linkages) as primary functional receptors on host epithelial cells (e.g., Chang C and A549) and a B lymphoblastoid cell line (Arnberg et al., 2000a; Arnberg et al., 2000b; Arnberg et al., 2002b; Burmeister et al., 2004; Cashman et al., 2004). Unlike HAdVs, bovine AdV-3 was reported to use both α2,3- and α2,6-linked sialic acids on target MDBK cells (Li et al., 2009). The interaction between the

HAdV fiber knob and cell surface SA was found to be charge-dependent as the first carried unusually high positive charges and the latter is negatively charged (Arnberg et al., 2002a). A recent study has revealed that the newly discovered gastroenteritis-causing HAdV-52 binds to sialic acid through its short fiber and to CAR via its short fiber (Lenman et al., 2015).

GD1a glycan: The GD1a is one of the four major sialylated glycosphingolipids of the gangliosides / glycolipids which is expressed on all types of cells at varying degrees (Hatano et al., 2011; Sturgill et al., 2012). Although several studies have shown that the EKC-causing subgroup D HAdVs use α2,3-linked sialic acid as functional receptors [Arnberg et al. (2000b); discussed in detail above], the sialic acid-containing glycan has not been identified. Recently, using glycan array screening assay as well as anti-glycan monoclonal antibodies and analysis of virus binding, it was discovered that HAdV-37 binds to the GD1a glycan on corneal epithelial cells (Nilsson et al., 2011). Using several advanced techniques including nuclear magnetic resonance and X-ray crystallography HAdV-37 fiber knob through two of its three sialic acid binding sites was found to interact at high affinity with the two terminal sialic acids of the GD1a glycan. Other EKC-causing (types 8 and 19a) and a non-causing (i.e., type 19p) subgroup D HAdVs are also capable of binding to GD1a, unlike the subgroup C HAdV-5 (Nilsson et al., 2011).

Desmoglein 2 (DSG-2): DSG-2 is a desmosomal transmembrane glycoproteins which belongs to the cadherin cell adhesion molecule superfamily. DSG-2 is expressed on human intestinal epithelial cells and a few other types of cells (Jiang et al., 2014) and plays a critical role in intercellular adhesion. Reduction or loss of DSG-2 on the border of intestinal epithelial cells was reported to play a role in the pathogenesis of Crohn's disease (Spindler et al., 2015). The full size of AdV-interacting DSG-2 has a MW of 160 kDa as indicated by immunoprecipitation and western blot analyses using HAdV-3 virions, anti-DSG-2 mAbs, and HeLa membrane proteins. Recent studies showed that DSG-2 is used as a primary receptor for the high-affinity attachment to host cells by the species B HAdV-3, -7, -11, and -14, which cause infections in the respiratory system and urinary tract (Wang et al., 2011). HAdV-3 binds to several types of cells including HeLa, K562, SKOV3, 293, HT29, SKHep1, Saos, and Y79 (human retinoblastoma), but not to

human Burkitt's lymphoma B cells or rodent cells. Also, HAdV-3 was found to bind DSG-2 on platelets and granulocytes. Follow-up studies by the same group revealed the aa residues within the HAdV-3 fiber knob which are critical for binding with DSG-2. These are N186, V189, S190, L296, D261, A263, and E299 and all are located within the extreme distal end of the fiber head domain. Virus-receptor binding is reduced or ablated by a mutation in one or two of these residues (Wang et al., 2013). The subgroup C HAdV-2 and -5 were found not to interact with DSG-2 (Wang et al., 2011). Contrary to findings of other researchers (see CD46 above), these authors reported the absence of HAdV-3 binding to CD46. Recent studies have shown that the newly emerging HAdV-B14p1 strain, which was linked to severe infections of the lower respiratory tract, binds to the apical surface of differentiated human bronchial epithelial cells (Lam et al., 2015). This strain was also shown to use DSG-2 as a binding molecule on susceptible cells (Wang et al., 2013).

Heparin sulfate glycosaminoglycans (or proteoglycans; HSPGs): HSPGs are cell surface structures expressed on almost all types of cells, and are composed of two major structural units: a protein core (known as proteoglycan) and glycosaminoglycans (a group of long carbohydrate chains containing one or more sulfated residues). HSPGs play important roles in cell-cell interaction and cell developmental and maturation (Poole, 1986). A few studies have shown that some HAdVs utilize HSPGs to mediate initial binding to target cells through pathways that are independent of their original, high-affinity attachment receptors. These interactions were found to be mediated through AdV non-fiber knob domain, e.g., fiber shaft. Early studies indicated that the subgroup B HAdV-2 and -5 belong to this receptor group (Dechecchi et al., 2001; Dechecchi et al., 2000). Studies have also shown that the subgroup B HAdV-3 and -35 utilize surface HSPGs as co-receptors on HeLa cells; the first through its fiber knob (low affinity binding), and the second though a non-fiber knob domain. Both viruses bind to the sulfated region within the HSPGs, a region that is naturally targeted for binding by extracellular ligands (Tuve et al., 2008).

Other surface attachment molecules: Like HSPGs, several molecules have been reported to be involved in the initial binding of HAdVs to susceptible cells, but not

necessarily lead to a complete infection process. Research efforts made in this area serve mainly towards the advancement in gene delivery mechanisms, cancer therapy, and virus detargeting and retargeting to certain tissues / cells, including those of the immune system. The molecules discovered by these studies include the following: 1) CD80 and CD86 were used for binding by HAdV-3 on dendritic cells (Short et al., 2004), and by all subgroup B HAdVs on permissive HeLa cells and CD80/CD86-transfected CHO cells (Hall et al., 2009; Short et al., 2006); 2) integrins αMβ2 and αLβ2, expressed on leukocytes and function as collagen receptors (Lahti et al., 2013); 3) α3β1 integrin, used by HAdV-5 and others (Salone et al., 2003); 4) major histocompatibility complex class I-α2 domain MHC I-α2 on human epithelial and transfected B lymphoblastoid cells, which interacted with HAdV-5 recombinant fiber knob (Hong et al., 1997). Other molecules also include vascular cell adhesion molecule 1 (VCAM-1), coagulation factors, dipalmitoyl phosphatidylcholine (DPPC), and lactoferrin [reviewed in Arnberg (2009); Zhang and Bergelson (2005)].

2.4.2.2. Internalization receptors - Integrins

While the attachment receptors that mediate the primary binding of AdVs to cells show a high variety of structure and function, the internalization co-receptors required for the secondary interaction of AdVs with cells are of only one type. All of the surface proteins discovered so far that mediate the step of AdV internalization belong to the integrins super family. One main reason for this is that most of the AdV penton base proteins contain an RGD (Arg-Gly-Asp) "signature" motif which is recognized by the integrin proteins. Integrins are hetermodimeric adhesions molecules composed of an α and a β subunit. The types of integrins used by AdVs for cell entry include αvβ3, αvβ5, α3β1, and α5β1 and the viruses types which have been found to utilize one or more of them include HAdV-2, -3, -4, and -5 (Davison et al., 2001; Mathias et al., 1994; Salone et al., 2003; Summerford et al., 1999; Wickham et al., 1993; Zhang and Bergelson, 2005). For THEV, only one report, based on analysis of the predicted THEV penton base aa sequence, has predicted that α4β1 integrin may be used by the virus as an internalization receptor (Suresh et al., 1995). This notion needs to be experimentally investigated. The Integrin α4β1 integrin is known to be expressed on many types of cells including

monocytes and lymphocytes. We may also speculate that THEV receptor molecule(s) is linked to an apoptosis signaling pathways, given that THEV has been shown to induce apoptosis in infected B cells of the spleen (Rautenschlein et al., 2000).

2.4.3. The use of virus overlay protein blot assay (VOPBA) for identifying novel viral receptors

VOPBA is a variation of the western blot technique modified for the specific detection of virus-binding proteins. The technique was originally developed by Gershoni et al. (1986) and was used for the first time to identify the cellular receptors of Sendi virus, a paramyxovirus, on human erythrocytes. A general description of the protocol is as follows. Proteins in the plasma membrane fraction of target cells are isolated and then separated on the basis of their molecular weights by using SDS-PAGE. These fractionated proteins are then blotted on a nitrocellulose or a polyvinylidene fluoride (PVDF) membrane and subsequently incubated with a solution of the virus of interest. Finally, the protein bands that had bound to the virus on the membrane are detected by incubation with antibodies against the virus, similar to what is followed with western blot. VOPBA has been widely utilized for the identification of unknown cell surface molecules, i.e., receptors, that specifically interact with infecting viruses. The unique advantage of this assay is that no previous knowledge is required about the potential cellular proteins to be identified. Moreover, virus-interacting protein bands recognized by VOPBA can be purified directly from the blot membrane, refined and digested by proteolytic enzymes, and then subjected to liquid chromatography and mass spectrometry for the analysis of aa composition (Koudelka et al., 2009; Trauger et al., 2004). This procedure can eventually lead to determining the actual virus receptor(s) of a virus on target cell(s). Using VOBPA, investigators have characterized numerous virus-binding proteins on the surface of various cell types for viruses belonging to different families. Table 2-1 summarizes the results from selected studies, displaying the virus name, target cell types, and the identified proteins.

Compared with other adenoviruses, THEV appears to have several unique characteristics: 1) it is the only adenovirus that naturally targets B lymphocytes for infection and replication, 2) as a *Siadenovirus* member, it contains the shortest adenovirus

genome known to date, 3) it is able to confer a long-lasting immunity in birds based upon a single-dose vaccination, 4) its vaccine strains are able to rapidly halt an ongoing infection of virulent strains, and 5) its virulent strains cause an immune-mediated disease characterized mainly by intestinal lesions; far from the primary site of virus replication in the spleen. Molecular mechanisms of the virus-induced immune responses and immunopathogenesis are still not well understood. In this dissertation, we sought to contribute to paving the way towards answering some fundamental questions about THEV, by exploring the virus-cell interaction. Specifically, the cellular receptor molecules with which THEV interacts on target B cells were studied. Additionally, a virus infectivity and titration assay was established to assist in performing the proposed research. The assay was also applied as a titration method for HE splenic and CC vaccines due to lack of modern assays for THEV infectivity titration.

Table 2-1
Examples of virus-cell interacting proteins identified by VOPBA.

Virus	Family, genus	Target cells	Identified molecule[1]	Reference
Human adenovirus-37	*Adenoviridae*, *Mastadenovirus*, subgroup D	Chang C[2]	50 kDa and 60 kDa (isoforms) membrane glycoproteins[3]	(Trauger et al., 2004; Wu et al., 2001; Wu et al., 2004)
Bovine adenovirus-3	*Adenoviridae*, *Mastadenovirus*	MDBK[4]	97 kDa and 34 kDa membrane glycoproteins (sialylated)	(Li et al., 2009)
Pseudorabies virus	*Herpesviridae*, alphaherpesvirus	MDBK[4]	140 kDa, HSPG[5] 85 kDa, integral membrane protein	(Karger and Mettenleiter, 1996)
Dengu virus Serotype 2 Serotype 3 Serotype 4	*Flaviviridae*, *Flavivirus*	HepG2[6]	 78-80, 90, 98, & 102 kDa 90, 130, & 182 kDa 90, & 130 kDa	(Jindadamrongwech and Smith, 2004)
Cowpea mosaic virus[7]	*Secoviridae*, *Comovirus*	BALB/C17[8] MC57[8] Human KB tumor cells Primary mouse DC[9] HUVEC[10] HeLa cells[11] Human KB tumor cells	 54 kDa non-glycosylated protein[12]	(Koudelka et al., 2007) (Koudelka et al., 2009)

[1]Identified molecules are designated as glycoproteins only if the investigators stated that, [2]conjunctival cell line, [3]This molecule was recognized later, by using lentil lectin chromatography and mass spectrometry, as a membrane cofactor protein (Trauger et al., 2004), [4]MDBK: Madin-Darby bovine kidney cell line, [5]HSPG: heparin sulfate proteoglycan; it was further identified by cosedimentation and affinity chromatography, [6]Human liver cell line, [7]plant-infecting virus, [8]fibroblast cell lines, [9]DC: dendritic cells, [10]HUVEC: human umbilical vein endothelial cells, [11]epithelial/cervix cell line, [12]This molecule was further identified by immune assays and proteomic analysis to be the cytoskeleton component, vimentin (Koudelka et al., 2009).

2.5. References

Ahmad, A.N., Hussain, I., Siddique, M. and Mahmood, M.S., 2005. Adaptation of indigenous infectious bursal disease virus (IBDV) in embryonated chicken eggs. Pakistan Veterinary Journal 25, 71-74.

Arnberg, N., 2009. Adenovirus receptors: implications for tropism, treatment and targeting. Reviews in Medical Virology 19, 165-178.

Arnberg, N., Edlund, K., Kidd, A.H. and Wadell, G., 2000a. Adenovirus Type 37 Uses Sialic Acid as a Cellular Receptor. J. Virol. 74, 42-48.

Arnberg, N., Kidd, A.H., Edlund, K., Nilsson, J., Pring-Åkerblom, P. and Wadell, G., 2002a. Adenovirus Type 37 Binds to Cell Surface Sialic Acid Through a Charge-Dependent Interaction. Virology 302, 33-43.

Arnberg, N., Kidd, A.H., Edlund, K., Olfat, F. and Wadell, G., 2000b. Initial Interactions of Subgenus D Adenoviruses with A549 Cellular Receptors: Sialic Acid versus alpha v Integrins. J. Virol. 74, 7691-7693.

Arnberg, N., Mei, Y.-F. and Wadell, G., 1997. Fiber Genes of Adenoviruses with Tropism for the Eye and the Genital Tract. Virology 227, 239-244.

Arnberg, N., Pring-Åkerblom, P. and Wadell, G., 2002b. Adenovirus Type 37 Uses Sialic Acid as a Cellular Receptor on Chang C Cells. Journal of Virology 76, 8834-8841.

Bachrach, H.L., Callis, J.J., Hess, W.R. and Patty, R.E., 1957. A plaque assay for foot-and-mouth disease virus and kinetics of virus reproduction. Virology 4, 224-236.

Bagriaçik, E.Ü. and Miller, K.S., 1999. Cell surface sialic acid and the regulation of immune cell interactions: the neuraminidase effect reconsidered. Glycobiology 9, 267-275.

Bankowski, R.A., 1958. A Tissue Culture-Modified Newcastle Disease Virus I. Modification, Propagation and Characteristics of the Tissue Culture Newcastle Disease Virus. Avian Diseases 2, 197-209.

Beach, N.M. 2006. Characterization of avirulent turkey hemorrhagic enteritis virus: a study of the molecular basis for variation in virulence and the occurrence of persistent infection, Virginia Polytechnic Institute and State University, Blacksburg, VA, USA, pp. 207.

Benkö, M. and Harrach, B., 1998. A proposal for a new (third) genus within the family Adenoviridae. *Arch Virol* 143, 829-837.

Bergelson, J.M., Cunningham, J.A., Droguett, G., Kurt-Jones, E.A., Krithivas, A., Hong, J.S., Horwitz, M.S., Crowell, R.L. and Finberg, R.W., 1997. Isolation of a Common

Receptor for Coxsackie B Viruses and Adenoviruses 2 and 5. Science 275, 1320-1323.

Biere, B. and Schweiger, B., 2010. Human adenoviruses in respiratory infections: Sequencing of the hexon hypervariable region reveals high sequence variability. Journal of Clinical Virology 47, 366-371.

Bora, D.P., Bhanuprakash, V., Venkatesan, G., Balamurugan, V., Prabhu, M. and Yogisharadhya, R., 2012. Quantitative polymerase chain reaction: another tool to evaluate viable virus content in live attenuated orf vaccine. Veterinaria italiana 48, 425-30.

Boulanger, P.A., Houdret, N., Scharfman, A. and Lemay, P., 1972. The Role of Surface Sialic Acid in Adenovirus-cell Adsorption. Journal of General Virology 16, 429-434.

Burmeister, W.P., Guilligay, D., Cusack, S., Wadell, G. and Arnberg, N., 2004. Crystal Structure of Species D Adenovirus Fiber Knobs and Their Sialic Acid Binding Sites. Journal of Virology 78, 7727-7736.

Calgua, B., Barardi, C.R.M., Bofill-Mas, S., Rodriguez-Manzano, J. and Girones, R., 2011. Detection and quantitation of infectious human adenoviruses and JC polyomaviruses in water by immunofluorescence assay. Journal of Virological Methods 171, 1-7.

Carbone, F.R. and Heath, W.R., 2003. The role of dendritic cell subsets in immunity to viruses. Current Opinion in Immunology 15, 416-420.

Carlson, H.C., Al-Sheikhly, F., Pettit, J.R. and Seawright, G.L., 1974. Virus Particles in Spleens and Intestines of Turkeys with Hemorrhagic Enteritis. Avian Diseases 18, 67-73.

Cashman, S.M., Morris, D.J. and Kumar-Singh, R., 2004. Adenovirus type 5 pseudotyped with adenovirus type 37 fiber uses sialic acid as a cellular receptor. Virology 324, 129-139.

Chary, P., Rautenschlein, S. and Sharma, J.M., 2002. Reduced Efficacy of Hemorrhagic Enteritis Virus Vaccine in Turkeys Exposed to Avian Pneumovirus. Avian Diseases 46, 353-359.

Clark, H.F. and Karzon, D.T., 1967. Terrapene heart (TH-1), a continuous cell line from the heart of the box turtle Terrapene carolina. Experimental Cell Research 48, 263-268.

Clark, H.F., Michalski, F., Tweedell, K.S., Yohn, D. and Zeigel, R.F., 1973. An adenovirus, FAV-1, isolated from the kidney of a frog (Rana pipiens). Virology 51, 392-400.

Cohen, C.J., Xiang, Z.Q., Gao, G.P., Ertl, H.C., Wilson, J.M. and Bergelson, J.M., 2002. Chimpanzee adenovirus CV-68 adapted as a gene delivery vector interacts with the coxsackievirus and adenovirus receptor. J Gen Virol 83, 151-5.

Cowen, B.S., 1988. Chicken Embryo Propagation of Type I Avian Adenoviruses. Avian Diseases 32, 347-352.

Crespo, H.J., Cabral, M.G., Teixeira, A.V., Lau, J.T., Trindade, H. and Videira, P.A., 2009. Effect of sialic acid loss on dendritic cell maturation. Immunology 128, e621-31.

Crespo, H.J., Lau, J.T. and Videira, P.A., 2013. Dendritic cells: a spot on sialic Acid. Front Immunol 4, 491.

Cromeans, T.L., Lu, X., Erdman, D.D., Humphrey, C.D. and Hill, V.R., 2008. Development of plaque assays for adenoviruses 40 and 41. Journal of Virological Methods 151, 140-145.

Cruz, D.J.M. and Shin, H.-J., 2007. Application of a focus formation assay for detection and titration of porcine epidemic diarrhea virus. Journal of Virological Methods 145, 56-61.

Cupelli, K., Muller, S., Persson, B.D., Jost, M., Arnberg, N. and Stehle, T., 2010. Structure of adenovirus type 21 knob in complex with CD46 reveals key differences in receptor contacts among species B adenoviruses. J Virol 84, 3189-200.

Cupelli, K. and Stehle, T., 2011. Viral attachment strategies: the many faces of adenoviruses. Current Opinion in Virology 1, 84-91.

Dan, A., Ruzsics, Z., Russell, W.C., Benko, M. and Harrach, B., 1998. Analysis of the hexon gene sequence of bovine adenovirus type 4 provides further support for a new adenovirus genus (Atadenovirus). J Gen Virol 79 (Pt 6), 1453-60.

Davison, A.J., Benko, M. and Harrach, B., 2003. Genetic content and evolution of adenoviruses. J Gen Virol 84, 2895-2908.

Davison, A.J., Wright, K.M. and Harrach, B., 2000. DNA sequence of frog adenovirus. J Gen Virol 81, 2431-2439.

Davison, E., Kirby, I., Whitehouse, J., Hart, I., Marshall, J.F. and Santis, G., 2001. Adenovirus type 5 uptake by lung adenocarcinoma cells in culture correlates with Ad5 fibre binding is mediated by alpha(v)beta1 integrin and can be modulated by changes in beta1 integrin function. J Gene Med 3, 550-9.

Dechecchi, M.C., Melotti, P., Bonizzato, A., Santacatterina, M., Chilosi, M. and Cabrini, G., 2001. Heparan sulfate glycosaminoglycans are receptors sufficient to mediate the initial binding of adenovirus types 2 and 5. J Virol 75, 8772-80.

Dechecchi, M.C., Tamanini, A., Bonizzato, A. and Cabrini, G., 2000. Heparan sulfate glycosaminoglycans are involved in adenovirus type 5 and 2-host cell interactions. Virology 268, 382-90.

Domermuth, C.H., Gross, W.B., Douglass, C.S., Dubose, R.T., Harris, J.R. and Davis, R.B., 1977. Vaccination for hemorrhagic enteritis of turkeys. Avian Dis 21, 557-565.

Domermuth, C.H., Gross, W.B. and DuBose, R.T., 1973. Microimmunodiffusion Test for Hemorrhagic Enteritis of Turkeys. Avian Diseases 17, 439-444.

Dulbecco, R., 1952. Production of Plaques in Monolayer Tissue Cultures by Single Particles of an Animal Virus. Proc Natl Acad Sci U S A 38, 747-52.

Dulbecco, R. 1980. The nature of viruses. In: Davis, B.D., Dulbecco, R., Eisen, H.N. and Ginsberg, H.S. (Eds), Microbiology, Harper and Row Publishers, Inc., New York, pp. 853-884.

Dulbecco, R. and Freeman, G., 1959. Plaque production by the polyoma virus. Virology 8, 396-397.

Dulbecco, R. and Vogt, M., 1954a. One-step growth curve of Western equine encephalomyelitis virus on chicken embryo cells grown in vitro and analysis of virus yields from single cells. The Journal of experimental medicine 99, 183-99.

Dulbecco, R. and Vogt, M., 1954b. Plaque formation and isolation of pure lines with poliomyelitis viruses. The Journal of experimental medicine 99, 167-82.

Durmort, C., Stehlin, C., Schoehn, G., Mitraki, A., Drouet, E., Cusack, S. and Burmeister, W.P., 2001. Structure of the Fiber Head of Ad3, a Non-CAR-Binding Serotype of Adenovirus. Virology 285, 302-312.

Elazhary, M.A. and Derbyshire, J.B., 1979. Aerosol stability of bovine adenovirus type 3. Can J Comp Med 43, 305-12.

Espmark, J.A., 1964. Tissue culture end-point titrations as a routine potency test for smallpox vaccine. Archiv fur die gesamte Virusforschung 15, 35-49.

Fadly, A.M. and Nazerian, K., 1984. Efficacy and Safety of a Cell-Culture Live Virus Vaccine for Hemorrhagic Enteritis of Turkeys: Laboratory Studies. Avian Diseases 28, 183-196.

Fadly, A.M., Nazerian, K., Nagaraja, K. and Below, G., 1985. Field vaccination against hemorrhagic enteritis of turkeys by a cell-culture live-virus vaccine. Avian Diseases 29, 768-77.

Fasina, S.O. and Fabricant, J., 1982. In vitro Studies of Hemorrhagic Enteritis Virus with Immunofluorescent Antibody Technique. Avian Diseases 26, 150-157.

Fleischli, C., Sirena, D., Lesage, G., Havenga, M.J., Cattaneo, R., Greber, U.F. and Hemmi, S., 2007. Species B adenovirus serotypes 3, 7, 11 and 35 share similar binding sites on the membrane cofactor protein CD46 receptor. J Gen Virol 88, 2925-34.

Furness, G. and Youngner, J.S., 1959. One-step growth curves for vaccinia virus in cultures of monkey kidney cells. Virology 9, 386-395.

Gershoni, J.M., Lapidot, M., Zakai, N. and Loyter, A., 1986. Protein blot analysis of virus receptors: identification and characterization of the sendai virus receptor. Biochimica et Biophysica Acta (BBA) - Biomembranes 856, 19-26.

Görög, P. and Kovács, I.B., 1978. Anti-inflammatory effect of sialic acid. Inflammation Research 8, 543-545.

Grimes, S.E. 2002. A Basic Laboratory Manual for the Small-Scale Production and Testing of I-2 Newcastle Disease Vaccine, RAP publication 2002/22, Food and Agriculture Organization of the United Nations (FAO), Bangkok, THAILAND, pp. 139.

Grimes, T.M., King, D.J. and Kleven, S.H., 1976. Application of a Microtiter Cell-Culture Method to Characterization of Avian Adenoviruses. Avian Diseases 20, 299-310.

Guardado-Calvo, P., Llamas-Saiz, A.L., Fox, G.C., Langlois, P. and van Raaij, M.J., 2007. Structure of the C-terminal head domain of the fowl adenovirus type 1 long fiber. Journal of General Virology 88, 2407-2416.

Hall, K., Blair Zajdel, M.E. and Blair, G.E., 2009. Defining the role of CD46, CD80 and CD86 in mediating adenovirus type 3 fiber interactions with host cells. Virology 392, 222-229.

Hammarlund, E., Amanna, I.J., Dubois, M.E., Barron, A., Engelmann, F., Messaoudi, I. and Slifka, M.K., 2012. A flow cytometry-based assay for quantifying non-plaque forming strains of yellow fever virus. PLoS One 7, e41707.

Hatano, K., Miyamoto, Y., Nonomura, N. and Kaneda, Y., 2011. Expression of gangliosides, GD1a, and sialyl paragloboside is regulated by NF-κB-dependent transcriptional control of α2,3-sialyltransferase I, II, and VI in human castration-resistant prostate cancer cells. International Journal of Cancer 129, 1838-1847.

Hierholzer, J.C. and Killington, R.A. 1996. Virus isolation and quantitation. In: Mahy, B.W.J. and Kangro, H.O. (Eds), Virology Methods Manual, Academic Press, London, pp. 25-46.

Hong, S.S., Karayan, L., Tournier, J., Curiel, D.T. and Boulanger, P.A., 1997. Adenovirus type 5 fiber knob binds to MHC class I [alpha]2 domain at the surface of human epithelial and B lymphoblastoid cells. EMBO J 16, 2294-2306.

Houri, N., Huang, K.-C. and Nalbantoglu, J., 2013. The Coxsackievirus and Adenovirus Receptor (CAR) Undergoes Ectodomain Shedding and Regulated Intramembrane Proteolysis (RIP). PLoS ONE 8, e73296.

Hussain, I., Nagaraja, K.V. and Newman, J.A., 1993. Efficacy of splenic and cell culture haemorrhagic enteritis vaccines in commercial and specific-pathogen-free turkeys. Pak. J. Agri. Sci 30, 388-392.

Jeffrey M, B., 1999. Receptors mediating adenovirus attachment and internalization. Biochemical Pharmacology 57, 975-979.

Jiang, K., Rankin, C.R., Nava, P., Sumagin, R., Kamekura, R., Stowell, S.R., Feng, M., Parkos, C.A. and Nusrat, A., 2014. Galectin-3 regulates desmoglein-2 and intestinal epithelial intercellular adhesion. J Biol Chem 289, 10510-7.

Jindadamrongwech, S. and Smith, D.R., 2004. Virus Overlay Protein Binding Assay (VOPBA) Reveals Serotype Specific Heterogeneity of Dengue Virus Binding Proteins on HepG2 Human Liver Cells. Intervirology 47, 370-373.

Joseph, H.M., Ballmann, M.Z., Garner, M.M., Hanley, C.S., Berlinski, R., Erdélyi, K., Childress, A.L., Fish, S.S., Harrach, B. and Wellehan Jr, J.F.X., 2014. A novel siadenovirus detected in the kidneys and liver of Gouldian finches (Erythura gouldiae). Veterinary Microbiology 172, 35-43.

Juarez, D., Long, K.C., Aguilar, P., Kochel, T.J. and Halsey, E.S., 2013. Assessment of plaque assay methods for alphaviruses. Journal of Virological Methods 187, 185-189.

Kallesh, D.J., Hosamani, M., Balamurugan, V., Bhanuprakash, V., Yadav, V. and Singh, R.K., 2009. Quantitative PCR: a quality control assay for estimation of viable virus content in live attenuated goat pox vaccine. Indian journal of experimental biology 47, 911-5.

Kärber, G., 1931. 50% end-point calculation. Arch. Exp. Pathol. Pharmak 162, 480-483.

Karger, A. and Mettenleiter, T.C., 1996. Identification of cell surface molecules that interact with pseudorabies virus. Journal of Virology 70, 2138-45.

Katoh, H., Ohya, K., Kubo, M., Murata, K., Yanai, T. and Fukushi, H., 2009. A novel budgerigar-adenovirus belonging to group II avian adenovirus of Siadenovirus. Virus Res 144, 294-7.

Katz, D., Ben-Moshe, H. and Alon, S., 1976. Titration of Newcastle disease virus and its neutralizing antibodies in microplates by a modified hemadsorption and hemadsorption inhibition method. Journal of Clinical Microbiology 3, 227-232.

Katz, D. and Kohn, A., 1971. Isolation and Identification of Marek's Disease Herpesvirus by Yolk-Sac Inoculation Method. Avian Diseases 15, 187-198.

Kidd, A.H., Chroboczek, J., Cusack, S. and Ruigrok, R.W.H., 1993. Adenovirus Type 40 Virions Contain Two Distinct Fibers. Virology 192, 73-84.

King, D.J. and Seal, B.S., 1997. Biological and molecular characterization of Newcastle disease virus isolates from surveillance of live bird markets in the northeastern United States. Avian Dis. 41, 683-9.

Koudelka, K.J., Destito, G., Plummer, E.M., Trauger, S.A., Siuzdak, G. and Manchester, M., 2009. Endothelial Targeting of Cowpea Mosaic Virus (CPMV) via Surface Vimentin. PLoS Pathog 5, e1000417.

Koudelka, K.J., Rae, C.S., Gonzalez, M.J. and Manchester, M., 2007. Interaction between a 54-Kilodalton Mammalian Cell Surface Protein and Cowpea Mosaic Virus. Journal of Virology 81, 1632-1640.

Kournikakis, B. and Fildes, J., 1988. Titration of avirulent Newcastle disease virus by the plaque assay method. Journal of Virological Methods 20, 285-293.

Kovács, E.R. and Benkő, M., 2009. Confirmation of a novel siadenovirus species detected in raptors: partial sequence and phylogenetic analysis. Virus Res 140, 64-70.

Kovács, E.R. and Benkő, M., 2011. Complete sequence of raptor adenovirus 1 confirms the characteristic genome organization of siadenoviruses. Infection, Genetics and Evolution 11, 1058-1065.

Kovács, E.R., Janoska, M., Dan, A., Harrach, B. and Benkő, M., 2010. Recognition and partial genome characterization by non-specific DNA amplification and PCR of a new siadenovirus species in a sample originating from Parus major, a great tit. J Virol Methods 163, 262-8.

LaBarre, D.D. and Lowy, R.J., 2001. Improvements in methods for calculating virus titer estimates from TCID50 and plaque assays. Journal of Virological Methods 96, 107-126.

Lahti, M., Heino, J. and Kapyla, J., 2013. Leukocyte integrins alphaLbeta2, alphaMbeta2 and alphaXbeta2 as collagen receptors--receptor activation and recognition of GFOGER motif. Int J Biochem Cell Biol 45, 1204-11.

Lam, E., Ramke, M., Warnecke, G., Schrepfer, S., Kopfnagel, V., Dobner, T. and Heim, A., 2015. Effective Apical Infection of Differentiated Human Bronchial Epithelial Cells and Induction of Proinflammatory Chemokines by the Highly Pneumotropic Human Adenovirus Type 14p1. PLoS One 10, e0131201.

Lambeth, C.R., White, L.J., Johnston, R.E. and de Silva, A.M., 2005. Flow cytometry-based assay for titrating dengue virus. J Clin Microbiol 43, 3267-72.

Lee, S.Y., Kim, J.H., Park, Y.M., Shin, O.S., Kim, H., Choi, H.G. and Song, J.W., 2014. A novel adenovirus in Chinstrap penguins (Pygoscelis antarctica) in Antarctica. Viruses 6, 2052-61.

Lenman, A., Liaci, A.M., Liu, Y., Ardahl, C., Rajan, A., Nilsson, E., Bradford, W., Kaeshammer, L., Jones, M.S., Frangsmyr, L., Feizi, T., Stehle, T. and Arnberg, N., 2015. Human adenovirus 52 uses sialic acid-containing glycoproteins and the coxsackie and adenovirus receptor for binding to target cells. PLoS Pathog 11, e1004657.

Li, X., Bangari, D.S., Sharma, A. and Mittal, S.K., 2009. Bovine adenovirus serotype 3 utilizes sialic acid as a cellular receptor for virus entry. Virology 392, 162-8.

Lonberg-Holm, K., Crowell, R.L. and Philipson, L., 1976. Unrelated animal viruses share receptors. Nature 259, 679-681.

Malenovska, H., 2013. Virus quantitation by transmission electron microscopy, TCID50, and the role of timing virus harvesting: A case study of three animal viruses. Journal of Virological Methods 191, 136-140.

Mathias, P., Wickham, T., Moore, M. and Nemerow, G., 1994. Multiple adenovirus serotypes use alpha v integrins for infection. Journal of Virology 68, 6811-6814.

Mayginnes, J.P., Reed, S.E., Berg, H.G., Staley, E.M., Pintel, D.J. and Tullis, G.E., 2006. Quantitation of encapsidated recombinant adeno-associated virus DNA in crude cell lysates and tissue culture medium by quantitative, real-time PCR. J Virol Methods 137, 193-204.

Melnick, J.L. and Opton, E.M., 1956. Assay of poliomyelitis neutralizing antibody in disposable plastic panels. Bulletin of the World Health Organization 14, 129-46.

Nazerian, K., Elmubarak, A. and Sharma, J.M., 1982. Establishment of B-lymphoblastoid cell lines from Marek's disease virus-induced tumors in turkeys. International Journal of Cancer 29, 63-68.

Nazerian, K. and Fadly, A.M., 1982. Propagation of virulent and avirulent turkey hemorrhagic enteritis virus in cell culture. Avian Diseases 26, 816-27.

Nazerian, K. and Fadly, A.M., 1987. Further studies on in vitro and in vivo assays of hemorrhagic enteritis virus (HEV). Avian Diseases 31, 234-40.

Nazerian, K.E.L., MI), Fadly, Aly M. (Holt, MI). 1983. Propagation of hemorrhagic enteritis virus in a turkey cell line and vaccine produced, The United States of America as represented by the Secretary of Agriculture (Washington, DC), United States.

Nemerow, G.R., 2000. Cell Receptors Involved in Adenovirus Entry. Virology 274, 1-4.

Nemerow, G.R., Pache, L., Reddy, V. and Stewart, P.L., 2009. Insights into adenovirus host cell interactions from structural studies. Virology 384, 380-8.

Nemerow, G.R., Stewart, P.L. and Reddy, V.S., 2012. Structure of human adenovirus. Current Opinion in Virology 2, 115-121.

Nielsen, L.K., Smyth, G.K. and Greenfield, P.F., 1992. Accuracy of the endpoint assay for virus titration. Cytotechnology. 8, 231-6.

Nilsson, E.C., Storm, R.J., Bauer, J., Johansson, S.M.C., Lookene, A., Angstrom, J., Hedenstrom, M., Eriksson, T.L., Frangsmyr, L., Rinaldi, S., Willison, H.J., Domellof, F.P., Stehle, T. and Arnberg, N., 2011. The GD1a glycan is a cellular receptor for adenoviruses causing epidemic keratoconjunctivitis. Nat Med 17, 105-109.

Ossa, J.E., Bates, R.C. and Schurig, G.G., 1983. Hemorrhagic Enteritis in Turkeys: Purification and Quantification of the Virus. Avian Diseases 27, 235-245.

Park, Y.M., Kim, J.-H., Gu, S.H., Lee, S.Y., Lee, M.-G., Kang, Y.K., Kang, S.-H., Kim, H.J. and Song, J.-W., 2012. Full genome analysis of a novel adenovirus from the South Polar skua (Catharacta maccormicki) in Antarctica. Virology 422, 144-150.

Payne, A.F., Binduga-Gajewska, I., Kauffman, E.B. and Kramer, L.D., 2006. Quantitation of flaviviruses by fluorescent focus assay. Journal of Virological Methods 134, 183-189.

Philipson, L., Lonberg-Holm, K. and Pettersson, U., 1968. Virus-Receptor Interaction in an Adenovirus System. Journal of Virology 2, 1064-1075.

Pierson, F.W. and Fitzgerald, S.D. 2008. Hemorrhagic Enteritis and Related Infections. In: Saif, Y.M., Fadly, A.M., Glisson, J.R., McDougald, L.R., Nolan, L.K. and Swayne, D.E. (Eds), Diseases of Poultry, Wiley-Blackwell, Iowa, pp. 276-286.

Pitcovski, J., Mualem, M., Rei-Koren, Z., Krispel, S., Shmueli, E., Peretz, Y., Gutter, B., Gallili, G.E., Michael, A. and Goldberg, D., 1998. The Complete DNA Sequence and Genome Organization of the Avian Adenovirus, Hemorrhagic Enteritis Virus. Virol 249, 307–315.

Poole, A.R., 1986. Proteoglycans in health and disease: structures and functions. Biochemical Journal 236, 1-14.

Prabhu, M., Siva Sankar, M.S., Bhanuprakash, V., Venkatesan, G., Bora, D.P., Yogisharadhya, R. and Balamurugan, V., 2012. Real time PCR: a rapid tool for potency estimation of live attenuated camelpox and buffalopox vaccines. Biologicals 40, 92-5.

Ranheim, T., Mathis, P.K., Joelsson, D.B., Smith, M.E., Campbell, K.M., Lucas, G., Barmat, S., Melissen, E., Benz, R., Lewis, J.A., Chen, J., Schofield, T., Sitrin, R.D.

and Hennessey, J.P., Jr., 2006. Development and application of a quantitative RT-PCR potency assay for a pentavalent rotavirus vaccine (RotaTeq). J Virol Methods 131, 193-201.

Rautenschlein, S. and Sharma, J.M., 1999. Response of turkeys to simultaneous vaccination with hemorrhagic enteritis and Newcastle disease viruses. Avian Dis 43, 286-92.

Rautenschlein, S., Suresh, M., Neumann, U. and Sharma, J.M., 1996. Pathogenic mechanisms of avian adenovirus type II. International Symposium on Adenovirus and Reovirus Infections in Poultry, 41–50.

Rautenschlein, S., Suresh, M. and Sharma, J.M., 2000. Pathogenic avian adenovirus type II induces apoptosis in turkey spleen cells. Arch Virol 145, 1671-83.

Reed, L.J. and Muench, H., 1938. A simple method of estimating fifty per cent endpoints. The American Journal of Hygiene 27, 493-497.

Rightsel, W.A., Schultz, P., Muething, D. and McLean, I.W., Jr., 1956. Use of vinyl plastic containers in tissue cultures for virus assays. J Immunol 76, 464-74.

Rivera, S., Wellehan, J.F., Jr., McManamon, R., Innis, C.J., Garner, M.M., Raphael, B.L., Gregory, C.R., Latimer, K.S., Rodriguez, C.E., Diaz-Figueroa, O., Marlar, A.B., Nyaoke, A., Gates, A.E., Gilbert, K., Childress, A.L., Risatti, G.R. and Frasca, S., Jr., 2009. Systemic adenovirus infection in Sulawesi tortoises (Indotestudo forsteni) caused by a novel siadenovirus. J Vet Diagn Invest 21, 415-26.

Roelvink, P.W., Lizonova, A., Lee, J.G.M., Li, Y., Bergelson, J.M., Finberg, R.W., Brough, D.E., Kovesdi, I. and Wickham, T.J., 1998. The Coxsackievirus-Adenovirus Receptor Protein Can Function as a Cellular Attachment Protein for Adenovirus Serotypes from Subgroups A, C, D, E, and F. J. Virol. 72, 7909-7915.

Rohr, U.P., Heyd, F., Neukirchen, J., Wulf, M.A., Queitsch, I., Kroener-Lux, G., Steidl, U., Fenk, R., Haas, R. and Kronenwett, R., 2005. Quantitative real-time PCR for titration of infectious recombinant AAV-2 particles. J Virol Methods 127, 40-5.

Salone, B., Martina, Y., Piersanti, S., Cundari, E., Cherubini, G., Franqueville, L., Failla, C.M., Boulanger, P. and Saggio, I., 2003. Integrin α3β1 Is an Alternative Cellular Receptor for Adenovirus Serotype 5. Journal of Virology 77, 13448-13454.

Schalk, J.A., van den Elzen, C., Ovelgonne, H., Baas, C. and Jongen, P.M., 2004. Estimation of the number of infectious measles viruses in live virus vaccines using quantitative real-time PCR. J Virol Methods 117, 179-87.

Schmidt, N.J., Lennette, E.H. and King, C.J., 1966. Neutralizing, hemagglutination-inhibiting and group complement-fixing antibody responses in human adenovirus infections. J Immunol 97, 64-74.

Schoepp, R.J. and Beaty, B.J., 1984. Titration of dengue viruses by immunofluorescence in microtiter plates. Journal of Clinical Microbiology 20, 1017-1019.

Scotti, P.D., 1977. End-point Dilution and Plaque Assay Methods for Titration of Cricket Paralysis Virus in Cultured Drosophila Cells. J Gen Virol 35, 393-396.

Segerman, A., Atkinson, J.P., Marttila, M., Dennerquist, V., Wadell, G. and Arnberg, N., 2003. Adenovirus Type 11 Uses CD46 as a Cellular Receptor. Journal of Virology 77, 9183-9191.

Sellers, R.F., 1955. Growth and Titration of the Viruses of Foot-and-Mouth Disease and Vesicular Stomatitis in Kidney Monolayer Tissue Cultures. Nature 176, 547-549.

Senne, D.A. 2008. Virus propagation in embryonating chicken eggs. In: Dufour-Zavala, L. (Ed), Isolation, Identification, and Characterization of Avian Pathogens, The American Association of Avian Pathologists, Athens, GA, pp. 204-208.

Seya, T., Nomura, M., Murakami, Y., Begum, N.A., Matsumoto, M. and Nagasawa, S., 1998. CD46 (membrane cofactor protein of complement, measles virus receptor): structural and functional divergence among species (review). International journal of molecular medicine 1, 809-16.

Sharma, A., Li, X., Bangari, D.S. and Mittal, S.K., 2009. Adenovirus receptors and their implications in gene delivery. Virus Res 143, 184-94.

Sharma, J.M., 1994. Response of specific-pathogen-free turkeys to vaccines derived from marble spleen disease virus and hemorrhagic enteritis virus. Avian Dis 38, 523-30.

Sharma, J.M., Coulson, B.D. and Young, E., 1976. Effect of in vitro adaptation of Marek's disease virus on pock induction on the chorioallantoic membrane of embryonated chicken eggs. Infect Immun 13, 292-5.

Shayakhmetov, D.M., Li, Z.-Y., Ternovoi, V., Gaggar, A., Gharwan, H. and Lieber, A., 2003. The Interaction between the Fiber Knob Domain and the Cellular Attachment Receptor Determines the Intracellular Trafficking Route of Adenoviruses. Journal of Virology 77, 3712-3723.

Shinozaki, T., Araki, K., Fujita, Y., Kobayashi, M., Tajima, T. and Abe, T., 1991. Epidemiology of enteric adenoviruses 40 and 41 in acute gastroenteritis in infants and young children in the Tokyo area. Scand J Infect Dis. 23, 543-7.

Short, J.J., Pereboev, A.V., Kawakami, Y., Vasu, C., Holterman, M.J. and Curiel, D.T., 2004. Adenovirus serotype 3 utilizes CD80 (B7.1) and CD86 (B7.2) as cellular attachment receptors. Virology 322, 349-59.

Short, J.J., Vasu, C., Holterman, M.J., Curiel, D.T. and Pereboev, A., 2006. Members of adenovirus species B utilize CD80 and CD86 as cellular attachment receptors. Virus Res 122, 144-53.

Singh, A.K., Ballmann, M.Z., Benko, M., Harrach, B. and van Raaij, M.J., 2013. Crystallization of the C-terminal head domain of the fibre protein from a siadenovirus, turkey adenovirus 3. Acta Crystallographica Section F 69, 1135-1139.

Sirena, D., Lilienfeld, B., Eisenhut, M., Kälin, S., Boucke, K., Beerli, R.R., Vogt, L., Ruedl, C., Bachmann, M.F., Greber, U.F. and Hemmi, S., 2004. The Human Membrane Cofactor CD46 Is a Receptor for Species B Adenovirus Serotype 3. Journal of Virology 78, 4454-4462.

Smither, S.J., Lear-Rooney, C., Biggins, J., Pettitt, J., Lever, M.S. and Olinger Jr, G.G., 2013. Comparison of the plaque assay and 50% tissue culture infectious dose assay as methods for measuring filovirus infectivity. Journal of Virological Methods 193, 565-571.

Soudais, C., Boutin, S., Hong, S.S., Chillon, M., Danos, O., Bergelson, J.M., Boulanger, P. and Kremer, E.J., 2000. Canine Adenovirus Type 2 Attachment and Internalization: Coxsackievirus-Adenovirus Receptor, Alternative Receptors, and an RGD-Independent Pathway. Journal of Virology 74, 10639-10649.

Spackman, E. and Killian, M. 2014. Avian Influenza Virus Isolation, Propagation, and Titration in Embryonated Chicken Eggs. In: Spackman, E. (Ed), Animal Influenza Virus, Springer New York, pp. 125-140.

Spindler, V., Meir, M., Vigh, B., Flemming, S., Hutz, K., Germer, C.T., Waschke, J. and Schlegel, N., 2015. Loss of Desmoglein 2 Contributes to the Pathogenesis of Crohn's Disease. Inflammatory bowel diseases 21, 2349-59.

Strauss, R., Sova, P., Liu, Y., Li, Z.Y., Tuve, S., Pritchard, D., Brinkkoetter, P., Moller, T., Wildner, O., Pesonen, S., Hemminki, A., Urban, N., Drescher, C. and Lieber, A., 2009. Epithelial phenotype confers resistance of ovarian cancer cells to oncolytic adenoviruses. Cancer Res 69, 5115-25.

Sturgill, E.R., Aoki, K., Lopez, P.H., Colacurcio, D., Vajn, K., Lorenzini, I., Majić, S., Yang, W.H., Heffer, M., Tiemeyer, M., Marth, J.D. and Schnaar, R.L., 2012. Biosynthesis of the major brain gangliosides GD1a and GT1b. Glycobiology 22, 1289-1301.

Summerford, C., Bartlett, J.S. and Samulski, R.J., 1999. [alpha]V[beta]5 integrin: a co-receptor for adeno-associated virus type 2 infection. Nat Med 5, 78-82.

Suresh, M., Cyr, S.S. and Sharma, J.M., 1995. Molecular cloning and sequence analysis of the penton base genes of type II avian adenoviruses. Virus Res 39, 289-297.

Swenson, P.D., Lowens, M.S., Celum, C.L. and Hierholzer, J.C., 1995. Adenovirus types 2, 8, and 37 associated with genital infections in patients attending a sexually transmitted disease clinic. Journal of Clinical Microbiology 33, 2728-2731.

Taharaguchi, S., Fukazawa, R., Kitazume, M., Harima, H., Taira, K., Oonaka, K. and Hara, M., 2012. Biology of fowl adenovirus type 1 infection of heterologous cells. Arch Virol 157, 2223-6.

Tan, P.K., Michou, A.-I., Bergelson, J.M. and Cotten, M., 2001. Defining CAR as a cellular receptor for the avian adenovirus CELO using a genetic analysis of the two viral fibre proteins. Journal of General Virology 82, 1465-1472.

Taylor, J. and Graham, A.F., 1961. Analysis of a plaque assay method for purified poliovirus MEF-1. Virology 13, 427-438.

Thiel, J.F. and Smith, K.O., 1967. Fluorescent Focus Assay of Viruses on Cell Monolayers in Plastic Petri Plates. Experimental Biology and Medicine 125, 892-895.

Thorsen, J., Weninger, N., Weber, L. and Dijk, C.V., 1982. Field Trials of an Immunization Procedure against Hemorrhagic Enteritis of Turkeys. Avian Diseases 26, 473-477.

Tomko, R.P., Xu, R. and Philipson, L., 1997. HCAR and MCAR: The human and mouse cellular receptors for subgroup C adenoviruses and group B coxsackieviruses. Proceedings of the National Academy of Sciences 94, 3352-3356.

Trauger, S.A., Wu, E., Bark, S.J., Nemerow, G.R. and Siuzdak, G., 2004. The Identification of an Adenovirus Receptor by Using Affinity Capture and Mass Spectrometry. ChemBioChem 5, 1095-1099.

Tuve, S., Wang, H., Jacobs, J.D., Yumul, R.C., Smith, D.F. and Lieber, A., 2008. Role of cellular heparan sulfate proteoglycans in infection of human adenovirus serotype 3 and 35. PLoS Pathog 4, e1000189.

Ulloa, F. and Real, F.X., 2001. Differential Distribution of Sialic Acid in α2,3 and α2,6 Linkages in the Apical Membrane of Cultured Epithelial Cells and Tissues. Journal of Histochemistry & Cytochemistry 49, 501-509.

van den Hurk, J.V., 1990. Propagation of group II avian adenoviruses in turkey and chicken leukocytes. Avian Dis 34, 12-25.

Villegas, P. 2008. Titration of biological suspensions. In: Dufour-Zavala, L. (Ed), Isolation, Identification, and Characterization of Avian Pathogens, The American Association of Avian Pathologists, Athens, GA, pp. 217-221.

Wang, F., Puddy, A.C., Mathis, B.C., Montalvo, A.G., Louis, A.A., McMackin, J.L., Xu, J., Zhang, Y., Tan, C.Y., Schofield, T.L., Wolf, J.J. and Lewis, J.A., 2005. Using QPCR to assign infectious potencies to adenovirus based vaccines and vectors for gene therapy: toward a universal method for the facile quantitation of virus and vector potency. Vaccine 23, 4500-8.

Wang, H., Li, Z.-Y., Liu, Y., Persson, J., Beyer, I., Moller, T., Koyuncu, D., Drescher, M.R., Strauss, R., Zhang, X.-B., Wahl, J.K., Urban, N., Drescher, C., Hemminki, A., Fender, P. and Lieber, A., 2011. Desmoglein 2 is a receptor for adenovirus serotypes 3, 7, 11 and 14. Nat Med 17, 96-104.

Wang, H., Liaw, Y.-C., Stone, D., Kalyuzhniy, O., Amiraslanov, I., Tuve, S., Verlinde, C.L.M.J., Shayakhmetov, D., Stehle, T., Roffler, S. and Lieber, A., 2007. Identification of CD46 Binding Sites within the Adenovirus Serotype 35 Fiber Knob. Journal of Virology 81, 12785-12792.

Wang, H., Yumul, R., Cao, H., Ran, L., Fan, X., Richter, M., Epstein, F., Gralow, J., Zubieta, C., Fender, P. and Lieber, A., 2013. Structural and functional studies on the interaction of adenovirus fiber knobs and desmoglein 2. J Virol 87, 11346-62.

Weber, J., 1972. Titration of Adenovirus by Counting Cells Containing Virus-Induced Inclusion Bodies. Applied Microbiology 23, 1025-1026.

Wellehan, J.F., Jr., Greenacre, C.B., Fleming, G.J., Stetter, M.D., Childress, A.L. and Terrell, S.P., 2009. Siadenovirus infection in two psittacine bird species. Avian Pathol 38, 413-7.

Wickham, T.J., Mathias, P., Cheresh, D.A. and Nemerow, G.R., 1993. Integrins αvβ3 and αvβ5 promote adenovirus internalization but not virus attachment. Cell 73, 309-319.

Wiig, J.N. and Mæhle, B.O., 1975. Distribution of sialic acid in thymocytes, T- and B-cells of the mouse. Experimental Cell Research 93, 31-38.

Winocour, E. and Sachs, L., 1959. A plaque assay for the polyoma virus. Virology 8, 397-400.

Winship, T.R. and Thacore, H.R., 1980. A sensitive method for quantification of vesicular stomatitis virus defective interfering particles: focus forming assay. J Gen Virol 48, 237-40.

Wolf, J.J., Wang, L. and Wang, F., 2007. Application of PCR technology in vaccine product development. Expert review of vaccines 6, 547-58.

Wu, E., Fernandez, J., Fleck, S.K., Von Seggern, D.J., Huang, S. and Nemerow, G.R., 2001. A 50-kDa Membrane Protein Mediates Sialic Acid-Independent Binding and Infection of Conjunctival Cells by Adenovirus Type 37. Virology 279, 78-89.

Wu, E., Trauger, S.A., Pache, L., Mullen, T.-M., Von Seggern, D.J., Siuzdak, G. and Nemerow, G.R., 2004. Membrane Cofactor Protein Is a Receptor for Adenoviruses Associated with Epidemic Keratoconjunctivitis. Journal of Virology 78, 3897-3905.

Yadav, S., Dash, B.B., Kataria, J.M., Dhama, K., Gupta, S.K. and Rahul, S., 2007. Pathogenicity study of different avipoxviruses in embryonated chicken eggs and cell cultures. Indian J. Vet. Pathol. 31, 17-20.

Yamaguchi, S., Imada, T. and Kawamura, H., 1981. Growth and infectivity titration of virulent infectious bursal disease virus in established cell lines from lymphoid leukosis tumors. Avian Dis 25, 927-35.

Young, M., Alders, R., Grimes, S., Spradbrow, P., Dias, P., da Silva, A. and Lobo, Q. 2002. Controlling Newcastle Disease in Village Chickens: A Laboratory Manual, ACIAR MONOGRAPH SERIES, Australian Centre for International Agricultural Research (ACIAR), Canberra, Australia, pp. 144.

Youngner, J.S., 1956. Virus Adsorption and Plaque Formation in Monolayer Cultures of Trypsin-Dispersed Monkey Kidney. The Journal of Immunology 76, 288-292.

Zhang, Y. and Bergelson, J.M., 2005. Adenovirus Receptors. J. Virol. 79, 12125-12131.

Zsivanovits, P., Monks, D.J., Forbes, N.A., Ursu, K., Raue, R. and Benkö, M., 2006. Presumptive Identification of a Novel Adenovirus in a Harris Hawk (Parabuteo unicinctus), a Bengal Eagle Owl (Bubo bengalensis), and a Verreaux's Eagle Owl (Bubo lacteus). Journal of Avian Medicine and Surgery 20, 105-112.

Chapter 3

Development and Applications of Real-Time PCR for Quantification of Turkey Hemorrhagic Enteritis Virus Genomes (THEV): Genomic Titration of HE Live Vaccines and Assessment of Virus Replication in Cell Culture Systems

3.1. Abstract

In this chapter the development and optimization of a new SYBR Green I-based qPCR assay for the quantification of THEV genomes are described in compliance with the MIQE guidelines (Bustin et al., 2009), which states the minimum information for publication of quantitative real-time PCR experiments. The assay is rapid, sensitive, specific, and highly reproducible with a limit of quantification of 10 genome copies per reaction. It was validated for use with a variety of samples including, splenic vaccines, cell-free cell culture vaccines, infected cell cultures, and intestinal tissues.

The THEV genomic titers in splenic vaccine batches, obtained from two different sources, ranged from 8.10E+06 to 1.39E+08 and from 6.32E+07 to 4.10E+08 genome copies/dose. Differences among batches from each source were statistically significant. The establishment of this precise and fast qPCR assay should be beneficial for HE vaccine producers to generate more standardized products and to minimize batch-to-batch variations. The assay can function as either a complementary or a substitute for the agar gel immunodiffusion (AGID) test, which is currently used for splenic vaccine titration.

The qPCR assay was used for studying the kinetics of THEV replication in cultured cells by means of growth curve experiments. The application of this approach is an excellent research tool for investigating the effect of various factors on virus replication under controlled experimental conditions. It was found that the inoculation vessel, e.g., tubes *vs.* culture plates, and the virus-cell ratio are factors that substantially affect the efficiency of virus replication and its growth characteristics in cell culture.

In addition to the above-mentioned uses, the developed qPCR assay was used in conjunction with cell culture system for the establishment of a novel infectivity method for THEV, which is described in detail in Chapter 4 of this dissertation.

3.2. Introduction

Turkey hemorrhagic enteritis virus (THEV) is responsible for causing the hemorrhagic enteritis (HE) disease in turkeys and primarily affects birds at 4-12 weeks of age. It is a non-enveloped double-stranded DNA virus in the genus *Siadenovirus*, family *Adenoviridae*. Clinical signs of HE include depression, splenomegaly, intestinal hemorrhage, bloody droppings, and death. The mortality rate ranges from <1 – 60% in susceptible turkeys depending on the virulence of the infecting THEV strain and the accompanying secondary infections (Davison and Harrach, 2011; Gross and Moore, 1967; Pierson and Fitzgerald, 2008).

Protection of commercial turkeys against HE is conferred by two types of vaccines: the first is propagated in live turkeys, processed as a crude splenic homogenate (Domermuth et al., 1977), and produced locally through turkey companies; while the second is propagated in susceptible B cells (Fadly and Nazerian, 1984; Nazerian, 1983) and commercially marketed as lyophilized or liquid cell-free products. At present, an agar gel immunodiffusion (AGID) test (Domermuth et al., 1973; Domermuth et al., 1972) is the only quality control assay for the assessment of THEV titers in splenic vaccines. The test determines the highest vaccine dilution that gives positive results (i.e., forming a precipitation line). A minimum "positive" dilution (i.e., 1:16) is required to indicate the presence of sufficient amount of virus in a batch of vaccine. As can be noticed, the test gives a rough estimation of the amount of viral antigens (mainly the capsid proteins which interact with THEV-specific serum antibodies) in splenic vaccines, rather than estimating the actual infectious virus titers. Moreover, the test is very subjective and its results vary greatly based on the quality of the test reagents including the virus-specific polyclonal antibodies (i.e., hyperimmune serum collected for infected birds), the positive control splenic material, and the storage time of the agar plates. These components have not been well-optimized for the AGID test and were found to substantially affect the accuracy of results. Moreover, the test takes two days before a confirmative result can be obtained; and, at times, needs to be repeated due to the above-mentioned issues.

In the present study, the establishment and optimization of a simple, rapid, and sensitive SYBR Green-based qPCR assay for the precise quantification of THEV genome copies and its application on determining the viral genomic titers in HE live vaccines are

described. The reproducibility, sensitivity, and specificity of the assay were demonstrated using DNA templates extracted from various types of samples. The assay was used to compare the virus genomic titer in multiple splenic vaccine batches produced in two different facilities. Additionally, the assay was employed, for the first time, to study the kinetics of THEV replication in infected RP19 cells though growth curve experiments.

3.3. Materials and Methods

3.3.1. Primers design and synthesis

Oligonucleotide primers were designed based on the published sequence of the hexon (*hex*) gene of the Virginia avirulent strain of THEV (GenBank accession number, whole genome, AY849321). Primers were designed using Primer3 software (v. 0.4.0) (Koressaar and Remm, 2007; Untergasser et al., 2012), available at http://bioinfo.ut.ee/primer3-0.4.0/, to generate a 445-bp amplicon for the conventional PCR and a 115-bp amplicon for the qPCR assays described below. All primers were synthesized by Sigma-Aldrich (St. Louis, MO). To ensure the uniqueness of target THEV fragments for standard PCR and qPCR assays, the expected sequences (445 bp and 115 bp, respectively) were subjected to in silico specificity screening through the BLAST search on the NCBI website (http://blast.ncbi.nlm.nih.gov/Blast.cgi). Nucleotide sequence of the mentioned fragments as well as the homology results can be found in Appendix A. Results show that no sequence similarities were found to any DNA from other organisms than THEV. The amplification specificity of the standard PCR primer set was verified with PCR and gel electrophoresis (Fig. 3-1), while the specificity of the qPCR primer set was verified using the melt curve analysis (Fig. 3-4). The absence of non-specific amplification was confirmed for both primer sets. Primer sequences and positions within the THEV genome are shown in Table 3-1.

Table 3-1
Nucleotide sequences of the primers used in the standard and real-time PCR assays.

Name	Sequence (5' to 3')	Position*	Melting T (°C)	Amplicon size (bp)
Conventional PCR primers				
THEVhexfragF (forward)	GCGGATTTGATGAGTAGGAATC	14594	63.5	445
THEVhexfragR (reverse)	TATAACGCCCGCCAATATGT	15038	63.8	
Real-time PCR primers				
THEVqPCRhexF (forward)	GGCATGGGCAACTATCCTAA	14726	63.6	115
THEVqPCRhexR (reverse)	GAACACTGCCAAAACCCATC	14840	64.3	

*Oligonucleotide primers were designed based on the published sequence of the hexon gene of the Virginia avirulent strain of THEV (GenBank accession number AY849321). Positions of primers are relative to the published genome sequence. Primers were designed using the online software Primer3 (http://frodo.wi.mit.edu/primer3/) and were manufactured by Sigma-Aldrich.

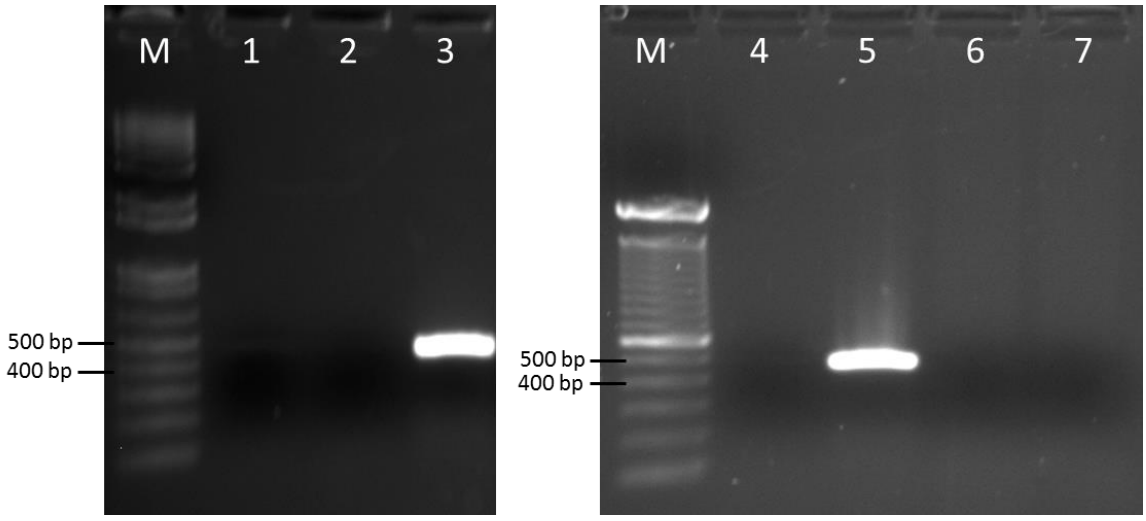

Fig. 3-1. Agarose gel electrophoresis showing the specificity of the conventional PCR primer set listed in Table 3-1. PCR assay was run on DNA templates extracted from THEV-infected spleens (200 ng/µl; lanes 3 & 5) as positive controls or regular RP19 cells (lanes 6 & 7) as negative controls. One microliter DNA/reaction was used. The amplification products were electrophoresed on a 1% agarose gel containing ethidium bromide at 100 V for 45 min and visualized under UV light. Lanes 1, 2, & 4: NTC (i.e., water). Lane M: 1 kb DNA ladder. One distinguished band was amplified from the positive control samples and no non-specific amplifications or primer dimers were detected.

3.3.2. Preparation of plasmid DNA standard

Total DNA was extracted from THEV-infected RP19 cells using QIAamp DNA mini kit (Qiagen, Valencia, CA), following the Blood or Body Fluids Spin Protocol. The DNA was eluted in 50 µl of UltraPure™ DNase/RNase-free distilled water (Life Technologies, Carlsbad, CA). Using the extracted DNA and specific primers (Table 3-1), a 445-bp fragment of THEV *hex* gene was amplified by a conventional PCR assay. The PCR reaction (50 µl final volume) contained 45 µl of Platinum® PCR SuperMix High Fidelity (Invitrogen, Grand Island, NY), 2 µl of each of forward and reverse primers at 10 µM (final concentration 400 nM), and 1 µl of DNA. PCR cycling conditions included an initial incubation step for template denaturation at 95°C for 2 min and polymerase activation, 35 cycles of amplification at 95°C for 30 s, 58°C for 30 sec, and 65°C for 45 sec, and a final elongation step at 72°C for 10 min. PCR amplification products (50 µl volume) were electrophoresed at 100 V for 45 min, on a 1% agarose gel in TBE buffer

(89 mM Tris-borate, 2 mM EDTA, pH 8.3; Sigma-Aldrich) containing ethidium bromide for DNA staining. The PCR products were confirmed under an ultraviolet transilluminator using the Kodak Gel Logic 200 Imaging System (Kodak, Rochester, NY). Next, the 445-bp DNA band was cut out of the gel and purified using the QIAquick Gel Extraction Kit (Qiagen), according to the manufacturer's instructions and eluted in 30 µl of DNase/RNase-free distilled water. The concentration of recovered DNA fragment was measured using NanoDrop spectrophotometer (ND-1000; Thermo Fisher Scientific, Wilmington, DE) and found to be 18.64 ng/µl. The purified *hex* fragment was then cloned into the vector pCR®2.1-TOPO® (Invitrogen, Carlsbad, CA) by TA cloning, following the manufacturer's recommended protocol. The plasmids were then used to transform One Shot® TOP10 (Invitrogen) chemically competent *E. coli* cells, which were grown overnight at 37°C on an ampicillin-positive Luria-Bertani (amp^+ LB) agar plate containing X-gal (5-bromo-4-chloro-3-indolyl-b-D-galactopyranoside; Qiagen). White colonies with the potentially correct insert (445-bp fragment) were selected and grown overnight at 37°C in amp^+ LB broth while shaken at 200 rpm. The recombinant plasmid was then extracted from the transformed *E. coli* cells using the QIAprep Spin Miniprep Kit (Qiagen). The recombinant plasmid with the 445-bp fragment (named pCR2.1-hex) was confirmed by EcoRI restriction digestion analysis (Fig. 3-2), followed by agarose gel electrophoresis. The concentration (nanogram/µl) of the purified stock of plasmid DNA was measured by NanoDrop 1000 spectrophotometer (Thermo Fisher Scientific) and plasmid copy number was calculated using the formula: copy number = (plasmid concentration [ng/µl] × 6.022 × 10^{23}) / (nucleotide length × 1 × 10^9 × 650), which is available in an electronic format at http://cels.uri.edu/gsc/cndna.html. Plasmid stock solution was diluted with DNase/RNase-free distilled water and 10-fold serial dilutions containing 10^6 to 10 plasmid copies/µl were made and aliquots were stored at -80°C for future use in generating qPCR standard curves.

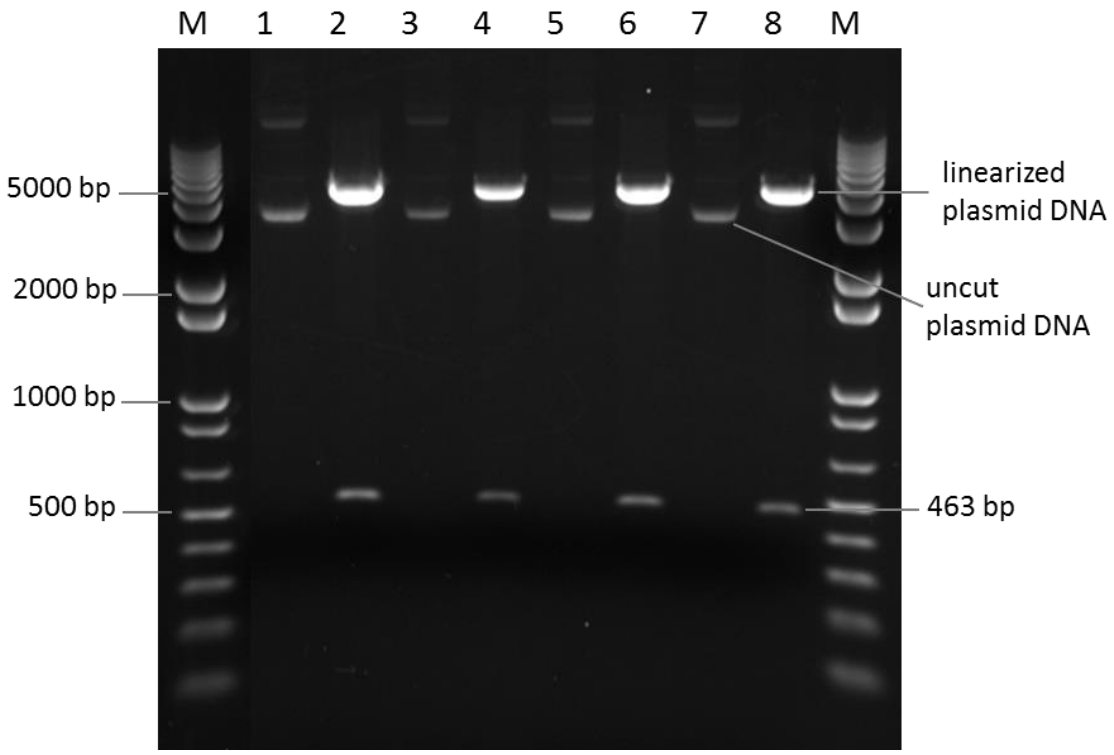

Fig. 3-2. Restriction digestion analysis of the recombinant plasmid (pCR2.1-hex) using EcoRI enzyme. Digestion reactions were made on 4 batches of purified plasmid DNA from transformed *E. coli*. Lanes 1, 3, 5, & 7 show the bands of the uncut, supercoiled plasmid DNA, while lanes 2, 4, 6, & 8 show the digestion products of these same plasmids: one large band representing the cut, linearized plasmid DNA and one small band (463 bp) containing the 445-bp *hex* fragment insert (+ 18 plasmid nucleotides). Lane M: 1 kb DNA ladder for molecular size.

3.3.3. Real-time PCR (qPCR) assay for THEV: performance, precision, and reproducibility

All qPCR runs were carried out in an iCycler® thermal cycler instrument (Bio-Rad, Hercules, CA). The qPCR mixtures (25 µl final volume) were made in Eppendorf™ real-time PCR Tube Strips (white color, 8 tubes/strip) with Masterclear™ Cap Strips (Fisher Scientific) and contained 12.5 µl of 2× SYBR Green I mastermix (SensiMix™ SYBR® & Fluorescein Kit; Bioline, Taunton, MA), 0.5 µl of each of forward and reverse primers at 10 µM (final concentration is 200 nM), 10.5 µl DNase/RNase-free distilled water, and 1 µl of DNA template. No changes were made in the $MgCl_2$ concentration

which was 3 mM in 1× reaction mix. The PCR cycling conditions included an initial DNA denaturation and polymerase activation step at 95°C for 10 min, 40 cycles of amplification at 95°C for 15 sec, 56°C for 15 sec (primer annealing temperature; confirmed by a thermal gradient experiments), and 72°C for 15 sec. Immediately after the end of the amplification protocol, melt curve analysis was performed to verify the specificity of the amplified products. The melt curve conditions were 1 cycle of denaturation at 95°C for 1 min, 1 cycle of annealing at 55°C for 1 min, and 80 cycles of temperature increment at a rate of 0.5°C/10 sec starting at 55°C (data collection). Post-run qPCR amplification and melt-curve data were analyzed using the Bio-Rad iCycler IQ software (v 3.1.7050).

Performance parameters as well as reproducibility of the qPCR assay were determined using duplicates, triplicates, or five replicates from each tenfold dilution of the plasmid DNA standard. This wide range of replicates was used to ensure that similar qPCR quality can be obtained under different conditions of assay stringency. This experiment was also used to determine the sensitivity of the assay where the lowest concentration of standard DNA used was always 10 copies/µl. In addition, the assay precision, i.e., intra-assay variation, was determined by running a single round of qPCR using five replicates from each plasmid DNA dilution and calculating the coefficient of variation (CV[%]) for each dilution. The assay reproducibility (i.e., inter-assay variation) was determined by running the qPCR assay for six rounds on different days with using two different batches of SYBR Green reagents and calculating the CV(%) for each dilution.

3.3.4. Specificity of the qPCR assay

Samples collected and tested: Two duodena and 12 spleens were collected from uninoculated turkey poults, 5.5 weeks of age, raised in isolation at Virginia Polytechnic Institute and State University under an approved IACUC protocol. All of the samples were used as negative controls. For positive controls, one sample from homogenized splenic (i.e., live bird-propagated) HE vaccine prepared as described previously (Domermuth et al., 1977) was used. Preparation of negative control samples before DNA extraction: In 2-ml microcentrifuge tubes, 250 mg from each spleen were weighed and

250 µl of PBS were added. Samples were then homogenized using stainless steel beads and vortexing. The duodenal samples were difficult to homogenize using the method for spleens and thus, used in the DNA purification protocol without complete homogenization. Total DNA was extracted from all samples using QIAamp DNA Mini Kit (Qiagen), following the tissue protocol according to the manufacturer's instructions. The DNA was eluted in 200 µl of DNase/RNase-free distilled water. DNA extracts were diluted at 1:10 with DNase/RNase-free distilled water and 1 µl per reaction was used in the qPCR assay for determination of virus genome copy number.

3.3.5. Optimization of qPCR for quantification of THEV genomes in splenic (live-bird) HE vaccines

HE splenic vaccines used in this section were propagated following a method described previously (Domermuth et al., 1977), with some adjustments. Briefly, susceptible turkey poults at 5.5 to 6 weeks of age were intravenously inoculated with a cell culture-based HE inoculum, euthanized 3 days post-inoculation, and spleens were harvested and stored at -20°C. Spleens were then thawed, ground, and blended at 1:1 (v/v) with sterile PBS to form a homogenous suspension.

Splenic HE vaccines are typically heavily loaded with THEV particles due to the very high level of virus replication in inoculated susceptible turkeys. Also, in total DNA preparations from tissues (e.g., spleens) the ratio of host chromosomal to pathogen (i.e., virus) DNA is usually high. Such DNA extractions, when used in their undiluted form, often lead to the appearance of nonspecific fluorescence signals in SYBR Green-based real-time PCR assays. In order to empirically determine the optimal amount of total DNA (genomic + viral) which can be used in qPCR without showing nonspecific signals, we ran the following qPCR experiment. DNA was extracted from four batches of HE splenic vaccine (30 mg) using QIAamp DNA Mini Kit (Qiagen), following the tissues protocol according to the manufacturer's instructions. The DNA was eluted in 200 µl of DNase/RNase-free distilled water. qPCR assay was run using the following DNA amounts: 1) 4 µl of neat DNA, 2) 1 µl of neat DNA, or 3) 1 µl of DNA diluted at 1:10, 1:100, or 1:1000 with water. The quality of amplification from each DNA amount used

per reaction (i.e., concentration) was evaluated based on the features of the corresponding amplification curve and the melt / dissociation curve analysis.

The qPCR assay was applied on numerous splenic vaccine batches for the quantification of THEV genomic titers. The majority of tested vaccine batches were obtained from two separate locations and one batch was received from a different location. DNA was purified using QIAamp DNA Mini Kit (Qiagen), following the tissue protocol as illustrated by the manufacturer. DNA was extracted from either 30 mg or 25-30 µl of splenic vaccine. For the majority of samples, DNA was initially eluted in 600 µl of DNase/RNase-free distilled water, and diluted further at 1:10 before used in qPCR, while for a few samples these values were 200 µl elution volume and 3:10 dilution for qPCR. These DNA elution volumes and dilution factors were based on results from the qPCR validation and optimization experiments. The following formula was used to calculate the qPCR titer in any given sample:

$$Titer\ (vGCN/dose) = vGCN/1\mu l \times DNA\ elution\ volume\ (\mu l) \times DNA\ DF \times CF$$

Where:

vGCN	= Viral genome copy number determined by qPCR.
DNA DF	= Dilution factor: A factor to compensate for the dilution of DNA before used in qPCR
CF	= Conversion factor: A factor used to calculate the vGCN per dose based on the sample weight or volume used for DNA extraction; DNA was extracted from slightly varying amounts of vaccine.

3.3.6. Agar gel immunodiffusion (AGID) test for splenic HE vaccines

AGID test was performed on splenic HE vaccines based on methods described previously (Domermuth et al., 1972), with modifications. The agar gel was composed of 0.8% agarose, 8% sodium chloride, and 0.2% sodium azide in dH_2O. Into rectangular immunodiffusion plates (Miles Laboratories, Pittsburgh, PA), ~13 ml of the heated / microwaved agar were poured, allowed to solidify at RT, and then stored in a humidified container in the refrigerator. The splenic vaccines were prepared for the test by making

twofold dilutions in PBS. The THEV-positive serum used in the test was hyperimmune serum collected from poults inoculated with THEV-A. A high anti-THEV titer was confirmed by using PROFLOK® HEV ELISA Antibody Test Kit (Zoetis, Florham Park, NJ). Into the designated test wells 25 µl of the respective reagent were added. The AGID plates were incubated in dark at RT, in a humidified chamber. The results were read after ~48 hours.

3.3.7. Validation of qPCR for use with HE cell culture (CC) vaccines and determination of assay reproducibility

One vial of a commercial HE-CC vaccine product (lyophilized) was reconstituted in 5 ml of serum-reduced Leibovitz-McCoy (SRLM) media (see Table 3-2 for composition). A tenfold dilution series (10^{-1} to 10^{-6}) and a 1 label dose solution (1:40 dilution) were prepared. Total DNA was extracted from triplicate samples (200 µl) at each dilution using the QIAamp DNA Mini Kit (Qiagen) following the Blood or Body Fluids spin protocol and eluted in 50 µl of DNase/RNase-free distilled water. qPCR was performed using 1 µl of DNA per reaction and the vGCN for each dilution was calculated using the formula described above. The correlations between the vaccine dilution factor and the corresponding qPCR Cq values were determined.

Also, reproducibility was examined by repeating the assay three times on three different days using the same set of serially-diluted DNA samples. As a measure of reproducibility, CV(%) for the mean Cq values from the three qPCR runs was calculated for each dilution.

3.3.8. Growth curve of THEV in RP19 cells

MDTC-RP19 (RP19), a B-lymphoblastoid cell line established from a Marek's disease virus-induced tumor (Nazerian et al., 1982), was purchased from the American Type Culture Collection (Manassas, VA) and used in the experiments below. The cells were grown as suspension cultures in complete Liebovitz-McCoy (CLM) media (see Table 3-2 for composition) at 41°C in a humidified atmosphere with 5% CO_2. When infected with THEV, the cells were maintained in serum-reduced Liebovitz-McCoy (SRLM) media (see Table 3-2 for composition). The growth of THEV in RP19 cell

cultures was studied using different inoculum-to-cell ratios and under various inoculation conditions. For inoculation purposes, a THEV inoculum was made by reconstituting one vial of a lyophilized HE CC vaccine in 5 ml of SRLM growth media. The inoculum was stored in small aliquots at -20°C and used as needed.

Table 3-2
Composition of complete and serum-reduced Leibovitz-McCoy growth media for RP19 cells; CLM and SRLM, respectively.

Media component (Manufacturer)	CLM (%)	SRLM (%)
Leibovitz's L-15 Medium* (ATCC)	32	45.15
McCoy's 5A Medium† (ATCC)	32	45.15
Chicken serum (Sigma-Aldrich, St. Louis, MO)	20	5
Fetal bovine serum, heat inactivated (FBS; Sigma-Aldrich)	10	2.5
Tryptose phosphate broth (Millipore, Solon, OH)	5	1.2
Penicillin-Streptomycin Solution‡ (ATCC)	1	1

*Medium contains 2 mM L-glutamine and no sodium bicarbonate
†Medium contains 1.5 mM L-glutamine and 2200 mg/l sodium bicarbonate
‡The solution provides a final concentration of 100 I.U./ml penicillin and 100 μg/ml streptomycin.

Expt. 1A: Aliquots of 2.5×10^6 of cultured RP19 cells were pelleted by centrifugation at 1200 rpm for 10 minutes and resuspended in 2 ml of SRLM media. In two 15-ml conical tubes, the cells were inoculated with 250 μl of either undiluted or 1:10-diluted HE inoculum, followed by incubation for 1 h at 41°C. Since virus titer in the HE inoculum used was not known, the infectious doses were expressed as "volume of undiluted inoculum (μl)/cell". Accordingly, the two infectious doses used in this experiment were 0.0001 and 0.00001 μl/cell. Post-incubation, cells were pelleted, washed 3 times with sterile PBS to remove unbound virus, and resuspended in 12.5 ml of SRLM media. To the designated wells of 48-well tissue culture-treated plates, 0.5 ml of inoculated cells (i.e., 10^5 cells/well) was added and the plates were incubated at 41°C in a humidified incubator with 5%CO_2 in the air. Triplicate cell samples were then collected from each inoculation group at 12-h intervals for 72 h and stored at -20°C until DNA

extraction. No CPE was observed in inoculated cells from both treatments when examined under light microscope. Cells were lysed using three freeze-thaw cycles and DNA was extracted from cell lysates (200 µl) using QIAamp DNA Blood Mini Kit (Qiagen), following the Blood or Body Fluids Spin Protocol. DNA was eluted in 50 µl of DNase/RNase-free distilled water. DNA (1 µl/reaction) was used in THEV qPCR assay to quantify the virus genomes in different treatment samples, following the protocol described above.

Expt. 1B: Aliquots of cultured RP19 cells (2.5×10^6) were pelleted and resuspended in 2 ml of SRLM media. To three wells of a 12-well, flat bottom, tissue culture-treated plate, cells were added and then inoculated with 1.25 ml or 250 µl of undiluted HE inoculum, or 250 µl of 1:10 diluted inoculum. The amounts of inoculum corresponded to infectious doses of 0.0005, 0.0001, or 0.00001 µl/cell, respectively. Cells were then incubated for 1 h at 41°C in a humidified CO_2 incubator. The rest of the experimental procedure was carried out essentially as described in Expt. 1 above; with one exception of extending the sampling period till 96 h instead of 72 h. Cells from the three treatment groups did not show CPE when observed under light microscope.

Expt. 2: The purpose of this experiment was to establish a relationship between the stage of THEV replication and the development of evident CPE in infected RP19 cells. Two experiments were run in parallel; one for sampling of infected cells and the other for imaging. *Expt. 2A*: A cell suspension of RP19 cells (1.79×10^7) in 10 ml of SRLM media was made and incubated at 41°C for 1.5 h. Cells were then inoculated with THEV in SRLM media (25.8 ml) at 50 infectious viral particles/cell (titer was determined by qPCR infectivity assay; see Chapter 4 for details). The final density of cells after inoculation was 5×10^5 cells/ml. To the wells of 96-well culture plates, 300 µl of inoculated cells (i.e., 1.5×10^5) were added. Cell samples were harvested every 12 h from 1 to 168 hpi. Triplicate samples were used for DNA extraction and qPCR as described above. *Expt. 2B*: For cell imaging, 1.2 ml of inoculated cell solution prepared in *Expt. 2A* was added to each of four wells of a 12-well culture plates. Non-inoculated cells were used as negative control. Several images were taken from both cell groups every 12-24 hpi using an inverted light microscope (Olympus BX60; Olympus America Inc., Center

Valley, PA) at 400× magnification and a digital camera. Images were processed using QCapture ProTM 6.0 software (QImaging, Surrey, BC, Canada).

3.3.9. Statistical analysis

Data was analyzed by one-way analysis of variance (ANOVA), and when statistical significance exists, multiple comparisons between treatment means were performed by Tukey-Kramer HSD (Honestly Significant Difference) test using JMP® Pro (v. 10.0.0, SAS Institute, Inc., Cary, NC). The significance level was set at $P \leq 0.05$. Data from the qPCR assay was transformed to the $\log_{10}$ format to achieve a normal distribution, before statistically analyzed with ANOVA.

3.4. Results

3.4.1. Performance of THEV qPCR assay: precision (intra-assay variation), variability (reproducibility; inter-assay variation), sensitivity, and limit of detection

Three independent qPCR runs were performed using tenfold dilution series (from 10^6 to 10 copies) of the standard pCR2.1-hex, to evaluate the performance parameters of the developed assay. Amplification plots, melting / dissociation curves, and standard curves generated from the three runs are shown in Fig. 3-3. The standard curve parameters which measure the qPCR performance are summarized in Table 3-2. Three standard curves were generated using 2, 3, or 5 replicates of the standard plasmid DNA dilutions. Very tight correlations were obtained ($R \geq 0.998$) between the log copy numbers of the input standard DNA (i.e., pCR2.1-hex) and the corresponding Cq values. Likewise, the PCR efficiency (> 98.4%) and the standard curve slope values (average -3.325) from the three runs indicate the high performance of the assay under the three replicate conditions. Moreover, NTC (water) reactions did not show any trace of amplification; i.e., no fluorescence signals were detected, which is also an indication of the absence of primer dimer formation. The assay limit of detection was consistently found to be as low as 10 copies per 1 µl which was detected at an average Cq of 31.53±0.34; calculated from the three runs. Overall, results show that using from 2 to 5 replicates of standard DNA dilutions can result in high-quality standard curves with

equally-well performance parameters. These standard curves can be reliably used for accurate quantification of THEV genome copies. The consistent results from the three runs prove that the assay is highly reproducible. Also, this result has a useful practical value when a large number of samples need to be accommodated in a single qPCR run. For example, using duplicates instead of triplicates, a researcher can save 7 wells/tubes to be used for experimental samples, rather than for standard curve templates. As shown in Table 3-4, the intra-assay and inter-assay variation (mean CV%) were within the acceptable range seen in the literature. These values ranged from 0.53 to 1.54 and from 3.2 to 8.1, respectively, confirming the high precision and reproducibility of the developed qPCR assay.

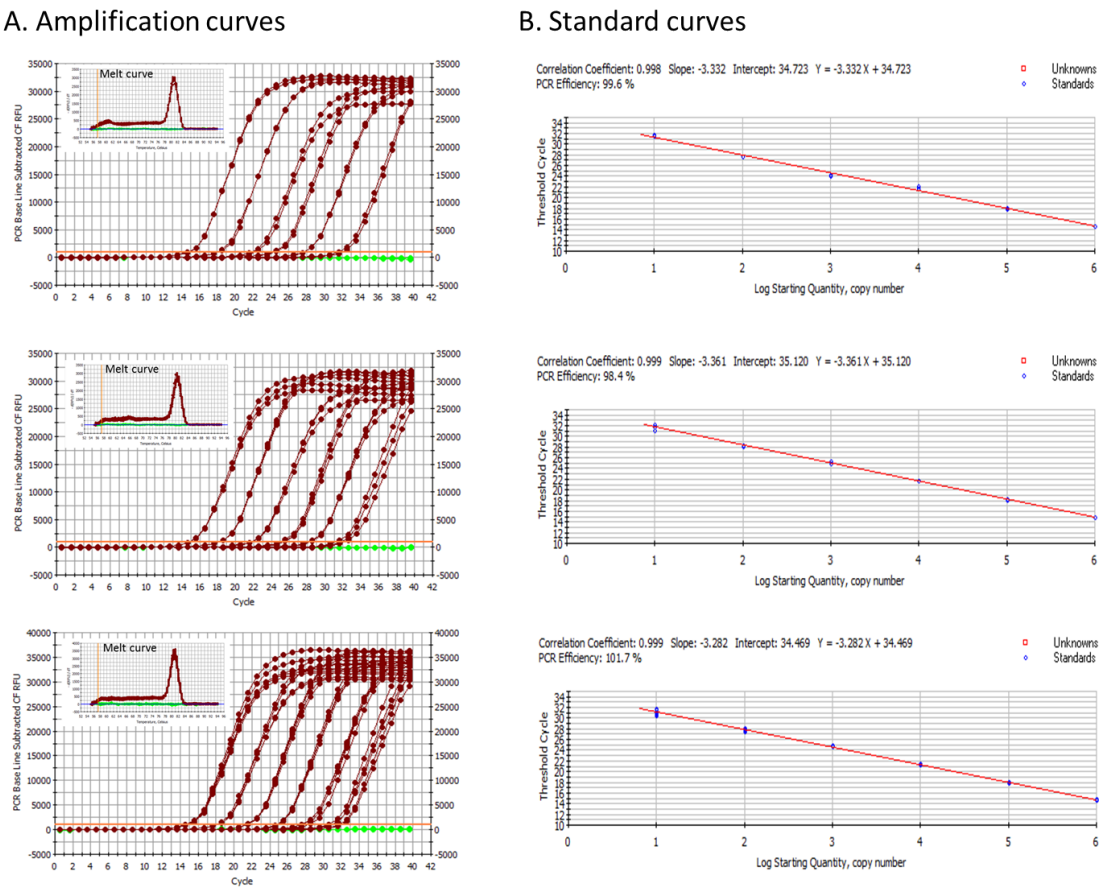

Fig. 3-3. SYBR Green-based qPCR assay for THEV. Representative amplification plots (A), linear standard curves/regression lines showing the linear dynamic range of standard DNA (B), and melt curve charts (embedded in panel A graphs) obtained with 10-fold serial dilutions (ranging from 10 to 10^6 copies/µl) of plasmid DNA standard (pCR2.1-hex). The assay was performed on three sets of replicates: 2 (top panels), 3 (middle panels), or 5 (bottom panels) replicates from each standard dilution. Only one peak of ~81ºC was generated indicating the specific target amplification (115-bp hexon fragment) and the absence of primer dimer formation. The melt curves are generated by plotting the temperature (ºC) on x-axis against the –dRFU/dT (the change in fluorescence/change in temperature) on y-axis. RFU: relative fluorescence unit.

Table 3-3
qPCR assay performance parameters using 2, 3, or 5 replicates of the plasmid DNA standards for generating standard curves.

Standard DNA replicates*	PCR efficiency	R	Slope	Y-intercept
2	99.6%	0.998	-3.332	34.723
3	98.4%	0.999	-3.361	35.120
5	101.7%	0.999	-3.282	34.469

*The number of replicates used from each dilution of plasmid DNA standard.
R: correlation coefficient.

Table 3-4
Intra-assay (precision) and inter-assay (reproducibility) variation of the qPCR as measured with standard plasmid DNA templates using Cq values.

Plasmid copies	Intra-assay (single run; 5 replicates/dilution)			Inter-assay (5 runs/different days)*		
	Mean	SD	CV(%)	Mean	SD	CV(%)
10^1	33.03	0.51	1.54	32.4	1.0	3.2
10^2	29.85	0.82	0.82	28.6	1.0	3.6
10^3	26.63	0.06	0.21	25.3	1.3	5.2
10^4	23.33	0.07	0.30	22.2	1.2	5.6
10^5	20.06	0.05	0.27	18.7	1.2	6.3
10^6	16.84	0.09	0.53	15.2	1.2	8.1

*Plasmid DNA was used in triplicates
SD: Standard deviation

3.4.2. Specificity of THEV qPCR assay

The specificity of the SYBR Green-based THEV qPCR assay for the target gene was assessed using DNA mixtures purified from a range of THEV-negative and positive tissue samples, which were collected from field turkey poults, in addition to the NTC reactions. The qPCR amplification plot and the corresponding melt peak chart generated from running the assay on these DNA templates are displayed in Fig. 3-4. As expected, a very strong fluorescence signal (i.e., amplification curve) was observed from the THEV-positive sample (i.e., HE splenic vaccine); while the signals obtained from the THEV-

negative splenic and duodenal tissue samples and the NTC reactions were below the baseline level. The melt curve chart shows one specific peak from HE splenic vaccine, but no peaks at all were observed from the rest of the THEV-negative DNA templates. Together, results from the amplification plot and the melt curve analysis indicate the absence of either nonspecific amplification or primer dimer formation, confirming the high specificity of the developed qPCR assay for the target virus DNA.

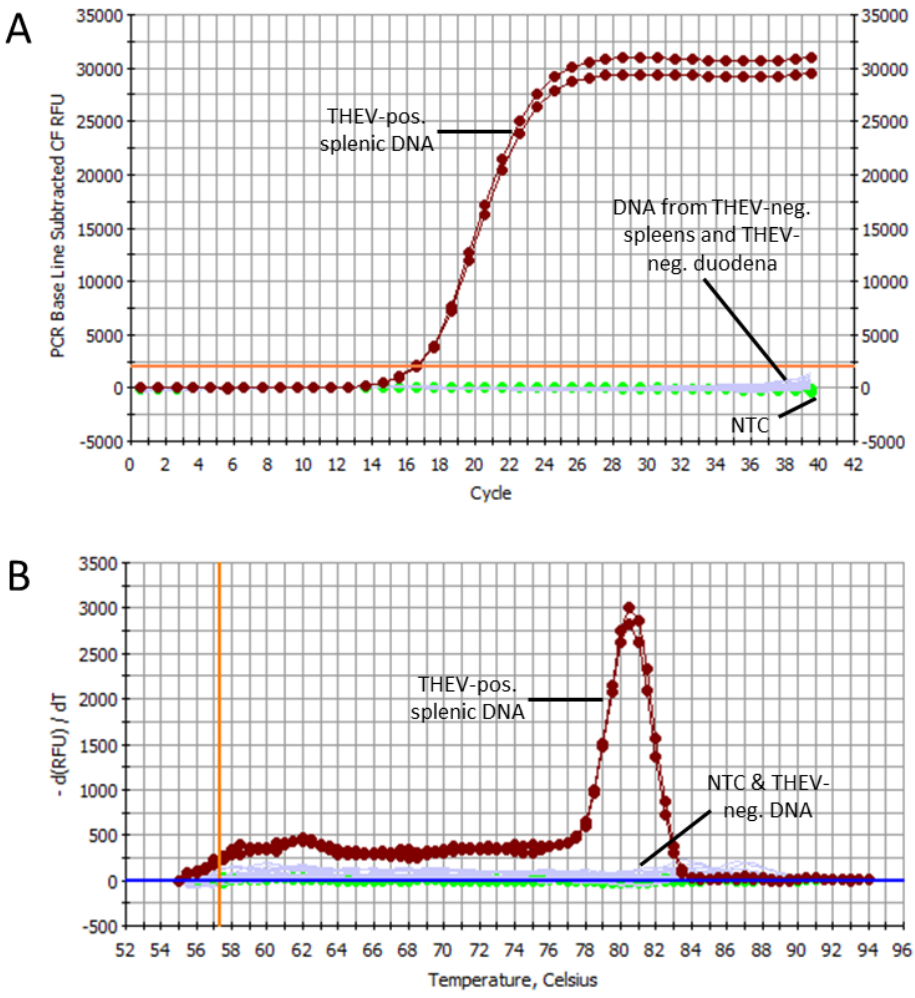

Fig. 3-4. Specificity of the SYBR Green-based qPCR assay. Total DNA was isolated from HE splenic vaccine (n=1; pos. control), and spleens (n=12; neg. control) and duodena (n=2; neg. control) from susceptible, commercial turkey poults and used to evaluate the specificity. The amplification plot (A) and the corresponding melt curve (B) are shown. RFU: relative fluorescence unit. NTC: no-template control (water). For other explanations see Fig. 3-3.

3.4.3. Optimization of THEV qPCR assay for HE splenic vaccines

qPCR was run on different amounts of total DNA extracted from HE splenic vaccines. The amplification plots and melt curve charts from these runs are displayed in Fig. 3-5. The optimal template concentration for use in SYBR Green-based qPCR to specifically and reliably quantify target THEV genomes was determined by two criteria: 1) generation of a sigmoidal-shape amplification curve that shows the exponential and non-exponential plateau phases; and 2) melting/dissociation curve that displays one single peak close to the expected melt temperature of the target DNA fragment. As shown in Fig. 3-5 (panels A-D), the amplification curves from reactions in which 4 or 1 µl of neat DNA extracts were used are not normal and the related melt curves showed nonspecific signals (two peaks; ~80 and 85°C); as compared with those obtained from the standard DNA (melt temperature = 81°C). These are signs of highly concentrated DNA which occur because of two reasons: 1) PCR reagents are depleted quickly and before amplification cycles are fully complete, and 2) SYBR Green I dye binds nonspecifically to non-target double-stranded DNA which outweighs target DNA in the reaction mixture. When DNA templates were diluted at 10^{-1}, 10^{-2}, or 10^{-3}, normal amplification plots and a desired melt peak of 81°C were obtained. The two dilutions of 10^{-2} and 10^{-3} fell within the range of standard curve as their Cq values were close to or lower than that of the maximum limit of the 10^6 copies, respectively. Although the 10^{-1} dilution of DNA was detected at a relatively earlier / lower Cq value than that of the maximum standard curve limit (i.e., outside the designed quantification range), the assay provided a very accurate prediction of vGCN at this dilution. This result was also supported by the statistically significant correlation ($R^2 = 0.998$; $P < 0.0001$) found between the measured $\log_{10}$ vGCN in the three template dilutions and their corresponding Cq values (Fig. 3-6).

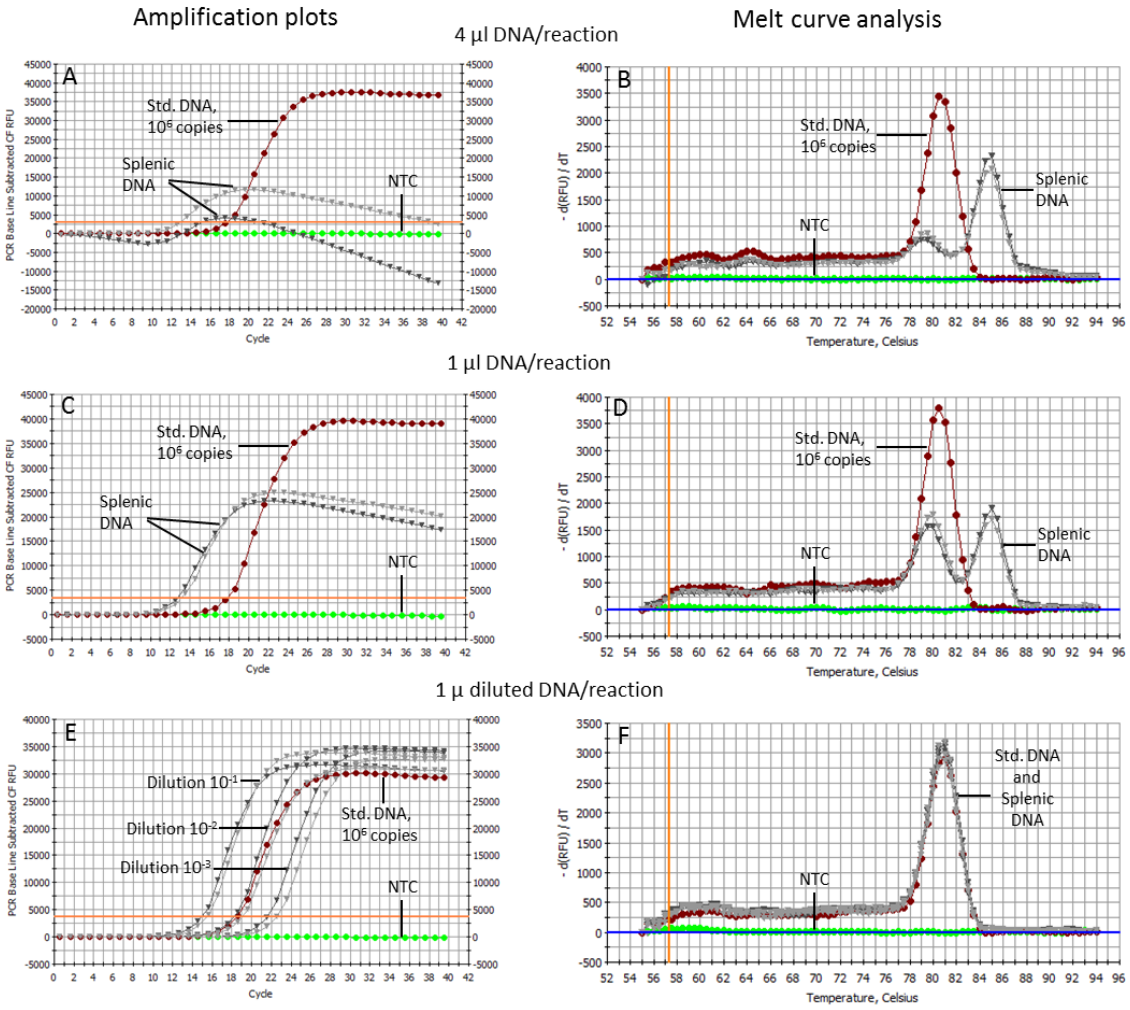

Fig. 3-5. Validation and optimization of qPCR for reliable quantification of THEV genomes in infected spleens. Amplification plots (A, C, E) and the corresponding melt curves (B, D, F) were generated from running qPCR on different dilutions of DNA extracted from splenic vaccine samples. RFU: relative fluorescence unit. NTC: no-template control (water). For more explanations of the melt curve and amplification curve plots see Fig. 3-3 and 3-4.

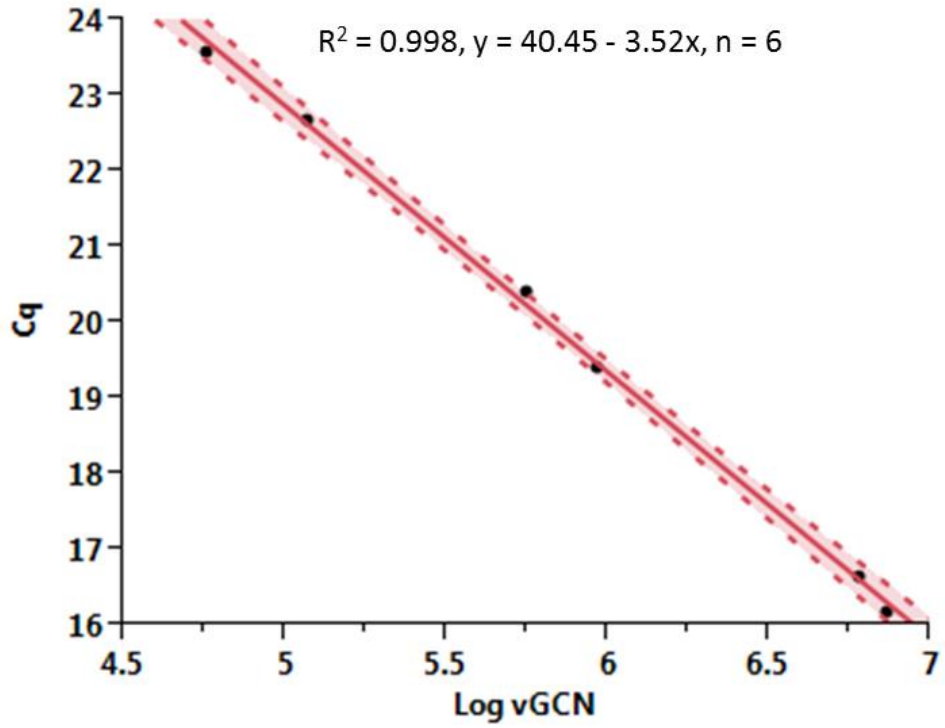

Fig. 3-6. Correlation between $\log_{10}$ viral genome copy numbers (vGCN) from three tenfold-diluted DNA templates extracted from splenic vaccines and their corresponding quantification cycle (Cq) values. This step was performed to optimize the amount of input splenic DNA in qPCR.

The optimized qPCR assay was applied for the determination of THEV genomic titers of numerous batches of HE splenic vaccine. As presented in Table 3-5, titers of vaccine batches from source B ranged from 8.1E+06 to 1.39E+08 genome copies/dose, while those from source VA ranged from 6.32E+07 to 4.1E+08 genome copies/dose. When analyzed individually within each source (i.e., B or VA) and as a whole, THEV genomic titers per dose were found to be significantly different ($P < 0.0001$ for all analyses). Using the current data set (Table 3-5), no correlation was found between the genomic titers and their corresponding AGID titers. This may be, in large part, due to similar genomic titers falling under different AGID titer groups. Similar observation has been reported before (Beach, 2006).

Table 3-5
qPCR-based titration of HE splenic (live-bird) vaccines.

Batch*	Genomic titer (vGCN/dose)†	AGID titer
B01	1.27E+08 ± 2.19E+06	1:16
B02	5.84E+07 ± 7.12E+06	1:16
B03	1.15E+08 ± 2.19E+06	1:32
B04	1.39E+08 ± 1.35E+07	1:32
B05	8.66E+06 ± 3.90E+05	ND‡
B06	8.10E+06 ± 1.74E+06	ND
B07	3.78E+07 ± 2.26E+06	ND
B08	8.68E+06 ± 4.85E+05	1:8
P01	7.78E+07 ± 1.71E+07	ND
VA01L	6.32E+07 ± 5.20E+06	1:64
VA01S	1.25E+06 ± 6.23E+04	ND
VA02	2.00E+08 ± 1.27E+07	1:64
VA03	1.46E+08 ± 9.39E+06	1:32
VA04	2.41E+08 ± 1.78E+07	1:32
VA05	2.13E+08 ± 6.11E+06	1:32
VA06	1.66E+08 ± 9.84E+06	1:32
VA07	1.04E+08 ± 7.47E+06	1:32
VA08	1.21E+08 ± 1.15E+07	1:32
VA09	1.38E+08 ± 5.69E+06	1:32
VA10	1.22E+08 ± 7.94E+06	1:32
VA11a	3.91E+08 ± 8.23E+07	ND
VA11b	4.10E+08 ± 3.72E+07	1:16
VA12	9.79E+07 ± 6.66E+06	1:16
VA13	9.41E+07 ± 3.12E+06	1:16
AGID	1.10E+08 ± 3.43E+07	ND

*Highlighted vaccine batches P01, VA01S, VA11a, and AGID were not included in the statistical analyses as they were included in the study for control purposes only.
†vGCN: viral genome copy number; titers are presented as means of three aliquots from each batch ± standard error.
‡ND: not determined.

3.4.4. Validation of THEV qPCR for HE CC vaccines and assay repeatability

The qPCR assay was performed on DNA extracts purified from tenfold serial dilutions of a commercial HE CC vaccine. It was an important validation step for the developed assays to examine whether the DNA extraction procedure will affect its accuracy. Therefore, instead of serially diluting the DNA from an initial DNA extract and

running the qPCR on this dilution series, the DNA was extracted directly from the actual 10-fold dilutions of an HE cell-culture vaccine batch. This approach confirms the reliability and accuracy of this assay in determining the differences in virus genome copies amongst samples of different virus content. As shown in Fig. 3-7, a statistically significant correlation (R^2 = 0.974; P < 0.001) between the log HE inoculum dilution factor and the corresponding Cq values were found. This indicates a minimal effect of DNA extraction procedure on the accuracy of developed qPCR and that the obtained results reflect the actual differences among tested samples.

Another way to determine the reproducibility of the qPCR assay was to run the assay three times in three different days using the same set of DNA extracts and calculate the CV. Values of CV ranged from 0.82% to 2.96% for the 7 inoculum dilutions used, which confirms a very low variability among the results of the three qPCR runs (Table 3-6).

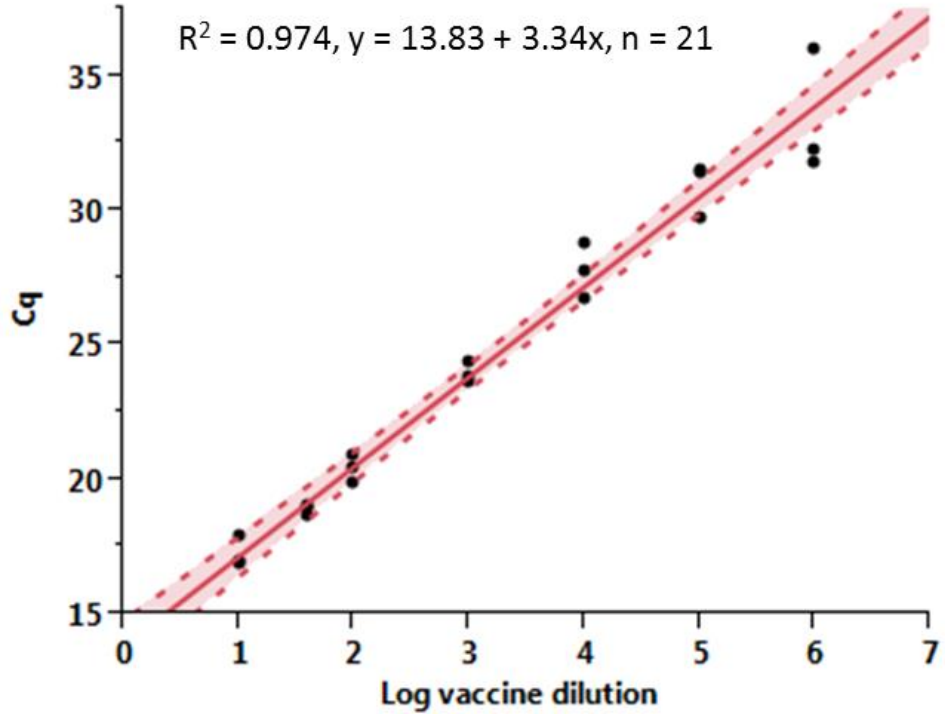

Fig. 3-7. Correlation between the dilution factor of a HE virus stock, i.e., CC vaccine inoculum, and the corresponding qPCR Cq values.

Table 3-6
Variation in qPCR results as determined by coefficient of variation (CV%) from three repeated runs on three different days.

Log dilution	Cq values from qPCR/run day			Mean	SD	CV%
	1	2	3			
1	12.98	12.61	12.75	12.78	0.19	1.46
1.6*	15.50	15.40	15.72	15.54	0.16	1.05
2	16.61	16.05	16.79	16.48	0.39	2.34
3	20.78	19.68	19.97	20.14	0.57	2.83
4	24.48	23.34	24.66	24.16	0.72	2.96
5	28.34	29.08	28.85	28.76	0.38	1.32
6	N/A†	32.40	32.78	32.59	0.27	0.82

*This dilution represents one vaccine label dose.
†N/A: the dilution was not tested in this run.
Cq: quantification cycle.
SD: standard deviation.
CV%: coefficient of variation.

3.4.5. Growth curve of THEV in RP19 cells

Growth curve experiments were performed to explore the growth kinetics of THEV in cultured RP19 cells. Changes in THEV genome replication were monitored over time using the qPCR assay developed in this study. Two experiments were carried out under different inoculation conditions (i.e., in 15-ml conical tubes or in 12-well culture plate) and using different infectious doses. In experiment 1, the cells were initially inoculated in a 15-ml tube at a dose of 0.00001, the increase in viral DNA was observed as early as 12 hpi. Over a period of 72 h, the fold increase in vGCN reached 158 times compared to the genomic titer at 1 hpi (Fig. 3-8). In experiment 2, the cells were initially inoculated in a tissue culture-treated plate, the change in vGCN was found to be dose-dependent, with the lowest dose showing the higher virus titer. vGCN increased over a period of 96 h by 10, 35, or 257 folds as compared to the initial values measured at 1 hpi, when doses of 0.0005, 0.0001, or 0.00001 were used, respectively (Fig. 3-9).

When compared together at the dose of 0.00001, at the time point 72 hpi, it was found that the fold increase in vGCN in cells initially inoculated in a 15-ml conical tube was much higher than that of cells inoculated in a 12-well tissue-culture treated plate

(158 *vs.* 19, respectively; Fig. 3-10). Possible explanations of these observations are mentioned in the discussion section.

In another experiment, the relationship between the appearance of CPE in THEV-inoculated RP19 cells and the level of virus replication was investigated. Fig. 3-11 displays representative micrographs of inoculated cells at different time points post-inoculation starting from 12 hpi until 168 hpi (i.e., 7 dpi). Fig. 3-12 shows the corresponding THEV DNA growth curve. An evident CPE (cell enlargement/ballooning) in inoculated cells was first observed at 48 hpi and became more pronounced at 72 hpi. From this point on, cells began to burst as indicated by the increasing number of lysed cells. At the DNA level, a gradual decline in viral DNA was observed until 24 hpi, at which point vGCN was considered as the initial or base value. vGCN started to increase at 36 hpi which indicated the initiation of viral DNA replication. At 48 hpi (when CPE was first noticed), vGCN has increased by 2.28 fold, compared with that at 24 hpi. vGCN continued to grow until reaching its peak at 120 hpi (i.e., 5 dpi), where it showed a 17-fold increase over the 24 hpi value. After this point and for the next two days, vGCN started to drop and became (at 7 dpi) about 11 times the value determined at 24 hpi. By this point (i.e., 7 dpi) most of the cells (infected & non-infected) in the culture have already been lysed. The decline in vGCN which started after 5 dpi is most likely due to the degradation of the non-packaged viral DNA by cellular nucleases after cell burst. The vGCN determined at 7 dpi is expected to be mainly from capsidated THEV virions; it may, however, include a small percentage of yet non-degraded free viral genomes. A similar pattern of growth characteristics has been reported for other viruses. Infectious bursal disease virus was found to reach its peak titer at 60 hpi in infected cell cultures and decline thereafter (Rekha et al., 2014).

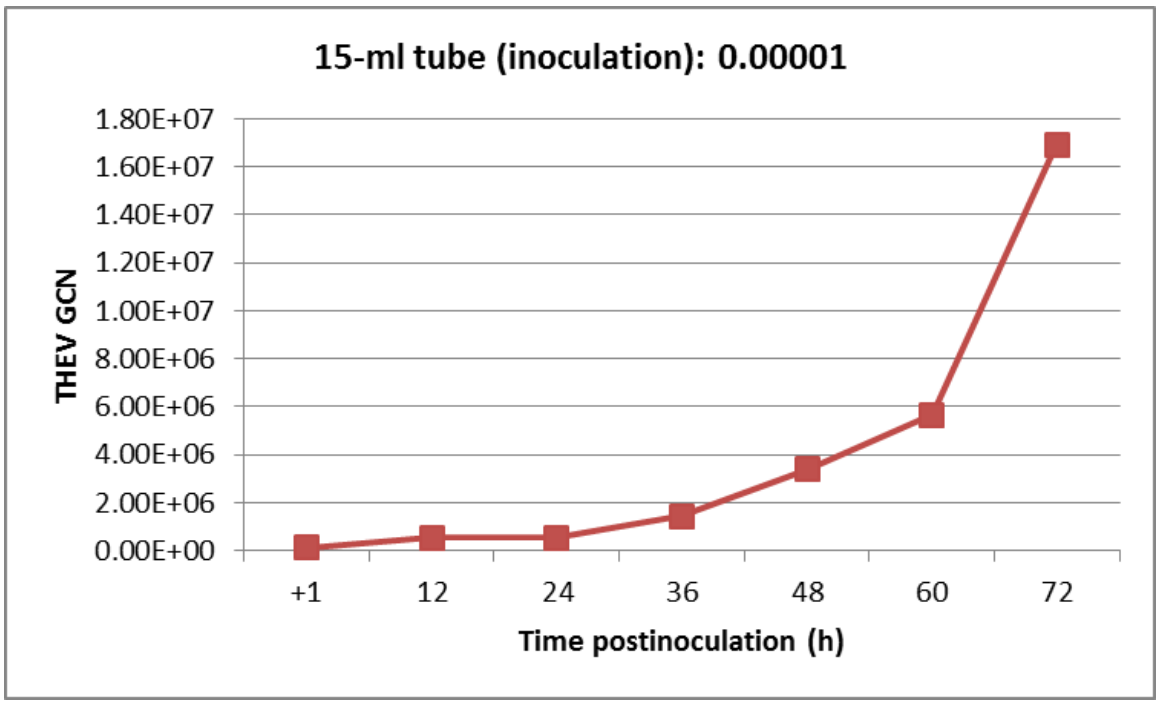

Fig. 3-8. Growth characteristics of THEV in RP19 cells inoculated at 0.00001 µl/cell in a 15-ml conical tube for 1 h. After inoculation, cells were washed, resuspended in media, and dispensed in a 48-well culture plate (10^5 cells/well). Each data point represents the mean vGCN of triplicate samples.

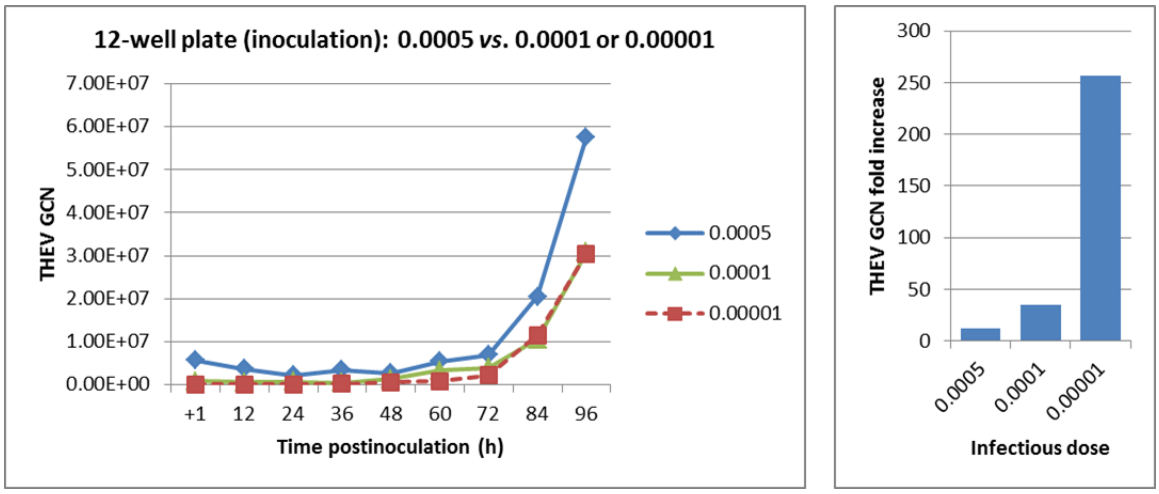

Fig. 3-9. Growth characteristics of THEV in RP19 cells inoculated at 0.0005, 0.0001, or 0.00001 µl/cell in a 12-well tissue culture-treated plate for 1 h. After inoculation, cells were washed, resuspended in media, and dispensed in a 48-well culture plate (10^5 cells/well). Each data point represents the mean vGCN of triplicate samples.

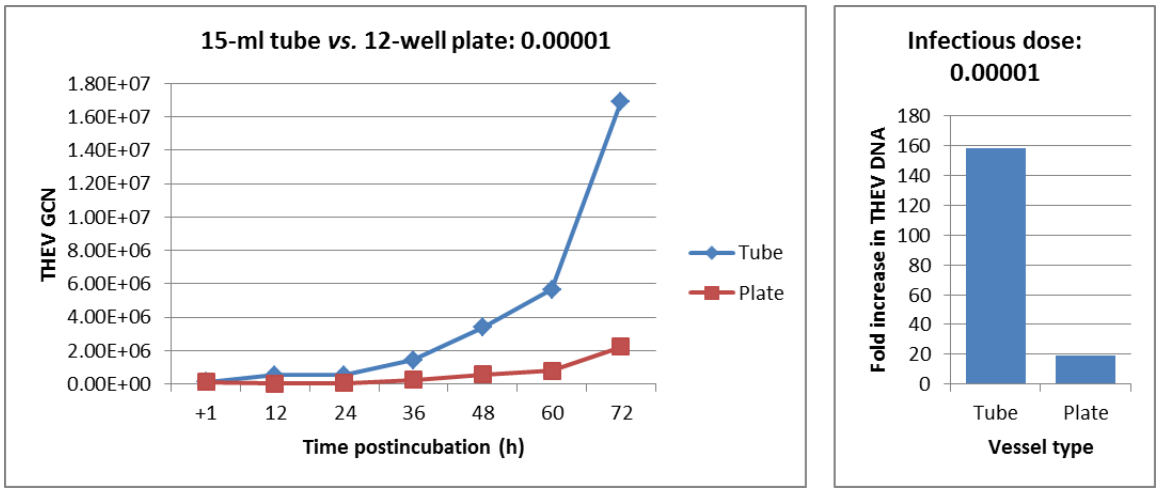

Fig. 3-10. Comparison of the growth characteristics of THEV in RP19 cells inoculated in either 15-ml conical tube or 12-well tissue culture-treated plate at 0.00001 µl/cell. Each data point represents the mean vGCN of triplicate samples.

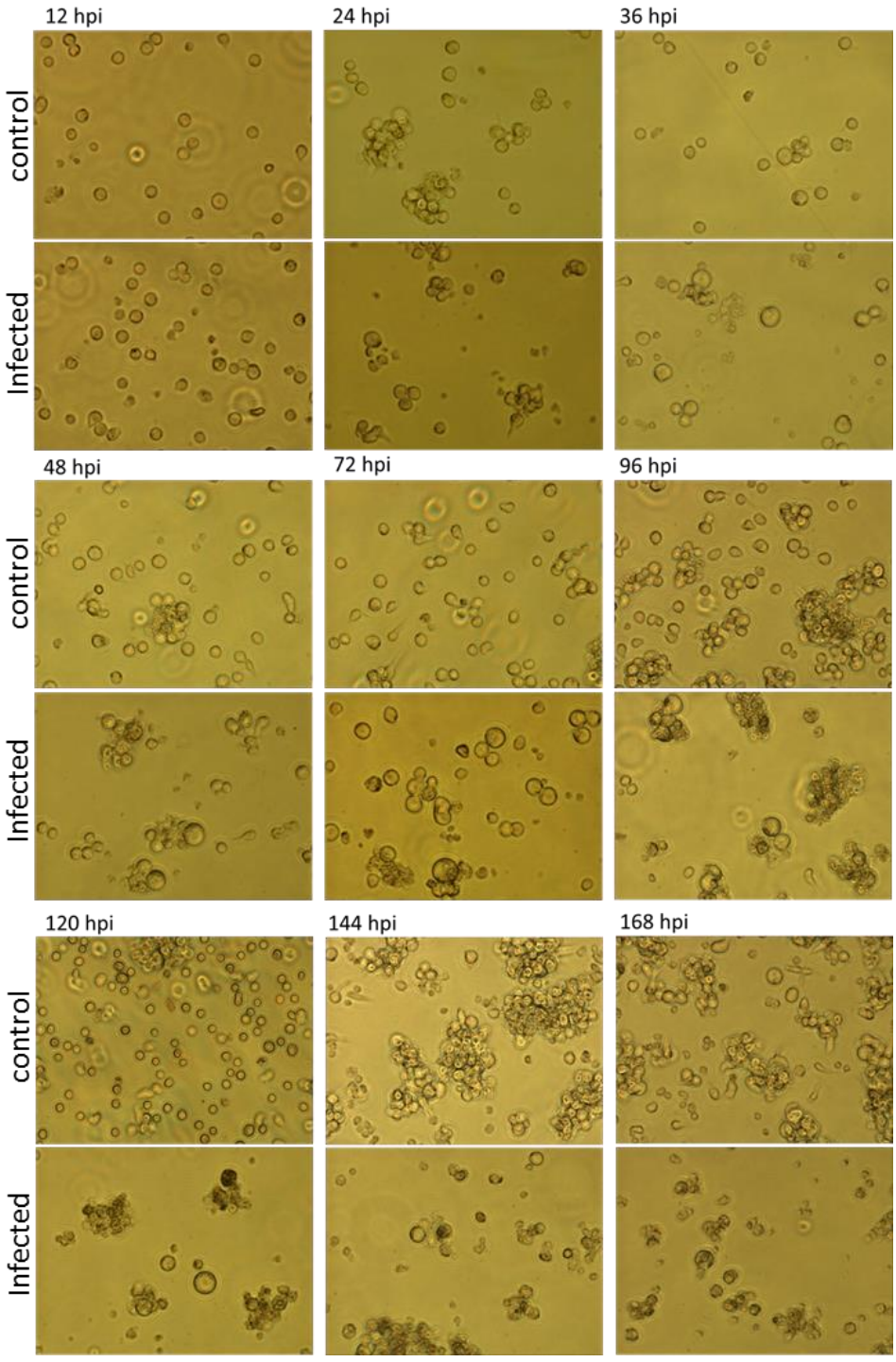

Fig. 3-11. Photomicrographs showing the cytopathic effects (cell enlargement and rupture, followed by pyknosis) of turkey hemorrhagic enteritis virus (THEV) in RP19 suspension cell cultures observed by inverted light microscopy. Images were taken at various subsequent time points post-inoculation from 12 h to 168 h at a 400× magnification. Cells were inoculated at MOI of 50 and control cells were mock-inoculated with SRLM media. hpi: hour post-inoculation.

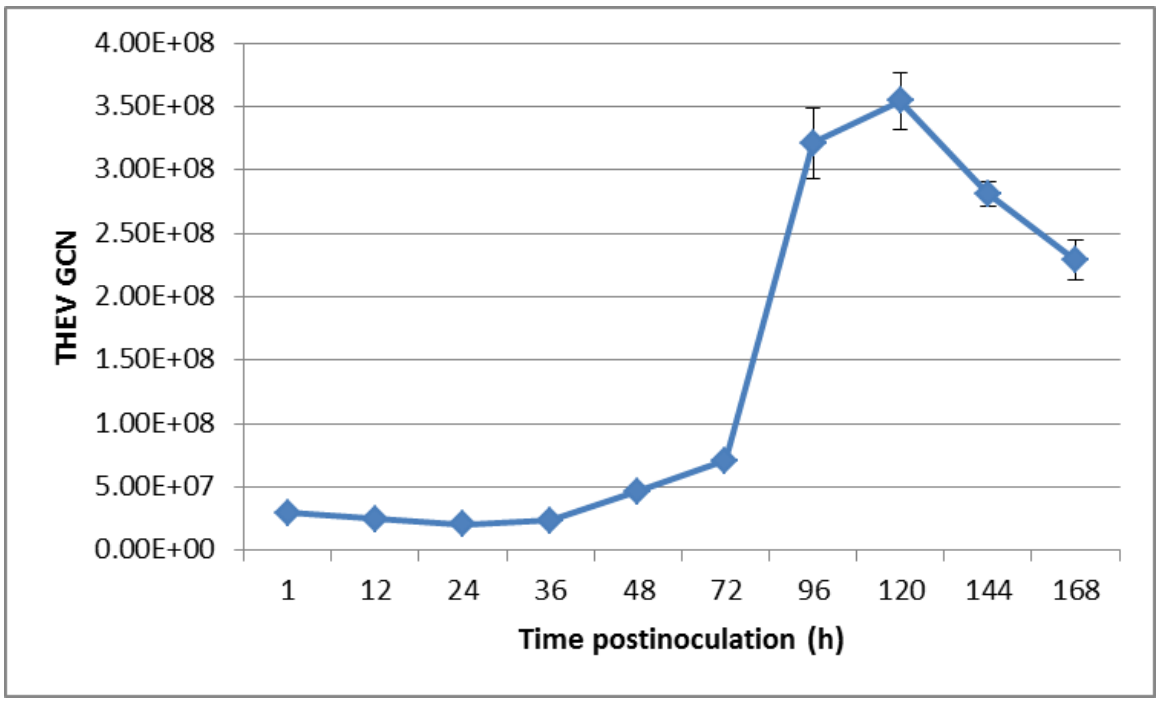

Fig. 3-12. Growth curve of THEV in RP19 cells inoculated at MOI of 50. Each time point represents the mean±SEM of vGCN from three replicate samples.

3.5. Discussion

In order to obtain a steady level of immunity against diseases in vaccinated birds, it is important to carefully examine the quality of the vaccines administered. One important quality control measure in viral vaccine development is ensuring the presence of sufficient amount of virus particles per label dose. This is especially important in live vaccines as they are administered in relatively low numbers and expected to replicate inside the animal and eventually confer a good protective immunity. There are two main types of HE live vaccines, in vivo and in vitro, which are currently produced according to standard procedures established previously (Domermuth et al., 1977; Fadly and Nazerian, 1984; Fadly et al., 1985; Nazerian, 1983; Thorsen et al., 1982). These vaccines are used widely in the US for the prevention of HE in domestic turkeys through the administration in drinking water. There is tendency by the turkey production companies to use the cell culture vaccines for breeder flocks and the splenic vaccines for growers. Current quality control methods used for live HE vaccines (i.e., AGID test for splenic vaccine and CPE-

based microscopic examination for CC vaccines) have several downsides. They are time consuming (two to several days), have very low sensitivity and accuracy, and their results depend highly on the experience of the performing individual. Moreover, AGID test results vary greatly based on the reagents used. Likewise, CPE observations in inoculated suspension cell cultures are highly affected by the culturing microenvironment and it is common to get confused with "normal" changes in non-inoculated cells. The cell culture-endpoint method is not suitable for splenic vaccine due to the toxic materials (e.g., free viral proteins and inflammatory cytokines) that are contained in the infected spleens. Such materials need to be removed before a splenic suspension can be used with cultured cells for titration, which is feasibly a complicated process.

Real-time quantitative PCR (qPCR) has been originated as a quick diagnostic tool in veterinary virology and used for the detection of numerous pathogens of interest (Mackay et al., 2002). Recently, qPCR has been extensively used in determining the genomic titers of viral live vaccines and virus suspensions. qPCR genomic titers have been found to strongly correlate with those obtained by the gold standard functional titration methods for several viruses including adenoviruses and adenoviral vectors, reoviruses, adeno-associated viruses, and lentiviral Vectors (Guo et al., 2011; Rohr et al., 2005; Sastry et al., 2002; Segura et al., 2010; Veldwijk et al., 2002). This means that, by determining the genomic titer of a vaccine batch, one can get an insight into what the functional titer of this batch could be. Previously, two qPCR assays have been developed for primarily detecting THEV genomes and were used for quantification of the virus DNA as well (Beach, 2006; Shah et al., 2013). Because the main objective of these assays was for use in diagnostics or to validate other techniques that may by less-expensive (i.e., competitive PCR), they have not been well-optimized for use with HE live vaccines. In addition, some downsides of these assays include: 1) the requirement of constructing special standard DNA molecules for generating standard curves, which entails the use of techniques and/or special plasmid vectors that may not be attainable in most laboratories; 2) the relatively high limit of detection (LOD) (i.e., 439 and 23.8 genome copies, respectively) compared with what can be generally achieved by qPCR assays; 3) the relatively long running times of thermal cycling protocols (i.e., 3-4 h) as compared with other qPCR assays. Unlike these assays, THEV qPCR established in this

study have the following advantages: 1) shorter running time (~2 h), 2) it has a lower LOD (10 copies/reaction), 3) the standard plasmid DNA was made with a PCR-amplified *hex* fragment that was inserted in a commercially available plasmid vector, a technique that can be easily reproduced by most laboratories, 4) it was optimized for use with templates purified from a variety of samples including live HE vaccines, which means that the assay can be used as a sensitive diagnostics tool as well as a quality control tool for vaccine titer assessment. Moreover, the majority of the essential and most of the desirable information recommended by the MIQE guidelines (Bustin et al., 2009) were reported for the different development stages of the assay. The assay was described in a detailed manner, so that it can be easily reproduced by other researchers and service laboratories.

Due to the exponential nature of the qPCR assay, differences among samples can be exacerbated by inaccuracy in sampling practices and DNA extraction procedures (Kulski, 1994). These variations can be further aggravated when using qPCR for absolute quantification of genome copies, where test samples are usually not normalized against a reference template. In order to ensure the absence of variations in THEV-qPCR results due to the mentioned factors, we ran the assay on templates extracted individually from seven dilutions of a commercial HE vaccine. The assay precisely distinguished the differences in virus genome content among tested dilutions, which indicates its high reliability for estimating the viral load in a wide variety of unknown samples.

Titration of HE vaccines: The precision and sensitivity of qPCR can be improved by removing the non-specific signals obtained from non-target DNA molecules (Kulski, 1994). The amount of total DNA (genomic + viral) from HE splenic vaccines that can be used in qPCR was optimized by serially diluting the sample DNA and determining the optimal dilution. This step successfully eliminated the generation of nonspecific signals, which can affect the accuracy of the calculated viral genomic titers. This optimization will also help gain a better judgment when comparing between titers from different vaccine batches. This is because the total DNA concentration usually varies from batch to batch, and thus the level of nonspecific amplification will vary causing considerable untrue variations in titers. The optimized THEV qPCR assay was applied to samples from HE splenic vaccines and from non-infected splenic and intestinal tissues. The assay was

highly specific as no signals were detected from negative controls, while titers from vaccine batches were accurately measured. The optimized qPCR procedure can be used as a quality control measure to quantitatively evaluate the quality of HE splenic vaccines as compared to the much less accurate and very subjective AGID test. The assay was also optimized and applied for use with HE cell culture vaccines. It was able to accurately determine the variations in genomic titers among various vaccine batches from different companies.

Growth curve for THEV replication: The method of growth curve has been proposed by Ellis and Delbruck (1939) to quantitatively monitor the multiplication of phages in bacterial hosts. Soon after its establishment, this method was extensively employed for investigating the kinetics of viral replication under various conditions in infected cell cultures or live animals for many DNA and RNA viruses (Bachrach et al., 1957; Dulbecco and Vogt, 1954; Furness and Youngner, 1959; Massin et al., 2010; Ranheim et al., 2006; Reddy et al., 2000; Rekha et al., 2014). From these studies, growth curve of viruses can be established based on the infectious (or functional) titers or qPCR genomic titers measured in samples collected at different points over a certain period of time. To our knowledge, the tremendous literature of HE contains only one study concerning the kinetics of THEV multiplication in vitro, which was conducted by van den Hurk (1990). The author adapted an indirect immunofluorescent staining protocol to determine the percentage of positively infected turkey primary leukocyte cultures over a 96-h course. This technique was restricted to measure the number of infected cells without any reflection of the changes in the virus replication within these positively infected cells. In the present work we reported, for the first time, the implementation of qPCR assay for studying the kinetics of THEV replication in infected cultured cells, which adds a significant value to the developed assay. Furthermore, THEV qPCR was used in studying the effect of some factors on the replication of THEV in cell culture, including the amount of inoculum used (i.e., multiplicity of infection or virus-cell ratio), and the vessel used during the inoculation step. We have observed that THEV replication was more efficient at lower inoculation doses than at higher doses. This might be due to a competition of the internalized virus particles, when using higher virus doses, on the microtubules and the dynein molecules used for virus transportation. Adenovirus

particles via their hexon units binds with dynein motor proteins which carry them to the nuclear envelope, where the particles accumulate (Medina-Kauwe, 2003). It is expected that, in case virus particles outnumber dynein molecules, a portion of the particles may not be transported from the cytosol to the nucleus in a timely manner and; therefore, they might be subjected to destruction by the cellular clearance mechanisms. This explanation is supported by the observed reduction in virus numbers (i.e., genome copies) within the first 12-24 hpi. The difference in virus replication found between the cells inoculated in 15-ml conical tubes and those inoculated in 12-well culture plate might be difficult to explain and, therefore, further work is planned to investigate this phenomena. However, one reason could be that the culturing microenvironment in the tubes was more supporting for virus uptake by suspended cells than that in culture plates. In this study, it was noticed that culture plates tend to limit the mobility of cells and cells tend to settle down at the bottom very quickly. This may reduce the random chance for virus particles to encounter their specific receptors on cells and subsequently, reduce virus attachment and entry. It has been reported that THEV production in spinner cultures of leukocytes was higher than that in stationary cultures (van den Hurk, 1990).

In conclusion, the present study showed that qPCR is a valuable tool in determining the variations among splenic vaccine batches produced from different facilities over extended periods of time. The qPCR assay was also proven to be useful in studying THEV growth kinetics and characteristics under different culturing conditions. Moreover, the assay was beneficial in delineating a relationship between the virus replication and the development of cytopathology in inoculated cell cultures and has the capacity to be applied for similar studied in live birds.

3.6. References

Bachrach, H.L., Callis, J.J., Hess, W.R. and Patty, R.E., 1957. A plaque assay for foot-and-mouth disease virus and kinetics of virus reproduction. Virology 4, 224-236.

Beach, N.M. 2006. Characterization of avirulent turkey hemorrhagic enteritis virus: a study of the molecular basis for variation in virulence and the occurrence of persistent infection, Virginia Polytechnic Institute and State University, Blacksburg, VA, USA, pp. 207.

Bustin, S.A., Benes, V., Garson, J.A., Hellemans, J., Huggett, J., Kubista, M., Mueller, R., Nolan, T., Pfaffl, M.W., Shipley, G.L., Vandesompele, J. and Wittwer, C.T., 2009. The MIQE Guidelines: Minimum Information for Publication of Quantitative Real-Time PCR Experiments. Clin Chem 55, 611-622.

Davison, A. and Harrach, B. 2011. Siadenovirus. In: Tidona, C. and Darai, G. (Eds), The Springer Index of Viruses, Springer New York, pp. 49-56.

Domermuth, C.H., Gross, W.B., Douglass, C.S., Dubose, R.T., Harris, J.R. and Davis, R.B., 1977. Vaccination for hemorrhagic enteritis of turkeys. Avian Dis 21, 557-565.

Domermuth, C.H., Gross, W.B. and DuBose, R.T., 1973. Microimmunodiffusion Test for Hemorrhagic Enteritis of Turkeys. Avian Diseases 17, 439-444.

Domermuth, C.H., Gross, W.B., DuBose, R.T., Douglass, C.S. and Reubush, C.B., Jr., 1972. Agar Gel Diffusion Precipitin Test for Hemorrhagic Enteritis of Turkeys. Avian Diseases 16, 852-857.

Dulbecco, R. and Vogt, M., 1954. One-step growth curve of Western equine encephalomyelitis virus on chicken embryo cells grown in vitro and analysis of virus yields from single cells. The Journal of experimental medicine 99, 183-99.

Ellis, E.L. and Delbruck, M., 1939. THE GROWTH OF BACTERIOPHAGE. The Journal of general physiology 22, 365-84.

Fadly, A.M. and Nazerian, K., 1984. Efficacy and Safety of a Cell-Culture Live Virus Vaccine for Hemorrhagic Enteritis of Turkeys: Laboratory Studies. Avian Diseases 28, 183-196.

Fadly, A.M., Nazerian, K., Nagaraja, K. and Below, G., 1985. Field vaccination against hemorrhagic enteritis of turkeys by a cell-culture live-virus vaccine. Avian Diseases 29, 768-77.

Furness, G. and Youngner, J.S., 1959. One-step growth curves for vaccinia virus in cultures of monkey kidney cells. Virology 9, 386-395.

Gross, W.B. and Moore, W.E.C., 1967. Hemorrhagic Enteritis of Turkeys. Avian Diseases 11, 296-307.

Guo, K., Dormitorio, T.V., Ou, S.-C. and Giambrone, J.J., 2011. Development of TaqMan real-time RT-PCR for detection of avian reoviruses. Journal of Virological Methods 177, 75-79.

Koressaar, T. and Remm, M., 2007. Enhancements and modifications of primer design program Primer3. Bioinformatics 23, 1289-91.

Kulski, J.K., 1994. Quantitation of human cytomegalovirus DNA in leukocytes by end-point titration and duplex polymerase chain reaction. J Virol Methods 49, 195-208.

Mackay, I.M., Arden, K.E. and Nitsche, A., 2002. Real-time PCR in virology. Nucleic Acids Research 30, 1292-1305.

Massin, P., Kuntz-Simon, G., Barbezange, C., Deblanc, C., Oger, A., Marquet-Blouin, E., Bougeard, S., van der Werf, S. and Jestin, V., 2010. Temperature sensitivity on growth and/or replication of H1N1, H1N2 and H3N2 influenza A viruses isolated from pigs and birds in mammalian cells. Veterinary Microbiology 142, 232-241.

Medina-Kauwe, L.K., 2003. Endocytosis of adenovirus and adenovirus capsid proteins. Adv Drug Deliv Rev 55, 1485-96.

Nazerian, K., Elmubarak, A. and Sharma, J.M., 1982. Establishment of B-lymphoblastoid cell lines from Marek's disease virus-induced tumors in turkeys. International Journal of Cancer 29, 63-68.

Nazerian, K.E.L., MI), Fadly, Aly M. (Holt, MI). 1983. Propagation of hemorrhagic enteritis virus in a turkey cell line and vaccine produced, The United States of America as represented by the Secretary of Agriculture (Washington, DC), United States.

Pierson, F.W. and Fitzgerald, S.D. 2008. Hemorrhagic Enteritis and Related Infections. In: Saif, Y.M., Fadly, A.M., Glisson, J.R., McDougald, L.R., Nolan, L.K. and Swayne, D.E. (Eds), Diseases of Poultry, Wiley-Blackwell, Iowa.

Ranheim, T., Mathis, P.K., Joelsson, D.B., Smith, M.E., Campbell, K.M., Lucas, G., Barmat, S., Melissen, E., Benz, R., Lewis, J.A., Chen, J., Schofield, T., Sitrin, R.D. and Hennessey, J.P., Jr., 2006. Development and application of a quantitative RT-PCR potency assay for a pentavalent rotavirus vaccine (RotaTeq). J Virol Methods 131, 193-201.

Reddy, S.M., Witter, R.L. and Gimeno, I., 2000. Development of a Quantitative-Competitive Polymerase Chain Reaction Assay for Serotype 1 Marek's Disease Virus. Avian Diseases 44, 770-775.

Rekha, K., Sivasubramanian, C., Chung, I.M. and Thiruvengadam, M., 2014. Growth and replication of infectious bursal disease virus in the DF-1 cell line and chicken embryo fibroblasts. BioMed research international 2014, 494835.

Rohr, U.P., Heyd, F., Neukirchen, J., Wulf, M.A., Queitsch, I., Kroener-Lux, G., Steidl, U., Fenk, R., Haas, R. and Kronenwett, R., 2005. Quantitative real-time PCR for titration of infectious recombinant AAV-2 particles. J Virol Methods 127, 40-5.

Sastry, L., Johnson, T., Hobson, M.J., Smucker, B. and Cornetta, K., 2002. Titering lentiviral vectors: comparison of DNA, RNA and marker expression methods. Gene therapy 9, 1155-62.

Segura, M.M., Monfar, M., Puig, M., Mennechet, F., Ibanes, S. and Chillon, M., 2010. A real-time PCR assay for quantification of canine adenoviral vectors. J Virol Methods 163, 129-36.

Shah, J.D., Scharber, S.K. and Cardona, C.J., 2013. Development and Application of Quantitative Real-Time PCR for the Rapid Detection of Hemorrhagic Enteritis Virus in Tissue Samples. Avian Diseases 57, 300-302.

Thorsen, J., Weninger, N., Weber, L. and Dijk, C.V., 1982. Field Trials of an Immunization Procedure against Hemorrhagic Enteritis of Turkeys. Avian Diseases 26, 473-477.

Untergasser, A., Cutcutache, I., Koressaar, T., Ye, J., Faircloth, B.C., Remm, M. and Rozen, S.G., 2012. Primer3--new capabilities and interfaces. Nucleic Acids Res 40, e115.

van den Hurk, J.V., 1990. Propagation of group II avian adenoviruses in turkey and chicken leukocytes. Avian Dis 34, 12-25.

Veldwijk, M.R., Topaly, J., Laufs, S., Hengge, U.R., Wenz, F., Zeller, W.J. and Fruehauf, S., 2002. Development and optimization of a real-time quantitative PCR-based method for the titration of AAV-2 vector stocks. Mol Ther 6, 272-8.

Chapter 4

A Novel Real-Time PCR-Based Infectivity Assay for Turkey Hemorrhages Enteritis Virus: Application on the Titration of Cell Culture Vaccines

4.1. Abstract

Assuring the presence of accurate virus infective titers in live vaccines is an important step in vaccine development and production. A novel approach for the infectivity titration of turkey hemorrhagic enteritis virus (THEV) in live vaccines combining a SYBR Green I-based qPCR assay and a cell culture system is reported. qPCR was used to enumerate the viral genome copy number (vGCN) of the internalized (infective) virus particles following an *in vitro* infection of cultured MDTC-RP19 cells. The measured vGCN will represent the amount of infectious viral particle (IVPs) in tested vaccine. The method was applied to compare nine batches of HE cell culture (CC)-propagated vaccines from three different companies. Also, the relationships between vaccine qPCR-infectious titer (IVPs/1 label dose) and both the genomic titer (vGCN/dose) and the progeny virus genomes at 72 hour post-inoculation (hpi) in cell culture were determined. Results showed that the qPCR-infectious titer of tested vaccine lots varied significantly ($P < 0.0001$) from lot to lot and among companies. The mean values (±SEM) ranged between 6.84E+03 (±1.32E+03) and 2.39E+05 (±3.59E+04) IVPs/dose. For the three companies tested, the differences in infectious titers among batches were 6.36E+03, 8.03E+04, and 1.52E+05 IVPs/dose. Strong positive linear relationships were found between the qPCR infectious titer and both the genomic titer ($R^2 = 0.92$ and $P < 0.0001$) and the virus progeny in cell culture at 72 hpi ($R^2 = 0.78$ and $P = 0.0015$). Further, $CCID_{50}$ titers were determined on the nine vaccine lots using the endpoint dilution assay in RP19 cells. Calculated titers ranged from 7.92E+01 to 1.26E+03 $CCID_{50}$/vaccine label dose and did not correlate well with the qPCR infectious titers. The ratios of vGCN:IVP ranged from 5:1 to 98:1, and those of IVP:$CCID_{50}$ ranged from 41:1 to 467:1. In conclusion, the present study revealed moderate to significant lot-to-lot variations in THEV titer per label dose among HE CC vaccine products from different companies, which indicate inaccuracy of current titration protocols used for

THEV. The new approach proved an excellent alternative to traditional titration methods and a useful tool for a more consistent titer of HE CC vaccines. The utilization of this method to standardize virus titers among vaccine batches would presumably help improve vaccine performance in the field by providing consistent levels of protection. Moreover, this assay has proven to be an instrumental research tool. It was utilized in most of the experiments described in Chapter 5 of this dissertation for determining the effect of various treatments on virus infectivity.

4.2. Introduction

Turkey hemorrhagic enteritis virus (THEV), a member of the genus *Siadenovirus*, family *Adenoviridae*, is the etiologic agent of the hemorrhagic enteritis (HE) disease in turkeys. The different strains of THEV cause immunosuppression in susceptible birds, disposing them to secondary infections (e.g., *E. coli*), and can lead to high rates of mortality. The clinical HE disease caused by virulent THEV can be prevented effectively by vaccination of 4½-6 weeks-of-age turkey poults with naturally occurring avirulent THEV strains (Davison and Harrach, 2011; Domermuth et al., 1977; Larsen et al., 1985; Newberry et al., 1993). The only USDA-licensable vaccines for HE prevention are live-virus cell culture (CC)-propagated products. Another type of vaccine is generated through turkey production companies as splenic homogenate from infected birds, but cannot be commercialized.

Currently, two titration methods can be applied to THEV; both are quantal assays. The first one is endpoint dilution in poults at 6 weeks of age (Domermuth et al., 1977). The drawbacks of this method are that it is cost prohibitive, time consuming, labor-intensive, subject to individual variations among birds, and requires the killing of many birds. The second method is *in vitro* endpoint dilution in cultured MDTC-RP19, B cell line (RP19 cells) to determine the tissue culture infectious dose 50 ($TCID_{50}$) (Nazerian and Fadly, 1987; Sharma, 1994). This method relies solely on visual evaluation of infected cells in suspension for cytopathic effect (CPE; i.e., enlargement and ballooning of cells), the only manifestation of successful infection and viral replication. In suspension cultures, CPE can be easily confused with the enlargement of cells

undergoing necrosis. Moreover, the protocol is laborious and it takes from 3 to 12 days for inoculated cell culture to show evident CPE (Fadly et al., 1985).

Plaque assay and similar methods cannot be used for THEV due to the lack of a susceptible adherent cell line (Nazerian and Fadly, 1987). No fully quantitative infectivity assays are available to accurately quantify THEV. Thus, there was an urgent need for a more accurate method for THEV titration. The technology of real-time PCR has been intensively applied for quantification of viruses with promising results, compared with traditional methods. Despite the establishment of THEV-susceptible RP19 cells more than three decades ago; development of a reliable titration method for THEV has yet to be achieved. The time and effort, as well as inherent inaccuracy, associated with traditional titration methods in general and with THEV titration in particular, made it necessary to develop a new assay for virus titration. The aim of the present study was to establish a fully quantitative, facile method for the titration of THEV in live vaccines using a combination of RP19 cell culture and qPCR assay. The method was applied to compare the virus titers in HE live vaccines produced by three manufacturers in the US. qPCR infectious titers were also compared with those obtained by the traditional $TCID_{50}$ protocol. The established method is intended for use as a reliable alternative for traditional, less-accurate titration methods and to minimize the amount of work needed for vaccine titration. It will also help standardize the virus titers in HE vaccines produced by various manufacturers.

4.3. Materials and methods

4.3.1. Cells and growth conditions

RP19 cells, growth conditions, and the composition of Leibovitz-McCoy growth and maintenance media (CLM and SRLM, respectively; Table 3-2) were all described in detail in Chapter 3 under “Materials and methods” section.

4.3.2. Optimization of the infection procedure to be used in the qPCR-based infectivity assay

Two experiments were carried out for the optimization of infection protocol to be used in the qPCR infectivity assay. The purpose of the first experiment was to determine the optimal time point post-inoculation at which most of infective viral particles are internalized. At this point the cells would be collected to estimate the virus infectious titer in samples. This time point is expected to be after the complete entry of infective virus particles into inoculated cells and before the initiation of genome replication. The purpose of the second experiment was to determine the appropriate number of cells to be used for the inoculation step and whether a certain cell number will support virus replication better than the other.

The first experiment was designed based on the following facts. As an adenovirus, THEV is expected to be adsorbed in a few minutes after cell inoculation, and then internalized after relatively various time spans (Chardonnet and Dales, 1970a; Chardonnet and Dales, 1970b). Also, THEV genome is not expected to start active replication before 18 to 24 hpi, the time by which virus particles reach the nucleus as reported by van den Hurk (1990). Thus, the optimal time point to quantify the infective THEV particles was expected to be between a few minutes and 24 hpi. In this experiment, RP19 cells (5×10^5) were added to 1.5-ml tubes and pelleted at 2000 rpm for 7 min at 4°C. To each cell pellet, 100 µl of a THEV inoculum in SRLM media was added and mixed well. Inoculated cells were then transferred to the wells of a round-bottom 96-well culture plate and incubated at 41ºC. Triplicate cell samples were collected at 0.25, 0.5, 0.75, 1, 6, 12, 18, or 24 hpi. Upon collection, cells were pelleted, washed thrice with 500 µl aliquots of PBS to remove unbound virus and free-floating genomes, resuspended in 200 µl of PBS, and stored at -20ºC. Cells were lysed through 3 freeze-thaws and DNA was extracted from cell lysates using the QIAamp DNA Mini Kit (Qiagen), following the Blood or Body Fluids Spin Protocol. DNA was eluted in 200 µl of DNase/RNase-free distilled water. THEV qPCR (described in Chapter 3, Subsection 3.3.3) was run on DNA templates (4 µl/reaction) with the SensiMix™ SYBR® & Fluorescein Kit (Bioline) to quantify virus genome copy number (vGCN) in the inoculated cell samples.

Using the qPCR data, the mean vGCN at each time point post-inoculation was calculated and plotted against the corresponding virus incubation length (Fig. 4-1). Results indicated that no significant differences existed in vGCN starting 15 min post-

inoculation till 18 hpi. However, at 1 hpi vGCN was slightly higher than other time points. Significant difference in vGCN was mainly seen at 24 hpi ($P < 0.0001$). These observations are in agreement with those reported by van den Hurk (1990), who found that THEV virions were seen in the nucleus of cultured leukocytes at 18 to 24 hpi. Based on these results, the 1 h virus incubation time was chosen to be used in all qPCR infectivity assay experiments. To conclude, vGCN determined by qPCR in inoculated RP19 cells at 1 hpi reflects the actual infectious viral particles (IVPs) of THEV in a given inoculum.

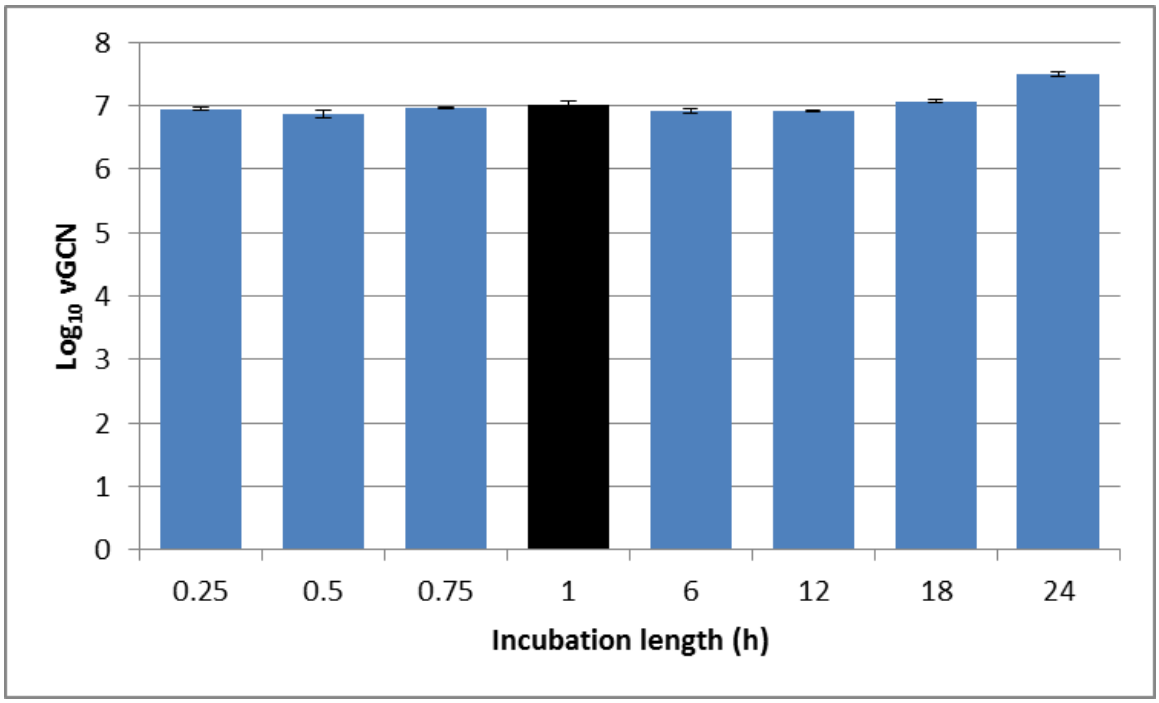

Fig. 4-1. Effect of virus incubation period (h) in cultured RP19 cells on the level of virus entry as measured by the qPCR assay. RP19 cells (5×10^5) were inoculated with THEV and triplicate samples were collected at different time points post-inoculation for DNA extraction and vGCN quantification. Each column represents the mean from triplicate cell samples. Bars show standard errors of the means.

In the second experiment, four groups of cultured RP19 cells; 0.5×10^6, 1×10^6, 2×10^6, or 4×10^6, were pelleted and resuspended in 1 ml of SRLM media in 1.5-ml Eppendorf tubes. A stock inoculum of THEV was made by reconstituting a vial of

lyophilized HE CC vaccine product (1000 dose) in 5 ml of SRLM media. A working dilution of the stock inoculum was made at 1:10 in SRLM media and used here. Each cell pellet was resuspended in 200 µl of the THEV inoculum and incubated at 41ºC for 1 h. Cells were then washed thrice with PBS, pelleted, resuspended in SRLM media, and stored at -20ºC. DNA extraction from cells and qPCR assay for vGCN determination were essentially performed as illustrated in the first optimization experiment. The total vGCN was calculated for each sample, and mean vGCN per cell number group was calculated and plotted against the corresponding cell number (Fig. 4-2). Results showed that there were no significant differences (P = 0.8454) in vGCN among the four groups of cell numbers tested (Fig. 4-2). Therefore, for the qPCR infectivity assay, the lowest number of cells (5×10^5) was chosen to be used in all experiments.

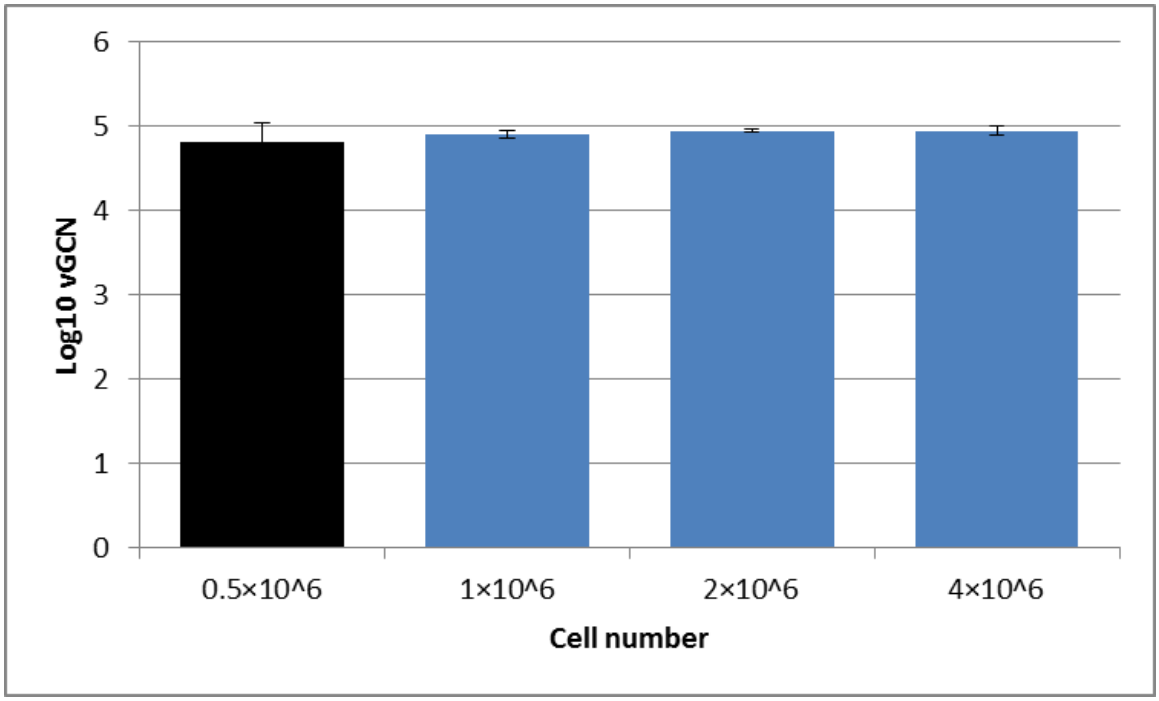

Fig. 4-2. Effect of cell number used for the inoculation with THVE on the level of virus entry as measured by qPCR assay. Cells were inoculated with virus, incubated for 1 h, washed, and resuspended in SRLM media. DNA was extracted from triplicate samples per cell group and vGCN was determined by qPCR. Each column represents the mean from duplicate cell samples. Bars show standard errors of the means. No significant differences were found in virus entry (P = 0.8454).

4.3.3. Preparation of HE CC vaccine products for titration

HE live vaccines evaluated in this study are commercially available products and offered in either liquid or lyophilized form. These vaccines are cell-free virus suspensions which are obtained through the propagation of avirulent THEV strains in RP19 cells using standard methods previously described (Nazerian and Fadly, 1982; Nazerian, 1983). For this study, three vaccine batches/lots produced by three different vaccine companies were purchased. Once received, vaccine vials were stored according to the manufacturer's recommendations or reconstituted immediately (for lyophilized products) in SRLM media and stored at -20ºC. Regardless of the dosage per vial, the vaccine material in each vial was resuspended in a total of 50 ml of SRLM media and these were considered stock solutions. Based on the dosage of each vial, the appropriate dilution in SRLM media was made so that every 100 µl of inoculum contained 1 vaccine label dose. The entire process of vaccine reconstitution and dilution was performed on ice. The l-dose suspensions were filtered through 0.45 μm syringe filters to remove possible impurities, divided into small aliquots, and then stored at -20ºC. When needed for use in the titration experiments, aliquots of vaccines were thawed slowly on ice, and then equilibrated at RT before cell inoculation.

Table 4-1
Information of HE CC vaccine products evaluated in this study.

Vaccine ID*	Expiry date†	Vial dosage‡
A1	10/25/14	1000
A2	01/17/15	1000
A3	01/13/15	5000
B1	10/08/13	2000
B2	11/29/13	5000
B3	03/13/14	5000
C1	01/06/14	2000
C2	05/22/14	5000
C3	09/18/15	5000

*A different letter was assigned to each vaccine manufacturer and does not associate in any way to the manufacturer's identity. A number from 1 to 3 was assigned to each of the three vaccine lots from each manufacturer. Example: A1 refers to company A, lot 1, and so on.
†At the time the titration experiment were performed, all vaccine lots were still valid (i.e., did not pass the label expiry date).
‡Total label doses per vial.

4.3.4. Determining the genomic titers of HC CC vaccines

Triplicate samples of one label dose (100 µl) were taken from each of the nine vaccine lot to be tested (Table 4-1). To each vaccine sample 100 µl of PBS was added to bring the total volume to 200 µl and DNA was extracted using the QIAamp DNA Mini Kit (Qiagen), following the Blood or Body Fluids Spin Protocol. DNA was eluted in 200 µl of DNase/RNase-free distilled water. THEV qPCR was run on DNA extracts (4 µl/reaction) with the SensiMix™ SYBR® & Fluorescein Kit (Bioline) and total vGCN per label dose was calculated for each vaccine lot.

4.3.5. qPCR-based infectivity assay for titration of HE CC vaccines and measurement of vaccine potency

Fig. 4-3 displays a schematic of the steps involved in the new qPCR-based infectivity assay. To the wells of a V-bottom 96-well culture plate, 100 µl of cells (5×10^5) in SRLM media were dispensed, followed by incubation at 41ºC for 1 h. Cells in

triplicate were then individually inoculated with one label dose of each vaccine product and incubated for 1 h (time sufficient for virus entry). Inoculated cells were transferred from the culture plate wells to 1.5-ml tubes and pelleted by centrifugation at 3000 rpm for 7 min at 4ºC. Cells were then washed thrice with 500 µl aliquots of PBS+2%FBS to remove unbound virus particles and free-floating virus genomes. Cell pellets were then resuspended in 200 µl of PBS and stored at -20ºC until DNA extraction and THEV qPCR as described above. vGCN determined by qPCR was used to calculate the virus infectious titer in tested vaccine lots and expressed as IVPs/label dose. This experiment was repeated twice. A correlation between genomic titers and IVPs per label dose was demonstrated.

Differences in potency among tested vaccine lots were assessed by measuring the virus replication after 3 days in culture. Cells that were inoculated with 1 label dose from each vaccine lot were harvested at 72 hpi, followed by DNA extraction and qPCR as described above. Total vGCN at 72 hpi was used as an indicator of virus progeny. The correlation between IVPs per label dose and virus progeny was studied.

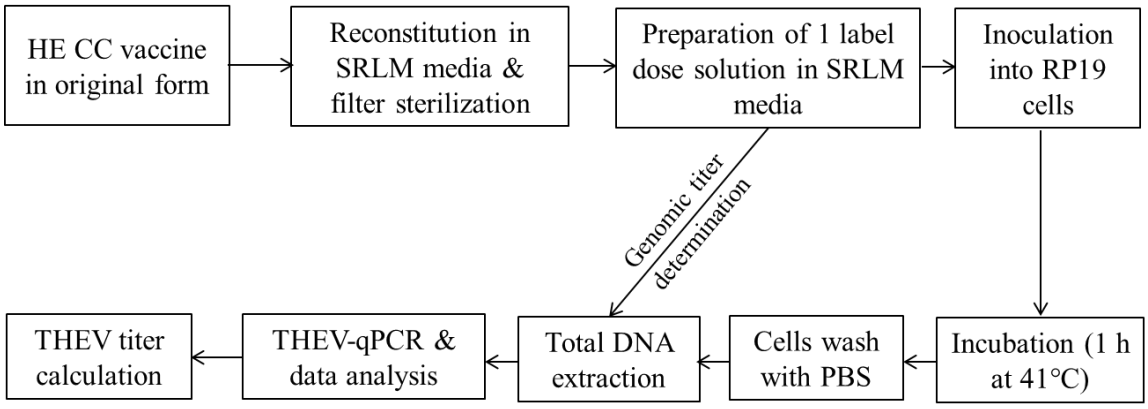

Fig. 4-3. Schematic summarizing the principal steps of the novel qPCR-based infectivity assay developed in this study for THEV titration.

4.3.6. Cell culture infectious dose 50 ($CCID_{50}$) endpoint dilution assay for titration of HE CC vaccines

To the wells of 96-well flat-bottom, non-tissue culture treated, culture plates, RP19 cells (1×10^4) in 100 µl of SRLM media were added, followed by incubation overnight at 41ºC. A total of nine plates were prepared; one plate per vaccine lot. In a V-bottom 96-well culture plate, a tenfold dilutions series (10^{-1}-10^{-5}) in SRLM media was prepared from each of the vaccine stock solutions described above (Subsection 4.3.3.). The flat-bottom cell culture plates were removed one by one from the incubator and cells were inoculated with 100 µl of one vaccine dilution; 10 wells/dilution. The first two wells of each row were mock-inoculated with 100 µl of SRLM media as negative controls. Inoculation of the plates with vaccine dilutions was performed sequentially starting with lot A1 ending with lot C3. Once inoculated the plate was returned to the incubator at 41ºC. The cells were monitored daily for 7 days with an inverted light microscope at the same order of inoculation, for the development of CPE (i.e., cell enlargement and ballooning). Inoculated wells were scored as positive or negative. Virus titer of each vaccine stock solution was estimated based on the formula of Spearman-Kärber (Kärber, 1931; Villegas, 2008), and $CCID_{50}$/dose was then calculated.

4.3.7. Statistical analysis

Data was analyzed by one-way analysis of variance (ANOVA), and when statistical significance exists, multiple comparisons between treatment means were performed by Tukey-Kramer HSD (Honestly Significant Difference) test using JMP® Pro (v. 10.0.0, SAS Institute, Inc., Cary, NC). The significance level was set at $P \leq 0.05$. Data from the qPCR assay and $CCID_{50}$ protocol was transformed to the $\log_{10}$ format to achieve a normal distribution, before being statistically analyzed with ANOVA.

4.4. Results

4.4.1. Determining the qPCR infectious titers in nine HE vaccine batches from three companies

The new qPCR-based infectivity titration method was employed to quantify the virus infectious titer (expressed as infectious viral particles; IVPs) in HE vaccine products from three different companies in the US; three batches per company were evaluated. Also, the genomic titers (expressed as viral genome copies; vGC) per label dose and virus progeny (expressed as viral genome copies at 72 hpi; vGC-72h) in cell culture per label dose were determined. Results showed that, overall, there were statistically significant differences in the virus genomic titers (vGCN; $P < 0.0001$), the infectious titers (IVPs; $P < 0.0001$), and the virus progeny (vGCN-72h; $P < 0.0001$) per label dose among the tested vaccine lots from the three companies (Figures 4-4, 4-5, and 4-6). Significant variations in genomic titers were found among vaccine batches of one out of three (1/3) companies, in infectious titers among batches of 3/3 companies, and in virus progeny at 72 hpi among batches of 2/3 companies. In order to get a better idea about the titer variations, the real values (before transformation) of titers per label dose as determined by qPCR assay were listed in Table 4-2. These values were used to make the following calculations. The overall range of difference in virus genomic titers, infectious titers, and virus progeny at 72 hpi between the highest and the lowest vaccine lots tested were 8.53E+06 vGC, 2.32E+05 IVPs, and 4.88E+08 vGC-72h per label dose. Within each company, these variations were found to be 2.33E+05, 6.36E+03, and 8.83E+06; 8.00E+06, 8.03E+04, and 3.54E+08; or 3.33E+06, 1.52E+05, and 3.70E+08 per label dose for company A, B, or C, respectively. When the cell-culture endpoint dilution assay was applied on these vaccine lots, high variations in titers were also detected (Table 4-2). The difference between the highest- and lowest-titer lot was 2.37E+02, 4.99E+02, and 2.64E+02 $CCID_{50}$/label dose for company A, B, or C, respectively. When differences in qPCR infectious titers were calculated per 2000-dose vial, an estimate of 1.27E+07, 1.61E+08, or 3.54E+08 IVPs per vial was found when comparing the high-titer and low-titer vaccine lots from company A, B, or C, respectively. This large variation among

batches reflects the monetary value a vaccine manufacturer can potentially save when a precise titration method, such as the one developed in this study, is followed.

The ratios of vGCN:IVP (the number of virus genome copies for each infectious particle) and IVP:$CCID_{50}$ (the number of virus infectious particles for each $CCID_{50}$) were calculated and found to vary considerably among the tested vaccine lots within each company. Overall, the range of these ratios was 5:1 (lot B2) to 98:1 (lot A2) and 41:1 (lot C3) to 467:1 (lot B2), respectively (Table 4-2). It is expected that, once the titration process is standardized within a given company and low variations among batches are maintained, genomic titers can be used as a direct indicator of the infectious titer. The vGCN:IVP ratio can be used to estimate the IVPs/dose for a vaccine product by only determining its genomic titer. In some cases a vaccine batch can be subjected to further dilution or concentration, based on its determined infectious titer. In order to ensure that this batch contains the expected infectious titer after the change made to its concentration, one can just determine the genomic titer and use the above ratio to obtain an estimation of the current infectious titer. The same concept can be applied to the IVP:$CCID_{50}$ ratio, which can be used to adjust a vaccine batch content of $CCID_{50}$ based on the determined IVPs values.

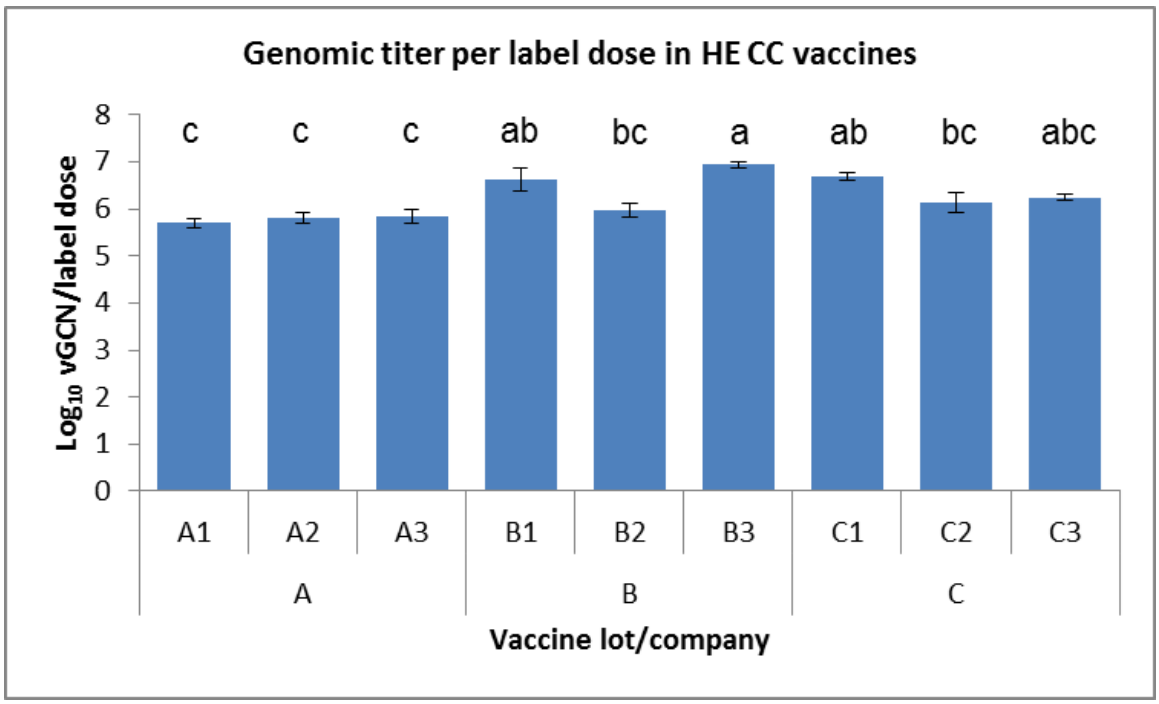

Fig. 4-4. Variations in genomic titers (vGCN/label dose) of THEV among nine hemorrhagic enteritis cell culture (HE CC) vaccine lots from three companies. Each column represents the mean from triplicate DNA extracts per vaccine lot. Bars show standard errors. Significance: $P < 0.0001$. Means / columns with different letters differ significantly.

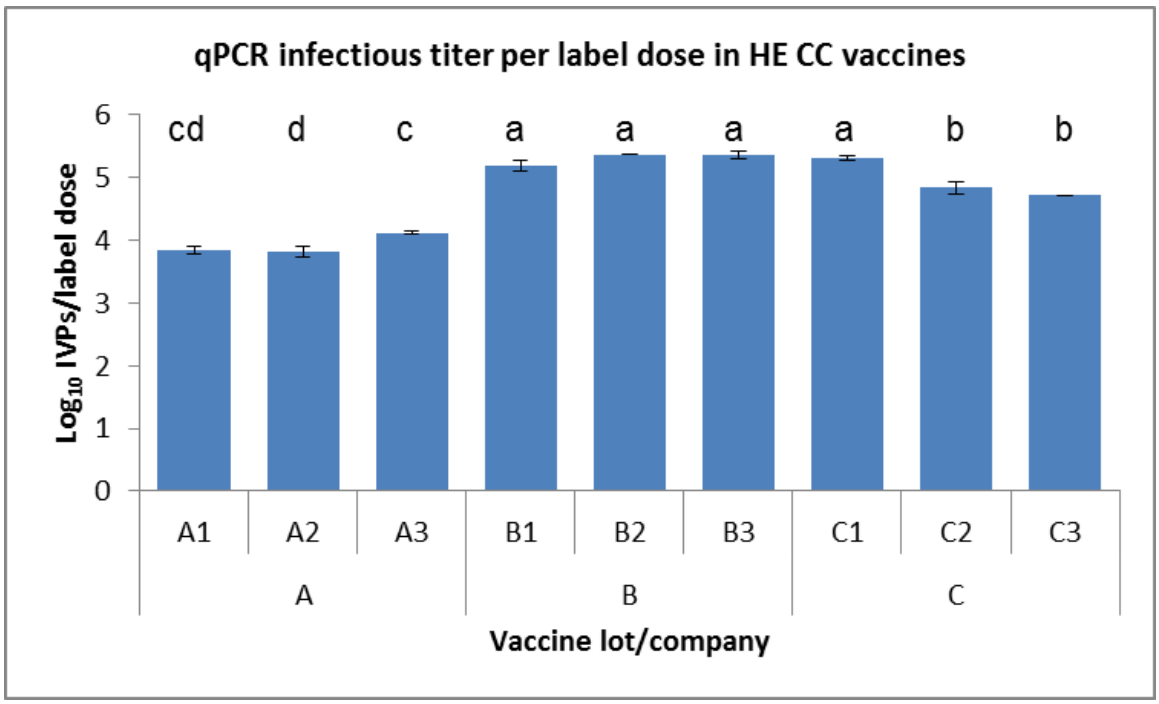

Fig. 4-5. Variations in qPCR-based infectious titers (IVPs/label dose) of THEV among nine hemorrhagic enteritis cell culture (HE CC) vaccine lots from three companies. Each column represents the mean from individually treated triplicate cell samples. Bars show standard errors. Significance: $P < 0.0001$. Means / columns with different letters differ significantly.

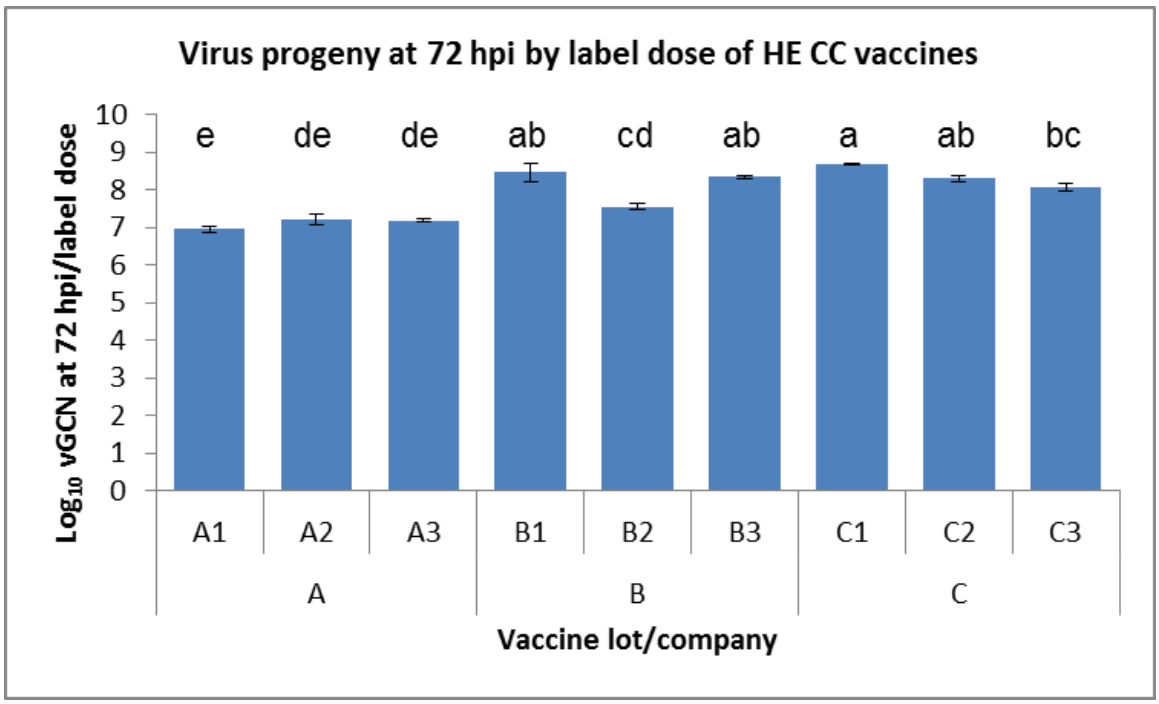

Fig. 4-6. Variations in **v**irus progeny per vaccine label dose (vGCN at 72 hpi) among nine hemorrhagic enteritis cell culture (HE CC) vaccine lots from three companies. Each column represents the mean from individually treated triplicate cell samples. Bars show standard errors. Significance: $P < 0.0001$. Means / columns with different letters differ significantly.

Table 4-2
Comparison between genomic titer, qPCR-based infectious titer, and CCID50 titer per label dose, vGCN:IVP ratios, and IVP:$CCID_{50}$ ratios in nine CC HE vaccine batches from three companies.

Company	Lot	Genomic titer (vGCN/dose)* (±SEM)	qPCR infectious titer (IVPs/dose)† (±SEM)	$CCID_{50}$/dose‡	vGCN:IVP ratio	IVP:$CCID_{50}$ ratio
A	1	5.33E+05 (1.11E+05)	6.97E+03 (1.04E+03)	7.92E+01	77:1	88:1
	2	6.71E+05 (1.52E+05)	6.84E+03 (1.32E+03)	9.98E+01	98:1	69:1
	3	7.66E+05 (2.13E+05)	1.32E+04 (8.19E+02)	3.16E+02	58:1	42:1
B	1	5.31E+06 (2.22E+06)	1.59E+05 (3.00E+04)	7.91E+02	33:1	201:1
	2	1.07E+06 (3.25E+05)	2.34E+05 (4.37E+03)	5.01E+02	5:1	467:1
	3	9.07E+06 (2.49E+06)	2.39E+05 (3.59E+04)	1.00E+03	38:1	239:1
C	1	5.03E+06 (8.70E+05)	2.04E+05 (1.80E+04)	9.95E+02	25:1	205:1
	2	1.70E+06 (7.26E+05)	7.21E+04 (1.51E+04)	1.26E+03	24:1	57:1
	3	1.82E+06 (3.03E+05)	5.22E+04 (5.20E+02)	1.26E+03	35:1	41:1

*vGCN, viral genome copy number; values represent means±SEM from triplicate samples/DNA extracts.
†IVPs, infectious virus particles; values represent means±SEM from duplicate experiments with triplicate samples each.
‡CPE scores have been recorded at 7 dpi and used for calculating CCID50 titer using Spearman-Kärber method.

4.4.2. Correlation between qPCR infectious titer and each of genomic titers, virus progeny/potency, and $CCID_{50}$

A statistically positive linear relationship was found between the qPCR infectious titer and the genomic titer per vaccine label dose (R^2 = 0.92 and $P < 0.0001$; n = 9; Fig. 4-7A). This strong relationship means that the virus genomic titer in HE vaccines can be used as indicator of the infectious titer. Since determining genomic titers takes only a few hours (for DNA extraction and qPCR assay), a quick decision can be made on whether a certain vaccine batch needs to be further diluted out or concentrated. Afterwards the infectivity assay can be run to determine the actual infectious titer of the adjusted batch. Likewise, a statistically positive correlation was found between the qPCR infectious titer and the virus progeny in cell culture after 72 h (R^2 = 0.78 and P = 0.0015; n = 9; Fig. 4-7B). This relationship is a strong indication that the qPCR infectious titer can be related directly to the expected vaccine potency in live birds upon vaccination. No correlation was found between titers obtained from the $CCID_{50}$ protocol and those from the qPCR-based infectivity assay. This absence of linear relationship was expected because of the high variability and lower accuracy of the $CCID_{50}$ endpoint dilution method, especially when applied to suspended cells. In cells growing in suspension cultures, like RP19 cells, often times the CPE (mainly ballooning of cells) may be easily recognized or does not develop within the recommended duration for the protocol, i.e., 7 days as recommended by Rautenschlein and Sharma (1999).

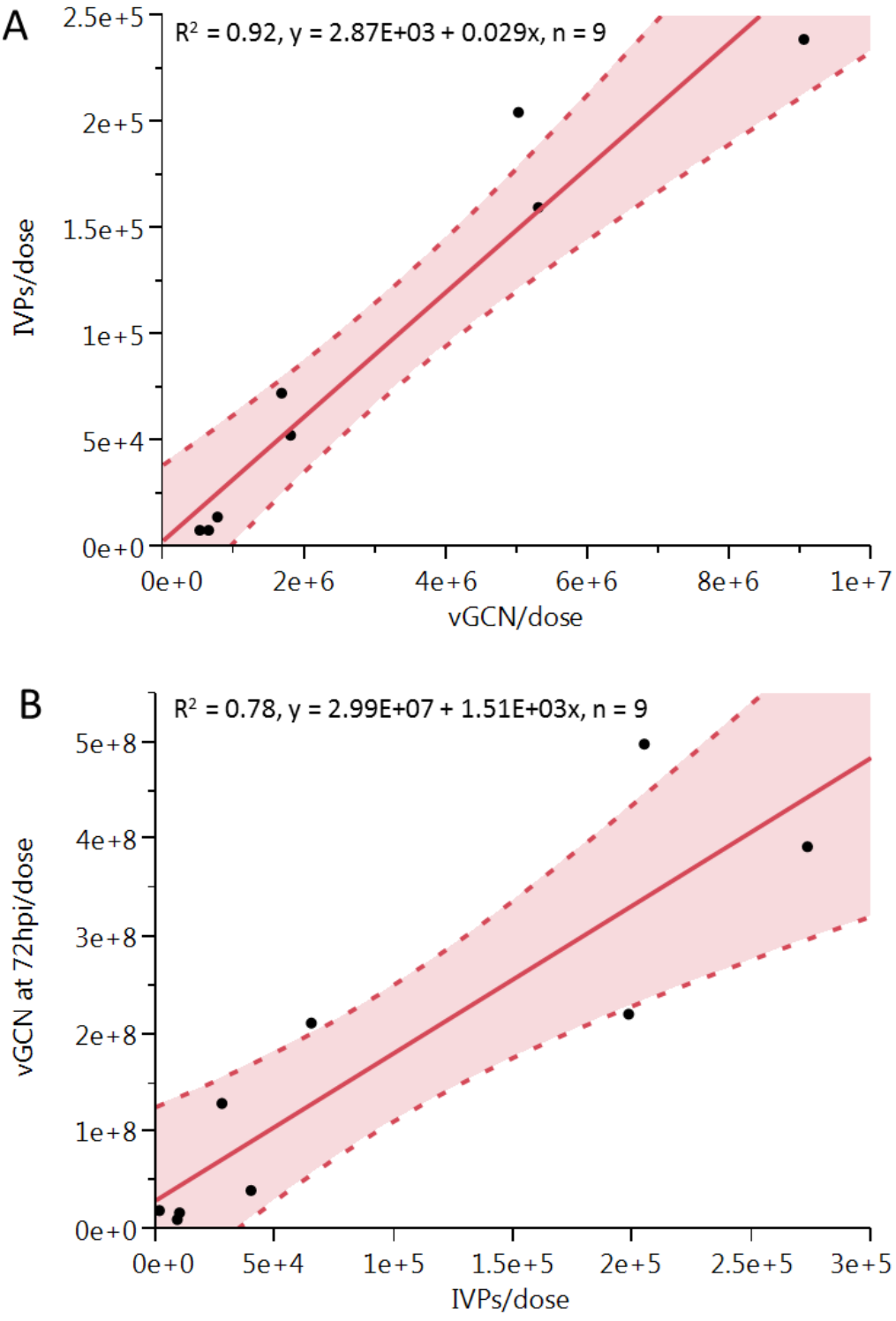

Fig. 4-7. Correlation between the qPCR-based infectious titer (IVPs/dose) and both the virus genomic titer (vGCN/dose; A; $P < 0.0001$) and the virus progeny at 72 hpi (B; $P = 0.0015$) in HE CC vaccines.

4.5. Discussion

The development of accurate and precise infectivity assays has been and still is a very active area of research in many laboratories working on human and animal viruses. qPCR assays in conjunction with cell culture systems have been utilized extensively as a tool to achieve precise virus titers. This approach has been applied for the infectivity titration of many viruses including adenoviral vectors, adeno-associated viruses, reoviruses, measles, mumps, and rubella viruses, rotaviruses, and poxviruses, among others (Ammour et al., 2013; Guo et al., 2011; Kallesh et al., 2009; Ranheim et al., 2006; Rohr et al., 2005; Schalk et al., 2004; Segura et al., 2010; Veldwijk et al., 2002; Wang et al., 2005). The common concept of the qPCR-based infectivity methods is that the genomic titer (determined by qPCR) of cell-internalized virus particles (at a certain time point post-inoculation) is strongly correlated with the infectivity of the virus inoculum (Wolf et al., 2007). qPCR-based infectious titers have been found to correlate with the functional titers estimated by traditional methods such as plaque assay, focus forming assay, and $TCID_{50}$ protocol, as reported in the studies mentioned above.

Only a few traditional protocols have been previously described for the infectivity titration of HE live vaccines. The gold standard infectivity titration methods for most viruses are end point titration in susceptible cell-culture systems or live animals/birds. For THEV, a method for determining the infectious titers by applying an endpoint dilution protocol in live turkeys to determine the "poult infective dose" has been reported by Domermuth et al. (1977). Cell culture-based endpoint assays for the titration of THEV have been reported a few times in the literature. In these assays, RP19 cells (Rautenschlein and Sharma, 1999; Sharma, 1994) or primary leukocytes (van den Hurk, 1990) were inoculated with the virus dilutions and scored for CPE. The infection in inoculated cells was also confirmed using staining procedures, apparently because the non-infected cells undergoing necrosis can be easily confused with cells developing infection-based CPE. With the disadvantages of these assays (e.g., intensive labor, very lengthy protocols, high cost, inaccuracy, and complexity, etc.), a novel, fully quantitative, and rapid method for THEV titration was an urgent need for both research and the vaccine industry.

In this study the development of a novel and simple qPCR-based infectivity assay for the accurate titration of THEV was described. The assay is rapid and can give final results in less than a day, as compared with several days for the less-accurate CCID50 protocol. The assay only shares the step of cell preparation with the traditional protocols, but does not require the cells to

be incubated before inoculation. Once prepared, the cells can be inoculated immediately, incubated for 1 h, washed three times, resuspended in PBS, and stored at -20°C. Before the 1 h-DNA extraction procedure cells need to be lysed; this can be done by three cycles of freeze-thaws. In this study, cell lysis was done by freezing at -20°C, followed by thawing at room temperature, which took about 4 h for three cycles to be completed. The length of this step can be further shortened to less than 1 h by freezing at -80°C and thawing at 37°C, as reported previously for other protocols (Mayginnes et al., 2006). Other fast lysis procedures which are known not to affect the DNA quality may also be considered. After DNA extraction, qPCR can be run directly (3 h preparation and running time), followed by titer calculation and reporting as the final step. This assay was employed successfully in determining the infectious titers of fresh HE CC live vaccines from three different manufacturers. Nine vaccine batches were titrated and titers compared to each other within several hours.

A major drawback of the $CCID_{50}$ protocol observed specifically in this study is that it cannot be used to simultaneously compare the titers of vaccine batches with high variations in virus content. It was noticed that batches with higher virus titers showed CPE on inoculated cultures as early as 4 dpi, while batches of low titers did not develop a recognizable CPE until a few days later (i.e., up to 8 days). At the time low-titer vaccine batches showed CPE, the high-titer ones had already caused cell degeneration and death, which is a typical end result of THEV infection in cultures as reported by Nazerian and Fadly (1982).

In conclusion, the new THEV qPCR-based infectivity titration assay is a valuable and reliable addition to virological methods. It can achieve virus titration in a much shorter time than similar assays recently reported. It should be considered for use as either a quality control tool or an alternative titration method by vaccine companies to obtain reliable titers of their products. The assay cost may be relatively higher than the traditional methods; however, by lowering variations among batches and keeping titers within the optimal range, vaccine companies can save at least half of the cost per vial. Simple calculations based on current results have shown that one vaccine vial contained an estimate of 1.5 to 3.9 times the infectious doses of another vaccine vial within the same company. The monetary value of this variation can be exemplified based on the assumptions that a given company produces a batch of 1000 vials (2000-dose) of HE vaccine a month and each vial costs $20. The total cost of these vials will equal $20,000. If these vials are from a high titer batch, then each vial is expected to contain about 1.5 times the

doses of a low-titer vial. Therefore, the actual value of the produced batch will be 1500 vials; the total cost of which is $30,000. These simple calculations indicate a potential saving of $10,000/month when the vaccine titer per vial is optimized and standardized based on an accurate titration method. Finally, the qPCR assay has a very high sensitivity and, when used in research, was able to determine minor effects of several chemical and enzymatic treatments on virus infectivity (Chapter 5 of this dissertation).

4.6. References

Ammour, Y., Faizuloev, E., Borisova, T., Nikonova, A., Dmitriev, G., Lobodanov, S. and Zverev, V., 2013. Quantification of measles, mumps and rubella viruses using real-time quantitative TaqMan-based RT-PCR assay. J Virol Methods 187, 57-64.

Chardonnet, Y. and Dales, S., 1970a. Early events in the interaction of adenoviruses with HeLa cells. I. Penetration of type 5 and intracellular release of the DNA genome. Virology 40, 462-77.

Chardonnet, Y. and Dales, S., 1970b. Early events in the interaction of adenoviruses with HeLa cells. II. Comparative observations on the penetration of types 1, 5, 7, and 12. Virology 40, 478-85.

Davison, A. and Harrach, B. 2011. Siadenovirus. In: Tidona, C. and Darai, G. (Eds), The Springer Index of Viruses, Springer New York, pp. 49-56.

Domermuth, C.H., Gross, W.B., Douglass, C.S., Dubose, R.T., Harris, J.R. and Davis, R.B., 1977. Vaccination for hemorrhagic enteritis of turkeys. Avian Dis 21, 557-565.

Fadly, A.M., Nazerian, K., Nagaraja, K. and Below, G., 1985. Field vaccination against hemorrhagic enteritis of turkeys by a cell-culture live-virus vaccine. Avian Diseases 29, 768-77.

Guo, K., Dormitorio, T.V., Ou, S.-C. and Giambrone, J.J., 2011. Development of TaqMan real-time RT-PCR for detection of avian reoviruses. Journal of Virological Methods 177, 75-79.

Kallesh, D.J., Hosamani, M., Balamurugan, V., Bhanuprakash, V., Yadav, V. and Singh, R.K., 2009. Quantitative PCR: a quality control assay for estimation of viable virus content in live attenuated goat pox vaccine. Indian journal of experimental biology 47, 911-5.

Kärber, G., 1931. 50% end-point calculation. Arch. Exp. Pathol. Pharmak 162, 480-483.

Larsen, C.T., Domermuth, C.H., Sponenberg, D.P. and Gross, W.B., 1985. Colibacillosis of Turkeys Exacerbated by Hemorrhagic Enteritis Virus. Laboratory Studies. Avian Diseases 29, 729-732.

Mayginnes, J.P., Reed, S.E., Berg, H.G., Staley, E.M., Pintel, D.J. and Tullis, G.E., 2006. Quantitation of encapsidated recombinant adeno-associated virus DNA in crude cell lysates and tissue culture medium by quantitative, real-time PCR. J Virol Methods 137, 193-204.

Nazerian, K. and Fadly, A.M., 1982. Propagation of virulent and avirulent turkey hemorrhagic enteritis virus in cell culture. Avian Diseases 26, 816-27.

Nazerian, K. and Fadly, A.M., 1987. Further studies on in vitro and in vivo assays of hemorrhagic enteritis virus (HEV). Avian Diseases 31, 234-40.

Nazerian, K.E.L., MI), Fadly, Aly M. (Holt, MI). 1983. Propagation of hemorrhagic enteritis virus in a turkey cell line and vaccine produced, The United States of America as represented by the Secretary of Agriculture (Washington, DC), United States.

Newberry, L.A., Skeeles, J.K., Kreider, D.L., Beasley, J.N., Story, J.D., McNew, R.W. and Berridge, B.R., 1993. Use of virulent hemorrhagic enteritis virus for the induction of colibacillosis in turkeys. Avian Dis 37, 1-5.

Ranheim, T., Mathis, P.K., Joelsson, D.B., Smith, M.E., Campbell, K.M., Lucas, G., Barmat, S., Melissen, E., Benz, R., Lewis, J.A., Chen, J., Schofield, T., Sitrin, R.D. and Hennessey, J.P., Jr., 2006. Development and application of a quantitative RT-PCR potency assay for a pentavalent rotavirus vaccine (RotaTeq). J Virol Methods 131, 193-201.

Rautenschlein, S. and Sharma, J.M., 1999. Response of turkeys to simultaneous vaccination with hemorrhagic enteritis and Newcastle disease viruses. Avian Dis 43, 286-92.

Rohr, U.P., Heyd, F., Neukirchen, J., Wulf, M.A., Queitsch, I., Kroener-Lux, G., Steidl, U., Fenk, R., Haas, R. and Kronenwett, R., 2005. Quantitative real-time PCR for titration of infectious recombinant AAV-2 particles. J Virol Methods 127, 40-5.

Schalk, J.A., van den Elzen, C., Ovelgonne, H., Baas, C. and Jongen, P.M., 2004. Estimation of the number of infectious measles viruses in live virus vaccines using quantitative real-time PCR. J Virol Methods 117, 179-87.

Segura, M.M., Monfar, M., Puig, M., Mennechet, F., Ibanes, S. and Chillon, M., 2010. A real-time PCR assay for quantification of canine adenoviral vectors. J Virol Methods 163, 129-36.

Sharma, J.M., 1994. Response of specific-pathogen-free turkeys to vaccines derived from marble spleen disease virus and hemorrhagic enteritis virus. Avian Dis 38, 523-30.

van den Hurk, J.V., 1990. Propagation of group II avian adenoviruses in turkey and chicken leukocytes. Avian Dis 34, 12-25.

Veldwijk, M.R., Topaly, J., Laufs, S., Hengge, U.R., Wenz, F., Zeller, W.J. and Fruehauf, S., 2002. Development and optimization of a real-time quantitative PCR-based method for the titration of AAV-2 vector stocks. Mol Ther 6, 272-8.

Villegas, P. 2008. Titration of biological suspensions. In: Dufour-Zavala, L. (Ed), Isolation, Identification, and Characterization of Avian Pathogens, The American Association of Avian Pathologists, Athens, GA, pp. 217-221.

Wang, F., Puddy, A.C., Mathis, B.C., Montalvo, A.G., Louis, A.A., McMackin, J.L., Xu, J., Zhang, Y., Tan, C.Y., Schofield, T.L., Wolf, J.J. and Lewis, J.A., 2005. Using QPCR to assign infectious potencies to adenovirus based vaccines and vectors for gene therapy: toward a universal method for the facile quantitation of virus and vector potency. Vaccine 23, 4500-8.

Wolf, J.J., Wang, L. and Wang, F., 2007. Application of PCR technology in vaccine product development. Expert review of vaccines 6, 547-58.

Chapter 5

Characterization of Cellular Receptors for Turkey Hemorrhagic Enteritis Virus on MDTC-RP19, B Lymphoblastoid Cells

5.1. Abstract

Turkey hemorrhagic enteritis virus (THEV) is of economic importance to the poultry industry and can lead to devastating damage in an unprotected turkey population. THEV is a member of the genus *Siadenovirus*, family *Adenoviridae* and is known to specifically target B-lymphocytes in turkeys and other avian species. The cell receptors facilitating viral attachment and internalization have not yet been characterized. For our studies, a B-lymphoblastoid cell line (MDTC-RP19; RP19 cells for short), commonly used to produce hemorrhagic enteritis (HE) cell culture vaccines, was employed as the viral-specific target cell. To identify the surface components necessary for virus entry, cells were pre-treated with a number of reagents including neuraminidases and lectins (to cleave or block sialic acids, respectively), sodium periodate (to oxidize carbohydrates), and proteases. Cells were then centrifuged, rinsed, and re-suspended in media containing THEV. After 1 hour of incubation (time sufficient only for virus entry), cells were centrifuged, rinsed, and lysed (freeze-thaw). The effect on virus entry was measured by determining the residual virus genome copies using qPCR-based titration assay. Neuraminidases and sialic acid-specific lectins (i.e., MAA and SNA) inhibited, to various degrees, virus entry into RP19 cells, suggesting the use of surface α2,3-linked and α2,6-linked sialic acid as an attachment receptor. Moreover, virus entry was reduced by pre-treatment of cells with sodium periodate and proteases, indicating that THEV receptors contain carbohydrate and polypeptide components. THEV receptors were found to be sensitive to bromelain, ficin, and trypsin proteases, but not GluC endoproteinase, implying a unique structure of the virus protein receptors. Receptor proteins were further characterized using a virus overlay protein blot assay, which showed that THEV specifically binds to two cell surface proteins having molecular weights of 69 kDa and 87 kDa. Further work is required to unveil the identity of these protein components.

5.2. Introduction

THEV (also known as turkey adenovirus 3) affects turkeys of 4-12 weeks of age and exists naturally in two types of strains: virulent strains (THEV-V), which cause an immune-mediated disease (hemorrhagic enteritis; HE) characterized by intestinal hemorrhage, bloody droppings, and mortality rates of up to 60% (Gross and Moore, 1967); and avirulent strains (THEV-A), which are used as vaccines (Fadly and Nazerian, 1984; Fadly et al., 1985). Both virulent and avirulent strains cause splenomegaly in susceptible birds and a transient period of immunosuppression, during which secondary bacterial infections can occur (Pierson and Fitzgerald, 2008). THEV, the only member of the species *Turkey Siadenovirus A* (TAdV-A), belongs to the genus *Siadenovirus* of family *Adenoviridae* (Mayo, 2002). The virus has a typical adenovirus structure with an icosahedral capsid and a linear, non-segmented, dsDNA genome of about 26 kb (Davison and Harrach, 2011). The genus was so named because it contains an open reading frame (ORF 1) encompassing a sequence of high homology to the bacterial sialidases (Davison et al., 2000). Neither the transcription nor the expression and function of this sialidase homologue have been investigated during the THEV infectious cycle. Frog adenovirus 1 is the genus type species and the second member to be discovered (Clark et al., 1973). In the last few years, the genus has expanded remarkably upon the discovery of more siadenoviruses of avian origin, including raptor adenovirus 1 (Kovács and Benkő, 2009), budgerigar adenovirus 1 (Katoh et al., 2009), psittacine adenovirus 2 (Wellehan et al., 2009), great tit adenovirus 1 (Kovács et al., 2010), south polar skua adenovirus 1 (Park et al., 2012), gouldian finch adenovirus 1 (Joseph et al., 2014), Chinstrap penguin adenovirus 1 (Lee et al., 2014), and one more of reptilian origin, Sulawesi tortoise adenovirus 1 (Rivera et al., 2009).

Virus entry into target cells requires highly specific interactions among the molecules on the surface of both entities. In general, members of the family *Adenoviridae* access their host cells through a two-step clathrin-dependent receptor-mediated endocytosis; the first step is the attachment to a primary receptor through the protruding fiber proteins, and the second is the binding to a secondary receptor, through the penton proteins, which mediate virus internalization into cells (Nemerow, 2000; Zhang and Bergelson, 2005). Adenoviral fiber protein head/knob domains were found to interact

with a variety of primary receptors for attachment, including coxsackievirus-adenovirus receptor (CAR) (Bergelson et al., 1997; Roelvink et al., 1998), major histocompatibility (MHC) class I (Hong et al., 1997), vascular cell adhesion molecule-1 (VCAM-1) (Chu et al., 2001), heparan sulfate proteoglycan / glycosaminoglycans (HSPG / HS-GAGs) (Dechecchi et al., 2000; Summerford and Samulski, 1998; Tuve et al., 2008), sialic acids (Arnberg et al., 2000a; Lenman et al., 2015; Li et al., 2009), CD46 (a membrane cofactor protein) (Segerman et al., 2003; Wu et al., 2004), CD80 (B7.1) and CD86 (B7.2) (Short et al., 2004), desmoglein 2 (Wang et al., 2011), and ganglioside disialylated glycan (GD1a) (Nilsson et al., 2011); while the viral penton proteins were found to bind to several integrin molecules including αv, α3β1, and α5β1 integrins (Davison et al., 1997; Salone et al., 2003; Summerford et al., 1999; Wickham et al., 1993). CAR is constitutively expressed on the intercellular junctions and tight junctions of epithelial cells (Freimuth et al., 2008; Law and Davidson, 2005), but not on lymphocytes (Richardson et al., 2005). Therefore, THEV is not expected to bind to target lymphocytes through a CAR molecule. Likewise, αv integrins (vitronectin receptors) cannot be used for THEV internalization due to the absence of RGD motif on the penton protein. However, it was proposed that THEV may bind to α4β1 integrin (fibronectin receptor), which is known to be expressed on B cells among other cell types, as it contains an LDV motif (Suresh et al., 1995). Yet, no experimental evidence has been made to support this proposal.

Human blood lymphocytes were found nonpermissive to human adenovirus 2 (HAd-2) infection (Horvath and Weber, 1988), and it was reported that lymphocytes are not normally susceptible to adenoviral infections due to the absence or very low expression of the required attachment receptors (Leon et al., 1998). To the best of our knowledge, thus far, THEV is the only adenovirus found to naturally infect B lymphocytes (Suresh and Sharma, 1996). The virus has also been reported to provide a life-long immunity in vaccinated birds (Beach, 2006), which makes it a strong candidate as a vaccine and gene-delivery vector for various veterinary applications. To date, the mechanisms of the entry of THEV into host cells have not been investigated. Recent structural studies and glycan microarray analysis have shown that THEV fiber knob domain binds to 3'- and 5'-sialyllactose (Singh et al., 2015). Also, HAd-37 was reported

to attach to a B lymphoblastoid cell line through surface sialic acids (Arnberg et al., 2000a). The aim of the present study was to investigate the role, if any, of cell surface sialic acids in THEV entry and to determine the structural components of the virus receptors on RP19, B lymphoblastoid cells. The cells were subjected to different chemical and enzymatic treatments to inactivate or destroy a variety of cell surface components. The effect of these treatments on virus entry was then measured using a THEV-specific qPCR-based infectivity assay (Mahsoub et al., 2012). The protein moieties of potential THEV receptors were further characterized using a virus overlay protein blot assay.

5.3. Materials and methods

5.3.1. Cells and virus

RP19, a Marek's disease virus-induced B-lymphoblastoid cell line susceptible for THEV infection (Nazerian et al., 1982), was purchased from the American Type Culture Collection (ATCC, Manassas, VA) and used during the study. Cells were grown as suspension cultures in complete Liebovitz-McCoy (CLM) media (Table 3-2; Chapter 3) at 41°C in a humidified atmosphere with 5% CO_2. Cells inoculated with the virus were maintained in a serum-reduced (SR) LM media (SRLM; Table 3-2; Chapter 3) under the same incubation conditions stated above. The virus used in this work is the avirulent strain of THEV obtained from commercially available cell culture HE vaccines. A stock of virus suspension was prepared by reconstituting the lyophilized vaccine product in SRLM media and stored in small aliquots at -20°C. When needed, an aliquot of virus stock was diluted in SRLM media and used to inoculate the cells. The virus infectious titer, expressed as infectious viral particles (IVPs), was determined using a qPCR-based virus infectivity assay established in our laboratory (Mahsoub et al., 2011; Mahsoub et al., 2012). A brief description of this assay is described below. The infectious titer of the virus batch used in this study was 5.59×10^7 IVPs/0.1 ml. The multiplicity of infection (MOI) is, therefore, calculated as the number of IVPs per cell.

5.3.2. Virus infection and qPCR-based titration assay

A qPCR-based infectivity assay was developed and optimized in our laboratory to specifically measure the THEV infectivity in RP19 cell culture system (Mahsoub et al., 2011; Mahsoub et al., 2012). In this assay, RP19 cells are inoculated with THEV, washed 2-3 times with a washing buffer to remove unbound/non-internalized virus particles, resuspended in 200 µl of phosphate-buffered saline (PBS), and stored at -20°C until DNA extraction. The cells are then lysed by three freeze-thaw cycles and total DNA is extracted from cell lysates using QIAamp® DNA Mini kit (Qiagen, Valencia, CA) following the Blood or Body Fluids Spin Protocol. Using qPCR, the number of attached/internalized virus particles is estimated by determining the virus genome copy number (vGCN) in the extracted DNA. Reaction mixtures of 25 µl are made of SYBR Green I mastermix (12.5 µl; 2x SensiMix™ SYBR® & Fluorescein kit, Bioline, Taunton, MA), 10 mM forward and reverse primers (0.5 µl each; sequences are shown in Table 3-1; Chapter 3), UltraPure™ DNase and RNase-free distilled water (7.5-10.5 µl; Gibco®, Life Technologies, Grand Island, NY), and DNA template (1-4 µl). Reactions are loaded into Eppendorf™ real-time PCR tube strips with Masterclear™ cap strips (Fisher Scientific, Fair Lawn, NJ). The assay is carried out in an iCycler thermal cycler (Bio-Rad, Hercules, CA) with an initial incubation step at 95°C for 10 min for polymerase activation and template denaturation, followed by 40 cycles of amplification at 95°C for 15 s, 56°C for 15 s, and 72°C for 15 s. Melt curve analysis is always applied in every qPCR run for the detection of potential non-specific amplification. The total number of virus particles in a sample is then calculated by multiplying the vGCN/µl DNA (obtained from qPCR) by the total volume of DNA extract from that sample.

5.3.3. Flow cytometry for verification of sialic acid expression

The expression of sialic acid (SA) on RP19 cells was measured by staining with fluorescein isothiocyanate (FITC)-labeled wheat germ agglutinin (WGA; Sigma-Aldrich), followed by fluorescent-activated cell sorter (FACS) analysis. A stock solution of FITC-WGA at a concentration of 1 mg/ml was made by dissolving the lyophilized product in 2 ml of 50mM Tris-HCl (pH adjusted to 7.4). The solution was then stored in

small aliquots at -20°C until needed. The staining procedure was performed by incubating a total of 1×10^6 RP19 cells (washed once with PBS) with 1 µg of FITC-WGA in 1 ml of ice-cold PBS (pH 7.2) on ice for 1 h in darkness. Unbound WGA was removed by washing the cells 3 times with PBS. The cells were finally resuspended in 1 ml of cold PBS. The number of cells positive for WGA binding was assayed using a FACScan flow cytometer (Becton, Dickenson, and Company, Franklin Lakes, NJ). Data was analyzed and images were generated using FlowJo 7.6.3 software (FlowJo, Ashland, OR).

5.3.4. Neuraminidase treatments and sialic acid quantitation assay

The release of cell surface sialic acid from RP19 cells after neuraminidase treatment was verified and measured using Sialic Acid (NANA) Assay Kit (Abcam, Cambridge, MA) following the colorimetric assay protocol. Neuraminidase solutions at a concentration of 50 mU/ml were made in PBS containing 5%FBS (PBS-FBS Buffer 1; PFB-1) at pH 5.25 (adjusted with HCl and sterile-filtered through a 0.22 µm syringe filter) for CPN, VCP, and AUN or at pH 7.2 for CPN and VCP only. RP19 cells were washed once with PFB-1 and diluted at a density of 4×10^5 cells/ml. To seventy 1.5-ml Eppendorf microcentrifuge tubes, 0.5 ml of cell suspension (i.e., 2×10^5 cells) were added, pelleted, and divided into seven groups of ten. The pellets of each group were resuspended individually in 200 µl of a neuraminidase solution (i.e., 10 mU) and incubated at 37°C. Two groups were mock-treated with 200 µl of PFB-1 at pH 5.25 or 7.2 for use as negative controls and background calculations. Duplicate cell samples were collected from each group at 0, 30, 60, 90, and 120 min post-incubation (mpi) for the measurement of released cell surface SA. Cells were centrifuged at 3000 rpm for 7 min and supernatants (approx. 200 µl) were transferred into new tubes. Cell pellets were resuspended in SRLM media and placed in the incubator to be used later in infection experiment as described under subsection 5.2.5, Expt. 2. Small aliquots were taken from cells treated at pH 5.25 and their integrity was verified under a light microscope based on their appearance compared with the untreated control cells. All cells had normal morphology. One supernatant sample per time point was used for SA measurement in each treatment group (i.e., enzyme/pH). The assay was performed in a 96-well flat-bottom plate using 50 µl of the collected supernatants. The OD values were measured at

570 nm using SpectraMax® 340PC^{384} Microplate Reader and SoftMax Pro v5.4.5 software (Molecular Devices, Sunnyvale, CA). Since the sample volume for use in the assay is limited to 50 µl, the total amount of released SA in the original 200-µl samples (i.e., from 2×10^5 cells) was calculated by multiplying by a factor of 4.

5.3.5. Neuraminidase treatment

Expt. 1: RP19 cells were seeded at 4×10^5 cells/ml and incubated overnight. To 1.5-ml Eppendorf microcentrifuge tubes, 0.5 ml of cell suspension was added, washed once with PBS containing 2% FBS (PBS-FBS Buffer 2; PFB-2; pH7.2), and pelleted by centrifugation at 3000 rpm for 5 min. Duplicate cell pellets were each treated with 100 µl of neuraminidase from *Clostridium perfringens* (CPN; type V), *Vibrio cholera* (VCN; type III), or *Arthrobacter ureafaciens* (AUN) (all from Sigma-Aldrich) at a concentration of 0, 1, or 10 mU/ml in PFB-1 and incubated at 37°C for 1 h. Cells were washed twice with SRLM media and pelleted. Cell pellets were resuspended with 100 µl of virus in SRLM media and incubated for 1 h at 41°C. Cells were washed twice with SRLM media, resuspended in 200 µl PBS, and stored at -20°C until DNA extraction. Virus titer in different groups was measured and calculated as described in the infectivity assay.

Expt. 2: Neuraminidase-treated RP19 cells from the sialic acid assay described above were used in this experiment. The experiment included treating cells with 10 mU of NAs in PFB-2 at pH5.25 or 7.4. After the collection of supernatants for use in the assay, cell pellets were resuspended in SRLM media and incubated for about 2 h at 41°C. Post-incubation, cells were pelleted, resuspended in 200 µl of virus in SRLM media (MOI = 50), followed by incubation for 1 h at 41°C. Virus titer in different groups was measured and calculated as described in the infectivity assay.

Expt. 3: RP19 cells were washed once with PBS containing 2% serum (1:1 chicken serum & FBS; PBS-Serum Buffer; PSB) and 2×10^5 cells were added to 1.5-ml tubes and pelleted. Triplicate cell pellets were then resuspended with 100 µl of CPN or VCN at a concentration of 0, 1, or 10 mU/ml in PSB and incubated at 41°C for 1 h. After 3 washes with PSB, cells were inoculated with 100 µl of virus in SRLM media (MOI = 50). One hour post-incubation, cells were washed twice with PSB, resuspended in 200 µl

of PBS, and stored at -20°C. Virus titer in different groups was measured and calculated as described in the infectivity assay.

5.3.6. Lectin treatment

Expt. 1: RP19 cells (2×10^5) were washed once with PBS containing 1% FBS (PBS-FBS Buffer 3; PFB-3) and pelleted in 1.5-ml tubes. Three types of lectins (all from Sigma-Aldrich): WGA (molecular weight, 36 kDa), *Maackia amurensis* agglutinin (MAA; molecular weight, 130 kDa), and *Sambucus nigra* agglutinin (SNA; molecular weight, 140 kDa), were each dissolved in PBS and solutions of 10 µg per ml were made in PFB-3. To groups of triplicate cell pellets, 1 ml of lectin or PFB-3 for control was added, followed by incubation on ice for 1 h. Cells were washed twice with PFB-3 and pelleted. No pellets were formed from SNA treatment and therefore, samples of this group were discarded. Cell pellets were resuspended in 100 µl of virus in SRLM media (MOI = 20) for 1 h at 41°C. Cells were then washed twice with PFB-2, resuspended in 200 µl of PBS, and stored at -20°C. Virus titer in different groups was measured and calculated as described in the infectivity assay.

Expt. 2: RP19 cells (2×10^5) were washed once with PFB-1 and pelleted in 1.5-ml tubes. Cell pellets (in triplicates) were resuspended in 100 µl of WGA at concentration of 0, 10, 50, or 100 µg/ml in PFB-1 and incubated on ice for 1 h. Cells were washed twice with PFB-1 and inoculated with 200 µl of virus in SRLM media (MOI = 50). Post-inoculation cells were washed twice with PFB-1, resuspended in 200 µl of PBS, and stored at -20°C. Virus titer in different groups was measured and calculated as described in the infectivity assay.

Expt. 3: RP19 cells (2×10^5) were washed once with PSB and pelleted in 1.5-ml tubes. To cell pellets in triplicates, 100 µl of WGA, MAA, or SNA at a concentration of 10 or 100 µg/ml in PSB were added and mixed well. Control cells received 100 µl of PSB with no lectins. Treated cells were incubated at 41°C for 1 h. Cells were then washed thrice with PSB. No cells pellets were found in the tubes of all 100 µg treatments, most likely, due to some damaging effects of lectins at this concentration on the cells. Cell pellets from the 10 µg treatments were resuspended with 100 µl of virus in SRLM media (MOI = 50) and incubated at 41°C for 1 h. Cells were then washed twice with

PSB, resuspended in 200 µl of PBS, and stored at -20°C. Virus titer in different groups was measured and calculated as described in the infectivity assay.

Expt. 4: The procedure in Expt. 3 above was essentially followed, except with two main changes: 1) WGA, MAA, or SNA were used at concentrations of 10 or 50 µg/ml, 2) cells were inoculated with virus at MOI of 20. When this experiment was repeated under the exact same conditions, no cell pellets were formed after all the treatments of 50 µg/ml and the treatment of MAA at 10 µg/ml. The experiment was continued with the remaining samples.

5.3.7. Sodium periodate ($NaIO_4$) treatment

RP19 cells (2×10^5) were washed once and pelleted in 1.5-ml Eppendorf microcentrifuge tubes. Cell pellets (in triplicates) were resuspended with 100 µl of $NaIO_4$ (Acros Organics, Fisher Scientific) at a concentration of 0, 0.1, or 1 mM PBS (pH 7.2). Cells were incubated for 30 min at room temperate, in darkness. Post-incubation, 200 µl of 0.22% (v/v) glycerol solution in PBS was added to each tube to neutralize unreacted periodate (Stevenson et al., 2004). Cells were then washed twice and inoculated with 100 µl of virus in SRLM media (MOI = 50), followed by incubation for 1 h at 41°C. A small cell sample from each treatment was examined under a light microscope and all looked intact and healthy. Post-inoculation, cells were washed thrice, resuspended in 200 µl of PBS, and stored at -20°C until DNA extraction. Virus titer in different groups was measured and calculated as described in the infectivity assay.

5.3.8. Protease treatment

Expt. 1-2: Two experiments were run using the same proteases, but under different enzyme concentrations and MOI conditions. In the 1st experiment, RP19 cells (1×10^6) were washed once with HBSS (Gibco®, Life Technologies) and resuspended in 100 µl of PFB-2 in 1.5-ml Eppendorf microcentrifuge tubes. Suspended cells were mixed with 100 µl of bromelain (a cysteine endopeptidase from pineapple stem), ficin (a cysteine protease from fig tree latex), or V8-GluC (endoproteinase Glu-C; a glutamic or aspartic acid-specific serine endoproteinase expressed by *Staphylococcus aureus* protease V8 gene) (all purchased from Sigma-Aldrich) solution at concentrations of 0, 200, or

2000 mU/ml in PFB-2. The cells were incubated at 37°C for 30 min in a shaking water bath. Small cells samples were taken from untreated and 2000 mU/ml protease treatments and checked with a light microscope for damage or lysis. Cells in treated and untreated groups looked similar. Post-treatment, cells were washed twice with HBSS containing 2%FBS (HFB) and incubated with 200 µl virus suspension in SRLM media (i.e., MOI = 50) at 41°C for 1 h. Cells were then washed twice with HFB, resuspended in 200 µl of PBS, and stored at -20°C. Virus titer was measured and calculated for the different groups as described in the infectivity assay. In the 2nd experiment, the same procedure described above for Expt. 1 was essentially followed except for two main changes: 1) two sets of cell samples were used and treated with either 100 µl (similar to Expt. 1) or 200 µl of the mentioned proteases, 2) cells were inoculated at an MOI of 100 (i.e., twice the dose used in Expt. 1).

Expt. 3: In this experiment, the effect of cell treatment with high concentrations of bromelain on virus infection was investigated. RP19 cells (1×10^6) were washed once with PBS and pelleted. Cell pellets were resuspended in 200 µl of bromelain solution at concentrations of 0, 500, or 5000 mU/ml in PBS. Cells were washed twice with PF and incubated with 100 µl of virus suspension in SRLM media (MOI = 20) at 41°C for 1 h. Before inoculation, the cell viability was measured using the trypan blue exclusion test. Cells were washed twice with PF, resuspended in 200 µl of PBS, and stored at -20°C until used later for virus titration as described above. Every treatment included triplicate cell samples that were individually treated.

Expt. 4: RP19 cells (2×10^5) were pelleted, resuspended in 100 µl of trypsin (a serine protease; 500 mg/ml, Life Technologies) at a concentration of 0, 50, or 500 µg/ml in PBS, and incubated in a 37°C-water bath for 30 min with shaking every 10 min. Cells were washed twice with PF, inoculated with 100 µl of virus in SRLM media (MOI = 50), and then incubated as described above. Post-inoculation, cells were washed twice with PF, resuspended in 200 µl PBS, and stored at -20°C until used later for virus titration as described above. Every treatment included triplicate cell samples that were individually treated and data was reported as means from two independent experiments.

5.3.9. Virus overlay protein blot assay (VOPBA)

Preparation of RP19 cell membrane proteins: A variety of membrane protein isolation methods (including general protocols and commercial kits) have been tried to find the most suitable and productive procedure to use with the suspended RP19 cells. The concentration of protein fractions isolated from these methods was measured using the Pierce™ BCA Protein Assay Kit (Thermo Fisher Scientific, Waltham, MA), following the microplate procedure. Also, to explore the separation patterns of these protein in polyacrylamide gel, samples from the membrane and cytosolic protein preparations were mixed at 3:1 (v/v/) with 4× Laemmli sample buffer (Bio-Rad). Samples (45 µl) were loaded into a 4-12% TGX Mini-PROTEAN TGX precast gel (Bio-Rad) and subjected to sodium dodecyl sulfate-polyacrylamide gel electrophoresis (SDS-PAGE) at 180 V for 30-40 min to separate the proteins by molecular weight. The gel was then stained following the Coomassie Blue general staining procedure and images were taken with a photo scanner (HP Scanjet G3010, Hewlett-Packard Development Company, L.P., Palo Alto, CA). For the VOPBA, plasma membrane proteins were purified based on methods adapted from (Wu et al., 2001) and (Jindadamrongwech et al., 2004). RP19 cells were seeded at 1.5×10^6 cells/ml or 5×10^5 cells/ml and cultured for 2 or 3 days, respectively. Cells were harvested, washed twice with 20 or 10 ml, respectively, of PBS and pelleted by centrifugation at 1200 rpm for 10 min at 5°C. The two cell pellets were resuspended each in 5 ml of a cell resuspension solution (250 mM sucrose, 20 mM HEPES (pH 7.0), 1 mM EDTA, and 2 µg/ml aprotinin and leupeptin) containing 0.2% Triton X-100 and incubated for 5 min on ice, followed by vigorous vortexing for cell lysis. The complete lysis was verified by examining a cell sample under a light microscope for the absence of intact, shiny, plasma membranes. Cell lysates were centrifuged at 500 ×*g* for 15 min. Pellets containing subcellular organelles, nuclei, and cell debris were discarded and the supernatants containing the cell membranes were transferred into Thinwall,× Ultra-Clear™ centrifuge tubes (Beckman Coulter, Brea, CA) and stored at -20°C until next step. Tubes were centrifuged at 200,000 ×*g* (or 45,900 rpm) for 1 h at 4°C using Optima L-90K ultracentrifuge and SW 55 Ti rotor (Beckman Coulter). Supernatants were removed and the resultant pellets containing the membrane fraction were resuspended in 1 ml of ice-cold 10 mM Tris-HCl (pH 8.1) containing 10

µg/ml aprotinin and leupeptin (both from Sigma-Aldrich), mixed well by pipetting, and then vortexed for complete dissolution. Protein concentration in these extracts was measured using the BCA Protein Assay Kit (Thermo Fisher Scientific).

SDS-PAGE: Before use in the SDS-PAGE, protein samples were mixed at 1:1 (v/v) with 2× Laemmli sample buffer (Bio-Rad) containing 5% 2-Mercaptoethanol and incubated at 90°C for 2 min. Samples (~25 µl) were loaded into a 7.5% Mini-PROTEAN TGX precast gel (Bio-Rad) at 150 V for 1 h.

VOPBA: Proteins separated by SDS-PAGE were electroblotted onto a polyvinylidene fluoride membrane (PVDF; Immobilon®-P, Sigma-Aldrich) at 25 V for 7 min. The membrane was then blocked to prevent unspecific binding by incubation in the refrigerator overnight with 5% (w/v) skim milk in a solution of PBS (pH 7.4) containing 0.02% Tween-20 (PBS-T). After blocking, the membrane was washed 3 times with PBS-T, 3 min each; on a plate shaker. The membrane was then incubated for 1 h at room temperature (RT) with a THEV suspension (made from a lyophilized HE vaccine) in PBS-T containing 0.5% skim milk, followed by washing 3 times with PBS-T, 5 min each; on a plate shaker. The membrane was incubated with a 1:500 dilution of anti-THEV antibodies (hyperimmune serum from THEV-infected turkeys) in PBS-T containing 0.5% (w/v) milk, for 30 min at RT on a plate shaker, followed by 3 washes as described above to remove unbound primary antibodies. The membrane was then incubated with a 1:5000 dilution of horseradish peroxidase (HRP)-conjugated goat anti-turkey antibody (Kirkegaard & Perry Laboratories [KPL], Gaithersburg, MD) in PBS-T containing 0.5% (w/v) milk for 1 h at RT, on a plate shaker. To remove unbound secondary antibody, the membrane was washed 3 times with ample amounts of PBS-T. Protein bands that reacted with THEV were visualized by incubating the membrane with 8 ml of TMB membrane peroxidase substrate (KPL) for 10 minutes at RT. Images for the membrane were taken with an HP Scanjet photo scanner (Hewlett-Packard Development Company, L.P.).

5.3.10. Statistical analysis

Data from the qPCR-based virus titration/infectivity assay was transformed to the $\log_{10}$ format, before statistically analyzed with one-way analysis of variance (ANOVA).

When statistical significance existed, multiple comparisons between treatment means were performed by Tukey-Kramer HSD (Honestly Significant Difference) test using JMP® Pro (v. 10.0.0, SAS Institute, Inc., Cary, NC). The significance level was set at $P \leq 0.05$. Original qPCR titer data was used in ANOVA for calculation of treatment means. Virus titers in the different treatment groups were presented as percentages in relation to the virus titer in untreated control group, which was normalized as 100%. These percentages were used to create the graphs for results presentation.

5.4. Results

5.4.1. THEV attachment/entry requires sialic acid

The expression of sialic acid on the RP19 cell surface was confirmed by staining with a FITC-labelled WGA, a lectin that binds nonspecifically to all linkages of sialic acids. The stained RP19 cells showed a very strong fluorescence signal as compared to the unstained control (Fig.5-1). To examine the sensitivity of cell surface sialic acids to NA treatments, RP19 cells were pre-incubated for various times with 10 mU of different types of NAs at either acidic or neutral pH conditions, and a commercial sialic acid assay kit was used to quantitate the liberated SA in the supernatants. In general, SAs on RP19 cells were sensitive to all NAs used; however, as shown in Fig. 5-2, the incubation period at which NA treatment caused the maximum removal of cell surface SA varied. This period was found to be 60 min for VCN at pH5.25, 90 min for VCN at pH 7.4, and 120 min for CPN at both pH 5.25 and 7.4 and for AUN at pH 5.25. Based on this experiment, the amounts of SA released from NA-treated RP19 cells appear to be comparable to or even higher than what was described in the literature. One study reported the release of 32-33 nmol of SA after incubating 5×10^8 of lymphocytes from lymph nodes or thoracic duct with 50 U of VCN in culture media at 37°C for 30 min (Woodruff and Woodruff, 1972). This means that every 2×10^5 cells have received 20 mU of VCN and liberated 0.01 nmol of SA. Nevertheless, the proportion of released SA from NA-treated RP19 cells in relation to the overall amount expressed on cell surface is not known.

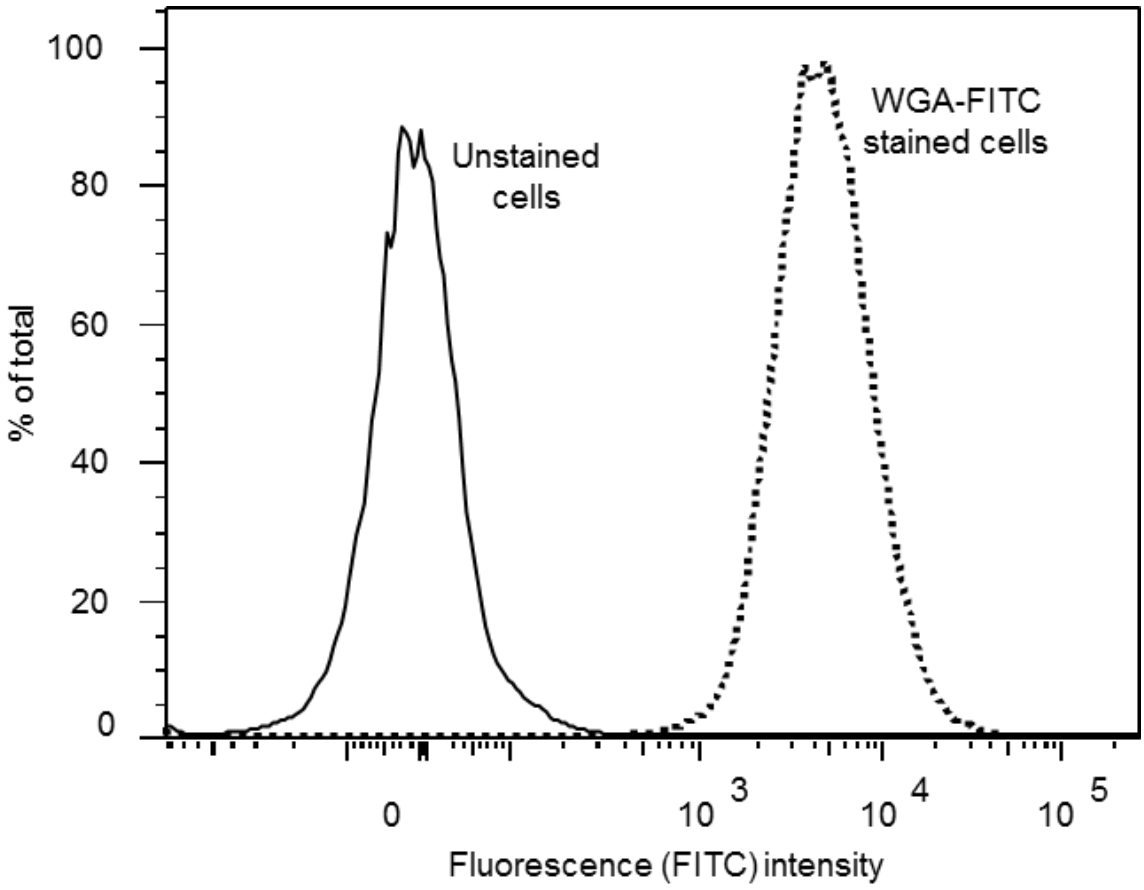

Fig. 5-1. Expression of sialic acid on RP19 cells, as measured by the use of FITC-conjugated WGA in a FACS assay. Cells were incubated on ice with 1 µg of FITC-WGA in PBS for 1 h. Control (unstained) cells were incubated with phosphate-buffered saline (PBS) for the calculation of background fluorescence. Fluorescence data (curve at left) shows that WGA binds to 100% of RP19 cells, indicating that SA is expressed on all cells.

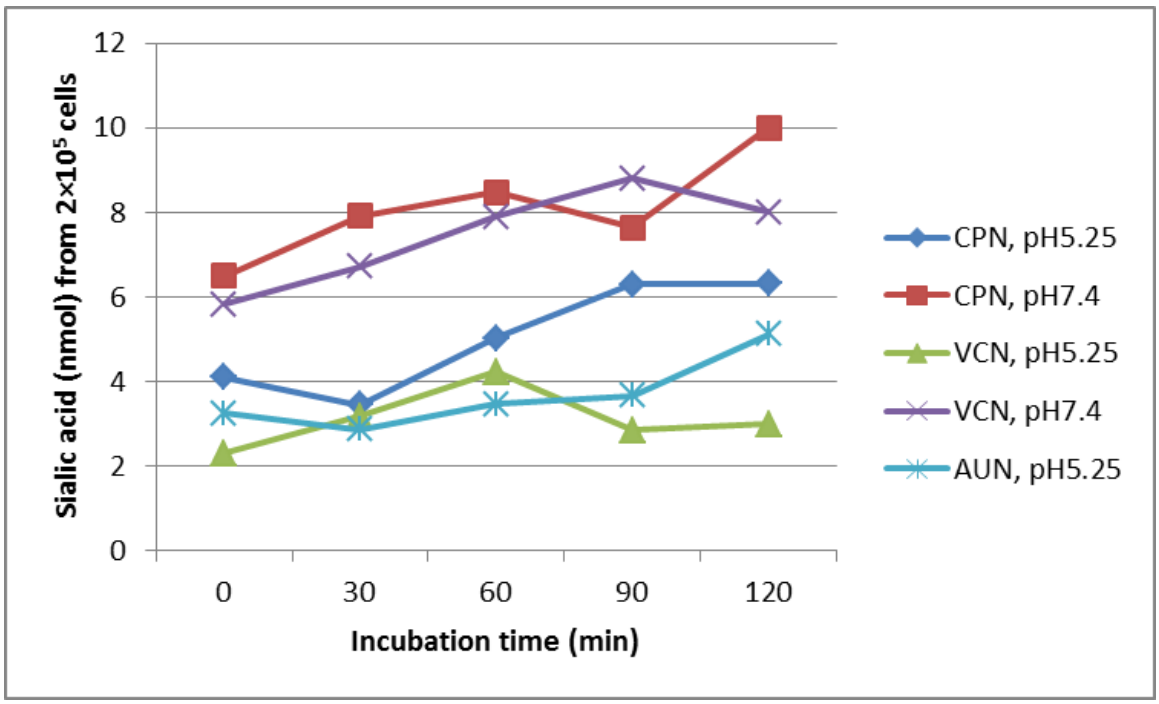

Fig. 5-2. Sialic acid (SA) on RP19 cells is sensitive to different neuraminidase treatments. Cells (2×10^5) were incubated with 10 mU of neuraminidase from *C. perfringens* (CPN), *V. cholerae* (VCN), or *A. ureafaciens* (AUN) under acidic or neutral pH conditions. At the mentioned time points post-incubation, cell samples were collected and the liberated SA was assayed in supernatants using a commercial kit. Untreated cells were used for background calculation which was subtracted from all treated cells.

The role of cell-surface sialic acids in THEV attachment to RP19 cells was investigated by treatment of cells with neuraminidases (NAs) from *Clostridium perfringens* (CPN), *Vibrio cholera* (VCN), or *Arthrobacter ureafaciens* (AUN); the first two NAs cleave α2,3-linked sialic acid residues at a much higher affinity than α2,6-linked and α2,8-linked sialic acid residues, while the AUN cleaves α2,6-linked sialic acid residues at a higher affinity than the other linkages. Experiments were performed under different pH and temperature conditions and the virus entry was measured by means of a qPCR assay. The experimental conditions were varied due to multiple reasons: 1) the effect of NA treatment at various concentrations on the integrity of RP19, B lymphoblastoid cells have not been reported before, 2) RP19 cells grow at temperature and pH conditions (i.e., 41°C; 7.4) different from those recommended for the optimal enzymatic activity (i.e., 37°C and 5.0), and 3) RP19 cells require a much higher serum

content in the growth media (i.e., 30 % for growth and 7.5% for maintenance) than what is used with the majority of other cell lines (i.e., 10% for growth and 0-2% for maintenance). Therefore, the working solutions of NAs were made in different buffers with different pH conditions and the incubation of cells with NAs was also done at 37°C or 41°C in an attempt to obtain the most accurate results possible.

In Expt. 1, where cells were pre-treated with NAs in PBS+2%FBS (pH7.4) and incubated at 37°C, THEV entry was reduced by 14% at 10 mU/ml of CPN, while VCN inhibited THEV entry in a dose-dependent fashion (up at 40% at 10 mU/ml). Surprisingly, under these conditions, AUN treatment increased virus entry (Fig. 5-3). In Expt. 2, cells were pre-treated with 10 mU/ml of NAs made in PBS+5%FBS (pH5.25 or 7.4) and incubated at 37°C for different intervals. When cells pre-treated with AUN, VCN, or CPN at pH5.25 for 30 min, THEV entry was reduced by 47%, 54%, or 23%, respectively as compared to the untreated control (Fig. 5-4). When cells were incubated for 60 min with AUN or VCN at pH5.25, THEV entry was further reduced by 49% or 60%, respectively. The maximum reduction in THEV entry (i.e., by 30%) by CPN at pH5.25 was shown when cells were incubated for 120 min (Fig. 5-4A). When cells were pre-treated with CPN at pH7.4 for 60 or 120 min, THEV entry was inhibited by 14% or 65%, respectively, while pre-treatment of cells with VCN at pH7.4 for 60 min showed a higher inhibition in virus entry than that at the other time points (i.e., by 56%) (Fig. 5-4B). In Expt. 3, where cells were pre-incubated with 1 or 10 mU/ml of NA at 41°C for 1 h, the effect of CPN on reducing virus entry was dose-dependent, while VCN at 10 mU/ml partially inhibited virus entry 21% (Fig. 5-5). From these experiments, it can generally be stated that the change in temperature for NA incubation (i.e., to 41°C) to ensure optimal cell conditions, improved the effect of CPN on reducing THEV entry. VCN treatment worked more efficiently at 37°C. Changing the pH condition to acidic values which favor the neuraminidase activity had a considerable impact on inhibiting THEV entry into RP19 cells, presumably due to an improved cleavage of surface sialic acid residues.

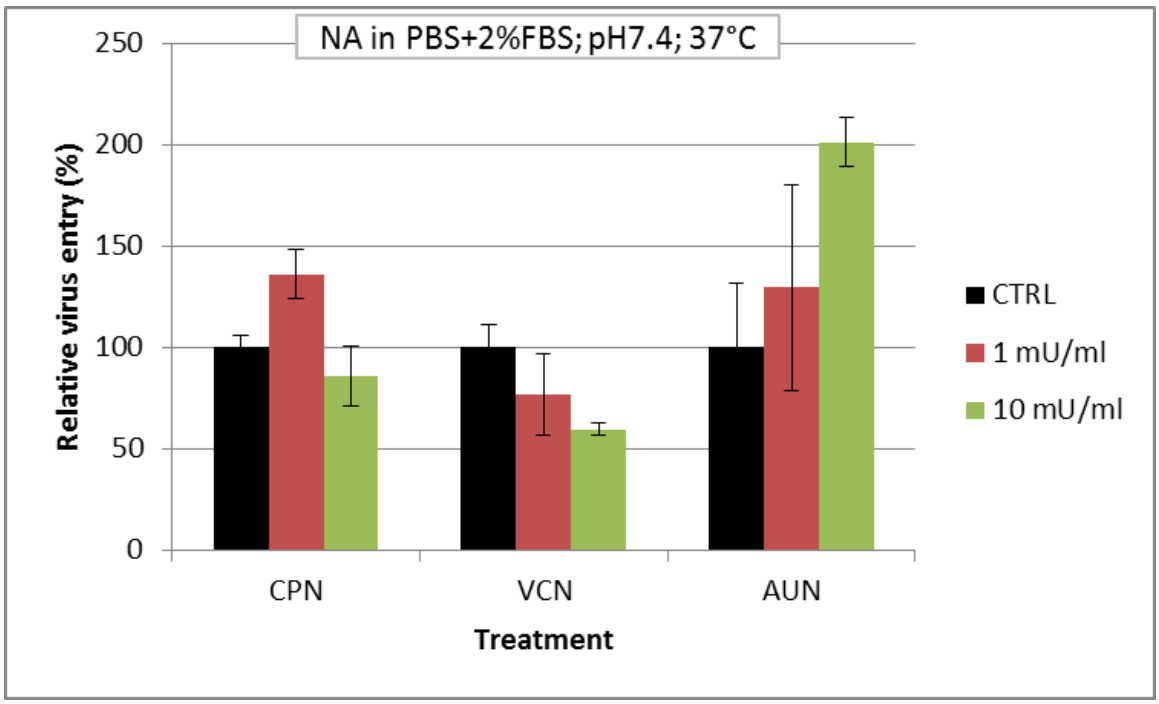

Fig. 5-3. Effect of neuraminidase treatment and incubation at 37°C of RP19 cells on THEV entry. RP19 cells (2×10^5) were pre-incubated at 37°C with 1 or 10 mU/ml of CPN, VCN, or AUN at pH7.4 for 1 h, followed by virus inoculation. Virus entry was measured using a qPCR-based infectivity assay. Percent relative virus entry of different groups is shown in relation to virus entry of untreated cells that was normalized to 100%. Each column represents mean±SEM from individually treated triplicate samples.

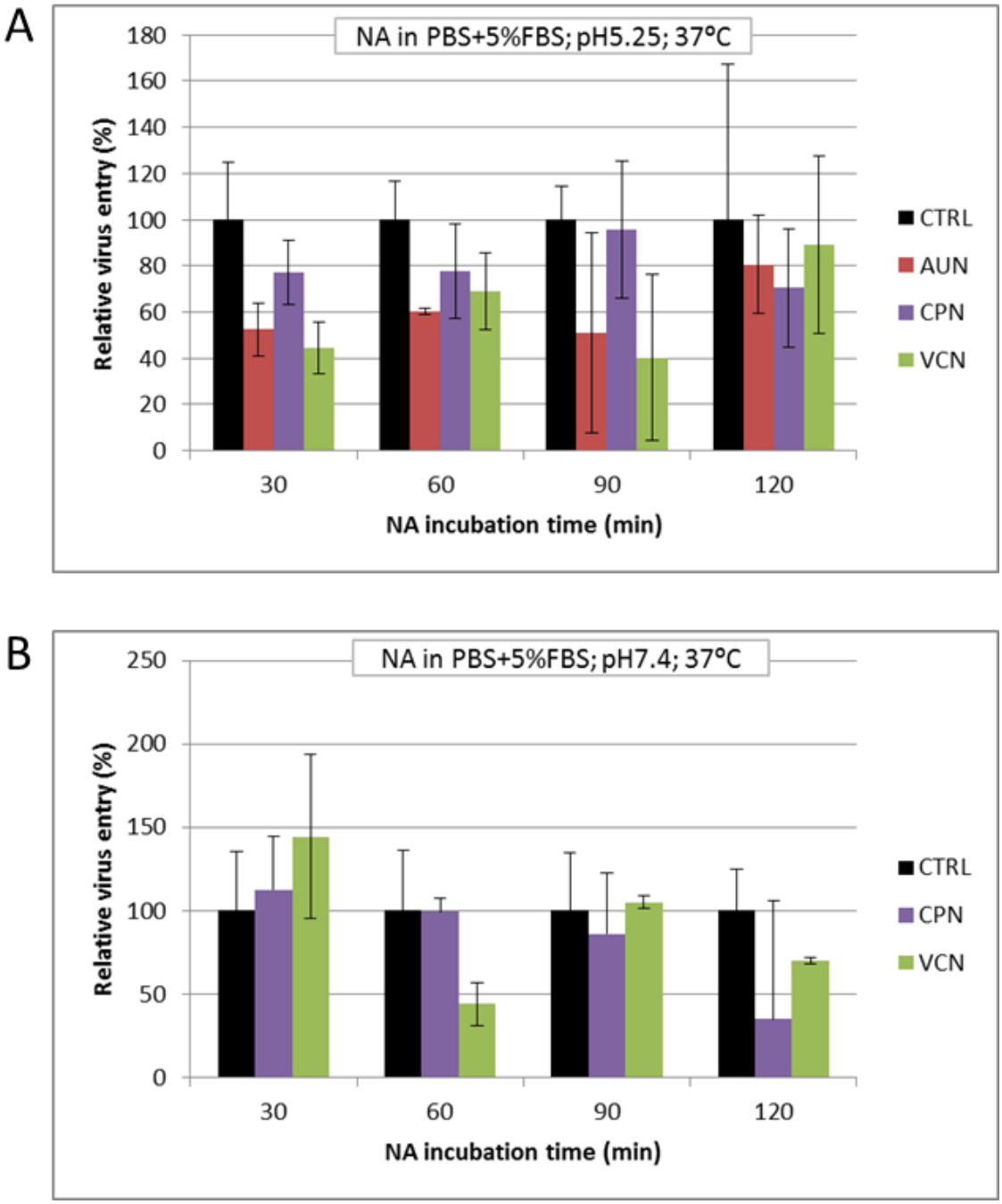

Fig. 5-4. Effect of neuraminidase treatment and incubation at 37°C of RP19 cells on THEV entry. RP19 cells (2×10^5) were pre-incubated with 10 mU/ml of CPN, VCN, or AUN at pH5.25 (A) or pH7.2 (B; AUN was not included) for different time periods, followed by virus inoculation at MOI of 50. Virus entry was measured using a qPCR-based infectivity assay. Percent relative virus entry of different groups is shown in relation to virus entry of untreated cells that was normalized to 100%. Each column represents mean±SEM from individually treated duplicate samples.

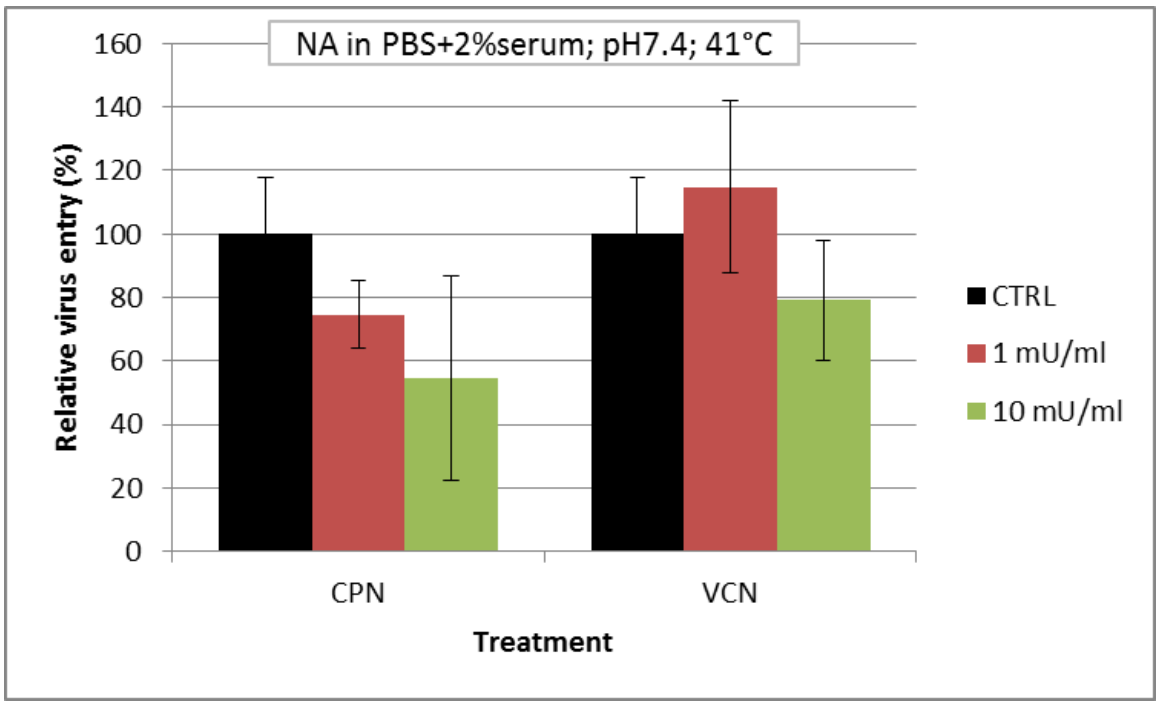

Fig. 5-5. Effect of neuraminidase treatment and incubation at 41°C of RP19 cells on THEV entry. RP19 cells (2×10^5) were pre-incubated with 1 or 10 mU/ml of CPN or VCN at pH7.2 for 1 h, followed by virus inoculation at MOI of 50. Virus entry was measured using a qPCR-based infectivity assay. Percent relative virus entry of different groups is shown in relation to virus entry of untreated cells that was normalized to 100%. Each column represents mean±SEM from individually treated triplicate samples.

To further confirm the role of surface sialic acid residues in THEV binding, RP19 cells were pre-treated with different sialic acid-specific lectins: WGA lectin, which binds nonspecifically at high affinity to all linkages of sialic acid, MAA lectin, which has a high affinity to α2,3-linked sialic acid, and SNA lectin, which has a high affinity to α2,6-linked sialic acids. As with the neuraminidase experiments, various experimental conditions were examined with the lectin treatments in an effort to keep the RP19 cells in good shape post-treatment and after virus inoculation. In the first attempt, RP19 cells (2×10^5) were incubated with a total of 100 µg of WGA, MAA, or SNA in 1 ml of PBS+1%FBS at 37°C for 1 h. When cells were centrifuged after the treatment, no cell pellets were formed, presumably due to some kind of cell-damaging effect. In a second experiment, cells were pre-incubated on ice for 1 h with 10 µg of WGA, MAA, or SNA in 1 ml of PBS+1%FBS and inoculated at 20 IVPs/cell. MAA treatment reduced THEV

entry by 8%, while WGA increased virus entry by 126%, compared with the untreated control (Fig. 5-6). Apparently, the SNA treatment at this concentration and incubation conditions had damaging effects on the cells, as no pellets were formed upon centrifugation immediately after the treatment. Cells from this experiment were examined under a light microscope. WGA treatment of 10 µg was found to cause a strong agglutination of RP19 cells, compared with the MAA and untreated control cells (see Fig. B-1, Appendix B). In a third experiment, the pre-incubation of cells on ice with a total of 5 or 10 µg of WGA in 100 µl of PBS+5%FBS for 1 h, followed by virus inoculation at 50 IVPs/cell, resulted in a slight reduction of virus entry, by 12% or 16%, respectively. Cells that received 1 µg of WGA did not differ in virus entry from the untreated control (Fig. 5-7). A fourth experiment was attempted, where cells were incubated on ice with 100 µl of 10, 50, 100, or 250 µg/ml of WGA, MAA, or SNA in PBS+2%FBS. This experiment was soon terminated because most of the treated cells failed to form pellets upon centrifugation and cell debris was observed in the tubes. This may indicate cytotoxic or other damaging effects of the treatments at the mentioned conditions. Although similar or higher concentrations of lectins have been successfully used at similar experimental conditions with other cell lines (Arnberg et al., 2002; Li et al., 2009), it was evident that these conditions were highly unfavorable for RP19 cells. The effect of lectins on the agglutination and viability of RP19 cells was investigated using light microscopy and flow cytometry (see Appendix B).

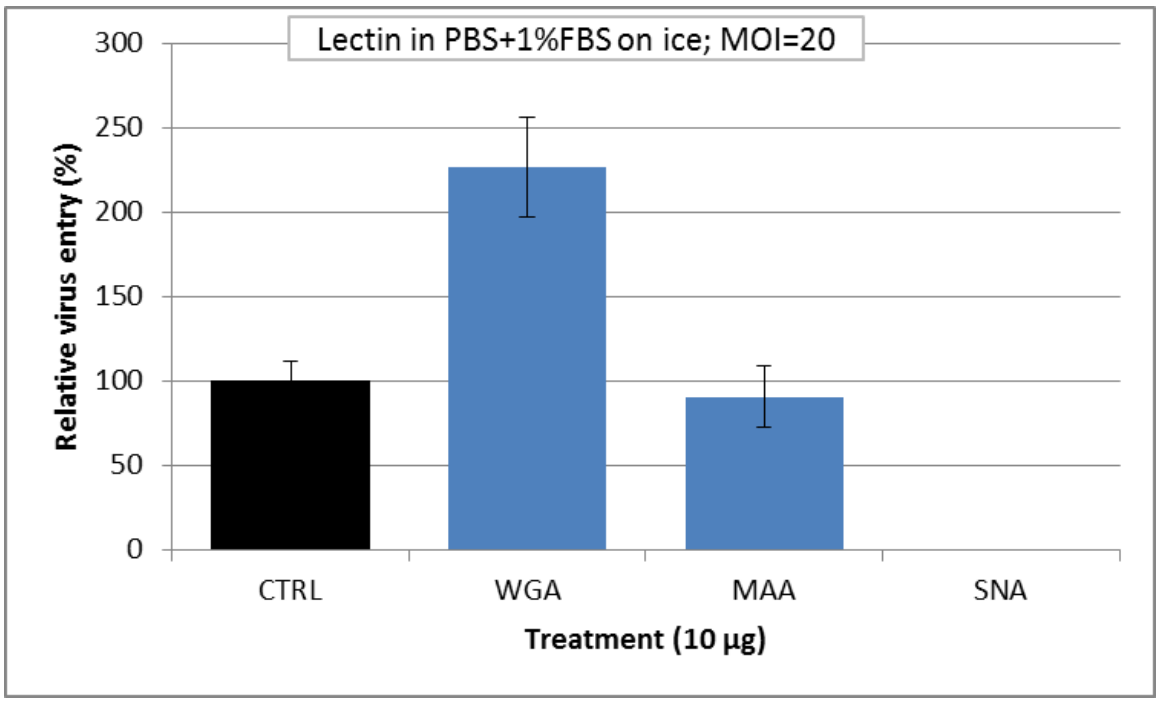

Fig. 5-6. Effect of lectin treatments and incubation on ice of RP19 cells on THEV entry. RP19 cells (2×10^5) were pre-incubated with 10 µg of WGA, MAA, or SNA (in 1 ml of PBS+1%FBS) on ice for 1 h, followed by virus inoculation at MOI of 20. Virus entry was measured using a qPCR-based infectivity assay. Percent relative virus entry of different groups is shown in relation to virus entry of untreated cells that was normalized to 100%. Each column represents mean±SEM from individually treated triplicate samples, except MAL that had duplicate samples only. No results are shown from the SNA treatment as cells were apparently killed by the treatment.

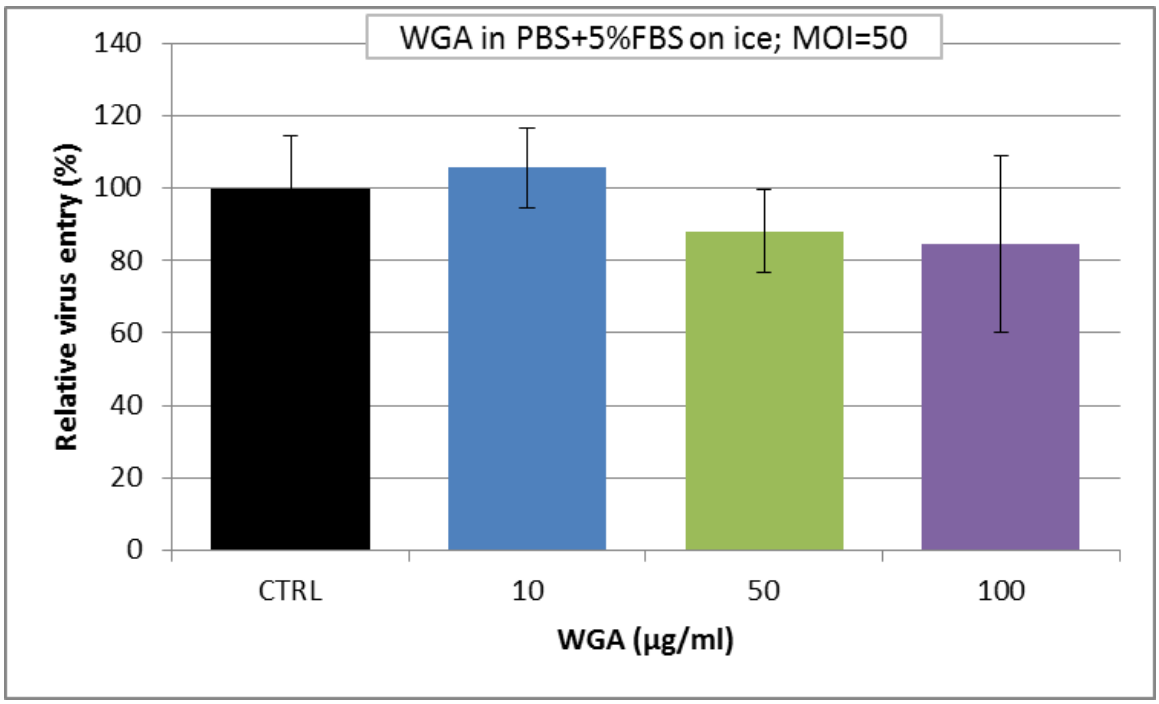

Fig. 5-7. Effect of WGA treatment and incubation on ice of RP19 cells on THEV entry. RP19 cells (2×10^5) were pre-incubated on ice for 1 h with 100 µl of 10, 50, or 100 µg/ml of WGA (in PBS+5%FBS), followed by virus inoculation at MOI of 50. Virus entry was measured using a qPCR-based infectivity assay. Percent relative virus entry of different groups is shown in relation to virus entry of untreated cells that was normalized to 100%. Each column represents mean±SEM from individually treated triplicate samples.

Since the above experimental conditions appeared damaging for RP19 cells, two more experiments were performed where cells were incubated with lectins at 41°C (the optimal temperature for cell growth), followed by virus inoculation at 50 or 20 IVPs/cell. In the 1st experiment, RP19 cells were pre-incubated with 1 or 10 µg of WGA, MAA, or SNA in 100 µl of PBS+2%serum, followed by virus inoculation at 50 IVPs/cell. Cells that received 1 µg of lectin, showed reduction in virus entry by 9%, 21%, or 13%, respectively, while those which received 10 µg did not survive the treatment; and therefore, no results were reported from them (Fig. 5-8A). In the 2nd experiment, cells were pre-treated with 1 or 5 µg of a lectin at the same conditions mentioned above, but inoculated at 20 IVPs/cell. The effect of lectins was not dose-dependent, and the maximum reduction in virus entry (i.e., by 27%, 48%, or 41%) was shown by the treatment of 5 µg of WGA, 1 µg of MAA, or 5 µg of SNA, respectively (Fig. 5-8B).

When an attempt was made to repeat the last experiment, the cells did not withstand the 5 µg treatment from the three lectins and the 1 µg of MAA. SNA and WGA treatments of 1 µg did not affect the virus entry (Fig. 5-8C). Combined together, regardless of the variations due to different experimental conditions, the overall results from neuraminidase and lectin experiments provide evidence of the involvement of surface sialic acid residues in THEV entry into RP19 cells.

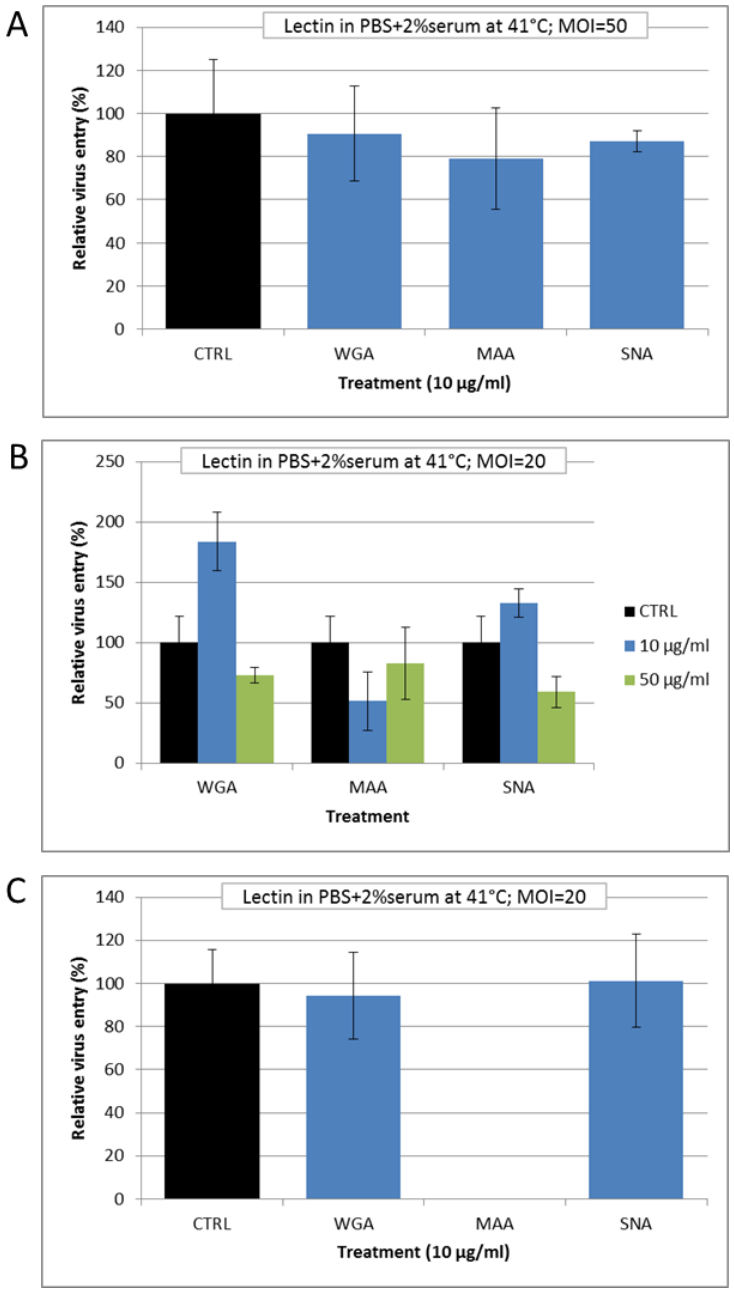

Fig. 5-8. Effect of lectin treatments (in PBS+2%serum) and incubation at 41°C of RP19 cells on THEV entry. Cells (2×10^5) were pre-incubated for 1 h with either 10 µg/ml of WGA, MAA, or SNA lectins, followed by virus inoculation at MOI of 50 (A), 10 or 50 µg/ml of the same lectins as in (A), followed by inoculation at MOI of 20 (B), or 10 µg/ml of the same lectins as in (A), followed by inoculation at MOI of 20 (C). The data from MAA treatment in (C) is not included as the cells did not survive post-treatment. Virus entry was measured using a qPCR-based infectivity assay. Percent relative virus entry of different groups is shown in relation to virus entry of untreated cells that was normalized to 100%. Each column represents mean±SEM from individually treated triplicate samples.

5.4.2. THEV cellular receptor contains a carbohydrate moiety

To examine the role of cell surface carbohydrates in THEV entry, RP19 cells were pre-treated with sodium periodate ($NaIO_4$) at room temperature, followed by virus inoculation. $NaIO_4$ can destroy carbohydrate chains by oxidation of neighboring hydroxyl groups on sugars to dialdehydes at acidic pH, with no alterations to the protein or lipid structures. $NaIO_4$ has also been shown to give satisfactory results at neutral pH (Stevenson et al., 2004; Woodward et al., 1985). Pre-treatment of RP19 cells with 0.1 or 1 mM $NaIO_4$ reduced THEV entry by 20-21% compared with the untreated cells (Fig. 5-9). Increasing the concentration of $NaIO_4$ to 2 or 10 mM did not cause a further reduction in virus entry. When RP19 cells were incubated with $NaIO_4$ at 41°C, the cells were killed, probably, due to cytotoxic effects of this reagent at high temperatures. Results from this experiment suggest that a carbohydrate moiety is an essential component of the THEV cell receptor.

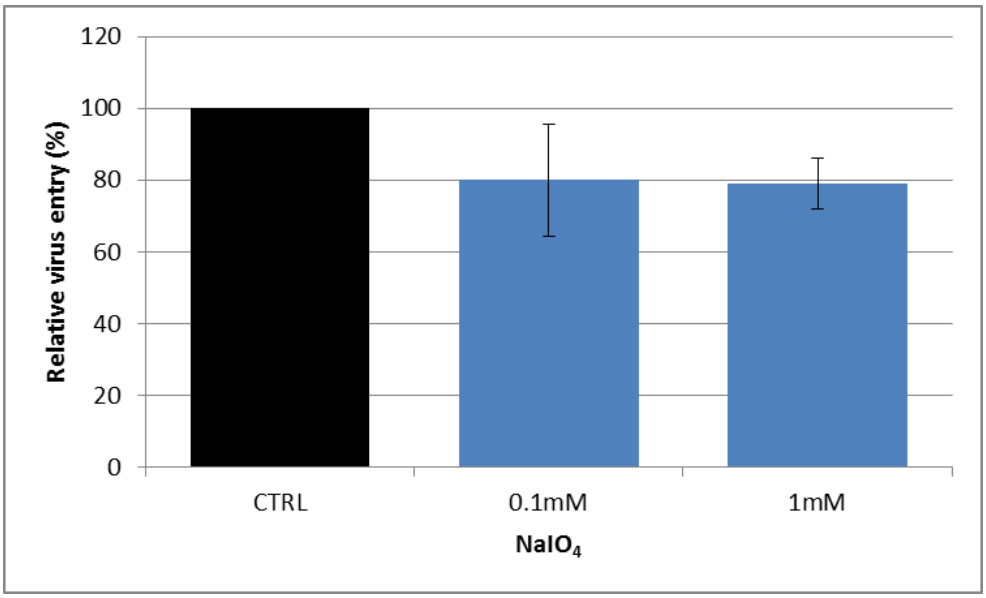

Fig. 5-9. THEV cellular receptor contains a carbohydrate moiety. RP19 cells were pre-incubated with mild concentrations of $NaIO_4$, followed by virus inoculation (MOI = 50). Virus entry was measured using a qPCR-based infectivity assay. Percent relative virus entry of different groups is shown in relation to virus entry of untreated cells that was normalized to 100%. Each column represents mean±SEM from two separate experiments each included individually treated duplicate or triplicate samples per group.

5.4.3. THEV cellular receptors contain protein moieties

Carbohydrate chains are known to be present on both glycoproteins and glycolipids (gangliosides). To examine whether a protein component is part of the THEV cell receptor, RP19 cells were pre-treated with various proteases at a range of concentrations, followed by virus inoculation at different MOIs. Pre-treatment of RP19 cells with a total of 200 mU of bromelain or ficin, followed by virus inoculation at MOI of 50, reduced THEV entry by 21% or 23%, respectively, while no inhibition occurred with using 20 mU (Fig. 5-10A). When these treatments were repeated and followed by inoculation at MOI of 100, no differences in virus reduction was noticed (Fig. 5-10B), probably due to overwhelming of the cells with virus. Using a total of 40 or 400 mU of bromelain or 400 mU of ficin, followed by inoculation at MOI of 100, reduced THEV entry by 30-30% or 35%, respectively (Fig. 5-10C). In a separate experiment, RP19 cells were pre-treated with 100 or 1000 mU of bromelain, followed by inoculation at MOI of 20. The inhibition in THEV entry was not dose-dependent, but reached a maximum of 67% at 100 mU of bromelain (Fig. 5-10D). In this experiment, immediately after treatment, cell count and viability was assessed using trypan blue exclusion test and a small reduction in cell number by 6% and cell viability by around 7% was found. In another experiment, digestion of RP19 cell surface proteins with 5 or 50 µg of trypsin, followed by inoculation at MOI of 50, reduced THEV entry in a dose-dependent manner, i.e., by 21 and 33%, respectively (Fig. 5-10E). In the literature, the selected MOI varies widely (from 0.1 to 10) based on the type of infectivity assays used (Chen and Benjamin, 1997; Kim et al., 2014; Stuart and Brown, 2007). From the present study, regardless of the treatments used, MOI of 20 appeared to be more suitable for the qPCR-based infectivity assay. Overall, these results suggest that THEV receptor on RP19 cells contains a protein component.

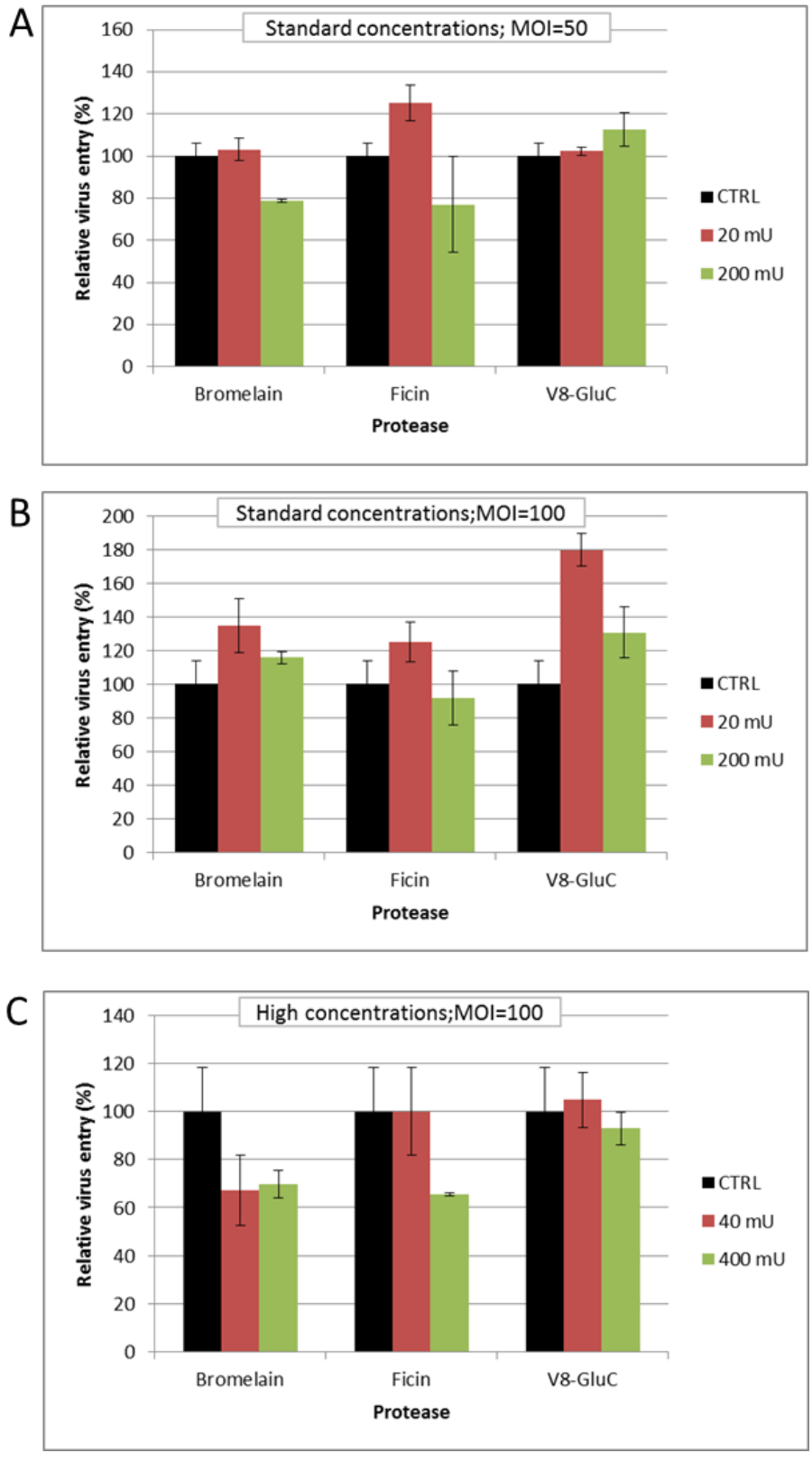

Fig. 5-10. THEV cell surface receptor contains a protein moiety. See next page for details.

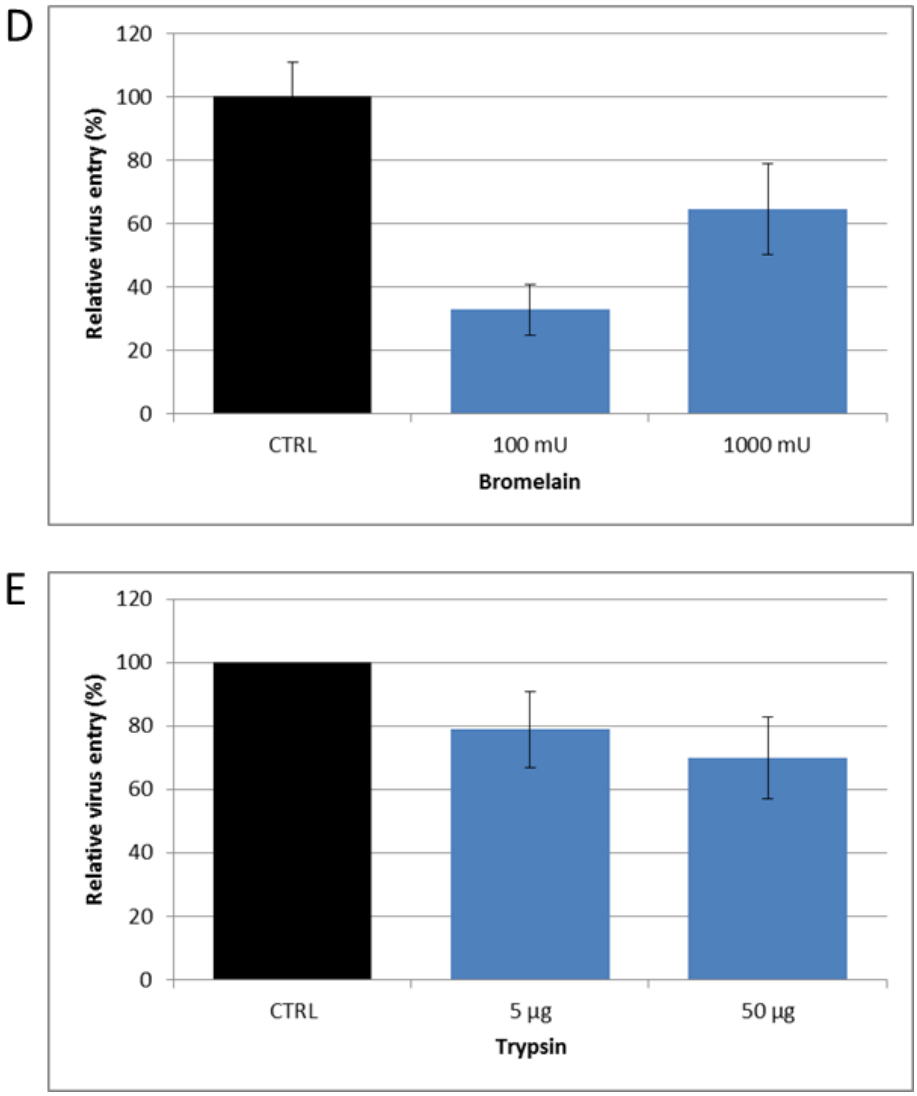

Fig. 5-10, cont'd. All treatments were performed at 37°C for 30 min. In two separate experiments, RP19 cells (1×10^6) were pre-treated with various proteases at the mentioned concentrations at 37°C for 30 min, followed by inoculation with THEV at MOI of 50 (A) or 100 (B & C). In a third experiment, cells (1×10^6) were pre-treated with bromelain, followed by virus inoculation (MOI=20) (D). In a fourth experiment, cells (2×10^5) were pre-treated with trypsin, followed by virus inoculation (MOI=50). (E). Virus entry was measured using a qPCR-based infectivity assay. Percent relative virus entry of different groups is shown in relation to virus entry of untreated cells that was normalized to 100%. A-D: Each column represents mean±SEM from individually treated triplicate samples. E: Each column represents mean± SEM from two separate experiments each included individually treated triplicate samples.

5.4.4. THEV binds to two B cell membrane proteins

To explore the variety in the membrane and cytosolic protein populations expressed by RP19 cells, different protein purifications were run on SDS-PAGE and stained with a general staining procedure using Coomassie blue. Fig. 5-11 displays the broad spectrum of protein molecules expressed on the membrane and in the cytosol of RP19 cells. VOPBA, a variant of the western blot assay, is a standard technique used to identify protein molecules that interact with viruses. After confirming the involvement of cell surface proteins in virus entry by proteolytic digestion experiments, VOPBA was performed to characterize the binding specificity of THEV to plasma membrane proteins from RP19 cells. Membrane proteins were purified from normally growing cells and separated based on molecular weight by electrophoresis though 7.5% SDS-PAGE. Proteins were transferred to a PVDF membrane by semi-dry electroblotting. The membrane was incubated with a virus suspension and the positions of virus binding were detected colorimetrically by HRP-specific reagents. Fig. 5-12 displays a digital image of the VOPBA membrane presenting the results of binding between THEV and RP19 cell membrane proteins. A faint band of approximately 87 kDa and a prominent band of approximately 69 kDa were detected. One or both of these proteins represent carbohydrate-containing potential receptors candidates for THEV. These two proteins will be further characterized in future work.

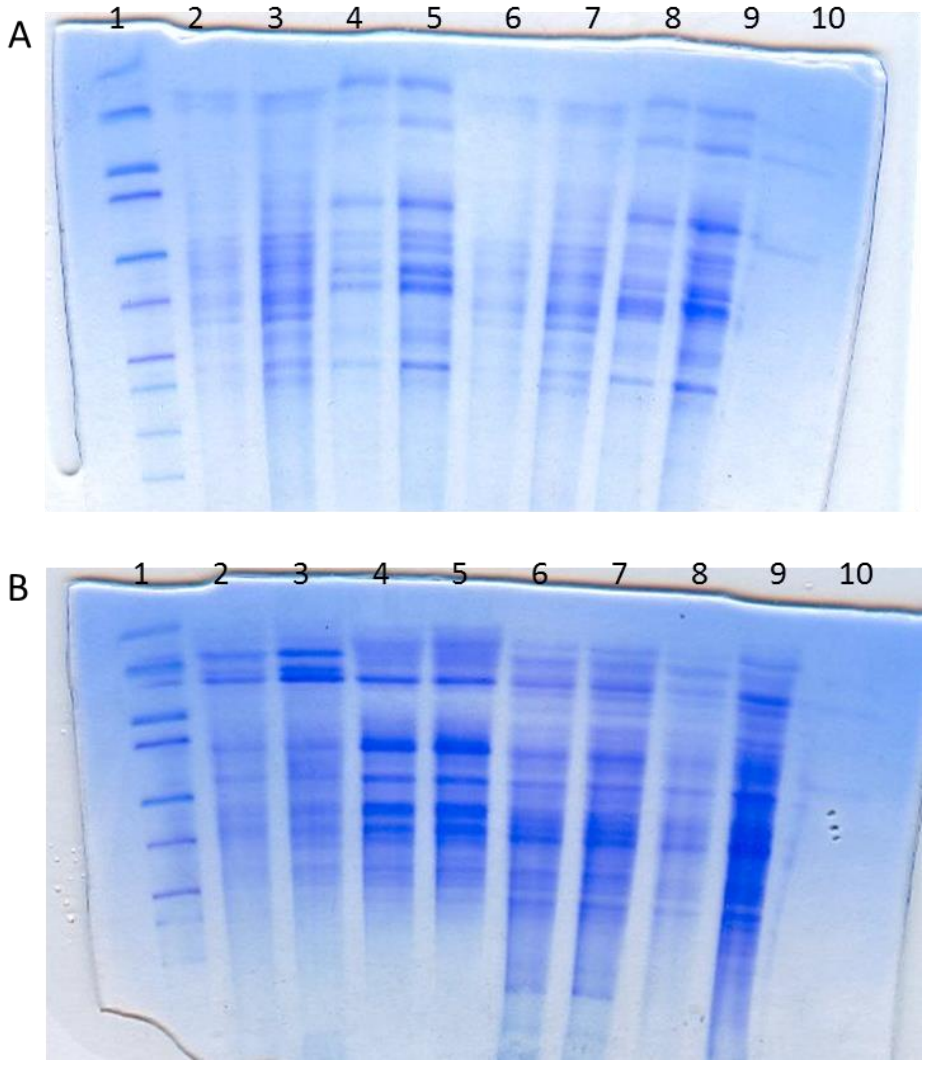

Fig. 5-11. SDS-PAGE analysis and Coomassie blue staining of the membrane and cytosolic proteins purified from cultured RP19 cells. Proteins were separated based on molecular weights on a 4-20% Mini-PROTEAN TGX precast gel (Bio-Rad), followed by general staining with Coomassie blue for visualization. Images represent a digital photo of the gels. In A & B gels, lane 1 contains a molecular weight (MW) marker. Gel A: lanes 2, 3, 6, & 7 contain membrane protein samples purified using Mem-PER™ Plus Membrane Protein Extraction Kit (Thermo Fisher Scientific); lane 10 contains a membrane protein sample isolated a method from Trauger et al. (2004); lanes 4, 5, 8, & 9 contain the cytosolic protein portions from the Mem-PER Plus kit isolations above. Gel B: lanes 2-3 contain resuspended pellets from the 6,000-RCF centrifugation step during preparation of lanes 6 & 7 protein samples, lanes 4 & 5 contain supernatants from the 20,000-RCF centrifugation step during preparation of lanes 6 & 7 protein samples; lanes 6 & 7 contain membrane proteins prepared as described by Jindadamrongwech and Smith (2004) with some modifications; lanes 8 & 9 contain membrane proteins prepared as described for the VOPBA in the Methods section; lane10 contains another sample purified as in gel A lane 10.

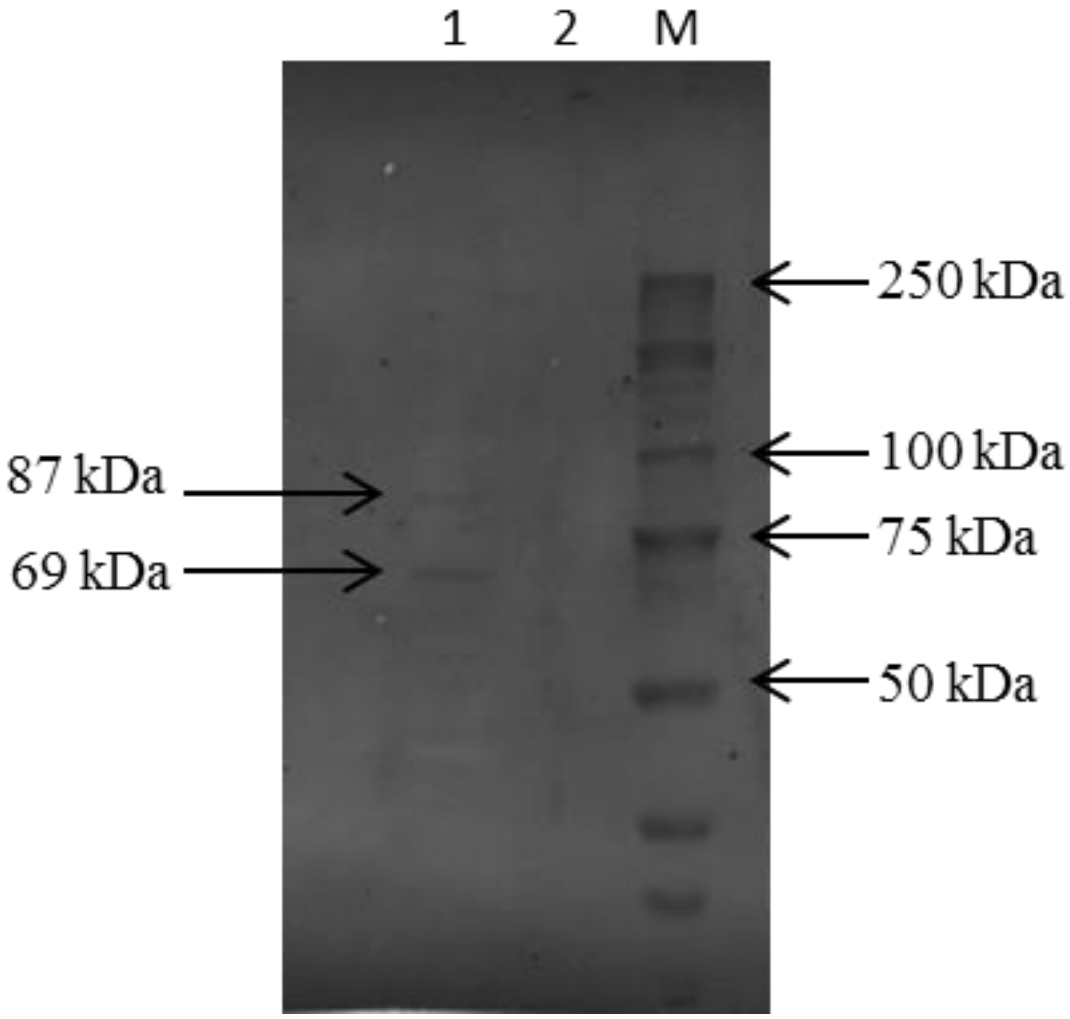

Fig. 5-12. THEV cell receptor is associated with approximately 87 and 69 kDa membrane proteins as analyzed by a virus overlay protein blot assay. RP19 cell membrane preparations were separated by 7.5% SDS-PAGE and transferred to a PVDF membrane. The blotted proteins were reacted with THEV and probed with hyperimmune serum against THEV and HRP-conjugated goat anti-turkey antibodies. Lane 1 and lane 2 were loaded with 9.0 µg or 3.4 µg, respectively, of RP19 membrane proteins from different purifications. Protein samples were prepared for the assay under reducing and denaturing conditions. Lane M: protein molecular weight marker.

5.5. Discussion

In this study, a set of experiments have been performed on the B lymphoblastoid, RP19 cells, to explore the nature of the THEV receptors. Due to the absence of a suitable virus binding/infectivity assay for THEV, a novel qPCR-based infectivity/titration assay has been developed in our laboratory (Mahsoub et al., 2011; Mahsoub et al., 2012) and used in this study to facilitate determining the effects of various treatments on virus entry. In these experiments, a panel of reagents has been used for the first time to pre-treat RP19 cells before virus inoculation and infectivity measurement. Thus, it may be worth noting that several factors were found to cause some discrepancy in the results and had to be optimized accordingly, such as the incubation temperature of treated RP19 cells, reagent concentration, and MOI for virus inoculation among others. Therefore, some experiments were re-run under varied conditions to reach the optimal experimental environment for both the cells and the treatment.

This work describes for the first time (based on the interaction between whole THEV particles and susceptible RP19 cells as well as a virus-protein binding assay) the general characteristics of the cellular receptors for THEV. We first showed that cell surface sialic acids are strongly involved in virus entry, and that a carbohydrate moiety and a protein moiety are key components of the THEV receptors. Results from multiple neuraminidase and lectin experiments indicated that both α2,3-linked and α2,6-linked sialic acids on RP19 cells function as a receptor for THEV entry. Our findings are in agreement with those recently reported by Singh et al. (2015), based on structural studies and glycan microarray analysis. The authors found that the THEV fiber head domain binds to 3'- and 6'-sialyllactose and proposed that "the THEV fiber protein may bind to a sialic acid-containing cell surface component, *in vivo*". They further demonstrated that the sialyllactose binding site is composed of six amino acids, which are located on the side of the fiber head, not on the top as with some human adenoviruses (Burmeister et al., 2004). Treatment of target cells with neuraminidases and α2,3-lniked or α2,6-lniked sialic acid-specific lectins (i.e., MAA or SNA, respectively) have been utilized to prove the use of cell surface sialic acids as attachment receptors for adenoviruses and non-adenoviruses (Arnberg et al., 2000b; Boulanger et al., 1972; Franca et al., 2013). Some viruses were found to attach to a single type of sialic acid linkages (i.e., α2,3 or α2,6) on cell surface,

like human adenovirus 37 (Arnberg et al., 2000a), equine rhinitis A virus (Stevenson et al., 2004), feline calicivirus (Stuart and Brown, 2007), enterovirus 70 (Nokhbeh et al., 2005), and human JC polyomavirus (Liu et al., 1998), and others, as the case of THEV, were found to use both, like adeno-associated viruses type 1 and 6 (Wu et al., 2006), bovine adenovirus 3 (Li et al., 2009) and porcine sapovirus (Kim et al., 2014). As for the THEV internalization receptor, a previous study based on the analyses of the predicted amino acid sequence of the putative penton protein, found that the common RGD motif which interacts with cell surface αv integrins and mediates human adenovirus entry is lacking in the THEV penton protein (Suresh et al., 1995). Interestingly, an alternative motif, LDV, was found which is known to be present in fibronectin and interact with cell surface α4β1 integrins. The latter integrin, also known as Very Late Antigen-4 and expressed on several cell types including lymphocytes, was then hypothesized to be used by THEV as an internalization receptor; yet, this hypothesis has never been experimentally tested.

As already mentioned, sodium periodate ($NaIO_4$) is most effective at room temperature and acidic pH conditions (Woodward et al., 1985). $NaIO_4$ treatment showed an observable effect in reducing THEV entry into RP19 cells; however, its effect could have been more evident, if it can be applied at a higher temperature, i.e., nearing that is required for optimal cell growth (i.e., 41°C). At suboptimal temperatures, RP19 cells tend to clump together forming large clusters of cells (Fig. 5-13). This characteristic prevents the treating agents (e.g., chemicals or enzymes) from contacting and affecting all cell surfaces, leaving a considerable portion of cell membranes "untreated". Post-treatment, the cells are incubated with the virus at 41°C; and therefore, they turn back to a single cell suspension and all cell surfaces (treated and untreated) become exposed for interaction with the virus particles. This process is expected to increase the chance for virus binding and entry into the incompletely-treated cells; and consequently, minimize the expected effect of the treatment.

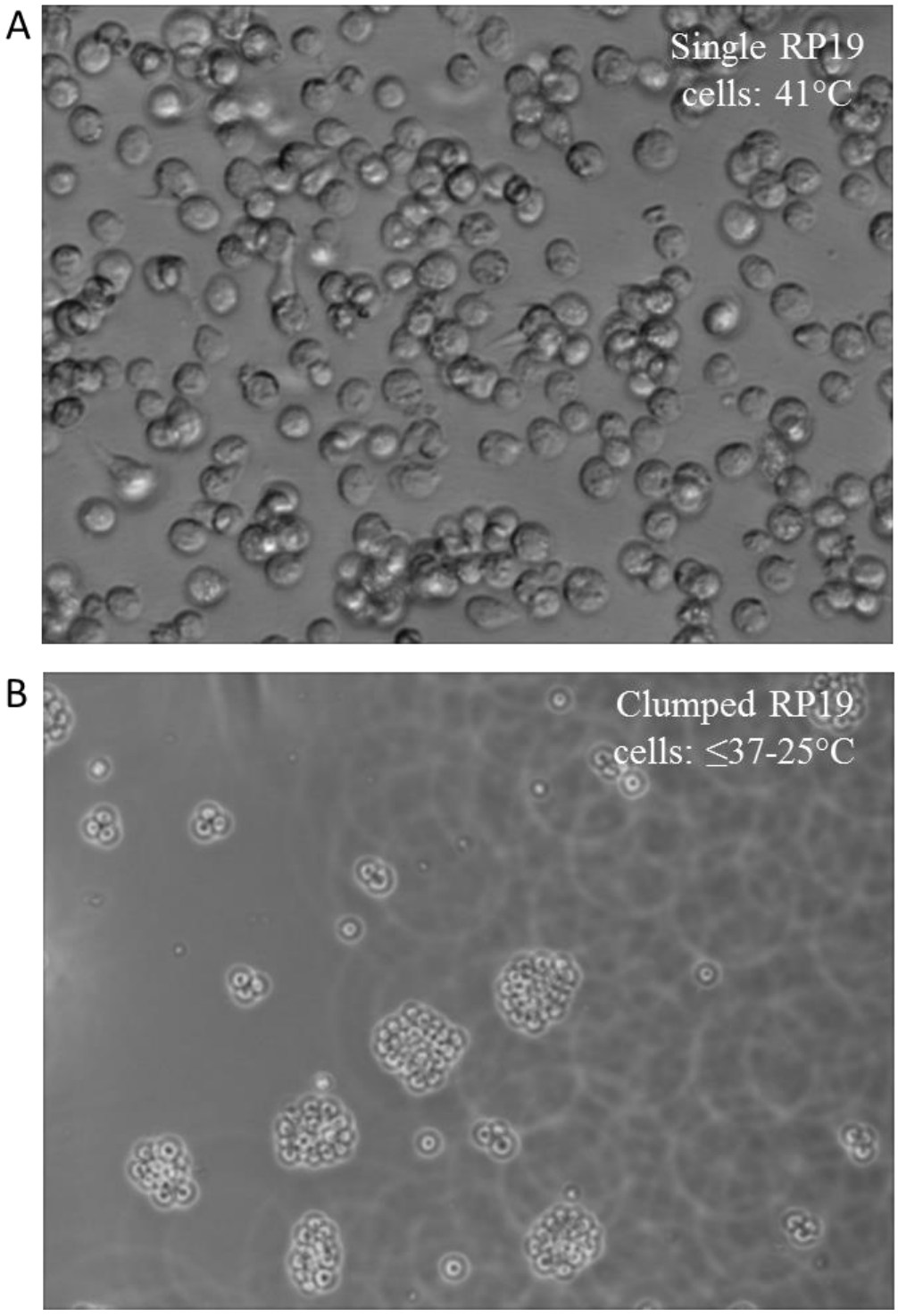

Fig. 5-13. Photomicrographs showing the behavior of RP19 cells at 41°C *vs.* 25-37°C. RP19 cells tend to clump together and form large clusters when incubated at suboptimal temperatures (i.e., under 41°C), as shown in panel B (100× magnification). Panel A (400× magnification) displays the normally suspended RP19 cells at the optimal growth temperature of 41°C.

Treatment of RP19 cells with proteases caused a noticeable reduction in THEV entry, which indicates that THEV receptor contains a protein moiety. However, since proteases destroy the polypeptides on the treated cell surface in a non-specific manner, it cannot be determined whether the reduction in virus entry is due to the impairment of the attachment or the internalization receptor of the virus. From the protease experiments, virus entry into cells was found to be sensitive to the treatment with two cysteine endopeptidases (bromelain and ficin), which have broad proteolytic specificities, and to a serine protease (trypsin), which cleaves polypeptides at the carboxylic side of Lys and Arg residues, but not to the serine protease endoproteinase Glu-C (from *S. aureus* V8), which specifically cleaves polypeptides at the carboxylic side of Glu and Aps residues. These findings suggest that the protein component of the THEV cell receptor(s) may have a unique structure lacking Glu and/or Asp amino acids. Unlike THEV cell receptor, human adenovirus 37 receptor was found to be destroyed by V8 protease treatment of host cells (Arnberg et al., 2000a).

VOPBA is a very useful technique which was developed as a modification of the western blot assay in 1986 to identify virus receptors (Gershoni et al.). It has since been used widely in virology for the specific detection of unknown proteins interacting with viruses. In this study, using VOPBA, THEV virions were found to bind specifically to two membrane proteins from RP19 cells with apparent molecular weights of 69 and 87 kDa. These two proteins may potentially represent a primary and a secondary receptor for THEV on target cells, like most adenoviruses. Future research is intended to further characterize these proteins using liquid chromatography and mass spectroscopy as well as antibody-blocking assays, as described for other adenoviruses (Trauger et al., 2004; Wu et al., 2004).

THEV is an important pathogen to the poultry industry in the US and several other countries around the world. Avirulent strains of THEV are widely used for vaccine production, while the virulent strains are responsible for an immune-mediated disease. Although remarkable progress has been made in the molecular studies on THEV, research on virus-host interactions at the molecular level remained inactive. The subcellular mechanisms involved in the immunogenesis and pathogenesis caused by THEV are yet unknown. Knowledge about THEV cell receptors and therefore, the

possibility to block them, would help design tightly-controlled experiments to study these phenomena. This may help design better strategies for vaccine development.

5.6. References

Arnberg, N., Edlund, K., Kidd, A.H. and Wadell, G., 2000a. Adenovirus Type 37 Uses Sialic Acid as a Cellular Receptor. J. Virol. 74, 42-48.

Arnberg, N., Kidd, A.H., Edlund, K., Olfat, F. and Wadell, G., 2000b. Initial Interactions of Subgenus D Adenoviruses with A549 Cellular Receptors: Sialic Acid versus alpha v Integrins. J. Virol. 74, 7691-7693.

Arnberg, N., Pring-Åkerblom, P. and Wadell, G., 2002. Adenovirus Type 37 Uses Sialic Acid as a Cellular Receptor on Chang C Cells. Journal of Virology 76, 8834-8841.

Beach, N.M. 2006. Characterization of avirulent turkey hemorrhagic enteritis virus: a study of the molecular basis for variation in virulence and the occurrence of persistent infection, Virginia Polytechnic Institute and State University, Blacksburg, VA, USA, pp. 207.

Bergelson, J.M., Cunningham, J.A., Droguett, G., Kurt-Jones, E.A., Krithivas, A., Hong, J.S., Horwitz, M.S., Crowell, R.L. and Finberg, R.W., 1997. Isolation of a Common Receptor for Coxsackie B Viruses and Adenoviruses 2 and 5. Science 275, 1320-1323.

Boulanger, P.A., Houdret, N., Scharfman, A. and Lemay, P., 1972. The Role of Surface Sialic Acid in Adenovirus-cell Adsorption. Journal of General Virology 16, 429-434.

Burmeister, W.P., Guilligay, D., Cusack, S., Wadell, G. and Arnberg, N., 2004. Crystal Structure of Species D Adenovirus Fiber Knobs and Their Sialic Acid Binding Sites. Journal of Virology 78, 7727-7736.

Chen, M.H. and Benjamin, T., 1997. Roles of N-Glycans with α2,6 as well as α2,3 Linked Sialic Acid in Infection by Polyoma Virus. Virology 233, 440-442.

Chu, Y., Heistad, D., Cybulsky, M.I. and Davidson, B.L., 2001. Vascular cell adhesion molecule-1 augments adenovirus-mediated gene transfer. Arteriosclerosis, thrombosis, and vascular biology 21, 238-42.

Clark, H.F., Michalski, F., Tweedell, K.S., Yohn, D. and Zeigel, R.F., 1973. An adenovirus, FAV-1, isolated from the kidney of a frog (Rana pipiens). Virology 51, 392-400.

Davison, A. and Harrach, B. 2011. Siadenovirus. In: Tidona, C. and Darai, G. (Eds), The Springer Index of Viruses, Springer New York, pp. 49-56.

Davison, A.J., Wright, K.M. and Harrach, B., 2000. DNA sequence of frog adenovirus. J Gen Virol 81, 2431-2439.

Davison, E., Diaz, R.M., Hart, I.R., Santis, G. and Marshall, J.F., 1997. Integrin alpha5beta1-mediated adenovirus infection is enhanced by the integrin-activating antibody TS2/16. Journal of Virology 71, 6204-6207.

Dechecchi, M.C., Tamanini, A., Bonizzato, A. and Cabrini, G., 2000. Heparan sulfate glycosaminoglycans are involved in adenovirus type 5 and 2-host cell interactions. Virology 268, 382-90.

Fadly, A.M. and Nazerian, K., 1984. Efficacy and Safety of a Cell-Culture Live Virus Vaccine for Hemorrhagic Enteritis of Turkeys: Laboratory Studies. Avian Diseases 28, 183-196.

Fadly, A.M., Nazerian, K., Nagaraja, K. and Below, G., 1985. Field vaccination against hemorrhagic enteritis of turkeys by a cell-culture live-virus vaccine. Avian Diseases 29, 768-77.

Franca, M., Stallknecht, D.E. and Howerth, E.W., 2013. Expression and distribution of sialic acid influenza virus receptors in wild birds. Avian Pathol 42, 60-71.

Freimuth, P., Philipson, L. and Carson, S.D. 2008. The Coxsackievirus and Adenovirus Receptor

Group B Coxsackieviruses. In: Tracy, S., Oberste, M.S. and Drescher, K.M. (Eds), Springer Berlin Heidelberg, pp. 67-87.

Gershoni, J.M., Lapidot, M., Zakai, N. and Loyter, A., 1986. Protein blot analysis of virus receptors: identification and characterization of the sendai virus receptor. Biochimica et Biophysica Acta (BBA) - Biomembranes 856, 19-26.

Gross, W.B. and Moore, W.E.C., 1967. Hemorrhagic Enteritis of Turkeys. Avian Diseases 11, 296-307.

Hong, S.S., Karayan, L., Tournier, J., Curiel, D.T. and Boulanger, P.A., 1997. Adenovirus type 5 fiber knob binds to MHC class I [alpha]2 domain at the surface of human epithelial and B lymphoblastoid cells. EMBO J 16, 2294-2306.

Horvath, J. and Weber, J.M., 1988. Nonpermissivity of human peripheral blood lymphocytes to adenovirus type 2 infection. Journal of Virology 62, 341-345.

Jindadamrongwech, S. and Smith, D.R., 2004. Virus Overlay Protein Binding Assay (VOPBA) Reveals Serotype Specific Heterogeneity of Dengue Virus Binding Proteins on HepG2 Human Liver Cells. Intervirology 47, 370-373.

Jindadamrongwech, S., Thepparit, C. and Smith, D.R., 2004. Identification of GRP 78 (BiP) as a liver cell expressed receptor element for dengue virus serotype 2. Archives of Virology 149, 915-927.

Joseph, H.M., Ballmann, M.Z., Garner, M.M., Hanley, C.S., Berlinski, R., Erdélyi, K., Childress, A.L., Fish, S.S., Harrach, B. and Wellehan Jr, J.F.X., 2014. A novel siadenovirus detected in the kidneys and liver of Gouldian finches (Erythura gouldiae). Veterinary Microbiology 172, 35-43.

Katoh, H., Ohya, K., Kubo, M., Murata, K., Yanai, T. and Fukushi, H., 2009. A novel budgerigar-adenovirus belonging to group II avian adenovirus of Siadenovirus. Virus Res 144, 294-7.

Kim, D.-S., Hosmillo, M., Alfajaro, M.M., Kim, J.-Y., Park, J.-G., Son, K.-Y., Ryu, E.-H., Sorgeloos, F., Kwon, H.-J., Park, S.-J., Lee, W.S., Cho, D., Kwon, J., Choi, J.-S., Kang, M.-I., Goodfellow, I. and Cho, K.-O., 2014. Both α2,3- and α2,6-Linked Sialic Acids on O-Linked Glycoproteins Act as Functional Receptors for Porcine Sapovirus. PLoS Pathog 10, e1004172.

Kovács, E.R. and Benkő, M., 2009. Confirmation of a novel siadenovirus species detected in raptors: partial sequence and phylogenetic analysis. Virus Res 140, 64-70.

Kovács, E.R., Janoska, M., Dan, A., Harrach, B. and Benkő, M., 2010. Recognition and partial genome characterization by non-specific DNA amplification and PCR of a new siadenovirus species in a sample originating from Parus major, a great tit. J Virol Methods 163, 262-8.

Law, L.K. and Davidson, B.L., 2005. What does it take to Bind CAR? Mol Ther 12, 599-609.

Lee, S.Y., Kim, J.H., Park, Y.M., Shin, O.S., Kim, H., Choi, H.G. and Song, J.W., 2014. A novel adenovirus in Chinstrap penguins (Pygoscelis antarctica) in Antarctica. Viruses 6, 2052-61.

Lenman, A., Liaci, A.M., Liu, Y., Ardahl, C., Rajan, A., Nilsson, E., Bradford, W., Kaeshammer, L., Jones, M.S., Frangsmyr, L., Feizi, T., Stehle, T. and Arnberg, N., 2015. Human adenovirus 52 uses sialic acid-containing glycoproteins and the coxsackie and adenovirus receptor for binding to target cells. PLoS Pathog 11, e1004657.

Leon, R.P., Hedlund, T., Meech, S.J., Li, S., Schaack, J., Hunger, S.P., Duke, R.C. and DeGregori, J., 1998. Adenoviral-mediated gene transfer in lymphocytes. Proc Natl Acad Sci U S A 95, 13159-64.

Li, X., Bangari, D.S., Sharma, A. and Mittal, S.K., 2009. Bovine adenovirus serotype 3 utilizes sialic acid as a cellular receptor for virus entry. Virology 392, 162-8.

Liu, C.K., Wei, G. and Atwood, W.J., 1998. Infection of glial cells by the human polyomavirus JC is mediated by an N-linked glycoprotein containing terminal alpha(2-6)-linked sialic acids. J Virol 72, 4643-9.

Mahsoub, H.M., Beach, N., Evans, N. and Pierson, F.W., 2011. Development of a Quantitative Real-Time Polymerase Chain Reaction (qPCR) Assay for Titration of Turkey Hemorrhagic Enteritis Virus Vaccines. Proceedings of the 83rd Northeastern Conference on Avian Diseases, 115.

Mahsoub, H.M., Beach, N. and Pierson, F.W., 2012. A Novel Approach for Quantifying Infectious Particles of Turkey Hemorrhagic Enteritis Virus Using SYBR Green-Based Real-time PCR and its Potential Applications. 84th Northeastern Conference on Avian Diseases.

Mayo, M.A., 2002. ICTV at the Paris ICV: Results of the Plenary Session and the Binomial Ballot. Archives of Virology 147, 2254-2260.

Nazerian, K., Elmubarak, A. and Sharma, J.M., 1982. Establishment of B-lymphoblastoid cell lines from Marek's disease virus-induced tumors in turkeys. International Journal of Cancer 29, 63-68.

Nemerow, G.R., 2000. Cell Receptors Involved in Adenovirus Entry. Virology 274, 1-4.

Nilsson, E.C., Storm, R.J., Bauer, J., Johansson, S.M.C., Lookene, A., Angstrom, J., Hedenstrom, M., Eriksson, T.L., Frangsmyr, L., Rinaldi, S., Willison, H.J., Domellof, F.P., Stehle, T. and Arnberg, N., 2011. The GD1a glycan is a cellular receptor for adenoviruses causing epidemic keratoconjunctivitis. Nat Med 17, 105-109.

Nokhbeh, M.R., Hazra, S., Alexander, D.A., Khan, A., McAllister, M., Suuronen, E.J., Griffith, M. and Dimock, K., 2005. Enterovirus 70 Binds to Different Glycoconjugates Containing α2,3-Linked Sialic Acid on Different Cell Lines. Journal of Virology 79, 7087-7094.

Park, Y.M., Kim, J.-H., Gu, S.H., Lee, S.Y., Lee, M.-G., Kang, Y.K., Kang, S.-H., Kim, H.J. and Song, J.-W., 2012. Full genome analysis of a novel adenovirus from the South Polar skua (Catharacta maccormicki) in Antarctica. Virology 422, 144-150.

Pierson, F.W. and Fitzgerald, S.D. 2008. Hemorrhagic Enteritis and Related Infections. In: Saif, Y.M., Fadly, A.M., Glisson, J.R., McDougald, L.R., Nolan, L.K. and Swayne, D.E. (Eds), Diseases of Poultry, Wiley-Blackwell, Iowa.

Richardson, C., Brennan, P., Powell, M., Prince, S., Chen, Y.H., Spiller, O.B. and Rowe, M., 2005. Susceptibility of B lymphocytes to adenovirus type 5 infection is dependent upon both coxsackie-adenovirus receptor and alphavbeta5 integrin expression. J Gen Virol 86, 1669-79.

Rivera, S., Wellehan, J.F., Jr., McManamon, R., Innis, C.J., Garner, M.M., Raphael, B.L., Gregory, C.R., Latimer, K.S., Rodriguez, C.E., Diaz-Figueroa, O., Marlar, A.B., Nyaoke, A., Gates, A.E., Gilbert, K., Childress, A.L., Risatti, G.R. and Frasca, S., Jr., 2009. Systemic adenovirus infection in Sulawesi tortoises (Indotestudo forsteni) caused by a novel siadenovirus. J Vet Diagn Invest 21, 415-26.

Roelvink, P.W., Lizonova, A., Lee, J.G.M., Li, Y., Bergelson, J.M., Finberg, R.W., Brough, D.E., Kovesdi, I. and Wickham, T.J., 1998. The Coxsackievirus-Adenovirus Receptor Protein Can Function as a Cellular Attachment Protein for Adenovirus Serotypes from Subgroups A, C, D, E, and F. J. Virol. 72, 7909-7915.

Salone, B., Martina, Y., Piersanti, S., Cundari, E., Cherubini, G., Franqueville, L., Failla, C.M., Boulanger, P. and Saggio, I., 2003. Integrin α3β1 Is an Alternative Cellular Receptor for Adenovirus Serotype 5. Journal of Virology 77, 13448-13454.

Segerman, A., Atkinson, J.P., Marttila, M., Dennerquist, V., Wadell, G. and Arnberg, N., 2003. Adenovirus Type 11 Uses CD46 as a Cellular Receptor. Journal of Virology 77, 9183-9191.

Short, J.J., Pereboev, A.V., Kawakami, Y., Vasu, C., Holterman, M.J. and Curiel, D.T., 2004. Adenovirus serotype 3 utilizes CD80 (B7.1) and CD86 (B7.2) as cellular attachment receptors. Virology 322, 349-59.

Singh, A.K., Berbis, M.A., Ballmann, M.Z., Kilcoyne, M., Menendez, M., Nguyen, T.H., Joshi, L., Canada, F.J., Jimenez-Barbero, J., Benko, M., Harrach, B. and van Raaij, M.J., 2015. Structure and Sialyllactose Binding of the Carboxy-Terminal Head Domain of the Fibre from a Siadenovirus, Turkey Adenovirus 3. PLoS One 10, e0139339.

Stevenson, R.A., Huang, J.A., Studdert, M.J. and Hartley, C.A., 2004. Sialic acid acts as a receptor for equine rhinitis A virus binding and infection. J Gen Virol 85, 2535-43.

Stuart, A.D. and Brown, T.D.K., 2007. α2,6-Linked sialic acid acts as a receptor for Feline calicivirus. Journal of General Virology 88, 177-186.

Summerford, C., Bartlett, J.S. and Samulski, R.J., 1999. [alpha]V[beta]5 integrin: a co-receptor for adeno-associated virus type 2 infection. Nat Med 5, 78-82.

Summerford, C. and Samulski, R.J., 1998. Membrane-Associated Heparan Sulfate Proteoglycan Is a Receptor for Adeno-Associated Virus Type 2 Virions. Journal of Virology 72, 1438-1445.

Suresh, M., Cyr, S.S. and Sharma, J.M., 1995. Molecular cloning and sequence analysis of the penton base genes of type II avian adenoviruses. Virus Res 39, 289-297.

Suresh, M. and Sharma, J., 1996. Pathogenesis of type II avian adenovirus infection in turkeys: in vivo immune cell tropism and tissue distribution of the virus. J. Virol. 70, 30-36.

Trauger, S.A., Wu, E., Bark, S.J., Nemerow, G.R. and Siuzdak, G., 2004. The Identification of an Adenovirus Receptor by Using Affinity Capture and Mass Spectrometry. ChemBioChem 5, 1095-1099.

Tuve, S., Wang, H., Jacobs, J.D., Yumul, R.C., Smith, D.F. and Lieber, A., 2008. Role of cellular heparan sulfate proteoglycans in infection of human adenovirus serotype 3 and 35. PLoS Pathog 4, e1000189.

Wang, H., Li, Z.-Y., Liu, Y., Persson, J., Beyer, I., Moller, T., Koyuncu, D., Drescher, M.R., Strauss, R., Zhang, X.-B., Wahl, J.K., Urban, N., Drescher, C., Hemminki, A., Fender, P. and Lieber, A., 2011. Desmoglein 2 is a receptor for adenovirus serotypes 3, 7, 11 and 14. Nat Med 17, 96-104.

Wellehan, J.F., Jr., Greenacre, C.B., Fleming, G.J., Stetter, M.D., Childress, A.L. and Terrell, S.P., 2009. Siadenovirus infection in two psittacine bird species. Avian Pathol 38, 413-7.

Wickham, T.J., Mathias, P., Cheresh, D.A. and Nemerow, G.R., 1993. Integrins αvβ3 and αvβ5 promote adenovirus internalization but not virus attachment. Cell 73, 309-319.

Woodruff, J.F. and Woodruff, J.J., 1972. Virus-induced alterations of lymphoid tissues: II. Lymphocyte receptors for Newcastle disease virus. Cellular Immunology 5, 296-306.

Woodward, M.P., Young Jr, W.W. and Bloodgood, R.A., 1985. Detection of monoclonal antibodies specific for carbohydrate epitopes using periodate oxidation. Journal of Immunological Methods 78, 143-153.

Wu, E., Fernandez, J., Fleck, S.K., Von Seggern, D.J., Huang, S. and Nemerow, G.R., 2001. A 50-kDa Membrane Protein Mediates Sialic Acid-Independent Binding and Infection of Conjunctival Cells by Adenovirus Type 37. Virology 279, 78-89.

Wu, E., Trauger, S.A., Pache, L., Mullen, T.-M., Von Seggern, D.J., Siuzdak, G. and Nemerow, G.R., 2004. Membrane Cofactor Protein Is a Receptor for Adenoviruses Associated with Epidemic Keratoconjunctivitis. Journal of Virology 78, 3897-3905.

Wu, Z., Miller, E., Agbandje-McKenna, M. and Samulski, R.J., 2006. Alpha2,3 and alpha2,6 N-linked sialic acids facilitate efficient binding and transduction by adeno-associated virus types 1 and 6. J Virol 80, 9093-103.

Zhang, Y. and Bergelson, J.M., 2005. Adenovirus Receptors. J. Virol. 79, 12125-12131.

Chapter 6

General Conclusions, Discussions, and Future Work

6.1. Summary

The work performed in this dissertation features the achievement of two distinct research projects. In the first project, a new SYBR Green-based qPCR assay for the quantification of THEV genomes was developed and optimized for use with different THEV-infected samples. The assay proved to be specific, sensitive, accurate, and highly reproducible with a limit of detection of 10 genome copies/reaction. It was used to determine the virus genomic titers in numerous HE splenic vaccines. High variations among tested vaccine batches were detected. These variations can be mainly attributed to original differences in virus titers from one batch to another. The qPCR assay is very helpful in that it can be used to determine whether a vaccine batch can be further diluted and what dilution factor can be used. This feature may lead to increasing the total vaccine doses per batch by two or three folds. The assay can be used as an alternative to the currently used AGID test. Several factors can affect the results of AGID including the positive controls of spleen and serum as well as the storage conditions of the agar plates. qPCR assays are not prone to inaccuracy due to such factors. In this study, no correlation was found between the AGID and qPCR titers, mainly due to the inherent insensitivity of AGID test. Vaccine batches of similar genomic titer showed different AGID titers and vice versa. An important use of the qPCR assay was the generation of one-step growth curves in cell cultures as proof of active viral replication. Traditionally, electron microscopy and immunofluorescent staining have been used to indicate the increase of viral particles in infected cells. Another method used to display viral replication was the development of CPE, which can be confused with enlargement of RP19 cells due to reasons other than infection. Because of the virtue of its high sensitivity, qPCR can detect the increase in virus genomes immediately once the replication starts, and before the formation of virus particles.

A suitable, *in vitro* infectivity assay for THEV has been lacking and was a major obstacle in advancing laboratory studies of the virus. A qPCR-based infectivity assay was developed to measure the infectious titer of THEV. The assay was employed in the

titration of several batches of HE cell culture vaccines. Significant batch-to-batch variation was found. No correlation was found between the $CCID_{50}$ and qPCR infectious titers. This is mainly a results of the high variations expected from using the $CCID_{50}$ protocol with suspended cells. It has an inherent inaccuracy in determining the CPE based only on the enlargement of cells. The qPCR infectivity assay cannot be applied directly to the splenic vaccines because of the presence of toxic materials and inflammatory cytokines that are detrimental to cells.

The invention of the qPCR-based infectivity assay was essential to further our studies on THEV. It was used in all of the infection experiment carried out in the second project of this dissertation. Alternative methods for the determination of virus infectivity include virus radiolabelling and the use of a scintillator. This is a relatively complicated technology and cannot be easily achieved in most small- and medium-sized laboratories. Other methods include the involvement of a reporter gene/protein (such as GFP or luciferase) into the virus genome and tracking its fluorescence activity. The absence of a THEV infectious clone and the difficulty to handle an entire virus genome of ~26 kb makes this step unachievable in the short run and beyond the scope of our present research. Indeed, the way the THEV qPCR infectivity assay was developed and optimized makes it an indispensable addition to laboratory techniques. It can be easily reproduced and employed in research by any small laboratory as long as a real-time PCR machine is available.

In the second project, the cell surface molecules utilized as receptors for THEV entry have been investigated. Using neuraminidase and lectin treatments of RP19 cells at different experimental conditions, it was found that cell surface sialic acids serve as functional receptors for THEV attachment. This finding is in agreement with the recent report that THEV fiber knob domain binds to sialyllactose (Singh et al., 2015). The authors suggested that, *in vivo*, THEV may bind to sialic acid-containing molecules. Sialic acids have been reported to function as binding receptors for many viruses, including human and animal adenoviruses (Arnberg et al., 2000; Li et al., 2009). Further, we found that cell surface carbohydrate and protein moieties are essential components of THEV receptors. Using virus overlay protein blot assay (VOPBA), it was found that THEV binds specifically to two membrane proteins on RP19 cells. Most likely, these

proteins represent the primary and secondary receptors for THEV. It is expected that one of these proteins is terminated with the sialic acid residues that are used for virus attachment. The second protein is expected to be the internalization receptor that interacts with the virus penton base protein and mediates the internalization step. Further experiments are planned to differentiate between the primary and secondary receptors for THEV. Previous research has shown that THEV induces apoptosis in splenic cells (Rautenschlein et al., 2000); thus, it is tempting to speculate that THEV receptors could be involved in apoptotic pathways.

6.2. Future research

6.2.1. Additional experiments for the confirmation of sialic acid as attachment receptor for THEV and distinguishing between primary and secondary receptors

6.2.1.1. Expt. 1: THEV-VOPBA on neuraminidase-treated RP19 cell membrane proteins

Table 6-1. Samples to be included in VOPBA for the effect of NA treatment on THEV binding to RP19 cell membrane proteins.

Lane	Sample + enzyme	Virus	Notes
1	Empty	Two sets of samples will be used and transferred to 2 PVDF membranes; 1 set will be incubated with virus & 1 set with no virus as negative controls.	VCN or AU removes α(2,3) or α(2,6)-linked surface sialic acids, respectively.
2	Protein molecular weight standard		
3	Sample 1: protein with no neuraminidase		
4	Sample 2: VCN with no protein		
5	Sample 3: AUN with no protein		
6	Sample 4: protein + VCN		
7	Sample 5: protein + AUN		
8	Empty		
9	Empty		
10	Empty		

Protein purification: RP19 cells will be grown for 2-3 days and plasma membrane proteins will be extracted using a commercial kit (e.g., Mem-PER^{TM} Plus Membrane Protein Extraction Kit, Thermo Scientific, Waltham, MA or Plasma Membrane Protein Extraction Kit, BioVision Inc., Milpitas, CA).

Sample preparation and neuraminidase treatment before the SDS-PAGE: Neuraminidases will be diluted at 100 mU in reaction buffer. Membrane protein samples will be individually incubated with the assigned NA (Table 1) at 37°C for 2 h. Alternatively, the membrane proteins will be extracted from NA (10 mU)-treated RP19 cells as described previously (Li et al., 2009; Wu et al., 2001).

SDS-PAGE and VOPBA: The protein samples prepared above will be mixed at a ratio of 1:4 with 4x Laemmli protein sample buffer (Bio-Rad) without β-mercaptoethanol or boiling (i.e., running under non-reducing and non-denaturing conditions). The protein mixtures will then be separated by molecular weight on a 4-16% polyacrylamide gel (Mini-PROTEAN TGX Precast Gel, Bio-Rad) at 180 V for 35-40 min. VOPBA will be performed as described in Chapter 5 and elsewhere (Wu et al., 2001).

6.2.1.2. Expt. 2: THEV-VOPBA and lectin western blot

Table 6-2. Samples to be included in VOPBA for the effect of lectin treatment on THEV binding to RP19 cell membrane proteins.

Lane	Sample	Virus	Notes
1	Empty	Two sets of samples will be used and transferred to 2 PVDF membranes; 1 set will be incubated with virus & 1 set with no virus as negative controls.	WGA (wheat germ agglutinin), MAA (*Maackia amurensis* agglutinin), or SNA (*Sambucus nigra* agglutinin) binds to all linkages of sialic acids, α(2,3)-linked, or α(2,6)-linked sialic acids, respectively.
2	Protein molecular weight standard		
3	Sample 1: protein with no lectin		
4	Sample 2: protein + WGA		
5	Sample 3: protein + MAA		
6	Sample 4: protein + SNA		
7	WGA with no protein		
8	MAA with no protein		
9	SNA with no protein		
10	Empty		

Protein purification and SDS-PAGE: Purification of RP19 cell membrane proteins and SDS-PAGE will be followed essentially as described in Experiment 6 above.

VOPBA/lectin western blot analysis: Proteins separated by SDS-PAGE will be transferred to a polyvinylidene fluoride membrane (Immun-Blot® PVDF Membrane; Bio-

Rad) and blocked for 1 h at room temperature (RT) with Buffer D to prevent non-specific binding. After blocking, the membrane will be rinsed once (5 min with shaking) with PBS-T and cut into strips corresponding to the different lectin groups. Membrane strips will be separately incubated for 30 min at RT with the assigned lectin diluted in Buffer D (see Table 3 for composition) at 0.1 µg/ ml. Protein sample in Lane 3 will serve as a positive control and will be incubate with Buffer D with no lectins. Lectins with no membrane proteins (i.e., Lanes 7, 8, & 9) will be incubated with Buffer D. After washing 4 times (5 min each) with Buffer D, the membrane strips will be separately incubated with a solution containing or not containing (negative controls) THEV. The assay will then be continued as in Experiment 4 above.

Table 6-3. Composition of Buffer D for dilution and blocking of lectins.

Component	Making 500 ml
0.5M HEPES (pH8)	10
0.5M $CaCl_2$	15
0.1M NaCl	5
Tween-20	0.5
ddH_2O	470

6.2.2. Identifying the receptor protein molecules for THEV on RP19 cells

6.2.2.1. Expt. 1: Liquid chromatography (LC) and mass spectrometry (MS) to identify THEV-bound cell-surface proteins and their amino acid sequences.

Methods:

1. In-gel digestion of THEV-reacted membrane proteins will be performed as follows. THEV-bound protein band(s) identified by SDS-PAGE/VOPBA will be excised from the blot membrane and treated with DL-Dithiothreitol (DTT; 10 mM; Sigma-Aldrich) to reduce disulfide linkages.
2. Alkylation will be performed with iodoacetamide (55 mM; Sigma-Aldrich) before digestion with trypsin (Trypsin Gold; Promega, Madison, WI) overnight at 37°C, with an estimated 1:30 enzyme/substrate ratio in ammonium bicarbonate (50 mM).

3. For suppression of proteolytic activity before deglycosylation, the glycoproteins extract will be incubated with soybean trypsin inhibitor (Sigma-Aldrich) in a 1:1 (w/w) ratio to trypsin for 1 h at 37°C.
4. Deglycosylation: The extract will be incubated for 2 h with PNGase F (Promega) as a general deglycosylation step for simplifying mass spectral interpretation.
5. LC and MS: Separation of extracted glycoproteins using LC (LC Packings Ultimate HPLC pump) and analysis of eluted complex protein mixture using LCQ DecaXP mass spectrometer (Thermo Finnigan, San Jose, CA) will be performed under the conditions described previously (Koudelka et al., 2009; Trauger et al., 2004). Instruments required are located in the Proteomics Core Facility at Virginia Bioinformatics Institute and Virginia Tech Center for Genomics, Virginia Tech.
6. The uninterpreted sequential mass spectra (MS/MS) obtained during the run will be searched with Mascot (Matrix Science, Limited) and SEQUEST (University of Washington, WA) database search programs using recommended criteria and search options (Koudelka et al., 2009; Trauger et al., 2004). These programs correlate mass spectral data of peptides with aa and nt data bases. Finally, the aa sequence and its corresponding protein(s) and organism(s) will be determined.

6.2.2.2. Expt. 2: Confirmation of the specificity of the identified receptor(s) to THEV by antibody inhibition of virus infection, followed by an infectivity assay.

Methods:

1. RP19 cells will be incubated with different dilutions of protein/receptor-blocking antibody (monoclonal or polyclonal). If more than one cell surface protein were found involved in THEV endocytosis and there were antibodies available for them, cells will be treated with each anti-protein antibody individually or in combination.
2. After washing with PBS to remove unbound antibodies, cells will be incubated with a THEV suspension for 1 h.
3. Non-internalized virus will be removed by washing with PBS and total DNA will be extracted from cell lysates.
4. THEV-qPCR will be performed as per the new infectivity assay in Aim #1 to evaluate the effect of treatment(s) on THEV infection.

Alternative approaches:

The planned experiment relies primarily on the availability of the appropriate antibodies for THEV receptor(s) identified from experiments 1 & 2 above. These antibodies may not be commercially available. This possibility will prevent the confirmation study from being conducted as described. Therefore, the following experiment will serve as an alternate for the receptor specificity confirmation.

Alternative experiment: Verification of THEV receptor specificity by receptor expression in non-permissive cells, e.g., peripheral T lymphocytes (PTL), followed by an infectivity assay.

Methods:

1. T-lymphocyte preparation from turkey peripheral blood:
    a. Peripheral blood lymphocytes (PBL) will be isolated as described previously (Berndt and Methner, 2001; Kapczynski, 2008), with some modifications. Briefly, heparinized blood will be drawn from wing vein turkey poults of less than 5 weeks of age using blood collection Vacutainer® tubes with heparin and Eclipse™ needles (Becton, Dickenson, and Company). With Histopaque 1077 (Sigma-Aldrich), PBL (aka. buffy coat) fraction will be collected from whole blood using density gradient centrifugation procedure. Cells will be washed with HBSS and finally resuspended in RPMI 1640 media. Cell viability and count will be assessed by trypan blue dye exclusion method with a hemacytometer (Strober, 2001).
    b. Flow cytometry and cell sorting for T cell isolation: Isolated PBL will be incubated with T cell-specific fluorescently labeled primary antibodies against CD4 (Mouse Anti-Chicken CD4-FITC), CD8α (Mouse Anti-Chicken CD8 α-CY5), and CD3 (Mouse Anti-Chicken CD3-R-PE) (all from Southern Biotech, Birmingham, AL) on ice for 30 min. Cells will be washed, resuspended in cold PBS, and then analyzed by flow cytometry. Using the flow cytometer cell sorter, T cell sub-populations will be separated in a clean tube and maintained thereafter in RPMI media containing 10% FBS until used in the transfection procedure.

2. Preparation of a cDNA clone encoding the identified receptor/protein for T-cell transfection:
    a. The nt sequence of the gene encoding a defined THEV receptor will be obtained by searching the NCBI GenBank nt sequence database. Obtained sequences will be used to design a primer pair spanning that gene using Primer3 software.
    b. Total RNA will be extracted from cultured RP19 cells using an RNeasy mini kit (Qiagen).
    c. First-strand complementary DNA (cDNA) will be synthesized by a SuperScript™ III Reverse Transcriptase kit (Invitrogen). This cDNA will be used to amplify the ds cDNA with gene-specific primers in a standard PCR reaction.
    d. The synthesized cDNA will be gel-purified based on its size and then inserted into an expression vector, generating a plasmid cDNA encoding the receptor protein.
    e. If more than one unique cell surface protein is found to be involved in THEV endocytosis, steps a through d will be repeated for each protein gene. Generated plasmids will be designated pTHEVrec1, pTHEVrec2, etc.
3. Transfection of T lymphocytes: T cells will be transfected with the prepared plasmid DNA through a lipid-based transfection technique using Lipofectamine® LTX with Plus™ Reagent (Invitrogen) according to the manufacturer's instructions and recommended modifications (Yahiro et al., 2012). Viability of transfected cells will be observed by trypan blue dye exclusion test.
4. Experimental design:
    a. RP19 cells, transfected T-cells, and non-transfected T-cells will be incubated with 100 µl of THEV suspension for 1 h.
    b. Steps 3 and 4 in Experiment 3 above (Aim #3) will be performed as described.

6.3. Conclusions

First, this dissertation describes the development of a simple and reproducible qPCR assay and a novel qPCR-based infectivity assay. These assays are excellent

laboratory tools to determine the genomic and the infectious titers of THEV in live vaccines as well as experimental samples. They can be used by vaccine producers to obtained more standardized vaccines with consistent titers. Additionally, qPCR was used to study virus replication in cultured cells. Second, we report for the first time based on virus-cell interaction studies, the nature of THEV receptors on target cells. Data that supports the use of sialic acid as a virus receptor was presented. The involvement of surface carbohydrates and proteins in THEV entry was demonstrated. Further, two membrane protein molecules were found to interact with THEV. Revealing the identity of these proteins should be given a high priority in future research.

6.4. References

Arnberg, N., Edlund, K., Kidd, A.H. and Wadell, G., 2000. Adenovirus Type 37 Uses Sialic Acid as a Cellular Receptor. J. Virol. 74, 42-48.

Berndt, A. and Methner, U., 2001. Gamma/delta T cell response of chickens after oral administration of attenuated and non-attenuated Salmonella typhimurium strains. Vet Immunol Immunopathol 78, 143-61.

Kapczynski, D.R., 2008. Evaluating the cell-mediated immune response of avian species to avian influenza viruses. Methods in molecular biology (Clifton, N.J.) 436, 113-26.

Koudelka, K.J., Destito, G., Plummer, E.M., Trauger, S.A., Siuzdak, G. and Manchester, M., 2009. Endothelial Targeting of Cowpea Mosaic Virus (CPMV) via Surface Vimentin. PLoS Pathog 5, e1000417.

Li, X., Bangari, D.S., Sharma, A. and Mittal, S.K., 2009. Bovine adenovirus serotype 3 utilizes sialic acid as a cellular receptor for virus entry. Virology 392, 162-8.

Rautenschlein, S., Suresh, M. and Sharma, J.M., 2000. Pathogenic avian adenovirus type II induces apoptosis in turkey spleen cells. Arch Virol 145, 1671-83.

Singh, A.K., Berbis, M.A., Ballmann, M.Z., Kilcoyne, M., Menendez, M., Nguyen, T.H., Joshi, L., Canada, F.J., Jimenez-Barbero, J., Benko, M., Harrach, B. and van Raaij, M.J., 2015. Structure and Sialyllactose Binding of the Carboxy-Terminal Head Domain of the Fibre from a Siadenovirus, Turkey Adenovirus 3. PLoS One 10, e0139339.

Strober, W. 2001. Trypan Blue Exclusion Test of Cell Viability, Current Protocols in Immunology, John Wiley & Sons, Inc.

Trauger, S.A., Wu, E., Bark, S.J., Nemerow, G.R. and Siuzdak, G., 2004. The Identification of an Adenovirus Receptor by Using Affinity Capture and Mass Spectrometry. ChemBioChem 5, 1095-1099.

Wu, E., Fernandez, J., Fleck, S.K., Von Seggern, D.J., Huang, S. and Nemerow, G.R., 2001. A 50-kDa Membrane Protein Mediates Sialic Acid-Independent Binding and Infection of Conjunctival Cells by Adenovirus Type 37. Virology 279, 78-89.

Yahiro, K., Satoh, M., Nakano, M., Hisatsune, J., Isomoto, H., Sap, J., Suzuki, H., Nomura, F., Noda, M., Moss, J. and Hirayama, T., 2012. Low-density Lipoprotein Receptor-related Protein-1 (LRP1) Mediates Autophagy and Apoptosis Caused by Helicobacter pylori VacA. Journal of Biological Chemistry 287, 31104-31115.

Appendix A

qPCR Assay Supplemental Data

A. *Nucleotide sequences of the 445 bp and the 115 bp (underlined) THEV hex fragments amplified by the standard PCR and the qPCR assays described in Chapter 3*

GCGGATTTGATGAGTAGGAATCATTATTATAGTCAGTGGAATCAAGCTGTAGATGATTATGATTTAAATG
TTAGAGTACTTACAAATATTGGTTATGAAGAGGGTCCTCCAGGTTACTGTTATCCAAGCACAGGCATGGG
CAACTATCCTAATACTGTCATGTCGGTTGGGACATTAGTGGATAATAATGGTACAACTGCTACAACAACG
TCAAATACTGTAGCTGTGATGGGTTTTGGCAGTGTTCCTACTATGGAAATTAACGTTCAAGCTTATTTGCA
AAAATGTTGGATGTATGCTAACATTGCAGAATATTTACCTGATAAGTATAAAAAAGCTATTCAAGGTACT
AGTGAAACTGATCCAACAACTTATAGTTATATGAATAGTAGGCTTCCTAATGTGAATATGGCTGATCTCTT
TACACATATTGGCGGGCGTTATA

B. *BLAST searches for the 445 bp and 115 bp THEV hex fragments used as targets for PCR assays*

A

Nucleotide Sequence (445 letters)

RID 141S76FH014 (Expires on 10-06 13:13 pm)

Query ID lcl|Query_31519
Description None
Molecule type nucleic acid
Query Length 445

Database Name nr
Description Nucleotide collection (nt)
Program BLASTN 2.2.32+

⊕Graphic Summary

⊖Descriptions

Sequences producing significant alignments:

Description	Max score	Total score	Query cover	E value	Ident	Accession
Avirulent turkey hemorrhagic enteritis virus strain Virginia, complete sequence	822	822	100%	0.0	100%	AY849321.1
Hemorrhagic enteritis virus, complete genome	822	822	100%	0.0	100%	AF074946.1
Turkey adenovirus A isolate THEV/IT/Ty/1037/09 hexon-like gene, partial sequence	817	817	100%	0.0	99%	KJ372213.1
Hemorrhagic enteritis virus hexon protein gene, partial cds	817	817	100%	0.0	99%	AF075681.1

B

Nucleotide Sequence (115 letters)

RID 142XC0UM01R (Expires on 10-06 13:33 pm)

Query ID lcl|Query_152939
Description None
Molecule type nucleic acid
Query Length 115

Database Name nr
Description Nucleotide collection (nt)
Program BLASTN 2.2.32+

⊕Graphic Summary

⊖Descriptions

Sequences producing significant alignments:

Description	Max score	Total score	Query cover	E value	Ident	Accession
Turkey adenovirus A isolate THEV/IT/Ty/1037/09 hexon-like gene, partial sequence	213	213	100%	5e-52	100%	KJ372213.1
Avirulent turkey hemorrhagic enteritis virus strain Virginia, complete sequence	213	213	100%	5e-52	100%	AY849321.1
Hemorrhagic enteritis virus hexon protein gene, partial cds	213	213	100%	5e-52	100%	AF075681.1
Hemorrhagic enteritis virus, complete genome	213	213	100%	5e-52	100%	AF074946.1

Fig. A-1. BLAST searches for the 445-nt (A) and 115-nt (B) *hex* fragments used as targets for the standard PCR and qPCR assays in this study. No sequence homology was found with DNA from other organisms; the only matching DNA sequences found were those from THEV isolates.

Appendix B

Effect of Lectins on RP19 Cells

Materials and methods

Expt. 1: Effect of WGA and MAA lectins on RP19 cells

Treatment of cells and other experimental details are described in *Expt. 1*, subsection 5.3.6, Chapter 5.

Expt. 2: Further experiments on the effect of lectin treatment on RP19 cells

Light microscopy: RP19 cells (2×10^5) were washed twice with PFB-3, pelleted, resuspended in 100 µg of WGA, MAA, or SNA in 1 ml PFB-3, and incubated at 37°C for 1 h. Post-incubation, cells were centrifuged and no pellets were obtained from any lectin group as compared to the PBS-treated control cells, which had normal cell pellets. Thus, in lectin-treated groups, the upper portions (~85%) of cell suspensions were discarded and the lower portions, which were expected to contain cells (non-pelleted), were mixed with 250 µl of PFB-3. Cell pellets of control group were resuspended in 250 µl of PFB-3. Samples were kept in the refrigerator for 12 h before microscopic examination and imaging was performed. Samples (10 µl) of cells were deposited on regular glass slides, observed with Olympus BX60 microscope (Olympus America Inc., Center Valley, PA) under bright field settings at 400× magnification, and images were captured using QCapture Pro^{TM} 6.0 software (QImaging, Surrey, BC, Canada). In addition to this experiment, images were taken for cell samples from lectin *Expt. 2* described above. Small samples were collected immediately after washing the cells from the lectin treatment. SNA treatment was not included as the cells lysed and no cell pellets were available for examination.

Flow cytometry: The effect of WGA lectin treatment on the integrity of RP19 cells was investigated using a Fluorescence Activated Cell Sorter (FACS) assay. RP19 cells (1×10^6) were washed once with PBS and incubated with different concentrations of FITC-conjugated WGA (i.e., 0, 1, 5, or 10 µg in 1 ml of PBS) for 1 h on ice. The cell integrity was assessed using a combination of forward scatter (FSC) and side scatter

(SSC) parameters. Data was collected and analyzed using the machine and software described under subsection 5.3.3, Chapter 5.

Results

WGA has cytotoxic and cytoagglutinating effects on lymphoblastoid, RP19 cells

Microscopic examination of cells in Fig. B-2 showed that WGA-treated cells incubated on ice experienced a strong condition of agglutination. Therefore, this phenomenon was further explored by studying the effect of WGA lectin on the viability and agglutination of RP19 cells using a standard WGA-FITC staining procure and flow cytometry. Also, the effect of WGA, MAA, and SNA on RP19 cells at the standard temperature of 37°C was examined by light microscopy.

Microscopic study: Fig. B-1 displays light micrographs of RP19 cells treated with three lectin types and incubated at 37°C. It was evident that WGA treatment of RP19 cells caused severe agglutination, as indicated by the large size of clumped cells, and mild to moderate lysis, which is more noticeable in panel "WGA-3". MAA- and SNA-treated cells were not agglutinated, but they had various degrees of cytolysis. WGA lectins were reported to have high cytoagglutinating and cytotoxic effects on various types of lymphoblastoid cells when used at certain concentrations (Ohba and Bakalova, 2003; Ohba et al., 2003).

Flow cytometric study: RP19 cells were incubated on ice with increasing amounts of FITC-conjugated WGA, which binds to surface sialic acids, for 1 h, followed by FACS analysis. Based on the forward and side scatter parameters of flow cytometry, the total number of cells and the portion of single cells were determined in each treatment groups (Fig. B-3 and B-4). Data from this experiment was calculated and summarized in Table B-1. It was found that WGA lectin treatment of RP19 cells adversely influenced the measured parameters in a dose-dependent manner. The total number of cells was reduced by 45 or 52% when treated with 5 or 10 µg of FITC-WGA, respectively, as compared with the untreated control, indicating the strong cytolytic effects of WGA at these concentrations. The number of single cells was decreased by 26, 43, or 47% with the treatment of 1, 5, or 10 µg of WGA, respectively, indicating the cytoagglutination of RP19 by WGA (Table B-1).

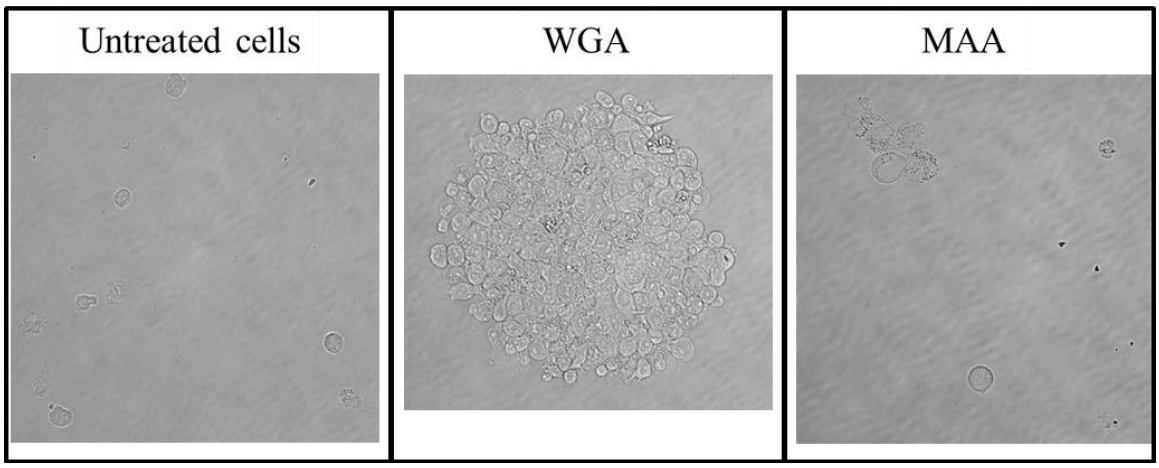

Fig. B-1. Photomicrographs showing the effects of WGA and MAA lectins (10 µg) on RP19 cells incubated on ice for 1 h. WGA caused severe agglutination of RP19 cells, while MAA did not show noticeable adverse effect on the cells compared with the untreated control. Image numbers under each treatment represent different microscopic fields on the same slide.

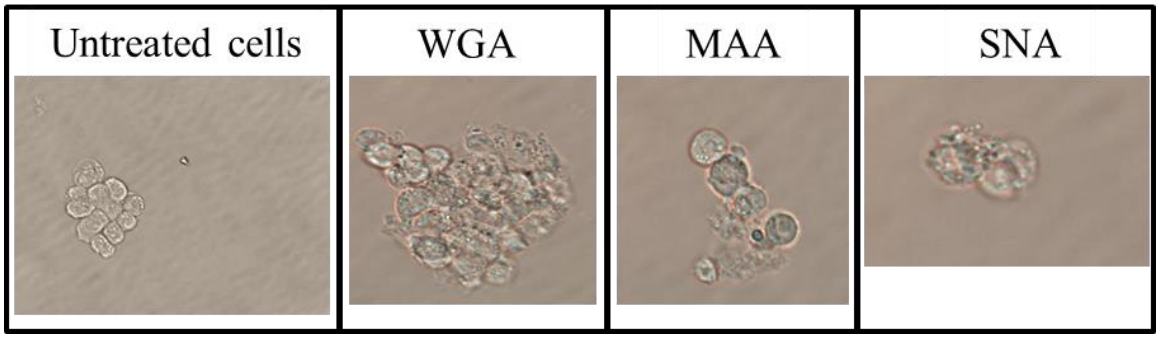

Fig. B-2. The cytotoxic and agglutinating effects of various lectin treatments on RP19, lymphoblastoid cells. Cells (2×10^5) were incubated with 100 µg (a relatively high concentration) of different plant lectins at 37°C for 1 h. WGA-treated cells became highly agglutinated, while MAA- and SNA-treated cells showed only mild signs of lysis. *Note: Clumping of untreated cells, which occurs naturally at temperatures below 41°C, can be distinguished from the severe "adhesive" effect of WGA.* All images were taken at 400× magnification.

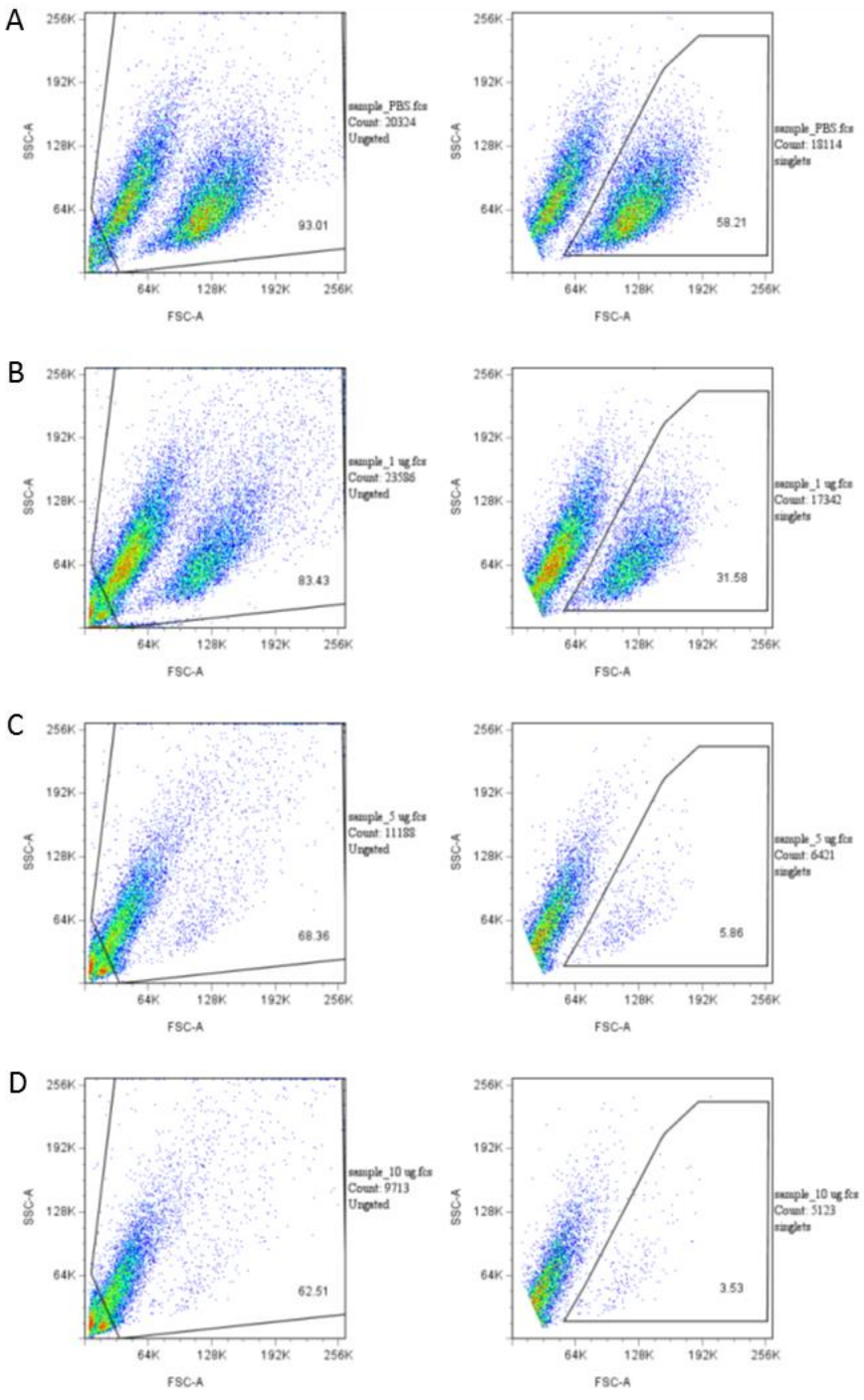

Fig. B-3. Dose-dependent agglutination and lysis of RP19 cells treated with WGA as determined by the forward and side scatter parameters of flow cytometric analysis. Cells (1×10^6) were incubated on ice for 1 h with various concentrations (0, 1, 5, or 10 µg/ml in PBS) of FITC-conjugated WGA and analyzed by a FACS assay. Panels A, B, C, and D represent the untreated, 1 µg, 5 µg, or 10 µg-treated cells, respectively. The cellular density plots at the left-side are used for total cell count, while those at the right are used for the single cells count.

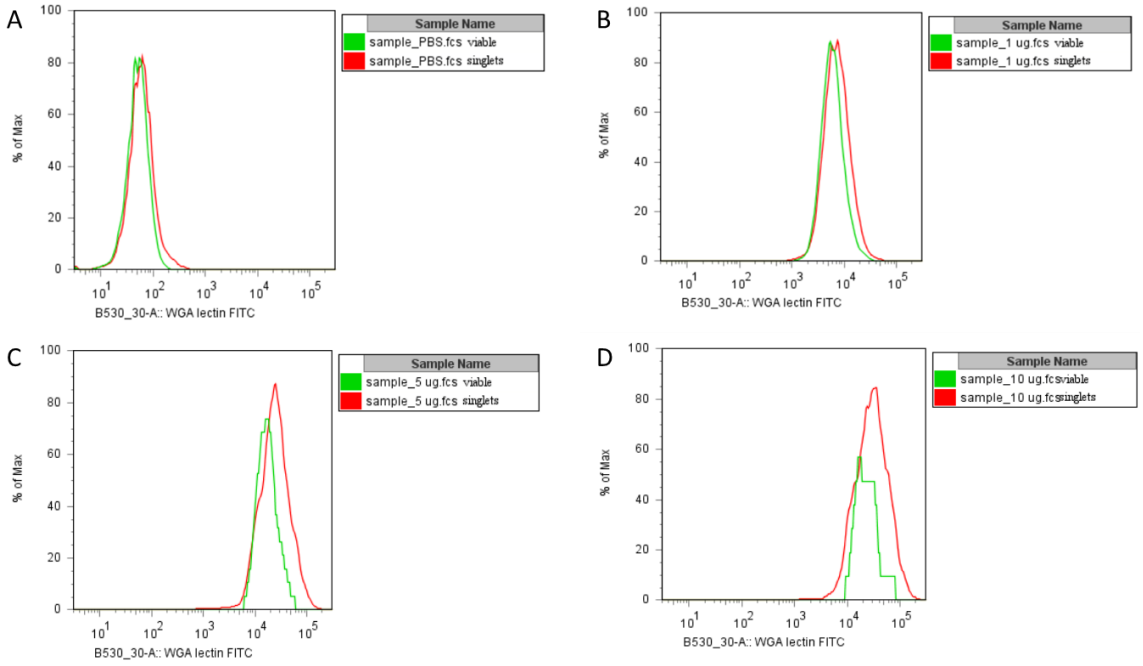

Fig. B-4. WGA treatment of RP19 cells reduced the cell viability in a dose-dependent manner as determined by FITC-staining and flow cytometry. For each treatment/panel, the number of total single cells analyzed is represented by a red-colored curve, while the proportion of the viable cells is represented by a green-colored curve. Panels A, B, C, and D represent the untreated, 1 µg, 5 µg, or 10 µg-treated cells, respectively.

Table B-1
Effect of WGA treatment on the agglutinability and viability of RP19 cells as determined by flow cytometry.

WGA concentration (µg)	Total no. of cells	Number of single cells (%)
0	20,324	18,114 (89.13)
1	23,586	17,342 (73.53)
5	11,188	6,421 (57.39)
10	9,713	5,123 (52.74)

References

Ohba, H. and Bakalova, R., 2003. Relationships between degree of binding, cytotoxicity and cytoagglutinating activity of plant-derived agglutinins in normal lymphocytes and cultured leukemic cell lines. Cancer chemotherapy and pharmacology 51, 451-8.

Ohba, H., Bakalova, R. and Muraki, M., 2003. Cytoagglutination and cytotoxicity of Wheat Germ Agglutinin isolectins against normal lymphocytes and cultured leukemic cell lines--relationship between structure and biological activity. Biochim Biophys Acta 1619, 144-50.